

1991

Novel Alumina-Based Stationary Phases for Liquid Chromatography.

Rene V. Arenas

Louisiana State University and Agricultural & Mechanical College

Follow this and additional works at: https://digitalcommons.lsu.edu/gradschool_disstheses

Recommended Citation

Arenas, Rene V., "Novel Alumina-Based Stationary Phases for Liquid Chromatography." (1991). *LSU Historical Dissertations and Theses*. 5221.

https://digitalcommons.lsu.edu/gradschool_disstheses/5221

This Dissertation is brought to you for free and open access by the Graduate School at LSU Digital Commons. It has been accepted for inclusion in LSU Historical Dissertations and Theses by an authorized administrator of LSU Digital Commons. For more information, please contact gradetd@lsu.edu.

INFORMATION TO USERS

This manuscript has been reproduced from the microfilm master. UMI films the text directly from the original or copy submitted. Thus, some thesis and dissertation copies are in typewriter face, while others may be from any type of computer printer.

The quality of this reproduction is dependent upon the quality of the copy submitted. Broken or indistinct print, colored or poor quality illustrations and photographs, print bleedthrough, substandard margins, and improper alignment can adversely affect reproduction.

In the unlikely event that the author did not send UMI a complete manuscript and there are missing pages, these will be noted. Also, if unauthorized copyright material had to be removed, a note will indicate the deletion.

Oversize materials (e.g., maps, drawings, charts) are reproduced by sectioning the original, beginning at the upper left-hand corner and continuing from left to right in equal sections with small overlaps. Each original is also photographed in one exposure and is included in reduced form at the back of the book.

Photographs included in the original manuscript have been reproduced xerographically in this copy. Higher quality 6" x 9" black and white photographic prints are available for any photographs or illustrations appearing in this copy for an additional charge. Contact UMI directly to order.

U·M·I

University Microfilms International
A Bell & Howell Information Company
300 North Zeeb Road, Ann Arbor, MI 48106-1346 USA
313/761-4700 800/521-0600

Order Number 9219520

Novel alumina-based stationary phases for liquid chromatography

Arenas, Rene V., Ph.D.

The Louisiana State University and Agricultural and Mechanical Col., 1991

U·M·I

300 N. Zeeb Rd.
Ann Arbor, MI 48106

**NOVEL ALUMINA-BASED STATIONARY PHASES
FOR LIQUID CHROMATOGRAPHY**

A Dissertation

**Submitted to the Graduate Faculty of the
Louisiana State University and
Agricultural and Mechanical College
in partial fulfillment of the
requirements for the degree of
Doctor of Philosophy**

in

The Department of Chemistry

**by
Rene V. Arenas
B.S., University of the Philippines at Los Baños, 1983
December 1991**

ACKNOWLEDGMENTS

To my research director, Professor Joe P. Foley, for sharing his knowledge of chromatography, I wish to extend my sincerest gratitude. His support and encouragement, and excellent suggestions during the conduct of my research, are very much appreciated.

Special thanks to the members of our research group (the Foleites) - Mark S. Jeansonne, Jeffrey A. Crow, Lori D. Payne, Edward L. Little, and Eric S. Ahuja, for our time together in the laboratory, in group meetings and social occasions.

I am also grateful to: Biotage, Inc. and LaRoche Chemicals, Inc., for providing the necessary materials and funds for the completion of this research; Dr. Kevin B. Holland (Biotage, Inc.) and Dr. John W. Novak, Jr. (LaRoche Chemicals, Inc.) for their helpful suggestions; Professors Kathleen M. Morden and Paul S. Russo for supplying the HPLC-grade water; and to all the faculty and staff of the Department of Chemistry at LSU for their academic and administrative support.

Finally, I would like to thank my Mom and Dad, my brother, Roehl, and sister Nancy, for their love and encouragement. And to my wife, Kellie, for her love and constant support, especially during our years of stay here in Baton Rouge, I am most grateful.

FOREWORD

This dissertation is about the chromatographic characterization of novel alumina-based stationary phases for high-performance liquid chromatography. For convenience, the material has been divided into two parts. Part A describes the unique chromatographic properties of polymer-coated Unisphere aluminas relative to conventional silica-based C₁₈ stationary phases for reversed-phase liquid chromatography, while Part B is about the optimization of the slurry-packing technique and chromatographic characterization of native Versal aluminas for normal-phase liquid chromatography. Although each part begins with general introduction and experimental chapters, additional introductory/experimental materials have been included in some chapters whenever appropriate. Finally, the chapters have been numbered consecutively, regardless of whether it belongs to Part A or Part B. It is hoped by the author that such an arrangement will result in easier comprehension of this dissertation.

TABLE OF CONTENTS

	<u>page</u>
ACKNOWLEDGEMENTS	ii
FOREWORD	iii
LIST OF TABLES	x
LIST OF FIGURES	xv
LIST OF SYMBOLS AND ABBREVIATIONS	xxii
ABSTRACT	xxvi
PART A. Polymer-Coated Unisphere Aluminas For Reversed-Phase Liquid Chromatography	1
CHAPTER	
I. General Introduction	2
A. Alkylbonded Silica-Based Stationary Phases	2
B. Polymer-Based Stationary Phases	3
Polystyrene-Divinylbenzene	3
C. Alumina-Based Stationary Phases	3
1. Chemically Bonded Stationary Phases On Alumina	4
2. Polymer-Coated Aluminas	5
Polymer Coating Of Support Material For RPLC	5
Polymer Coating Of Bare Alumina	7
D. Commercially Available Polymer-Coated Aluminas	8
1. Suppliers Of Polymer-Coated Aluminas	8
2. Unisphere Alumina	8
3. Unisphere Al-PBD, Unisphere Al-C ₁₈ And Unisphere Al-CN	9
References For Chapter I	12

II. Experimental	16
III. Solvent Strength Difference Between Acetonitrile And Methanol For The Polymer-Coated Aluminas And Si-C ₁₈	19
A. Comparison Of The Solvent Strengths Of MeCN And MeOH Based On k'	19
B. Relationship Between Log k' And Mobile Phase Composition	33
1. Using The Volume Fraction Of Organic Solvent	33
2. Using The $E_T(30)$ Solvent Polarity Scale	53
C. Comparison Of The S Values For The Different Columns	64
Limitations Of Using The S Value As A Measure Of Solvent Strength	69
D. Comparison Of The Difference In Solvent Strength Between MeCN And MeOH For The Polymer-Coated Aluminas And Si-C ₁₈ Columns Using The S Value	72
1. Unisphere And Millipore Al-PBD vs. Microsorb Si-C ₁₈	72
2. Unisphere Al-C ₁₈ And Unisphere Al-CN vs. LiChrospher Si-C ₁₈	75
E. Comparison Of The Solvent Strengths Of MeCN And MeOH Using ϵ	77
Relationship Between Log ϵ And Volume Fraction Of Organic Solvent	79
Conclusions	90
References For Chapter III	91
IV. Effect Of Binary Mobile Phase Composition And Stationary Phase Type On Methylene Selectivity	93
Introduction	93
Results And Discussion	94
A. Effect Of Mobile Phase Composition On Methylene Group Selectivity	101
B. Effect Of Stationary Phase Type On Methylene Group Selectivity	106

1. Toluene And Ethylbenzene	106
2. Hexane And Heptane	112
3. 2-Pentanone And 2-Hexanone	112
4. Acetophenone And Propiophenone	113
Conclusions	113
References For Chapter IV	115
V. Effect Of Temperature On Retention And Methylene Selectivity.....	116
Introduction	116
Experimental	117
Results And Discussion	118
A. Effect Of Temperature On Methylene Selectivity	118
B. Comparison Of ΔH° Values	123
References For Chapter V	131
VI. Polar Group Selectivity Of Polymer-Coated Aluminas	132
Introduction	132
Results And Discussion	132
A. Hydrophobic Selectivity	135
B. Polar Group Selectivity	135
1. Surface Hydroxyl Group Participation In Solute Retention	140
2. Effect Of Mobile Phase Composition On Polar Group Selectivity	147
Conclusions	149
References For Chapter VI	150
VII. Kinetic Performance Of Polymer-Coated Aluminas	151
Introduction	151
Reduced Parameters	152

Results And Discussion	155
A. Comparison Of Pertinent Kinetic Parameters At Optimum Flow Rates	155
B. Comparison Of Pertinent Kinetic Parameters At Practical Flow Rates	163
C. Comparison Of Pressure Drops Over A Range Of Flow Rates	167
D. Column Stability Of Al-CN And Al-C ₁₈	173
E. Combined Effects Of k' , α And $N_{0.5}$ On Resolution	176
Toluene And Ethylbenzene	178
Conclusions	186
References For Chapter VII	187
VIII. Column Re-Equilibration After Gradient Elution	189
Introduction	189
A. Gradient Elution In RPLC	189
B. Column Re-equilibration After Gradient Elution In RPLC	190
C. Literature Survey On Column Re-equilibration	190
1. Recommendations By Snyder's Group	191
2. Research Results Of Other Investigators	192
Experimental	195
Results And Discussion	198
A. Effect Of The Magnitude Of The Gradient Step ($\Delta\%B$)	198
B. Effect Of Flow Rate	203
C. Effect Of Temperature	209
References For Chapter VIII	215

PART B. Versal Aluminas for Normal-Phase Liquid Chromatography	216
IX. General Introduction	217
A. γ -Alumina For Normal-Phase Liquid Chromatography	217
Versal GL And Versal GH Aluminas	218
B. Packing of HPLC Columns	218
1. High-Pressure Slurry-Packing Of HPLC Columns	219
2. Dry-Packing Of HPLC Columns	222
References For Chapter IX	223
X. Experimental	224
A. Preparation Of Adsorbent And HPLC Column Blanks	224
B. High-Pressure, Slurry-Packing Procedure	225
C. Dry-Packing Procedure	228
1. "Tap-Fill" Method	228
2. "Lateral Tapping" Method	229
D. Conditioning The Column	229
E. Evaluation Of Column Performance	230
1. Instrumentation	230
2. Solvents And Solutes	231
3. "Reference" Stationary Phases	231
4. Chromatographic Parameters	231
5. Column Test Mixture	231
6. Alternative To Complete Column Conditioning For Evaluation Column Packing Efficiency	232
References For Chapter X	233
XI. Optimization Of HPLC Column Packing Procedure	234
A. γ -Alumina Samples Received From LaRoche Chemicals, Inc.	234

B. Particle Diameter, Particle Size Distribution And Particle Shape	241
C. Optimization Of HPLC Column Packing Procedure For LaRoche Aluminas And A Control Silica	244
1. Versal GL	250
$d_p = 10-15 \mu m$	250
$d_p = 37-44 \mu m$	253
2. Versal GH	257
$d_p = 5-10 \mu m$ and $10-15 \mu m$	257
$d_p = 15 \mu m$ ("air-classified")	263
$d_p = 37-44 \mu m$	264
3. IMPAQ RG2010Si	265
References For Chapter XI	269
XII. Chromatographic Characteristics Of Packed Versal HPLC Columns	270
Chromatographic Characteristics Of Various Aluminas	270
Conclusions	282
XIII. Summary And Conclusions	283
A. Polymer-Coated Unisphere Aluminas For Reversed-Phase Liquid Chromatography	283
B. Versal Aluminas For Normal-Phase Liquid Chromatography	290
APPENDIX	
Miscellaneous Figures	292
VITA	296

LIST OF TABLES

TABLE	<u>page</u>
2.1 List of reversed-phase columns used	17
3.1A Retention factors of selected compounds for the Unisphere Al-PBD column with MeCN/H ₂ O as mobile phase	21
3.1B Retention factors of selected compounds for the Unisphere Al-PBD column with MeOH/H ₂ O as mobile phase	22
3.2A Retention factors of selected compounds for the Millipore Al-PBD column with MeCN/H ₂ O as mobile phase	23
3.2B Retention factors of selected compounds for the Millipore Al-PBD column with MeOH/H ₂ O as mobile phase	24
3.3A Retention factors of selected compounds for the Unisphere Al-C ₁₈ column with MeCN/H ₂ O as mobile phase	25
3.3B Retention factors of selected compounds for the Unisphere Al-C ₁₈ column with MeOH/H ₂ O as mobile phase	26
3.4A Retention factors of selected compounds for the LiChrospher Si-C ₁₈ column with MeCN/H ₂ O as mobile phase	27
3.4B Retention factors of selected compounds for the LiChrospher Si-C ₁₈ column with MeOH/H ₂ O as mobile phase	28
3.5A Retention factors of selected compounds for the Microsorb Si-C ₁₈ column with MeCN/H ₂ O as mobile phase	29
3.5B Retention factors of selected compounds for the Microsorb Si-C ₁₈ column with MeOH/H ₂ O as mobile phase	29
3.6A Retention factors of selected compounds for the Unisphere Al-CN column with MeCN/H ₂ O as mobile phase	30
3.6B Retention factors of selected compounds for the Unisphere Al-CN column with MeOH/H ₂ O as mobile phase	31
3.7 Retention factors of toluene for the different stationary phases using 60/40 MeOH/H ₂ O as mobile phase	32
3.8A Linear and quadratic fits of plots of log k' vs. ϕ or E _T (30) polarity for the Unisphere Al-PBD column with MeCN/H ₂ O as mobile phase	35

3.8B	Linear and quadratic fits of plots of $\log k'$ vs. ϕ or $E_T(30)$ polarity for the Unisphere Al-PBD column with MeOH/H ₂ O as mobile phase	36
3.9A	Linear and quadratic fits of plots of $\log k'$ vs. ϕ or $E_T(30)$ polarity for the Millipore Al-PBD column with MeCN/H ₂ O as mobile phase	37
3.9B	Linear and quadratic fits of plots of $\log k'$ vs. ϕ or $E_T(30)$ polarity for the Millipore Al-PBD column with MeOH/H ₂ O as mobile phase	38
3.10A	Linear and quadratic fits of plots of $\log k'$ vs. ϕ or $E_T(30)$ polarity for the Microsorb Si-C ₁₈ column with MeCN/H ₂ O as mobile phase	39
3.10B	Linear and quadratic fits of plots of $\log k'$ vs. ϕ or $E_T(30)$ polarity for the Microsorb Si-C ₁₈ column with MeOH/H ₂ O as mobile phase	40
3.11A	Linear and quadratic fits of plots of $\log k'$ vs. ϕ or $E_T(30)$ polarity for the Unisphere Al-C ₁₈ column with MeCN/H ₂ O as mobile phase	41
3.11B	Linear and quadratic fits of plots of $\log k'$ vs. ϕ or $E_T(30)$ polarity for the Unisphere Al-C ₁₈ column with MeOH/H ₂ O as mobile phase	42
3.12A	Linear and quadratic fits of plots of $\log k'$ vs. ϕ or $E_T(30)$ polarity for the Unisphere Al-CN column with MeCN/H ₂ O as mobile phase	43
3.12B	Linear and quadratic fits of plots of $\log k'$ vs. ϕ or $E_T(30)$ polarity for the Unisphere Al-CN column with MeOH/H ₂ O as mobile phase	44
3.13A	Linear and quadratic fits of plots of $\log k'$ vs. ϕ or $E_T(30)$ polarity for the LiChrospher Si-C ₁₈ column with MeCN/H ₂ O as mobile phase	45
3.13B	Linear and quadratic fits of plots of $\log k'$ vs. ϕ or $E_T(30)$ polarity for the LiChrospher Si-C ₁₈ column with MeOH/H ₂ O as mobile phase	47
3.14	Improvement in R^2 values from linear to quadratic fit for $\log k'$ vs. ϕ for solutes with linear correlation coefficients (R^2) < 0.990	48
3.15	$E_T(30)$ polarity values at different concentrations of MeCN and MeOH for binary hydroorganic mobile phases	54

3.16	List of solutes with R^2 values ≥ 0.990 for linear fits of plots of $\log k'$ vs. ϕ that decreased to < 0.990 with $\log k'$ vs. $E_T(30)$ polarity	58
3.17	Average R^2 values for linear correlations in Tables 3.8A-3.13B	60
3.18	Comparison of R^2 values for linear fits of $\log k'$ vs. ϕ or $E_T(30)$ polarity for solutes with R^2 values < 0.990 for linear fits of $\log k'$ vs. ϕ	61
3.19	Frequency of cases where R^2 actually decreased for linear fits of $\log k'$ vs. ϕ to $\log k'$ vs. $E_T(30)$ polarity from published results of Johnson <i>et al.</i>	63
3.20	Comparison of S values for Unisphere Al-PBD, Millipore Al-PBD and Microsorb Si-C ₁₈	65
3.21	Comparison of S values for Unisphere Al-C ₁₈ , Unisphere Al-CN and LiChrospher Si-C ₁₈	66
3.22	Comparison of S values for all alumina-based and silica-based columns	67
4.1	Effect of binary mobile phase composition on methylene group selectivity of n-alkylbenzenes and n-alkanes for the Unisphere Al-PBD column	95
4.2	Effect of binary mobile phase composition on methylene group selectivity of n-alkylbenzenes and n-alkanes for the Millipore Al-PBD column	96
4.3	Effect of binary mobile phase composition on methylene group selectivity of n-alkylbenzenes and n-alkanes for the Microsorb Si-C ₁₈ column	97
4.4	Effect of binary mobile phase composition on methylene group selectivity of 2-ketones, alkylphenones and n-alkylbenzenes for the Unisphere Al-C ₁₈ column	98
4.5	Effect of binary mobile phase composition on methylene group selectivity of 2-ketones, alkylphenones and n-alkylbenzenes for the Unisphere Al-CN column	99
4.6	Effect of binary mobile phase composition on methylene group selectivity of 2-ketones, alkylphenones and n-alkylbenzenes for the LiChrospher Si-C ₁₈ column	100
5.1	Effect of temperature on the methylene group selectivity for the 2-ketones	119

5.2	Effect of temperature on the methylene group selectivity for the n-alkylphenones	119
5.3	Effect of temperature on the methylene group selectivity for the n-alkylbenzenes	120
5.4	Effect of temperature on the methylene group selectivity for the n-alkylbenzenes for the Unisphere and Millipore Al-PBD columns	120
5.5	Thermodynamic parameters for the Unisphere Al-PBD column	124
5.6	Thermodynamic parameters for the Unisphere Al-C ₁₈ column	125
5.7	Thermodynamic parameters for the LiChrospher Si-C ₁₈ column	126
5.8	Thermodynamic parameters for the Unisphere Al-CN column	127
5.9	Thermodynamic parameters for the Unisphere and Millipore Al-PBD columns	128
6.1	Retention factors of selected compounds for the various Unisphere polymer-coated aluminas and Si-C ₁₈ columns with 50/50 MeOH/H ₂ O as mobile phase	133
6.2	Retention factors of selected compounds for the Al-PBD column at different MeOH/H ₂ O concentrations	134
6.3	Retention factors of selected compounds for the Al-C ₁₈ column at different MeOH/H ₂ O concentrations	134
6.4	Group selectivity values for the various Unisphere polymer-coated aluminas and Si-C ₁₈ phases with 50/50 MeOH/H ₂ O as mobile phase	136
6.5	Group selectivity values for the Al-PBD column at different MeOH/H ₂ O concentrations	137
6.6	Group selectivity values for the Al-C ₁₈ column at different MeOH/H ₂ O concentrations	137
6.7	Peak asymmetry factors for the different columns with 50/50 MeOH/H ₂ O as mobile phase	143
7.1	Limiting values of reduced parameters for excellent columns	154
7.2	Comparison of pertinent kinetic parameters at optimum linear velocity	159

7.3	Comparison of pertinent kinetic parameters for the different polymer-coated aluminas and Si-C ₁₈ columns for nitrobenzene at practical flow rates	165
7.4	Comparison of pertinent kinetic parameters for the different polymer-coated aluminas and Si-C ₁₈ columns for toluene at practical flow rates	166
7.5	Linear regression parameters for the plots in Figs. 7.8-7.9	172
7.6	N values used for calculating R _s for the different columns	179
7.7	R _s values for toluene and ethylbenzene at different mobile phase compositions for the various columns	180
7.8A	Relevant parameters for the comparison of R _s values for toluene and ethylbenzene at equivalent retention for ethylbenzene with MeCN/H ₂ O as mobile phase	182
7.8B	Relevant parameters for the comparison of R _s values for toluene and ethylbenzene at equivalent retention for ethylbenzene with MeOH/H ₂ O as mobile phase	183
11.1	γ-Al ₂ O ₃ samples received from LaRoche Chemicals, Inc.	235
11.2	Typical amounts of adsorbent needed to slurry-pack 15 cm HPLC columns	235
11.3	pH of 5.0% slurry with water of various adsorbent	242
11.4A	Summary of results for HPLC columns prepared using the high-pressure slurry-packing procedure	246
11.4B	Summary of results for HPLC columns prepared using the dry-fill packing procedure (d _p = 37-44 μm)	249
12.1	Peak asymmetry and column efficiency (N and h) of benzene derivatives for Versal GH (column 20A) and Unisphere neutral aluminas at 25.0° C	276
12.2	Retention factors of benzene derivatives for Versal GH (column 20A), Unisphere and Versal GL (column 3A) aluminas at different temperatures.....	278
12.3	Selectivity of benzene derivatives on Versal GH (column 20A), Unisphere and Versal GL (column 3A) aluminas at different temperatures	279
12.4	Thermodynamic retention parameters of benzene derivatives for Versal GH (column 20A) and Unisphere neutral aluminas	280

LIST OF FIGURES

FIGURE	<u>page</u>
3.1 Characteristic curvature in plots of $\log k'$ vs. ϕ for solutes with retention data at 0% organic solvent for the Unisphere Al-PBD column	49
3.2 Characteristic curvature in plots of $\log k'$ vs. ϕ for solutes with retention data at 0% organic solvent for the Unisphere Al-C ₁₈ column	50
3.3 Characteristic curvature in plots of $\log k'$ vs. ϕ for solutes with retention data at 0% organic solvent for the Unisphere Al-CN column	51
3.4 Characteristic curvature in plots of $\log k'$ vs. ϕ for solutes with retention data at 0% organic solvent for the LiChrospher Si-C ₁₈ column	52
3.5 Frequency plots of R^2 for linear fits of (A) $\log k'$ vs. ϕ , and (B) $\log k'$ vs. $E_T(30)$	56
3.6 Examples of solutes that exhibit an approximately linear relationship for $\log k'$ vs. ϕ for the various stationary phases	68
3.7 Dependence of S on the mobile phase composition range over which it is measured for the Unisphere Al-PBD column	71
3.8 Difference in solvent strength between MeCN and MeOH as a function of mobile phase composition for the Unisphere Al-PBD column	80
3.9 Difference in solvent strength between MeCN and MeOH as a function of mobile phase composition for the Millipore Al-PBD column	81
3.10 Difference in solvent strength between MeCN and MeOH as a function of mobile phase composition for the Unisphere Al-C ₁₈ column	82
3.11 Difference in solvent strength between MeCN and MeOH as a function of mobile phase composition for the Unisphere Al-CN column	83
3.12 Difference in solvent strength between MeCN and MeOH as a function of mobile phase composition for the Microsorb Si-C ₁₈ column	84

3.13	Difference in solvent strength between MeCN and MeOH as a function of mobile phase composition for the LiChrospher Si-C ₁₈ column	85
3.14	Difference in solvent strength between MeCN and MeOH as a function of mobile phase composition for the Nucleosil 10-RP18 (silica-based) column	86
3.15	Relative proportion of free MeCN and free MeOH as a function of mobile phase composition	88
4.1	Effect of binary mobile phase composition of (A) MeCN/H ₂ O, and (B) MeOH/H ₂ O on the methylene group selectivity of n-alkylbenzenes for various polymer-coated aluminas and Si-C ₁₈ columns	102
4.2	Effect of binary mobile phase composition of (A) MeCN/H ₂ O, and (B) MeOH/H ₂ O on the methylene group selectivity of n-alkanes for various polymer-coated aluminas and Si-C ₁₈ columns	103
4.3	Effect of binary mobile phase composition of (A) MeCN/H ₂ O, and (B) MeOH/H ₂ O on the methylene group selectivity of 2-ketones for various polymer-coated aluminas and Si-C ₁₈ columns	104
4.4	Effect of binary mobile phase composition of (A) MeCN/H ₂ O, and (B) MeOH/H ₂ O on the methylene group selectivity of alkylphenones for various polymer-coated aluminas and Si-C ₁₈ columns	105
4.5	Linearity of plots of log (α_{CH_2}) vs. % organic solvent for 2-ketones for the LiChrospher Si-C ₁₈ column	107
4.6	Linearity of plots of log (α_{CH_2}) vs. % organic solvent for 2-ketones for the Unisphere Al-C ₁₈ column	107
4.7	Comparison of the α_{CH_2} values for the n-alkylbenzenes (toluene and ethylbenzene) using the ratio method with (A) MeCN/H ₂ O, and (B) MeOH/H ₂ O as mobile phases	108
4.8	Comparison of the α_{CH_2} values for the n-alkanes (hexane and heptane) using the ratio method with (A) MeCN/H ₂ O, and (B) MeOH/H ₂ O as mobile phases	109
4.9	Comparison of the α_{CH_2} values for the 2-ketones (2-pentanone and 2-hexanone) using the ratio method with (A) MeCN/H ₂ O, and (B) MeOH/H ₂ O as mobile phases	110

4.10	Comparison of the α_{CH_2} values for the alkylphenones (acetophenone and propiophenone) using the ratio method with (A) MeCN/H ₂ O, and (B) MeOH/H ₂ O as mobile phases	111
5.1	Effect of temperature on methylene selectivity for the 2-ketones for the various polymer-coated aluminas and Si-C ₁₈ column (same data as in Table 5.1)	122
5.2	Van't Hoff plots for the retention of 2-ketones for the Unisphere Al-C ₁₈ stationary phase using 30/70 MeCN/H ₂ O as mobile phase	129
6.1	Group selectivity for the various Unisphere polymer-coated aluminas and Si-C ₁₈ columns with 50/50 MeOH/H ₂ O as mobile phase at 25.0° C	138
6.2	Calculation of peak asymmetry	142
6.3	Surface hydroxyl group participation in solute retention as reflected in the selectivity values for phenol-aniline and methylbenzoate-methylaniline for the Unisphere polymer-coated aluminas and Si-C ₁₈ columns with 50/50 MeOH/H ₂ O as mobile phase at 25.0° C	146
6.4	Comparison of the nitro group selectivity for the various polymer-coated aluminas and Si-C ₁₈ column using 50% MeCN and 50% MeOH as mobile phases	148
7.1	Van Deemter plot for the Unisphere Al-PBD column	157
7.2	Van Deemter plot for the Unisphere Al-CN column	157
7.3	Van Deemter plot for the Unisphere Al-C ₁₈ column	158
7.4	Van Deemter plot for the Microsorb Si-C ₁₈ column	158
7.5	Van Deemter plots for retained solutes for all columns	162
7.6	Van Deemter plots for acetone for all columns	162
7.7	Comparison of normalized pressure drops ($\Delta P_{dp}^2/L$) for two porous Si-C ₁₈ and three Unisphere polymer-coated aluminas	171
7.8	Comparison of backpressures for hypothetical columns of equal column length (250 mm) and particle diameter (8 μ m) for the various silica- and alumina-based reversed-phase packings	171
7.9	Loss of stationary phase and change in column efficiency with time for the Unisphere Al-C ₁₈	175

7.10	Loss of stationary phase and change in column efficiency with time for the Unisphere Al-CN	175
7.11	Changes in ΔP and $As_{0.1}$ with time for the Unisphere Al-CN	177
7.12	Changes in ΔP and $As_{0.1}$ with time for the Unisphere Al-C ₁₈	177
8.1	Typical plot of k'/k'_{ss} vs. $(V-V_d)/V_m$ for 100 to 60% MeCN reversed step gradient for the Unisphere Al-CN column	196
8.2	Effect of initial mobile phase composition of the gradient run on column re-equilibration after gradient elution for the Microsorb Si-C ₁₈	199
8.3	Effect of initial mobile phase composition of the gradient run on column re-equilibration after gradient elution for the Unisphere Al-PBD	199
8.4	Effect of initial mobile phase composition of the gradient run on column re-equilibration after gradient elution for the Unisphere Al-C ₁₈	200
8.5	Effect of initial mobile phase composition of the gradient run on column re-equilibration after gradient elution for the Unisphere Al-CN	200
8.6	Plot of k'/k'_{ss} vs. $(V-V_d)/V_m$ for 100% MeCN to 100% H ₂ O reversed step gradient for the Microsorb Si-C ₁₈ column	202
8.7	Effect of flow rate on column re-equilibration volume after gradient elution for the Microsorb Si-C ₁₈	205
8.8	Effect of flow rate on column re-equilibration volume after gradient elution for the Unisphere Al-PBD	205
8.9	Effect of flow rate on column re-equilibration volume after gradient elution for the Unisphere Al-C ₁₈	206
8.10	Effect of flow rate on column re-equilibration volume after gradient elution for the Unisphere Al-CN	206
8.11	Effect of flow rate on column re-equilibration time after gradient elution for the Microsorb Si-C ₁₈	207
8.12	Effect of flow rate on column re-equilibration time after gradient elution for the Unisphere Al-PBD	207
8.13	Effect of flow rate on column re-equilibration time after gradient elution for the Unisphere Al-C ₁₈	208

8.14	Effect of flow rate on column re-equilibration time after gradient elution for the Unisphere Al-CN	208
8.15	Effect of temperature on column re-equilibration after gradient elution for the LiChrospher Si-C ₁₈	210
8.16	Effect of temperature on column re-equilibration after gradient elution for the Unisphere Al-PBD	210
8.17	Effect of temperature on column re-equilibration after gradient elution for the Unisphere Al-C ₁₈	211
8.18	Effect of temperature on column re-equilibration after gradient elution for the Unisphere Al-CN	211
8.19	Mobile phase viscosity at different compositions for hydroorganic mixtures of MeCN and MeOH	213
10.1	Diagram illustrating Alltech's high-pressure slurry packing apparatus	226
11.1	Scanning electron micrographs of Versal GH after removal of fines; $d_p = 37\text{-}44\ \mu\text{m}$	236
11.2	Scanning electron micrographs of Versal GH after removal of fines; $d_p = 10\text{-}15\ \mu\text{m}$	237
11.3	Scanning electron micrographs of Versal GL after removal of fines; $d_p = 10\text{-}15\ \mu\text{m}$	238
11.4	Scanning electron micrographs of Versal GH ("air-classified") with fines; $d_p = 15\ \mu\text{m}$	239
11.5	Scanning electron micrographs of Versal GH ("air-classified") after removal of fines; $d_p = 15\ \mu\text{m}$	240
11.6	Scanning electron micrographs of IMPAQ RG2010Si after removal of fines; $d_p = 8.8\ \mu\text{m}$	245
11.7	Chromatograms for toluene illustrating the column performance of 10-15 μm Versal GL aluminas slurry-packed at an inlet pressure of 7320 psi (6A) and 8540 psi (15A*)	251
11.8	Chromatograms for toluene illustrating the column performance of 37-44 μm Versal GL aluminas prepared by the dry-fill packing procedure involving "lateral tapping" only	255
11.9	Chromatograms for toluene illustrating the column performance of 37-44 μm Versal GL aluminas slurry-packed at an inlet pressure of 6100 psi	256

11.10	Chromatograms for toluene illustrating the column performance of 5-10 μm Versal GH aluminas slurry-packed at an inlet pressure of 9760 psi (16A) and 10980 psi (13A and 19A)	260
11.11	Chromatograms for toluene illustrating the column performance of 10-15 μm Versal GH aluminas slurry-packed at an inlet pressure of 6100 psi (5A), 9760 psi (17A) and 10980 psi (12A) ..	261
11.12	Chromatogram for toluene illustrating the column performance of 10-15 μm Versal GH alumina slurry-packed at an inlet pressure of 10980 psi (20A)	262
11.13	Chromatogram for toluene illustrating the column performance of 37-44 μm Versal GH alumina slurry-packed at an inlet pressure of 7320 psi (2A)	266
11.14	Chromatograms for toluene illustrating the column performance of 37-44 μm Versal GH aluminas prepared by the dry-fill packing procedure involving "lateral tapping" only	267
12.1	Normal-phase separation of benzene derivatives for 100 x 4.6 mm Versal GH Alumina (20A in Table 11.4A; d_p : 10-15 μm). Flow rate: 0.5 mL/min	271
12.2	Same as in Fig. 12.1. Flow rate: 1.0 mL/min	271
12.3	Normal-phase separation of benzene derivatives for 150 x 4.6 mm Versal GH Alumina (34A* in Table 11.4A; d_p : 15 μm). Flow rate: 0.5 mL/min	272
12.4	Same as in Fig. 12.3. Flow rate: 1.0 mL/min	272
12.5	Normal-phase separation of benzene derivatives for 150 x 4.6 mm Versal GH Alumina (35A* in Table 11.4A; d_p : 15 μm). Flow rate: 1.0 mL/min	273
12.6	Normal-phase separation of benzene derivatives for 100 x 4.6 mm Versal GL Alumina (3A in Table 11.4A; d_p : 37-44 μm). Flow rate: 0.5 mL/min	274
12.7	Same as in Fig. 12.6. Flow rate: 1.0 mL/min	274
12.8	Normal-phase separation of benzene derivatives for 250 x 4.6 mm Unisphere Neutral Alumina (SN 580ATC; d_p : 10 μm). Flow rate: 1.25 mL/min	275
12.9	Same as in Fig. 12.8. Flow rate: 2.0 mL/min	275
A.1	Plot of data in Table 5.2, illustrating the effect of temperature on α_{CH_2} for the n-alkylphenones for the various polymer-coated aluminas and LiChrospher Si-C ₁₈ column	293

A.2	Plot of data in Table 5.3, illustrating the effect of temperature on α_{CH_2} for the n-alkylbenzenes for the Unisphere Al-PBD and Al-C ₁₈ columns with 30% organic solvent as mobile phase	293
A.3	Plot of data in Table 5.4, illustrating the effect of temperature on α_{CH_2} for the n-alkylbenzenes for the Unisphere and Millipore Al-PBD phase with 60% organic solvent as mobile phase	294
A.4	Plot of data in Table 6.5, illustrating the effect of mobile phase composition (organic solvent = MeOH) on group selectivity for the Al-PBD phase	294
A.5	Plot of data in Table 6.6, illustrating the effect of mobile phase composition (organic solvent = MeOH) on group selectivity for the Al-C ₁₈ phase	295

LIST OF SYMBOLS AND ABBREVIATIONS

RPLC	Reversed-phase liquid chromatography
HPLC	High-performance liquid chromatography
PS-DVB	Polystyrene-divinylbenzene
ODA	Octadecylalumina; with octadecyl group chemically bonded onto the alumina
ODS	Octadecylsilica; synonymous to Si-C ₁₈
PBD	Polybutadiene
PMSC ₁₈	Polymethyloctadecylsiloxane
Al-PBD	Alumina coated with polybutadiene
Al-C ₁₈	Alumina coated with 2-octadecyl-1,3-butadiene
Al-CN	Alumina coated with a polymeric cyano phase
Al-C ₁	Alumina coated with polyisoprene
Si-C ₁₈	Octadecyl group chemically bonded onto silica; synonymous to ODS
MeCN	Acetonitrile
MeOH	Methanol
H ₂ O	Water
SN	Serial number
d_p	Particle diameter
k'	Retention factor (or capacity factor)
t_R	Solute retention time
t_m	Retention time for an unretained solute
RSD	Relative standard deviation
ϕ	Volume fraction of organic solvent in mobile phase
k'_w	Retention factor in pure water

S	Parameter used to measure the solvent strength of the organic modifier. S is equivalent to the negative of the slope from linear plots of log k' vs. ϕ
E_T(30) polarity scale	Mobile phase polarity scale based on the charge transfer absorption of 2,6-diphenyl-4-(2,4,6-triphenyl-N-pyridinio)phenolate
I	A constant which is a function of the partition coefficient, phase ratio, and adsorbed displacing agent
D_o	Concentration of organic solvent in mobile phase
z	Number of solvent molecules displaced
ε	Ratio of k' values for a given solute at equal % organic solvent for MeOH/H ₂ O and MeCN/H ₂ O
α_{CH₂}	Methylene group selectivity
α	Selectivity
K	Solute distribution coefficient
V_S	Stationary phase volume
V_M	Mobile phase volume
φ	Phase ratio
ΔG°	Change in Gibb's free energy
T	Absolute temperature
ΔH°	Change in enthalpy
ΔS°	Change in entropy
R	Universal gas constant
R_s	Resolution
N	Number of theoretical plates
As_{0.1}	Peak asymmetry at 10% of peak height
σ²	Peak variance
N_{0.5}	Plate count calculated using the half-height method
N_{Foley-Dorsey}	Plate count calculated using the Foley-Dorsey Equation

$W_{0.5}$	Peak width at half height
L	Column length
F	Flow rate
h	Reduced plate height
u	Reduced velocity
ϕ	Column resistance factor
E	Separation impedance
H	Plate height
D_m	Solute diffusion coefficient
ΔP	Pressure drop
η	Mobile phase viscosity
κ	Column permeability
ψ_2	Solvent association constant
M_2	Solvent molecular weight
V_1	Solute molar volume
u	Mobile phase linear velocity
u_{opt}	Mobile phase optimum linear velocity
ϵ_{Total}	Total column porosity
ϵ_e	Interstitial (or external) column porosity
ϵ_i	Intraparticle (or internal) column porosity
κ_o	Specific column permeability
D_c	Column inner diameter
$N_{Req'd}$	Required number of theoretical plates
Solvent A	The weak solvent, <i>e.g.</i> H ₂ O
Solvent B	The strong solvent, <i>e.g.</i> MeCN or MeOH
CR	Column re-equilibration

$\Delta\%B$	Change in % organic solvent during a gradient run
V_m	Column void volume
1-PrOH	1-Propanol
k'_{ss}	Retention factor at steady state (or equilibrium) condition
RCV	Re-equilibration column volume
V_t	Total volume of mobile phase that has passed through the column
V_d	Delay volume of the HPLC
SEM	Scanning electron micrograph(s)

ABSTRACT

The chromatographic properties of polymer-coated Unisphere aluminas for reversed-phase liquid chromatography were evaluated and compared to those of Si-C₁₈ phases. A greater difference in solvent strength between acetonitrile and methanol was observed for the Unisphere columns. Approximately equal methylene selectivity was also obtained for both stationary phase types. Evaluation of polar group selectivity showed the absence of hydroxyl group participation in solute retention for the aluminas. In terms of kinetic properties, acceptable reduced plate heights were obtained for the Unisphere columns at optimum velocities. However, the van Deemter curves for the aluminas showed a more rapid loss in efficiency with increasing solvent velocity. The applicability of the Unisphere columns for rapid analysis was also evaluated, and although a smaller normalized pressure drop was observed for the aluminas, especially at elevated flow rates, the larger reduced plate heights obtained for the aluminas at practical flow rates resulted in poorer resolution for the Unisphere columns. Finally, an investigation of the column re-equilibration process after gradient elution indicated that employing both high flow rate and high temperature will result in faster column equilibration, and that longer equilibration times are necessary for gradients started with pure water.

The slurry-packing process for Versal GH and Versal GL aluminas was also optimized for applications in normal-phase liquid chromatography. Due to their greater mechanical stability, the GH aluminas were determined to be more promising than the GL as HPLC adsorbents. Both Versal GH and GL provided retention and selectivities similar to that of Unisphere alumina, although the GL was found to be slightly less retentive. It was also concluded that the slurry-packing of the GL aluminas is problematic. At low pressures, the GL alumina particles cannot be consistently packed with good (adequate) efficiency. At the (higher) pressures necessary for efficient

column packing, GL aluminas fracture, producing fines which result in column blockage. Although the GH materials can be packed satisfactorily in the downward-flow mode using a density-balanced slurry, the costly, somewhat tedious density-balanced approach will probably not be necessary if an upward-flow packing mode is employed.

PART A

POLYMER-COATED UNISPHERE ALUMINAS FOR REVERSED-PHASE LIQUID CHROMATOGRAPHY

CHAPTER I

GENERAL INTRODUCTION

A. Alkylbonded Silica-Based Stationary Phases

Chemically bonded stationary phases on silica support (C_{18} and C_8) are presently the most popular stationary phase used in reversed-phase liquid chromatography (RPLC), primarily due to the high efficiency separations obtained. Silica-based stationary phases, however, have two major limitations. First is the presence of residual silanols which complicates the separation retention mechanism and often leads to peak tailing with polar solutes. Second, silica-based stationary phases are stable only over a pH range of 2-8.5 [1, 2], which limits the choice of mobile phases that can be used. Outside this pH range, the silica support and bonded phase decompose in aqueous solutions.

These two drawbacks severely limit the applicability of alkylbonded silica-based stationary phases for separating polar samples including organic bases, amino acids, peptides, proteins, and other important biological and pharmaceutical compounds. New silica-based columns for high-performance liquid chromatography (HPLC) introduced at the 1991 Pittsburgh Conference and Exposition have employed either (i) special synthesis procedures for silica supports; (ii) base-deactivated phases; (iii) exhaustive endcapping; (iv) shielding functional groups; (v) high-density coverage; or (vi) polymer coatings, to eliminate the effect of residual silanols and widen the pH range applicability of these phases [3]. Although these innovations have eliminated the use of amine modifiers or ion-pair reagents for the elution of polar compounds, these columns still cannot be used for extended periods of time outside the pH range 2-8.5.

B. Polymer-Based Stationary Phases

Polymer-based stationary phases can be classified as either lipophilic (*e.g.* polystyrene-divinylbenzene, polyacrylamide, polyvinylacetate, polymethyl methacrylate, polyethylene glycol methacrylate) or hydrophilic (*e.g.* polysaccharides) [4]. The greatest advantage of these materials is their chemical stability. Tanaka and Araki [5], and Lloyd [6] have published good reviews on polymer-based stationary phases for RPLC.

Polystyrene-Divinylbenzene

Highly crosslinked polystyrene-divinylbenzene (PS-DVB) , presently the most popular of this class of reversed-phase material, is stable from pH 0 to 14 [4]. It is also inert, ion-free, and insoluble in non-oxidizing solvents [7]. Although great improvements have been achieved recently, these phases are still limited by their lack of pressure stability, susceptibility to shrinking or swelling with changes in mobile phase composition, and poor column efficiency [2, 3, 5].

Unmodified PS-DVB can be used directly as stationary phase for RPLC. Unfortunately, it is very hydrophobic, and the high concentration of π -electrons in the stationary phase surface results in peak tailing and long retention times for aromatic solutes [5, 8, 9]. To overcome these difficulties, many researchers have tried to chemically modify the PS-DVB surface to shield the π -electrons [*e.g.* 7, 10, 11].

C. Alumina-Based Stationary Phases

As a result of the limitations of the above RPLC stationary phases, there is growing interest in developing more robust, high-efficiency, reversed-phases made from alternative support materials such as alumina (*vide infra*), carbon [12, 13], titania [14], zirconia [14-16], and hydroxyapatite [17]. Among these phases, alumina has to date received the most attention, in part due to its lower cost (an important factor for

preparative and industrial-scale separations), and its greater technological base. The most promising feature of alumina-based stationary phases is that they are stable over a pH range as wide as 2-13 [2, 18-21].

1. Chemically Bonded Stationary Phases On Alumina

Although it has been demonstrated by Knox and Pryde [22], and several other investigators [23-25] that alumina can be modified by reaction with silanes, conversion of alumina from inorganic adsorbent to reversed-phase material via silanization is not feasible because the Al-O-Si bonds are not stable under acidic conditions [2, 18-20]. Pesek and Lin [26] showed that bonded, alumina-based stationary phases which are stable from pH 1-12 can be achieved, however, by first chlorinating the surface hydroxyls of the alumina and then reacting them with *n*-butyllithium, producing a material with *n*-butyl groups chemically bonded to the alumina surface ($\text{=Al-O-(CH}_2\text{)}_3\text{CH}_3$). At present, such alkylalumina stationary phases needs further chromatographic characterization and stability testing.

Wieserman *et al.* [27] introduced Alcobond C-18 (which utilizes irregular alumina particles) and Unisphere C-18 (see section D.2 of this chapter for morphology of Unisphere alumina) at the 1988 Pittsburgh Conference, wherein the alkyl group is covalently bonded to the alumina support. The major disadvantage of this octadecylalumina (ODA) is that it cannot be used with phosphate or borate buffers.

As of this writing, four studies have been published which utilized the ODA column developed by Wieserman *et al.* [27]. Haky *et al.* [28] compared ODA with octadecylsilica (ODS) and found their selectivities and solute retention mechanisms to be similar. They observed (i) a higher degree of hydrogen-bonding solute-stationary phase interactions on ODA, and that (ii) multiple-ring aromatic compounds were more strongly adsorbed on the ODA surface. Differences in the solute-stationary phase interaction between the two phases were attributed to the difference in chemical properties of the

silica and alumina supports. Haky and Vemulapalli [29] also used ODA for the determination of lipophilicity values of organic compounds by HPLC and observed better linear correlation between $\log P$ (octanol-water partition coefficient) and $\log k'$ values for the ODA phase, compared to those obtained using either ODS, polybutadiene-coated alumina, or octadecyl-derivatized PS-DVB. Their use of the ODA column also allowed the estimation of the lipophilicity for organic bases in their neutral form, via the employment of alkaline mobile phases. More recently, Haky *et al.* [30] compared the utility of ODA and Vydac (polymeric) ODS for the separation of protein and peptide mixtures, and observed similar peak capacity for the two column types for the protein sample, although inferior resolution values were obtained for the ODA phase, and 50% less peak area was obtained for Cytochrome C for the ODA column. For the octapeptides, virtually identical peak areas were obtained for both phases, although higher peak capacity and resolution values were generally observed for the ODA phase. Finally, Park [31] showed that the active sites on ODA participate in solute retention, although alumina does not possess strong hydrogen-bonding active sites like residual silanols in ODS.

2. *Polymer-Coated Aluminas*

Polymer Coating Of Support Material For RPLC

An alternative to the preparation of bonded stationary phases for RPLC is to coat the support surface with a polymer of the desired polarity. This technique was first reported by Schomburg *et al.* in 1983 [32] as (i) an alternative to conventional silanization reactions for anchoring alkyl groups on silica, and as (ii) a way to provide good, if not complete coverage of the silanols on alkylbonded silicas. Polymer coating also provides an easy way for varying the phase ratio of the stationary phase by simply changing the thickness of the coating. Schomburg [2, 33] has given good reviews on

the different polymer coating procedures their group has developed, and on the unique properties of the various polymer-coated silicas and aluminas they have prepared.

The coating process developed by Schomburg *et al.* [32] consist essentially of two steps; (i) the coating of silica with the precursor (either polymers with siloxane bonds, *e.g.* polymethyloctylsiloxane or polymethyloctadecylsiloxane; or purely organic monomers or oligomers, *e.g.* polybutadiene (Bien-Vogelsang *et al.* [34]); and (ii) *in situ* polymerization and crosslinking of the coating by either thermal treatment, γ -irradiation, or addition of initiators [4]. Formation of mechanically stable polymer coatings (that can resist the high pressures involved during the separation) arises from the decrease in solubility of the polymerized molecules, and from the strong adsorption of the polymers onto the support surface (*e.g.* by dipole-dipole interaction or hydrogen bonding) [33].

Since 1983, several immobilization techniques and polymers have been employed primarily on bare silica or short-chain, alkyl-modified silica, resulting in highly-stable, polymer-coated stationary phases of comparable chromatographic characteristics and efficiencies as bonded silica-based stationary phases [34-42].

Aside from the work of Schomburg *et al.* [32], the most innovative technique for preparing polymer-coated silicas was by Ohtsu *et al.* [37]. Their procedure consists of first coating the support surface with silicone monomers. Then the silicone coating is subjected to polymerization, and finally the polysiloxane layer is modified with *n*-octyl or *n*-octadecyl groups. These silicone-coated supports are now popularly known as "capsule-type" supports.

The carbon load of the different polymer-coated silicas and aluminas that have been reported is 8-20%, while the coating film thickness is within 0.7-1.4 nm. The carbon content of chemically bonded stationary phases on silica is within 2-20% [4].

Polymer Coating Of Bare Alumina

Although silica is the preferred support material for polymer coating [2], due primarily to the more efficient columns obtained from silica, this technique has also been used extensively by commercial suppliers of alumina-based stationary phases. This trend is a result of the difficulty of preparing pH stable, chemically bonded stationary phases on alumina (e.g. octadecylalumina), which cannot withstand mobile phases containing phosphate and borate buffers.

Bien-Vogelsang *et al.* [34] were the first to report on polymer-coated aluminas. They were able to successfully coat 5 μm alumina particles (Spherisorb A5Y) with either polybutadiene (PBD) or polymethyloctadecylsiloxane (PMSC₁₈), and showed that these phases are mechanically stable and exhibit reversed-phase retention behavior. They observed no deterioration in column performance after more than 100 hours of use with an alkaline mobile phase of pH of 12.3 (0.1N Na₃PO₄ buffer and MeOH) in both isocratic and gradient elution modes, and demonstrated the absence of surface hydroxyl group participation in solute retention. It is emphasized that a mobile phase containing phosphate buffers cannot be used for the ODA column developed by Wieserman *et al.* [27]. Unfortunately, Bien-Vogelsang *et al.* [34] did observe a low separation efficiency for the alumina-based columns they used. For example, to obtain more than 5000 theoretical plates, it was necessary to lower the flow rate to about 0.4 mL/min for a 150 x 4.6 mm column.

The only other application of the PBD-coated (Spherisorb A5Y) alumina developed by Bien-Vogelsang *et al.* [34] was on the determination of the hydrophobicity of various compounds [43-46]. Except for some hydrophilic compounds, the hydrophobicity parameter obtained gave better correlation with theoretical log P values, and allowed the evaluation of the hydrophobicity of organic bases in their neutral form (at high pH), a virtual impossibility with the conventional silica-based alkyl-bonded stationary phases.

In a related study, Kaliszan and Osmialowski [47] also reported that the mechanism of retention (partitioning) for the PBD-coated alumina developed by Bien-Vogelsang *et al.* [34] was similar to that for an ODS stationary phase.

D. Commercially Available Polymer-Coated Aluminas

1. Suppliers Of Polymer-Coated Aluminas

To date, there are only two major suppliers of polymer-coated aluminas for HPLC: Biotage, Inc. (Charlottesville, VA) and ES Industries (Marlton, NJ). Millipore Corporation (Bedford, MA) has also developed a PBD-coated alumina stationary phase, but it is not yet commercially available

2. Unisphere Alumina

The technology for the production of Unisphere alumina, the alumina support being used by Biotage, was developed at Alcoa (New Kensington, PA).

Although Unisphere alumina is approximately spherical in shape, this material is unique in that the particles are made of crystalline platelets intersecting in the core region. Thus, it possesses both megapores (gaps between the platelets on the order of tenths of a micron or thousands of angstrom) and micropores (located within the platelets, between 40-200 Å in diameter) [48]. This unique morphology *supposedly allows the use of packed columns at higher flow rates with relatively lower back pressures, and results in rapid solvent equilibration* and higher sample capacity, compared to similarly-shaped spherical silica particles, while maintaining both the excellent mechanical strength and pH stability of conventional aluminas [27, 48-50]. This, in turn, should allow the packing of longer columns with Unisphere alumina, and the use of higher viscosity solvents, a definite advantage in HPLC.

3. *Unisphere Al-PBD, Unisphere Al-C₁₈ And Unisphere Al-CN*

It should be noted that Part A of this dissertation deals mainly with the determination of the chromatographic properties of three classes of polymer-coated Unisphere aluminas manufactured by Biotage (although two PBD-coated alumina columns from Millipore were also evaluated), namely: Unisphere Al-PBD, Unisphere Al-C₁₈, and Unisphere Al-CN. The alumina supports in these stationary phases have been coated with polymerized butadiene (-PBD), 2-octadecyl-1,3-butadiene (-C₁₈), and cyano phase (-CN), respectively. Groups in parentheses represent the components of the polymeric coating that are expected to determine the selectivity of the particular stationary phase. Preliminary work has already been performed on a Unisphere Al-C₁ phase (with polyisoprene coating). However, Biotage requested work on it to be terminated.

The polymer-coated aluminas produced by Biotage were synthesized based on the technology developed by Schomburg *et al.* [32]. In the case of the Al-PBD column, the polybutadiene copolymer used prior to crosslinking had an average molecular weight of 3000 [51].

Biotage formally introduced the Unisphere Al-PBD phase (particle diameter, $d_p = 8 \mu\text{m}$; pore size = 250 Å) at the 1990 Pittsburgh Conference [21], and the Unisphere Al-C₁₈, and Unisphere Al-CN phases at the 1991 Pittsburgh Conference [52].

Polybutadiene is a desirable polymer to use since it is stable against aqueous mobile phases at strongly basic pH [2]. On the other hand, the Unisphere Al-C₁₈ and Al-CN phases were synthesized primarily to duplicate the chromatographic selectivity and properties of silica-based -C₁₈ and -CN materials, while at the same time providing the pH stability of alumina, especially at alkaline pH. Additionally, the expected absence of surface hydroxyl group participation in solute retention for these various polymer-coated alumina phases make them very promising for RPLC.

As of this writing, only two comparisons of the chromatographic properties of Unisphere Al-PBD and ODS phases have been published [53, 54]. Haky and Vemulapalli [29], however, did report retention factors for 25 low molecular weight solutes for the Unisphere Al-PBD material using 25% methanol/75% phosphate buffer (0.05M) at pH 7.4 as mobile phase, and concluded that the octanol-water coefficients obtained on the Unisphere ODA were better than those obtained for the Unisphere Al-PBD stationary phase. Arenas and Foley [55-57] have also presented their preliminary results on the column re-equilibration after gradient elution of Unisphere Al-PBD and Millipore Al-PBD columns in several regional and national meetings (Chapter VIII).

Using acetonitrile-water mobile phase gradients with 0.1% trifluoroacetic acid for a mixture of ribonuclease A, cytochrome *c*, lysozyme and carbonic anhydrase, Haky *et al.* [53] showed that peak capacity and resolution were five times lower for the Unisphere Al-PBD than on a Vydac ODS column (packed with polymeric C₁₈ bonded to a highly-porous, spherical silica support). Irreversible adsorption was also observed for the same protein mixture on the PBD phase, resulting in increased column backpressure, and 50% reduction in peak areas. Comparable peak capacity, resolution, and peak areas were however observed for a synthetic mixture of octapeptides for both alumina-based and silica-based materials. Their results also suggested that the retention mechanism involved for the Unisphere Al-PBD and ODS phases are similar for the proteins, peptides, and low molecular weight solutes investigated. Haky *et al.* [53] also reported an increase in solute mass transfer resistance with solute size for the PBD phase, which was attributed to the unique morphology of the alumina support. The most surprising result reported by Haky *et al.* [53], was that *the column backpressure for the Unisphere Al-PBD phase was actually higher than that for the Vydac ODS material, when normalized for both column length and particle diameter*. In a similar study, the same group [30] reported that the normalized column backpressures observed for the

Unisphere ODA column were significantly lower than those of a Vydac ODS column. Unfortunately, no direct correlation between these two backpressure comparisons (Unisphere ODA and Vydac ODS [30], and Unisphere Al-PBD and Vydac ODS [53]) can be made since different normalization procedures were employed to adjust the original backpressure values to account for differences in particle diameter and column dimensions (Chapter VII).

The published results of Arenas and Foley [54] on the characterization of Unisphere Al-PBD were incorporated in this dissertation (Chapters III, IV and V).

As for both the Unisphere Al-C₁₈ and Al-CN stationary phases, no work has yet been published except for the presentations of Conroy *et al.* [58], and Holland *et al.* [59] at the 1991 Pittsburgh Conference, wherein the hydrolytic stability in both acidic and basic conditions, and the separation properties of these columns were illustrated. Arenas and Foley [60] also presented their preliminary results regarding the solvent strength difference between acetonitrile and methanol, and the column re-equilibration kinetics involved for these stationary phases (Chapters III and VIII).

The main objective of this research is to characterize and identify the unique chromatographic properties of the Unisphere Al-PBD, Al-C₁₈, and Al-CN stationary phases in terms of solvent strengths of acetonitrile and methanol, selectivity, active sites participation in solute retention, thermodynamic performance, van Deemter relationships (kinetic performance), column stability, and equilibration kinetics; and to compare these results to those of conventional, silica-based C₁₈ (Si-C₁₈) stationary phases.

REFERENCES FOR CHAPTER I

1. Snyder, L.R.; Kirkland, J.J. *Introduction to Modern Liquid Chromatography*, 2nd ed.; John Wiley & Sons, Inc.: New York, 1979; Chapter 7.
2. Schomburg, G. *LC-GC* 1988, 6, 36-50.
3. Majors, R.E. *LC-GC* 1991, 9, 192-203.
4. Unger, K.K. In *Packings and Stationary Phases in Chromatographic Techniques*; Unger, K.K., Ed.; Marcel Dekker, Inc.: New York, 1990; Chapter 6.
5. Tanaka, N.; Araki, M. In *Advances in Chromatography - Selectivity and Retention in Chromatography*; Giddings, J.C.; Grushka, E.; Brown, P.R., Eds.; Marcel Dekker, Inc.: New York, 1989; Vol. 30, Chapter 2.
6. Lloyd, L.L. *J. Chromatogr.* 1991, 544, 201-217.
7. Yang, Y.B.; Regnier, F.E. *J. Chromatogr.* 1991, 544, 233-247.
8. Benson, J.R.; Woo, D.J. *J. Chromatogr. Sci.* 1984, 22, 386-399.
9. Bowers, L.D.; Pedigo, S. *J. Chromatogr.* 1986, 371, 243-251.
10. Yang, Y.B.; Verzele, M. *J. Chromatogr.* 1987, 387, 197-205.
11. Sun, J.J.; Fritz, J.S. *J. Chromatogr.* 1990, 522, 95-105.
12. Knox, J.H.; Unger, K.K.; Mueller, H. *J. Liquid Chromatogr.* 1983, 6, 1-36.
13. Knox, J.H.; Kaur, B.; Millward, G.R. *J. Chromatogr.* 1986, 352, 3-25.
14. Trüdinger, U.; Müller, G.; Unger, K. Presented at the Fourteenth International Symposium on Column Liquid Chromatography, Boston, May 24, 1990, Paper L18.02.
15. Weber, T.P.; Carr, P.W. *Anal. Chem.* 1990, 62, 2620-2625.
16. Weber, T.P.; Carr, P.W.; Funkenbusch, E.F. *J. Chromatogr.* 1990, 519, 31-52.
17. Kawasaki, T. *J. Chromatogr.* 1991, 544, 147-184.
18. Laurent, C.; Billiet, H.A.H.; de Galan, L. *Chromatographia* 1983, 17, 253-258.
19. Laurent, C.J.M.; Billiet, H.A.H.; de Galan, L. *Chromatographia* 1983, 17, 394-399.
20. Billiet, H.; Laurent, C.; de Galan, L. *Tr. Anal. Chem.* 1985, 4, 100-103.
21. Majors, R.E. *LC-GC* 1990, 8, 198-210.

22. Knox, J.H.; Pryde, A.J. *J. Chromatogr.* **1975**, *112*, 171-188.
23. Pryde, A.; Darby, F.J. *J. Chromatogr.* **1975**, *115*, 107-116.
24. Hirata, Y.; Novotny, M.; Tsuda, T.; Ishii, D. *Anal. Chem.* **1979**, *51*, 1807-1809.
25. Hibi, K.; Ishii, D.; Tsuda, T. *J. Chromatogr.* **1980**, *189*, 179-185.
26. Pesek, J.J.; Lin, H.D. *Chromatographia* **1989**, *28*, 565-568.
27. Wieserman, L.F.; Martin, E.S.; Cross, K. Presented at the 1988 Pittsburgh Conference and Exposition on Analytical Chemistry and Applied Spectroscopy, New Orleans, February 23, 1988; Paper 391.
28. Haky, J.E.; Vemulapalli, S.; Wieserman, L.F. *J. Chromatogr.* **1990**, *505*, 307-318.
29. Haky, J.E.; Vemulapalli, S. *J. Liquid Chromatogr.* **1990**, *13*, 3111-3131.
30. Haky, J.E.; Raghani, A.R.; Dunn, B.M.; Wieserman, L.F. *Chromatographia* **1991**, *32*, 49-55.
31. Park, J.H. *Bull. Korean Chem. Soc.* **1990**, *11*, 568-570.
32. Schomburg, G.; Deege, A.; Köhler, J.; Bien-Vogelsang, U. *J. Chromatogr.* **1983**, *282*, 27-39.
33. Schomburg, G. *Tr. Anal. Chem.* **1991**, *10*, 163-169.
34. Bien-Vogelsang, U.; Deege, A.; Figge, H.; Köhler, J.; Schomburg, G. *Chromatographia* **1984**, *19*, 170-179.
35. Schomburg, G.; Köhler, J.; Figge, H.; Deege, A.; Bien-Vogelsang, U. *Chromatographia* **1984**, *18*, 265-274.
36. Figge, H.; Deege, A.; Köhler, J.; Schomburg, G. *J. Chromatogr.* **1986**, *351*, 393-408.
37. Ohtsu, Y.; Fukui, H.; Kanda, T.; Nakamura, K.; Nakano, M.; Nakata, O.; Fujiyama, Y. *Chromatographia* **1987**, *24*, 380-384.
38. Henry, R.A.; McKay, V.A.; Pollock, R.G.; Mallinsky, D.S. Presented at the 1989 Pittsburgh Conference and Exposition on Analytical Chemistry and Applied Spectroscopy, Atlanta, March 7, 1989; Paper 759.
39. Takeuchi, T.; Hu, W.; Haraguchi, H.; Ishii, D. *J. Chromatogr.* **1990**, *517*, 257-262.
40. Hanson, M.; Unger, K.K.; Schomburg, G. *J. Chromatogr.* **1990**, *517*, 269-284.
41. Shirota, O.; Ohtsu, Y.; Nakata, O. *J. Chromatogr. Sci.* **1990**, *28*, 553-558.

42. Hetem, M.J.J.; De Haan, J.W.; Claessens, H.A.; Cramers, C.A.; Deege, A.; Schomburg, G. *J. Chromatogr.* **1991**, *540*, 53-76.
43. Kaliszan, R.; Blain, R.W.; Hartwick, R.A. *Chromatographia* **1988**, *25*, 5-7.
44. Kaliszan, R.; Petrusiewicz, J.; Blain, R.W.; Hartwick, R.A. *J. Chromatogr.* **1988**, *458*, 395-404.
45. Kaliszan, R. In *High Performance Liquid Chromatography*; Brown, P.R.; Hartwick, R.A., Eds.; John Wiley & Sons, Inc.: New York, 1989; Chapter 14.
46. Gami Yilinkou, R.; Kaliszan, R. *Chromatographia* **1990**, *30*, 277-282.
47. Kaliszan, R.; Osmialowski, K. *J. Chromatogr.* **1990**, *506*, 3-16.
48. Wilhelmy, R.B. Presented at the 1988 Pittsburgh Conference and Exposition on Analytical Chemistry and Applied Spectroscopy, New Orleans, February 23, 1988; Paper 390.
49. Wieserman, L.F.; Burr, R.R.; Cross, K.; Simpson, Jr., F. Presented at the 1988 Pittsburgh Conference and Exposition on Analytical Chemistry and Applied Spectroscopy, New Orleans, February 23, 1988; Paper 393.
50. Biotage, Inc. *Unisphere-PBD Alumina*, 1990.
51. Holland, K.B., Biotage, Inc., personal communication by R.V. Arenas.
52. Stevenson, R. *Amer. Lab.* **1991**, *23*, 32Z-32KK.
53. Haky, J.E.; Raghani, A.; Dunn, B.M. *J. Chromatogr.* **1991**, *541*, 303-315.
54. Arenas, R.V.; Foley, J.P. *Anal. Chim. Acta* **1991**, *246*, 113-130.
55. Arenas, R.V.; Foley, J.P. Presented at the 45th Southwest Regional Meeting of the American Chemical Society, Baton Rouge, LA, December 6, 1989; Paper 19.
56. Arenas, R.V.; Foley, J.P. Presented at the 20th Annual Symposium - Advances in Applied Analytical Chemistry, New Orleans Chromatography-Analytical Discussion Group, Kenner, LA, May 3, 1990; Paper B-15.
57. Arenas, R.V.; Foley, J.P. Presented at the 14th International Symposium on Column Liquid Chromatography, Boston, May 22, 1990; Paper P432.
58. Conroy, C.M.; Washington, J.M.; Holland, K.B.; Zeller, K.; Burke, D.; Moe, D.C. Presented at the 1991 Pittsburgh Conference and Exposition on Analytical Chemistry and Applied Spectroscopy, Chicago, March 3, 1991; Paper 028P.
59. Holland, K.B.; Washington, J.M.; Zeller, K.; Burke, D.; Conroy, C.M.; Moe, D.C. Presented at the 1991 Pittsburgh Conference and Exposition on Analytical Chemistry and Applied Spectroscopy, Chicago, March 5, 1991, 1991; Paper 340P.

60. Arenas, R.V.; Foley, J.P. Presented at the 21st Annual Symposium - Advances in Applied Analytical Chemistry, New Orleans Chromatography-Analytical Discussion Group, Kenner, LA, May 23, 1991; Paper 41.

CHAPTER II

EXPERIMENTAL

The HPLC system consisted of (i) either a Rainin Model HP Liquid Chromatograph controlled by an Apple Machintosh Plus personal computer with the Dynamax HPLC method manager (Rainin Instrument Co., Inc., Woburn, MA), or a Series 400 Liquid Chromatograph and OMEGA-4 data collection and integration system (Perkin-Elmer, Norwalk, CT); (ii) a Model 7125-075 six-port injection valve (Rheodyne Inc., Cotati, CA) equipped with 6 μ L sample loop; and (iii) either a model V⁴ variable wavelength absorbance detector (ISCO, Lincoln, NE) set at 254 nm, or a Varian Aerograph Refractive Index Detector (Varian Instrument Division, Walnut Creek, CA). For temperature control, the columns were kept in glass water jackets connected to a model RMS-6 circulating bath (Brinkmann Instruments, Inc., Westbury, NY). Except for temperature dependent studies, all chromatographic measurements were conducted at $25.0 \pm 0.1^\circ \text{C}$, unless stated otherwise.

HPLC grade acetonitrile (MeCN), methanol (MeOH) and water (H₂O) were filtered using 0.45 μ m Nylon-66 membranes and degassed before use by ultrasonication under vacuum. The solvents were kept at room temperature during the analysis. All solutes were dissolved in solvents that were weaker or equal in strength to the mobile phase. The sample solutions were filtered using 0.2 μ m Nylon-66 membranes prior to injection. Retention measurements were not made until the column was fully equilibrated, i.e., until at least 15 column volumes of mobile phase had passed through the column.

The different polymer-coated alumina and silica-based C₁₈ columns used in the study are summarized in Table 2.1, with the corresponding column serial number (SN), column dimensions, particle diameter (d_p), and pore size. A flow rate of 2.0 mL/min

TABLE 2.1. List of reversed-phase columns used.

Column	Serial Number	Column Dimensions (mm)	d _p (μm)	Pore Size (Å)
Unisphere Al-PBD	593ATC	250 x 4.6	10	221
	003-0253	250 x 4.6	8	245
Millipore Al-PBD	B90441D2	150 x 3.9	5	92
	B00221C1	150 x 3.9	5	92
Unisphere Al-C ₁₈	B-0014	250 x 4.6	8	245
Unisphere Al-CN	262ATC	250 x 4.6	8	245
	B91-C-0049	250 x 4.6	8	245
Microsorb Si-C ₁₈	10053	50 x 4.6	3	100
	10412	150 x 4.6	5	100
	10788	150 x 4.6	5	100
LiChrospher Si-C ₁₈	86484701	125 x 4.0	5	100

was used for the different polymer-coated Unisphere alumina columns (Biotage, Inc., Charlottesville, VA), while a flow rate of 1.0 mL/min was used for the Millipore Al-PBD (Millipore Corporation, Bedford, MA), Microsorb Si-C₁₈ (Rainin Instrument Co., Inc., Woburn, MA), and LiChrospher Si-C₁₈ (E. Merck, Darmstadt, F.R. Germany) columns, unless stated otherwise.

The solute retention factor (k') was calculated using the equation below

$$k' = \frac{t_R - t_m}{t_m} \quad (2.1)$$

where t_R is the solute retention time, and t_m is the retention time for an unretained solute. The value for t_m was taken as the retention time of acetone using either MeCN or MeOH as the mobile phase. The reported k' for each test solute was based on the average of at least three values. *The relative standard deviation (RSD) was less than 0.5% for all reported k' values*, except in instances where the average value of k' was very small ($k' < 0.25$). The precision for the latter data was always better than 3.6%, although these data were generally excluded from our detailed analysis as a precaution.

Other experimental procedures specific to a given chapter are included where necessary.

CHAPTER III

SOLVENT STRENGTH DIFFERENCE BETWEEN ACETONITRILE AND METHANOL FOR THE POLYMER-COATED ALUMINAS AND Si-C₁₈

A. Comparison Of The Solvent Strengths Of MeCN And MeOH Based On k'

Retention data for several aromatic and (some) aliphatic compounds are reported in Tables 3.1A-3.6B for the different polymer-coated Unisphere aluminas, two Millipore Al-PBD and two silica-based C₁₈ columns using hydroorganic mixtures of MeCN and MeOH as mobile phases. Retention factors were determined only over a limited range of mobile phase composition since the corresponding k' values may be either excessively large (> 20) or small (< 0.25) at either extreme. It should be noted that all the data in Tables 3.1A-3.5B were determined at 25.0° C. The reported k' values in Tables 3.6A and 3.6B (for the Unisphere Al-CN column) were, however, obtained at 31.0° C. This occurred because the circulating bath capable of thermostating the column at 25.0° C was unavailable during the period when these retention data were being collected. Thus, calculated values (*e.g.* S , ϵ , selectivity, etc., reported in this chapter and the following chapters) based on the retention factors given in Tables 3.6A and 3.6B for the Unisphere Al-CN column are all at 31.0° C. It is emphasized that for the Al-CN column, no significant temperature effect is expected to arise due to a 6° C increase in temperature. This assumption is evident from a comparison of the k' values for a given solute at 25.0 and 31.0° C. For example, equivalent retentions were observed for acetophenone at both temperatures ($k' = 1.09$), while the k' values determined for butyrophenone at 25.0 and 31.0° C were 5.14 and 5.12, respectively, for the Al-CN phase.

By definition, strong solvents are those that provide small k' values (*i.e.*, less retention), while weak solvents are those that give larger k' values (*i.e.*, longer elution time). Consistent with the expected relationship between MeCN and MeOH in RPLC, MeCN is a stronger solvent than MeOH for all alumina-based and silica-based reversed-phase stationary phases. This simply reflects the fact that MeCN is less polar than MeOH. Thus, at equal percentages of organic solvent retention is less for the MeCN/H₂O system relative to the MeOH/H₂O system. For example, the retention factors for pentane for the Unisphere Al-PBD column (Tables 3.1A and 3.1B) are 1.00 and 2.83 using 60% MeCN and MeOH, respectively. Similarly, the retention factors for the same solute for the Microsorb Si-C₁₈ column (Tables 3.5A and 3.5B) are 6.18 and 16.76, respectively.

A closer look at the k' values in Tables 3.1A-3.6B also reveal that *solute retention for the alumina-based columns is in general considerably lower than that for the silica-based C₁₈ columns*. A good example of this is shown in Table 3.7 for toluene. At 60% MeOH the retention factors for toluene are < 2 for all alumina columns, while for both Si-C₁₈ columns, the retention factors are > 6. It is highly probable that an even greater difference in column strength exist between these alumina- and silica-based stationary phases, as both Si-C₁₈ columns have been used extensively prior to the study and may have experienced small to moderate losses of bonded stationary phase that is common for these phases. In general, however, the retention data reported for both Si-C₁₈ columns were generally comparable to similar data reported elsewhere for other silica-based C₁₈ columns [1].

TABLE 3.1A. Retention factors of selected compounds for the Unisphere Al-PBD column with MeCN/H₂O as mobile phase. ^a

Compound	Percent MeCN											
	0	10	20	30	40	50	60	70	80	90	100	
A. UV-absorbing compounds:												
Acetone	(0.02)											
2-Butanone	(0.13)	(0.09)	(0.06)									
3-Pentanone	0.46	0.29	(0.20)	(0.13)	—	—	—	—	—	—	—	
Acetophenone	3.22	1.42	0.66	0.32	—	—	—	—	—	—	—	
Nitrobenzene	3.66	2.52	1.32	0.62	—	—	—	—	—	—	—	
m-Nitrotoluene	—	8.02	3.41	1.38	—	—	—	—	—	—	—	
Toluene ^b	—	—	6.96	2.86	1.01	0.70	0.36	(0.16)	—	—	—	
	—	—	—	3.35	1.38	0.63	0.31	(0.15)	(0.09)	—	—	
Styrene ^c	—	—	—	4.23	1.56	0.67	0.31	(0.15)	(0.09)	—	—	
Ethylbenzene ^b	—	—	—	5.78	1.71	1.14	0.55	0.26	—	—	—	
	—	—	—	6.99	2.49	1.02	0.47	(0.23)	(0.11)	—	—	
Propylbenzene	—	—	—	12.80	3.05	1.94	0.87	0.42	—	—	—	
Butylbenzene	—	—	—	—	5.46	3.36	1.40	0.64	—	—	—	
B. Non-UV-absorbing compounds:												
Pentane	—	—	—	—	—	—	1.00	0.52	0.29	(0.14)	(0.08)	
Hexane	—	—	—	—	—	—	1.66	0.83	0.44	(0.21)	(0.11)	
Heptane	—	—	—	—	—	—	2.64	1.26	0.66	0.32	(0.14)	

^a Data reported are for the Unisphere Al-PBD column with serial number 593ATC.

^b Two sets of k' values are given for toluene and ethylbenzene. The first row of data was collected at the same time as the other k' values for the other test compounds. The second row of data was collected several months later. Unless stated otherwise, the second set of data for toluene and ethylbenzene are used for succeeding tables.

^c Data collected concurrently with the second set of toluene and ethylbenzene data.

TABLE 3.1B. Retention factors of selected compounds for the Unisphere Al-PBD column with MeOH/H₂O as mobile phase. ^a

Compound	Percent MeOH										
	0	10	20	30	40	50	60	70	80	90	100
A. UV-absorbing compounds:											
Acetone	(0.02)										
2-Butanone	(0.13)	(0.09)	(0.05)	(0.04)	(0.02)						
3-Pentanone	0.46	0.31	0.25	(0.13)	(0.08)	—	—	—	—	—	—
Acetophenone	3.22	1.83	1.09	0.62	0.32	0.27	—	—	—	—	—
Nitrobenzene	3.66	2.69	1.93	1.26	0.70	0.58	—	—	—	—	—
m-Nitrotoluene	—	9.49	6.13	3.51	1.73	—	—	—	—	—	—
Toluene ^b	—	—	11.98	7.45	3.89	3.10	1.37	0.61	0.28	(0.15)	—
					4.94	2.55	1.26	0.63	0.29	—	—
Styrene ^c	—	—	—	—	7.15	3.30	1.47	0.69	0.33	—	—
Ethylbenzene ^b	—	—	—	—	—	6.39	2.45	0.99	0.42	(0.17)	—
	—	—	—	—	10.96	4.96	2.13	0.95	0.43	—	—
Propylbenzene	—	—	—	—	—	—	4.53	1.64	0.62	(0.20)	—
Butylbenzene	—	—	—	—	—	—	8.88	2.84	0.95	0.29	—
B. Non-UV absorbing compounds:											
Pentane	—	—	—	—	—	—	2.83	1.16	0.48	(0.20)	(0.14)
Hexane	—	—	—	—	—	—	5.44	1.97	0.72	0.27	(0.10)
Heptane	—	—	—	—	—	—	9.82	3.23	1.07	0.36	(0.12)

^a Data reported are for the Unisphere Al-PBD column with serial number 593ATC.

^b Two sets of k' values are given for toluene and ethylbenzene. The first row of data was collected at the same time as the other k' values for the other test compounds. The second row of data was collected several months later. Unless stated otherwise, the second set of data for toluene and ethylbenzene are used for succeeding tables.

^c Data collected concurrently with the second set of toluene and ethylbenzene data.

TABLE 3.2A. Retention factors of selected compounds for the Millipore A1-PBD column with MeCN/H₂O as mobile phase. ^a

Compound	<u>Percent MeCN</u>										
	0	10	20	30	40	50	60	70	80	90	100
A. UV-absorbing compounds:											
Acetophenone	5.36	2.35	1.23	0.57	0.29	(0.19)	(0.04)	—	—	—	—
Nitrobenzene	—	—	2.40	1.18	—	—	—	—	—	—	—
m-Nitrotoluene	—	—	6.07	2.40	1.02	0.43	(0.17)	—	—	—	—
Toluene ^b	—	—	10.73	4.49	1.87	0.87	0.32	—	—	—	—
	—	—	—	—	1.65	0.73	0.35	(0.15)	—	—	—
Styrene ^c	—	—	—	—	1.98	0.85	0.38	(0.16)	—	—	—
Ethylbenzene ^b	—	—	—	—	—	—	0.54	—	—	—	—
	—	—	—	—	2.76	1.13	0.50	(0.22)	—	—	—
Propylbenzene	—	—	—	—	—	—	0.90	—	—	—	—
Butylbenzene	—	—	—	—	—	—	1.47	0.71	—	—	—
B. Non-UV-absorbing compounds:											
Pentane	—	—	—	—	—	—	1.22	0.60	0.31	(0.16)	(0.10)
Hexane	—	—	—	—	—	—	1.98	0.97	0.48	(0.23)	(0.14)
Heptane	—	—	—	—	—	—	3.15	1.48	0.74	0.35	(0.19)

^a Data reported are for the Millipore column with serial number B90441D2, unless indicated otherwise.

^b Two sets of k' values are given for toluene and ethylbenzene. The first row of data is for the Millipore column with serial number B90441D2. The second row is for the column with serial number B00221C1. Unless stated otherwise, the second set of data (serial number B00221C1) for toluene and ethylbenzene are used for succeeding tables.

^c The k' values for styrene are for the Millipore column with serial number B00221C1.

TABLE 3.2B. Retention factors of selected compounds for the Millipore Al-PBD column with MeOH/H₂O as mobile phase. ^a

Compound	Percent MeOH										
	0	10	20	30	40	50	60	70	80	90	100
A. UV-absorbing compounds:											
Acetophenone	—	—	1.88	1.19	0.69	0.42	0.27	—	—	—	—
Nitrobenzene	7.31	—	3.99	2.65	1.58	1.01	0.57	—	—	—	—
m-Nitrotoluene	—	—	—	6.81	3.49	2.05	1.06	0.55	—	—	—
Toluene ^b	—	—	—	—	7.00	3.46	1.89	0.88	—	—	—
	—	—	—	—	—	3.39	1.72	0.88	—	—	—
Styrene ^c	—	—	—	—	—	4.69	2.15	1.00	—	—	—
Ethylbenzene ^b	—	—	—	—	—	—	3.20	—	—	—	—
	—	—	—	—	—	6.01	2.67	1.20	—	—	—
Propylbenzene	—	—	—	—	—	—	5.64	—	—	—	—
Butylbenzene	—	—	—	—	—	—	10.53	—	—	—	—
B. Non-UV-absorbing compounds:											
Pentane	—	—	—	—	—	—	4.15	1.69	0.70	0.30	—
Hexane	—	—	—	—	—	—	7.79	2.80	1.04	0.39	—
Heptane	—	—	—	—	—	—	14.72	4.62	1.54	0.52	—

^a Data reported are for the Millipore column with serial number B90441D2, unless indicated otherwise.

^b Two sets of k' values are given for toluene and ethylbenzene. The first row of data is for the Millipore column with serial number B90441D2. The second row is for the column with serial number B00221C1. Unless stated otherwise, the second set of data (serial number B00221C1) for toluene and ethylbenzene are used for succeeding tables.

^c The k' values for styrene are for the Millipore column with serial number B00221C1.

TABLE 3.3A. Retention factors of selected compounds for the Unisphere Al-C₁₈ column with MeCN/H₂O as mobile phase.

Compound	Percent MeCN										
	0	10	20	30	40	50	60	70	80	90	100
2-Butanone	0.52	0.25	—	—	—	—	—	—	—	—	—
2-Pentanone	1.67	0.72	0.42	0.27	—	—	—	—	—	—	—
2-Hexanone	5.67	2.19	1.09	0.59	—	—	—	—	—	—	—
2-Heptanone	—	5.63	2.97	1.31	0.34	0.34	—	—	—	—	—
2-Octanone	—	—	8.03	2.88	1.19	0.55	0.29	—	—	—	—
2-Nonanone	—	—	—	6.55	2.22	0.95	0.46	—	—	—	—
Acetophenone	—	3.59	1.50	0.69	0.36	—	—	—	—	—	—
Propiophenone	—	10.38	3.89	1.56	0.72	0.38	—	—	—	—	—
Butyrophenone	—	—	9.32	3.20	1.31	0.59	0.31	—	—	—	—
Valerophenone	—	—	—	6.86	2.33	0.96	0.46	—	—	—	—
Nitrobenzene	—	5.91	2.87	1.30	0.62	0.33	—	—	—	—	—
m-Nitrotoluene	—	—	7.41	2.76	1.13	0.53	0.27	—	—	—	—
Toluene	—	—	11.16	4.55	1.90	0.90	0.47	0.26	—	—	—
Styrene	—	—	17.37	6.06	2.27	1.00	0.51	0.27	—	—	—
Ethylbenzene	—	—	—	9.20	3.30	1.40	0.68	0.36	—	—	—
Isopropylbenzene	—	—	—	16.52	5.15	1.98	0.90	0.46	—	—	—
Propylbenzene	—	—	—	—	6.14	2.33	1.04	0.53	0.28	—	—
Butylbenzene	—	—	—	—	11.60	3.80	1.60	0.77	0.40	—	—
Pentylbenzene	—	—	—	—	21.64	6.29	2.48	1.12	0.55	—	—
Hexylbenzene	—	—	—	—	—	10.55	3.81	1.65	0.78	—	—
Heptylbenzene	—	—	—	—	—	17.77	5.95	2.46	1.10	—	—
Octylbenzene	—	—	—	—	—	—	9.36	3.67	1.56	—	—
Nonylbenzene	—	—	—	—	—	—	14.64	5.47	2.24	—	—

TABLE 3.3B. Retention factors of selected compounds for the Unisphere Al-C₁₈ column with MeOH/H₂O as mobile phase.

Compound	Percent MeOH										
	0	10	20	30	40	50	60	70	80	90	100
2-Butanone	0.52	0.31	—	—	—	—	—	—	—	—	—
2-Pentanone	1.67	0.93	—	0.43	0.29	—	—	—	—	—	—
2-Hexanone	5.67	2.97	0.58	1.10	0.64	—	—	—	—	—	—
2-Heptanone	—	8.62	5.33	3.02	1.54	0.39	0.42	—	—	—	—
2-Octanone	—	—	—	8.53	3.73	1.17	0.74	0.37	—	—	—
2-Nonanone	—	—	—	—	9.15	3.63	1.34	0.57	0.25	—	—
Acetophenone	—	5.99	3.16	1.82	0.97	0.54	0.30	—	—	—	—
Propiophenone	—	—	8.85	4.73	2.24	1.11	0.55	0.30	—	—	—
Butyrophenone	—	—	—	11.42	4.84	2.13	0.92	0.44	—	—	—
Valerophenone	—	—	—	—	11.31	4.39	1.64	0.70	0.31	—	—
Nitrobenzene	—	7.69	5.33	3.42	1.97	1.11	0.59	0.34	—	—	—
m-Nitrotoluene	—	—	—	9.56	4.73	2.28	1.08	0.53	0.28	—	—
Toluene	—	—	—	—	7.04	3.68	1.67	0.85	0.40	—	—
Styrene	—	—	—	—	11.31	5.05	2.12	0.95	0.44	—	—
Ethylbenzene	—	—	—	—	—	—	2.80	1.21	0.54	—	—
Isopropylbenzene	—	—	—	—	—	—	4.20	1.64	0.66	—	—
Propylbenzene	—	—	—	—	—	—	5.09	1.93	0.76	—	—
Butylbenzene	—	—	—	—	—	—	9.61	3.20	1.12	—	—
Pentylbenzene	—	—	—	—	—	—	17.72	5.26	1.62	—	—
Hexylbenzene	—	—	—	—	—	—	—	8.68	2.37	—	—
Heptylbenzene	—	—	—	—	—	—	—	—	3.53	—	—
Octylbenzene	—	—	—	—	—	—	—	—	5.25	—	—
Nonylbenzene	—	—	—	—	—	—	—	—	7.84	—	—
										0.29	0.34

TABLE 3.4A. Retention factors of selected compounds for the LiChrospher Si-C₁₈ column with MeCN/H₂O as mobile phase.

Compound	Percent MeCN										
	0	10	20	30	40	50	60	70	80	90	100
Acetone	4.85	0.77	0.40	0.29	—	—	—	—	—	—	—
2-Butanone	16.62	2.63	1.33	0.91	0.59	0.44	—	—	—	—	—
2-Pentanone	—	8.77	3.88	2.29	1.40	0.90	0.56	0.35	—	—	—
2-Hexanone	—	—	11.31	5.52	2.89	1.68	0.98	0.59	0.34	—	—
2-Heptanone	—	—	—	13.41	5.82	3.02	1.65	0.96	0.54	0.31	—
2-Octanone	—	—	—	—	11.71	5.38	2.72	1.53	0.85	0.47	—
2-Nonanone	—	—	—	—	—	9.54	4.45	2.37	1.29	0.72	0.37
Acetophenone	—	—	12.43	5.50	2.71	1.49	0.82	0.48	0.26	—	—
Propiophenone	—	—	—	13.38	5.78	2.90	1.49	0.86	0.46	—	—
Butyrophenone	—	—	—	—	10.99	4.90	2.36	1.31	0.70	0.39	—
Valerophenone	—	—	—	—	—	8.38	3.76	1.99	1.03	0.53	0.25
Nitrobenzene	—	—	—	9.93	4.61	2.33	1.19	0.66	0.33	—	—
m-Nitrotoluene	—	—	—	22.71	8.94	4.07	1.94	1.04	0.53	0.25	—
Toluene	—	—	—	—	12.73	5.90	2.92	1.63	0.89	0.47	—
Styrene	—	—	—	—	15.66	6.64	3.17	1.72	0.91	0.46	—
Ethylbenzene	—	—	—	—	—	9.40	4.37	2.32	1.23	0.63	0.29
Isopropylbenzene	—	—	—	—	—	14.24	6.17	3.13	1.60	0.80	0.35
Propylbenzene	—	—	—	—	—	—	7.04	3.55	1.81	0.90	0.41
Butylbenzene	—	—	—	—	—	—	11.10	5.34	2.62	1.25	0.55
Pentylbenzene	—	—	—	—	—	—	—	8.12	3.80	1.74	0.71
Hexylbenzene	—	—	—	—	—	—	—	12.37	5.56	2.43	0.93
Heptylbenzene	—	—	—	—	—	—	—	19.08	8.14	3.40	1.24
Octylbenzene	—	—	—	—	—	—	—	—	12.02	4.76	1.60
Nonylbenzene	—	—	—	—	—	—	—	—	—	6.65	2.08

TABLE 3.4B. Retention factors of selected compounds for the LiChrospher Si-C₁₈ column with MeOH/H₂O as mobile phase.

Compound	Percent MeOH										
	0	10	20	30	40	50	60	70	80	90	100
Acetone	4.85	1.67	0.93	0.59	0.42	0.31	—	—	—	—	—
2-Butanone	16.62	5.47	2.79	1.66	1.09	0.70	0.46	0.29	—	—	—
2-Pentanone	—	18.51	8.87	4.76	2.80	1.63	0.94	0.56	0.32	—	—
2-Hexanone	—	—	—	13.67	7.09	3.62	1.78	0.95	0.51	—	—
2-Heptanone	—	—	—	—	18.75	8.24	3.82	1.64	0.78	0.36	—
2-Octanone	—	—	—	—	—	18.69	7.10	2.85	1.24	0.49	—
2-Nonanone	—	—	—	—	—	—	13.90	4.94	1.95	0.69	—
Acetophenone	—	—	—	16.76	7.71	3.61	1.72	0.88	0.49	—	—
Propiophenone	—	—	—	—	18.06	7.65	3.31	1.56	0.77	0.37	—
Butyrophenone	—	—	—	—	—	15.28	5.94	2.48	1.13	0.47	—
Valerophenone	—	—	—	—	—	—	11.34	4.09	1.67	0.64	0.27
Nitrobenzene	—	—	—	—	10.45	5.28	2.59	1.30	0.67	0.31	—
m-Nitrotoluene	—	—	—	—	—	11.58	5.03	2.30	1.09	0.45	—
Toluene	—	—	—	—	—	17.97	7.90	3.60	1.69	0.71	0.25
Styrene	—	—	—	—	—	—	9.73	4.10	1.78	0.74	—
Ethylbenzene	—	—	—	—	—	—	14.04	5.63	2.57	0.92	0.30
Isopropylbenzene	—	—	—	—	—	—	—	8.18	3.35	1.12	0.35
Propylbenzene	—	—	—	—	—	—	—	9.59	3.60	1.26	0.41
Butylbenzene	—	—	—	—	—	—	—	16.41	5.41	1.75	0.53
Pentylbenzene	—	—	—	—	—	—	—	—	8.22	2.36	0.63
Hexylbenzene	—	—	—	—	—	—	—	—	12.54	3.22	0.78
Heptylbenzene	—	—	—	—	—	—	—	—	—	4.54	1.01
Octylbenzene	—	—	—	—	—	—	—	—	—	6.17	1.23
Nonylbenzene	—	—	—	—	—	—	—	—	—	8.29	1.55

TABLE 3.5A. Retention factors of selected compounds for the Microsorb Si-C₁₈ column with MeCN/H₂O as mobile phase.

Compound	<u>Percent MeCN</u>					
	40	50	60	70	80	90 100
A. UV-absorbing compounds:						
Toluene	10.44	4.84	2.48	1.36	0.75	0.40 (0.20)
Styrene	12.76	5.51	2.70	1.43	0.77	0.40 (0.18)
Ethylbenzene	18.95	7.79	3.68	1.94	1.03	0.54 0.25
B. Non-UV-absorbing compounds:						
Pentane	—	—	6.18	3.25	1.84	0.97 0.47
Hexane	—	—	10.12	5.14	2.72	1.40 0.64
Heptane	—	—	16.53	7.95	4.11	2.05 0.85

TABLE 3.5B. Retention factors of selected compounds for the Microsorb Si-C₁₈ column with MeOH/H₂O as mobile phase.

Compound	<u>Percent MeOH</u>					
	40	50	60	70	80	90 100
A. UV-absorbing compounds:						
Toluene	—	13.54	6.26	2.91	1.31	0.58 (0.22)
Styrene	—	17.99	7.50	3.21	1.40	0.58 (0.15)
Ethylbenzene	—	27.53	11.12	4.54	1.88	0.76 (0.18)
B. Non-UV-absorbing compounds:						
Pentane	—	—	16.76	6.49	2.53	1.00 0.35
Hexane	—	—	—	7.26	3.95	1.41 0.44
Heptane	—	—	—	7.81	6.16	1.96 0.56

TABLE 3.6A. Retention factors of selected compounds for the Unisphere Al-CN column with MeCN/H₂O as mobile phase. ^a

Compound	Percent MeCN										
	0	10	20	30	40	50	60	70	80	90	100
2-Pentanone	0.53	0.55	0.45	0.30	—	—	—	—	—	—	—
2-Hexanone	1.79	1.58	1.16	0.66	0.37	—	—	—	—	—	—
2-Heptanone	6.09	4.82	2.97	1.42	0.67	0.34	—	—	—	—	—
2-Octanone	—	13.95	7.68	3.01	1.20	0.55	0.28	—	—	—	—
2-Nonanone	—	—	—	6.31	2.14	0.88	0.42	—	—	—	—
Acetophenone	5.62	3.86	2.17	1.09	0.55	0.31	—	—	—	—	—
Propiophenone	—	12.12	6.00	2.57	1.14	0.57	0.31	—	—	—	—
Butyrophenone	—	—	14.02	5.12	1.98	0.89	0.45	—	—	—	—
Valerophenone	—	—	—	10.56	3.47	1.39	0.66	0.33	—	—	—
Nitrobenzene	—	10.21	5.70	2.62	1.22	0.61	0.33	—	—	—	—
m-Nitrotoluene	—	—	13.96	5.28	2.12	0.95	0.48	0.26	—	—	—
Toluene	—	—	13.94	5.77	2.42	1.11	0.58	0.32	—	—	—
Styrene	—	—	—	8.66	3.28	1.42	0.70	0.37	—	—	—
Ethylbenzene	—	—	—	10.90	3.93	1.64	0.78	0.41	—	—	—
Isopropylbenzene	—	—	—	18.18	5.74	2.16	0.97	0.49	0.25	—	—
Propylbenzene	—	—	—	22.16	6.78	2.50	1.11	0.55	0.28	—	—
Butylbenzene	—	—	—	—	11.85	3.88	1.60	0.76	0.37	—	—
Pentylbenzene	—	—	—	—	—	—	—	1.00	0.47	—	—
Hexylbenzene	—	—	—	—	—	—	—	1.36	0.61	0.26	—
Heptylbenzene	—	—	—	—	—	—	—	1.82	0.79	0.33	—
Octylbenzene	—	—	—	—	—	—	—	2.47	1.02	0.40	—
Nonylbenzene	—	—	—	—	—	—	—	3.33	1.32	0.49	—

^a Data reported were obtained at 31.0 °C.

TABLE 3.6B. Retention factors of selected compounds for the Unisphere Al-CN column with MeOH/H₂O as mobile phase. ^a

Compound	Percent MeOH										
	0	10	20	30	40	50	60	70	80	90	100
2-Pentanone	0.53	0.44	0.39	0.34	0.25	—	—	—	—	—	—
2-Hexanone	1.79	1.38	1.10	0.85	0.56	0.38	0.25	—	—	—	—
2-Heptanone	6.09	4.37	3.20	2.22	1.27	0.75	0.43	—	—	—	—
2-Octanone	—	—	9.47	5.89	2.92	1.49	0.73	0.35	—	—	—
2-Nonanone	—	—	—	15.81	6.75	2.94	1.25	0.52	0.25	—	—
Acetophenone	5.62	4.20	3.13	2.14	1.29	0.79	0.48	0.28	—	—	—
Propiophenone	—	13.40	9.21	5.71	3.07	1.67	0.90	0.48	0.27	—	—
Butyrophenone	—	—	—	13.18	6.33	3.06	1.46	0.69	0.37	—	—
Valerophenone	—	—	—	—	14.16	6.09	2.51	1.05	0.50	—	—
Nitrobenzene	—	10.90	8.53	5.98	3.62	2.13	1.22	0.70	—	—	—
m-Nitrotoluene	—	—	—	15.23	8.03	4.14	2.11	1.08	0.57	—	—
Toluene	—	—	—	13.19	7.28	3.77	1.89	0.94	0.47	—	—
Styrene	—	—	—	—	12.87	6.03	2.76	1.27	0.61	0.29	—
Ethylbenzene	—	—	—	—	14.56	6.68	2.97	1.32	0.60	0.27	—
Isopropylbenzene	—	—	—	—	—	10.43	4.15	1.67	0.70	0.29	—
Propylbenzene	—	—	—	—	—	12.75	4.94	1.93	0.79	0.32	—
Butylbenzene	—	—	—	—	—	25.56	8.68	3.00	1.10	0.40	—
Pentylbenzene	—	—	—	—	—	—	—	4.51	1.47	0.50	—
Hexylbenzene	—	—	—	—	—	—	—	6.85	1.98	0.61	—
Heptylbenzene	—	—	—	—	—	—	—	10.68	2.74	0.76	—
Octylbenzene	—	—	—	—	—	—	—	—	3.86	0.93	—
Nonylbenzene	—	—	—	—	—	—	—	—	5.26	1.14	—

^a Data reported were obtained at 31.0 °C.

TABLE 3.7 Retention factors of toluene for the different stationary phases using 60/40 MeOH/H₂O as mobile phase. ^a

Column	k'
Unisphere Al-PBD	1.26
Unisphere Al-C ₁₈	1.67
Millipore Al-PBD	1.72
Unisphere Al-CN	1.89
Microsorb Si-C ₁₈	6.26
LiChrospher Si-C ₁₈	7.90

^a These values were obtained from Tables 3.1A-3.6B.

B. Relationship Between Log k' And Mobile Phase Composition

1. Using The Volume Fraction Of Organic Solvent

Although several investigators [2, 3] have shown that $\log k'$ varies quadratically with the volume fraction of organic modifier (ϕ), at least between 10-100% organic solvent [4], this quadratic dependence (Eqn. 3.1) has been disputed by other

$$\log k' = A\phi^2 + B\phi + C \quad (3.1)$$

researchers [5-7], and to a first approximation, the dependence of $\log k'$ on ϕ is given by the linear relationship

$$\log k' = \log k'_w - S\phi \quad (3.2)$$

where k'_w is the retention factor in pure water, and S is a parameter related to the solvent strength of the pure organic solvent [5]. According to Snyder *et al.* [5], the value of S is determined experimentally as the negative of the slope from linear plots of $\log k'$ vs. ϕ . A larger S value means that solute retention (k') decreases faster for a given increase in the volume fraction of organic solvent. Therefore, a larger S value corresponds to a stronger solvent. This simple approach makes qualitative comparisons of solvent strength easier for various types of reversed-phase packings, although it should be noted that the value of S obtained varies with solute structure, and from column to column [8]. For the quadratic relationship given in Eqn. 3.1, A is usually positive, B is large and negative, and C is the $\log k'$ value in pure water [9].

According to Ahuja [10], better linearity is obtained by most chromatographers from plots of $\log k'$ vs. ϕ for MeOH/H₂O compared to MeCN/H₂O. Conflicting results have been reported for the MeCN/H₂O solvent system. Karger *et al.* [11] observed a

pronounced deviation from linearity in MeCN-rich mobile phases, while Abbott *et al.* [12] reported otherwise. It should be noted, however, that Karger *et al.* [11] determined k' values over a wider range of mobile phase composition (10-100% MeCN) compared to Abbott *et al.* [12] (60-90% MeCN).

Tables 3.8A-3.13B show the linear correlation coefficients (R^2 values) obtained from linear and quadratics fits of plots of $\log k'$ vs. ϕ for the retention factors given in Tables 3.1A-3.6B. From Tables 3.8A-3.13B, it can be seen that *for both Si-C₁₈ and polymer-coated aluminas, a quadratic function provides a better description of the relationship between $\log k'$ and ϕ than does a linear function.* A very good example of this is illustrated by acetophenone for the Unisphere Al-CN column wherein retention data were determined from 0% to 70% MeOH (Table 3.12B). For the latter solute, the R^2 value increased from 0.988 for a linear fit, to 0.999 for a quadratic fit. More significant, however, is the better quadratic correlation obtained for plots of $\log k'$ vs. ϕ where pronounced deviations from linearity have been observed (defined in this study as those for solutes with $R^2 < 0.990$). The improvement in R^2 values from linear to quadratic fits for these solutes are given in Table 3.14. For the alumina columns, the poorest correlation for the linear fit of $\log k'$ vs. ϕ given in Table 3.14 was for 2-pentanone for the Al-CN phase with 0-30% MeCN as mobile phase. For this solute, R^2 increased from 0.783 for a linear fit to 0.999 for a quadratic fit. Similarly, the poorest correlation obtained for the silica-based column was for 2-butanone for the LiChrospher column with 0-50% MeCN, wherein R^2 increased from 0.868 to 0.971, respectively.

In general, deviations from linearity were observed at or near 0% organic solvent. Examples of these deviations are illustrated in Figs. 3.1-3.4. Only a slight deviation from linearity was observed for both Unisphere Al-PBD and Al-C₁₈ columns (Figs. 3.1 and 3.2). However, a more significant curvature was observed for both Al-CN and

TABLE 3.8A. Linear and quadratic fits of plots of $\log k'$ vs. ϕ or $E_T(30)$ polarity for the Unisphere Al-PBD column with MeCN/H₂O as mobile phase.

Compound	Log k' vs. ϕ				Log k' vs. $E_T(30)$ polarity				Range (%)
	<u>Linear</u>		<u>Quadratic</u>		<u>Linear</u>		<u>Quadratic</u>		
	- Slope ($\times 10^2$)	R ²	- B ($\times 10^2$)	R ²	- Slope	R ²	- B	R ²	
2-Butanone	1.66	1.000	1.57	1.000	-0.10	0.999	-0.44	1.000	0-20
3-Pentanone	1.86	0.999	1.98	1.000	-0.12	0.999	-0.36	0.999	0-30
Acetophenone	3.32	0.999	3.70	1.000	-0.21	1.000	-0.39	1.000	0-30
Nitrobenzene	2.58	0.980	1.36	0.999	-0.16	0.966	-2.89	1.000	0-30
m-Nitrotoluene	3.83	1.000	3.38	1.000	-0.26	0.996	-2.58	1.000	10-30
Toluene	3.13	0.993	5.04	1.000	-0.48	0.995	-1.83	0.996	30-80
Styrene	3.38	0.992	5.66	1.000	-0.52	0.996	-1.46	0.996	30-80
Ethylbenzene	3.54	0.994	5.46	0.999	-0.55	0.998	-2.42	0.999	30-80
Propylbenzene	3.52	0.970	6.76	0.981	-0.52	0.990	-0.29	0.990	30-70
Butylbenzene	3.16	0.988	-0.28	0.996	-0.53	0.976	-18.95	0.999	40-70
Pentane	2.77	0.999	2.88	0.999	—	—	—	—	60-100
	2.70	1.000	4.10	1.000	-0.49	0.991	16.10	1.000	60-80
Hexane	2.96	1.000	2.97	1.000	—	—	—	—	60-100
	2.90	1.000	4.44	1.000	-0.52	0.991	17.39	1.000	60-80
Heptane	3.13	0.998	1.92	0.999	—	—	—	—	60-100
	3.01	0.998	5.95	1.000	-0.54	0.987	21.63	1.000	60-80

TABLE 3.8B. Linear and quadratic fits of plots of $\log k'$ vs. ϕ or $E_T(30)$ polarity for the Unisphere A1-PBD column with MeOH/H₂O as mobile phase.

Compound	Log k' vs. ϕ				Log k' vs. $E_T(30)$ polarity				Range (%)
	<u>Linear</u>		<u>Quadratic</u>		<u>Linear</u>		<u>Quadratic</u>		
	- Slope ($\times 10^2$)	R ²	- B ($\times 10^2$)	R ²	- Slope	R ²	- B	R ²	
2-Butanone	2.21	0.978	1.28	0.993	-0.21	0.945	-4.04	0.968	0-40
3-Pentanone	1.93	0.974	1.06	0.991	-0.19	0.946	-4.24	0.980	0-40
Acetophenone	2.26	0.985	2.84	0.990	-0.23	0.984	-0.26	0.984	0-50
Nitrobenzene	1.70	0.985	1.54	0.986	-0.17	0.968	-1.80	0.979	0-50
m-Nitrotoluene	2.46	0.989	1.00	1.000	-0.24	0.942	-8.00	0.988	10-40
Toluene	3.06	0.999	2.36	1.000	-0.43	0.979	-8.94	0.998	40-80
Styrene	3.36	1.000	3.78	1.000	-0.47	0.988	-7.65	0.999	40-80
Ethylbenzene	3.53	1.000	3.72	1.000	-0.49	0.986	-8.59	0.999	40-80
Propylbenzene	4.52	0.999	2.33	1.000	-0.87	0.992	-19.30	1.000	60-90
Butylbenzene	4.94	1.000	4.07	1.000	-0.95	0.995	-17.13	1.000	60-90
Pentane	3.84	1.000	4.12	1.000	-0.74	0.996	-10.90	0.999	60-90
Hexane	4.34	1.000	4.66	1.000	-0.92	0.984	-22.72	0.997	60-100
Heptane	4.77	1.000	4.96	1.000	-1.01	0.984	-25.47	0.996	60-100

TABLE 3.9A. Linear and quadratic fits of plots of log k' vs. ϕ or $E_T(30)$ polarity for the Millipore Al-PBD column with MeCN/H₂O as mobile phase.

Compound	Log k' vs. ϕ				Log k' vs. $E_T(30)$ polarity				Range (%)
	<u>Linear</u>		<u>Quadratic</u>		<u>Linear</u>		<u>Quadratic</u>		
	- Slope ($\times 10^2$)	R ²	- B ($\times 10^2$)	R ²	- Slope	R ²	- B	R ²	
Acetophenone	3.49	0.990	2.55	0.996	-0.29	0.925	-4.59	0.978	0-60
Nitrobenzene	—	—	—	—	—	—	—	—	—
m-Nitrotoluene	3.86	1.000	3.80	1.000	-0.42	0.969	-8.42	0.999	20-60
Toluene	3.44	1.000	2.77	1.000	-0.58	0.993	-10.14	0.998	40-70
Styrene	3.63	1.000	3.22	1.000	-0.62	0.994	-9.72	0.998	40-70
Ethylbenzene	3.63	0.999	4.64	1.000	-0.62	0.997	-5.35	0.999	40-70
Pentane	2.75	0.995	5.18	0.999	—	—	—	—	60-100
	2.98	1.000	4.13	1.000	-0.54	0.992	16.72	1.000	60-80
Hexane	2.92	0.995	5.06	0.998	—	—	—	—	60-100
	3.09	1.000	3.30	1.000	-0.56	0.994	14.68	1.000	60-80
Heptane	3.07	0.999	4.28	0.999	—	—	—	—	60-100
	3.14	0.999	5.10	1.000	-0.57	0.990	19.61	1.000	60-80

TABLE 3.9B. Linear and quadratic fits of plots of $\log k'$ vs. ϕ or $E_T(30)$ polarity for the Millipore Al-PBD column with MeOH/H₂O as mobile phase.

Compound	Log k' vs. ϕ				Log k' vs. E _T (30) polarity				Range (%)
	<u>Linear</u>		<u>Quadratic</u>		<u>Linear</u>		<u>Quadratic</u>		
	- Slope (x 10 ²)	R ²	- B (x 10 ²)	R ²	- Slope	R ²	- B	R ²	
Acetophenone	2.13	0.998	2.43	0.999	-0.25	0.987	-1.09	0.988	20-60
Nitrobenzene	1.86	0.985	1.15	0.999	-0.20	0.955	-2.91	0.996	0-60
m-Nitrotoluene	2.70	0.999	2.37	0.999	-0.35	0.992	-1.32	0.992	30-70
Toluene	2.94	1.000	2.96	1.000	-0.40	0.992	-10.20	1.000	50-70
Styrene	3.35	1.000	3.73	1.000	-0.46	0.993	-10.96	1.000	50-70
Ethylbenzene	3.49	1.000	3.91	1.000	-0.48	0.993	-11.35	1.000	50-70
Pentane	3.79	1.000	4.54	1.000	-0.73	0.997	-9.47	0.999	60-90
Hexane	4.34	1.000	5.01	1.000	-0.83	0.997	-11.30	0.999	60-90
Heptane	4.82	1.000	6.14	1.000	-0.93	0.997	-11.01	0.999	60-90

TABLE 3.10A. Linear and quadratic fits of plots of log k' vs. ϕ or $E_T(30)$ polarity for the Microsorb Si-C₁₈ column with MeCN/H₂O as mobile phase.

Compound	Log k' vs. ϕ				Log k' vs. $E_T(30)$ polarity				Range (%)
	<u>Linear</u>		<u>Quadratic</u>		<u>Linear</u>		<u>Quadratic</u>		
	- Slope ($\times 10^2$)	R ²	- B ($\times 10^2$)	R ²	- Slope	R ²	- B	R ²	
Toluene	2.81	0.999	3.17	0.999	—	—	—	—	40-100
	2.84	0.997	4.37	1.000	-0.49	0.999	1.51	0.999	40-80
Styrene	2.99	0.998	3.45	0.998	—	—	—	—	40-100
	3.03	0.996	4.95	1.000	-0.52	0.998	2.38	0.999	40-80
Ethylbenzene	3.03	0.997	3.92	0.998	—	—	—	—	40-100
	3.13	0.994	5.49	1.000	-0.54	0.997	3.43	0.999	40-80
Pentane	2.70	0.999	2.13	1.000	—	—	—	—	60-100
	2.63	0.999	4.87	1.000	-0.47	0.988	18.02	1.000	60-80
Hexane	2.95	0.999	1.91	0.999	—	—	—	—	60-100
	2.88	1.000	3.79	1.000	-0.52	0.993	15.59	1.000	60-80
Heptane	3.16	0.997	1.52	0.999	—	—	—	—	60-100
	3.02	0.999	5.26	1.000	-0.55	0.989	19.81	1.000	60-80

TABLE 3.10B. Linear and quadratic fits of plots of log k' vs. ϕ or $E_T(30)$ polarity for the Microsorb Si-C₁₈ column with MeOH/H₂O as mobile phase.

Compound	Log k' vs. ϕ				Log k' vs. $E_T(30)$ polarity				Range (%)
	<u>Linear</u>		<u>Quadratic</u>		<u>Linear</u>		<u>Quadratic</u>		
	- Slope ($\times 10^2$)	R ²	- B ($\times 10^2$)	R ²	- Slope	R ²	- B	R ²	
Toluene	3.54	0.998	2.21	1.000	-0.64	0.958	-18.76	0.995	50-100
Styrene	4.04	0.991	0.94	0.996	-0.73	0.939	-23.87	0.985	50-100
Ethylbenzene	4.23	0.991	1.06	0.997	-0.77	0.940	-24.95	0.986	50-100
Pentane	4.18	0.999	3.15	1.000	-0.89	0.977	-25.52	0.994	60-100
Hexane	4.78	0.999	-0.88	1.000	-0.97	0.942	-77.65	0.995	70-100
Heptane	5.20	1.000	1.60	1.000	-0.92	0.881	-113.81	0.999	70-100

TABLE 3.11A. Linear and quadratic fits of plots of $\log k'$ vs. ϕ or $E_T(30)$ polarity for the Unisphere Al-C₁₈ column with MeCN/H₂O as mobile phase.

Compound	Log k' vs. ϕ				Log k' vs. $E_T(30)$ polarity				Range (%)
	Linear		Quadratic		Linear		Quadratic		
	- Slope ($\times 10^2$)	R ²	- B ($\times 10^2$)	R ²	- Slope	R ²	- B	R ²	
2-Pentanone	2.62	0.978	3.92	0.999	-0.17	0.988	1.41	0.999	0-30
2-Hexanone	3.02	0.988	4.11	0.999	-0.21	0.997	0.08	0.998	0-40
2-Heptanone	3.12	0.998	3.35	0.998	-0.26	0.975	-4.04	1.000	10-50
2-Octanone	3.61	0.992	5.78	1.000	-0.40	0.991	-4.29	0.999	20-60
2-Nonanone	3.84	0.992	7.26	1.000	-0.52	0.999	-2.33	0.999	30-60
Acetophenone	3.32	0.996	4.56	1.000	-0.25	0.998	-1.26	1.000	10-40
Propiophenone	3.60	0.993	5.13	1.000	-0.31	0.993	-2.60	0.999	10-50
Butyrophenone	3.69	0.991	6.03	1.000	-0.41	0.992	-4.17	0.999	20-60
Valerophenone	3.91	0.993	7.22	1.000	-0.53	0.998	-2.87	0.999	30-60
Nitrobenzene	3.17	0.998	3.64	0.999	-0.27	0.980	-3.69	0.999	10-50
m-Nitrotoluene	3.60	0.994	5.47	1.000	-0.40	0.989	-4.78	1.000	20-60
Toluene	3.28	0.993	4.93	1.000	-0.40	0.986	-4.93	0.999	20-70
Styrene	3.61	0.989	5.91	1.000	-0.44	0.990	-4.48	0.999	20-70
Ethylbenzene	3.50	0.990	6.40	1.000	-0.52	0.998	-2.87	0.999	30-70
Isopropylbenzene	3.87	0.988	7.42	1.000	-0.57	0.999	-2.36	0.999	30-70
Propylbenzene	3.32	0.992	6.37	1.000	-0.57	0.995	5.07	0.999	40-80
Butylbenzene	3.62	0.988	7.48	0.999	-0.62	0.993	6.99	0.999	40-80
Pentylbenzene	3.94	0.987	8.35	0.999	-0.68	0.992	8.16	0.999	40-80
Hexylbenzene	3.76	0.995	7.51	1.000	-0.66	0.994	8.11	0.998	50-80
Heptylbenzene	4.01	0.995	8.06	1.000	-0.71	0.994	8.80	0.999	50-80
Octylbenzene	3.89	0.999	6.27	1.000	-0.70	0.990	24.16	1.000	60-80
Nonylbenzene	4.08	0.999	6.84	1.000	-0.74	0.990	26.05	1.000	60-80

TABLE 3.11B. Linear and quadratic fits of plots of log k' vs. ϕ or $E_T(30)$ polarity for the Unisphere Al-C₁₈ column with MeOH/H₂O as mobile phase.

Compound	Log k' vs. ϕ				Log k' vs. $E_T(30)$ polarity				Range (%)
	<u>Linear</u>		<u>Quadratic</u>		<u>Linear</u>		<u>Quadratic</u>		
	- Slope ($\times 10^2$)	R ²	- B ($\times 10^2$)	R ²	- Slope	R ²	- B	R ²	
2-Pentanone	1.86	0.985	2.57	0.997	-0.18	0.981	1.35	0.986	0-40
2-Hexanone	2.28	0.996	2.62	0.998	-0.23	0.990	-0.75	0.991	0-50
2-Heptanone	2.67	0.997	2.02	0.999	-0.29	0.974	-3.76	0.994	10-60
2-Octanone	3.42	0.980	6.45	0.991	-0.45	0.979	6.83	0.991	30-70
2-Nonanone	3.92	0.999	5.19	1.000	-0.55	0.992	-7.46	0.999	40-80
Acetophenone	2.59	1.000	2.68	1.000	-0.28	0.989	-2.23	0.995	10-60
Propiophenone	2.98	0.999	3.21	0.999	-0.37	0.992	-2.32	0.995	20-70
Butyrophenone	3.56	0.999	4.23	1.000	-0.47	0.996	0.87	0.997	30-70
Valerophenone	3.92	0.999	5.33	1.000	-0.55	0.992	-7.10	0.999	40-80
Nitrobenzene	2.31	0.994	1.52	0.999	-0.26	0.966	-3.77	0.997	10-70
m-Nitrotoluene	3.10	0.999	3.47	1.000	-0.43	0.995	-2.86	0.997	30-80
Toluene	3.13	0.999	2.75	0.999	-0.44	0.982	-8.68	0.999	40-80
Styrene	3.55	1.000	4.01	1.000	-0.50	0.988	-8.11	0.999	40-80
Ethylbenzene	3.59	1.000	4.38	1.000	-0.65	0.995	-17.70	1.000	60-80
Isopropylbenzene	4.02	1.000	4.93	1.000	-0.73	0.995	-19.78	1.000	60-80
Propylbenzene	4.14	1.000	5.19	1.000	-0.76	0.995	-20.06	1.000	60-80
Butylbenzene	4.67	1.000	6.22	1.000	-0.85	0.996	-21.62	1.000	60-80
Pentylbenzene	5.19	1.000	6.35	1.000	-0.95	0.995	-25.64	1.000	60-80
Hexylbenzene	—	—	—	—	—	—	—	—	—
Heptylbenzene	—	—	—	—	—	—	—	—	—
Octylbenzene	—	—	—	—	—	—	—	—	—
Nonylbenzene	—	—	—	—	—	—	—	—	—

TABLE 3.12A. Linear and quadratic fits of plots of log k' vs. ϕ or $E_T(30)$ polarity for the Unisphere Al-CN column with MeCN/H₂O as mobile phase.

Compound	Log k' vs. ϕ				Log k' vs. $E_T(30)$ polarity				Range (%)
	<u>Linear</u>		<u>Quadratic</u>		<u>Linear</u>		<u>Quadratic</u>		
	- Slope ($\times 10^2$)	R^2	- B ($\times 10^2$)	R^2	- Slope	R^2	- B	R^2	
2-Pentanone	0.81	0.783	0.62	0.999	-0.05	0.746	-2.67	1.000	0-30
2-Hexanone	1.75	0.942	0.31	0.997	-0.12	0.890	-3.20	0.998	0-40
2-Heptanone	2.62	0.975	1.33	0.996	-0.20	0.911	-4.32	0.998	0-50
2-Octanone	3.52	0.996	3.66	0.996	-0.33	0.959	-5.64	0.999	10-60
2-Nonanone	3.93	0.993	7.21	1.000	-0.53	0.998	-2.95	0.999	30-60
Acetophenone	2.61	0.993	2.06	0.997	-0.20	0.952	-3.21	0.999	0-50
Propiophenone	3.25	0.997	3.83	0.999	-0.31	0.972	-4.36	1.000	10-60
Butyrophenone	3.75	0.994	5.70	1.000	-0.42	0.989	-5.09	0.999	20-60
Valerophenone	3.73	0.990	6.88	1.000	-0.55	0.998	-2.77	0.999	30-70
Nitrobenzene	3.05	0.998	3.15	0.998	-0.28	0.961	-4.77	1.000	10-60
m-Nitrotoluene	3.47	0.992	5.33	1.000	-0.43	0.987	-5.02	0.999	20-70
Toluene	3.29	0.993	4.95	1.000	-0.40	0.985	-5.04	0.999	20-70
Styrene	3.40	0.993	5.87	1.000	-0.50	0.997	-3.58	0.999	30-70
Ethylbenzene	3.56	0.992	6.28	1.000	-0.53	0.998	-3.51	0.999	30-70
Isopropylbenzene	3.67	0.987	6.75	1.000	-0.57	0.998	-0.16	0.998	30-80
Propylbenzene	3.74	0.987	6.95	1.000	-0.58	0.998	0.01	0.998	30-80
Butylbenzene	3.72	0.991	7.24	0.999	-0.64	0.995	5.99	0.999	40-80
Pentylbenzene	—	—	—	—	—	—	—	—	—
Hexylbenzene	3.62	0.999	0.74	1.000	—	—	—	—	70-90
Heptylbenzene	3.70	1.000	2.10	1.000	—	—	—	—	70-90
Octylbenzene	3.97	1.000	1.97	1.000	—	—	—	—	70-90
Nonylbenzene	4.16	1.000	1.76	1.000	—	—	—	—	70-90

TABLE 3.12B. Linear and quadratic fits of plots of $\log k'$ vs. ϕ or $E_T(30)$ polarity for the Unisphere Al-CN column with MeOH/H₂O as mobile phase.

Compound	Log k' vs. ϕ			Log k' vs. $E_T(30)$ polarity			Range (%)
	Linear		Quadratic	Linear		Quadratic	
	- Slope ($\times 10^2$)	R^2		- Slope	R^2		
			- B ($\times 10^2$)				
2-Pentanone	0.75	0.968	0.44	-0.07	0.924	-1.32	0.945
2-Hexanone	1.42	0.985	0.83	-0.15	0.955	-2.31	0.992
2-Heptanone	1.92	0.984	1.11	-0.20	0.955	-3.17	0.993
2-Octanone	2.92	0.996	1.95	-0.36	0.980	-4.48	0.995
2-Nonanone	3.63	1.000	3.99	-0.51	0.994	-3.51	0.996
Acetophenone	1.88	0.988	1.18	-0.20	0.958	-2.96	0.996
Propiophenone	2.50	0.996	1.89	-0.30	0.965	-4.16	0.997
Butyrophenone	3.13	0.999	3.54	-0.44	0.994	-2.82	0.996
Valerophenone	3.67	0.999	4.49	-0.51	0.990	-7.87	0.999
Nitrobenzene	2.04	0.986	0.98	-0.23	0.950	-4.01	0.997
m-Nitrotoluene	2.86	1.000	2.89	-0.40	0.993	-3.34	0.996
Toluene	2.92	0.999	2.35	-0.41	0.989	-4.78	0.996
Styrene	3.30	1.000	3.53	-0.50	0.983	-8.32	0.999
Ethylbenzene	3.47	1.000	3.44	-0.52	0.981	-9.31	0.999
Isopropylbenzene	3.89	1.000	4.31	-0.65	0.986	-12.73	1.000
Propylbenzene	3.99	1.000	4.64	-0.66	0.987	-12.66	1.000
Butylbenzene	4.51	1.000	5.32	-0.75	0.987	-14.16	1.000
Pentylbenzene	4.77	1.000	5.89	-1.00	1.000	5.00	1.000
Hexylbenzene	5.23	1.000	7.79	-1.10	0.999	9.65	1.000
Heptylbenzene	5.74	1.000	8.35	-1.21	0.999	9.95	1.000
Octylbenzene	—	—	—	—	—	—	—
Nonylbenzene	—	—	—	—	—	—	—

TABLE 3.13A. Linear and quadratic fits of plots of log k' vs. ϕ or $E_T(30)$ polarity for the LiChrospher Si-C₁₈ column with MeCN/H₂O as mobile phase.

Compound	Log k' vs. ϕ				Log k' vs. $E_T(30)$ polarity				Range (%)
	<u>Linear</u>		<u>Quadratic</u>		<u>Linear</u>		<u>Quadratic</u>		
	- Slope ($\times 10^2$)	R^2	- B ($\times 10^2$)	R^2	- Slope	R^2	- B	R^2	
2-Propanone	3.97	0.874	8.89	0.993	-0.26	0.899	7.22	0.995	0-30
2-Butanone	2.86	0.868	6.24	0.971	-0.23	0.932	3.30	0.979	0-50
2-Pentanone	2.25	0.990	3.09	0.997	-0.24	0.980	-2.27	0.994	10-70
2-Hexanone	2.49	0.996	3.28	0.999	-0.33	0.984	-3.63	1.000	20-80
2-Heptanone	2.67	0.995	3.86	0.999	—	—	—	—	30-90
	2.74	0.994	4.22	0.999	-0.42	0.998	-1.83	0.999	30-80
2-Octanone	2.76	0.997	4.04	0.999	—	—	—	—	40-90
	2.83	0.996	4.62	1.000	-0.48	0.998	2.21	1.000	40-80
2-Nonanone	2.77	0.998	3.56	0.999	—	—	—	—	50-100
	2.88	0.997	5.09	1.000	-0.51	0.996	4.58	0.999	50-80
Acetophenone	2.75	0.996	3.69	0.999	-0.36	0.985	-3.84	1.000	20-80
Propiophenone	2.89	0.995	4.26	0.999	-0.44	0.998	-2.41	0.999	30-80
Butyrophenone	2.87	0.996	4.39	0.999	—	—	—	—	40-90
	2.96	0.995	4.92	1.000	-0.51	0.998	2.53	1.000	40-80
Valerophenone	2.99	0.999	3.19	0.999	—	—	—	—	50-100
	3.01	0.997	5.02	0.999	-0.53	0.998	4.04	0.999	50-80
Nitrobenzene	2.92	0.999	3.57	1.000	-0.45	0.994	-4.09	0.999	30-80
m-Nitrotoluene	3.19	0.997	4.26	0.999	—	—	—	—	30-90
	3.23	0.995	4.84	1.000	-0.50	0.998	-2.55	0.999	30-80
Toluene	2.83	0.998	3.86	0.999	—	—	—	—	40-90
	2.87	0.996	4.54	1.000	-0.49	0.999	1.83	1.000	40-80
Styrene	3.01	0.997	4.27	0.999	—	—	—	—	40-90
	3.06	0.995	5.18	0.999	-0.52	0.998	2.87	1.000	40-80

TABLE 3.13A (continued).

Compound	Log k' vs. ϕ				Log k' vs. $E_T(30)$ polarity				Range (%)
	<u>Linear</u>		<u>Quadratic</u>		<u>Linear</u>		<u>Quadratic</u>		
	- Slope (x 10 ²)	R ²	- B (x 10 ²)	R ²	- Slope	R ²	- B	R ²	
Ethylbenzene	2.96	0.999	2.71	0.999	—	—	—	—	50-100
	2.92	0.998	4.81	1.000	-0.52	0.997	3.75	0.999	50-80
Isopropylbenzene	3.15	0.998	3.08	0.998	—	—	—	—	50-100
	3.14	0.997	5.47	1.000	-0.55	0.997	4.78	0.999	50-80
Propylbenzene	3.07	0.999	1.88	1.000	—	—	—	—	60-100
	2.95	1.000	3.37	1.000	-0.53	0.994	14.63	1.000	60-80
Butylbenzene	3.24	0.999	2.21	1.000	—	—	—	—	60-100
	3.14	1.000	3.65	1.000	-0.57	0.994	15.73	1.000	60-80
Pentylbenzene	3.52	0.998	0.93	1.000	—	—	—	—	70-100
Hexylbenzene	3.73	0.998	0.81	1.000	—	—	—	—	70-100
Heptylbenzene	3.94	0.998	1.05	1.000	—	—	—	—	70-100
Octylbenzene	4.38	0.998	2.11	1.000	—	—	—	—	70-100

TABLE 3.13B. Linear and quadratic fits of plots of log k' vs. ϕ or $E_T(30)$ polarity for the LiChrospher Si-C₁₈ column with MeOH/H₂O as mobile phase.

Compound	Log k' vs. ϕ				Log k' vs. $E_T(30)$ polarity				Range (%)
	<u>Linear</u>		<u>Quadratic</u>		<u>Linear</u>		<u>Quadratic</u>		
	- Slope ($\times 10^2$)	R ²	- B ($\times 10^2$)	R ²	- Slope	R ²	- B	R ²	
2-Propanone	2.28	0.941	4.14	0.994	-0.24	0.960	3.36	0.987	0-50
2-Butanone	2.34	0.969	3.59	0.991	-0.26	0.985	0.97	0.990	0-70
2-Pentanone	2.46	0.997	2.94	0.999	-0.30	0.993	-1.80	0.998	10-80
2-Hexanone	2.87	1.000	3.20	1.000	-0.40	0.995	-2.66	0.997	30-80
2-Heptanone	3.43	1.000	3.83	1.000	-0.52	0.984	-8.35	0.999	40-90
2-Octanone	3.92	0.999	4.61	1.000	-0.65	0.988	-12.10	1.000	50-90
2-Nonanone	4.31	1.000	4.28	1.000	-0.83	0.996	-12.87	1.000	60-90
Acetophenone	3.09	0.998	4.20	1.000	-0.43	0.996	-1.09	0.997	30-80
Propiophenone	3.36	0.998	4.53	1.000	-0.51	0.990	-6.41	0.999	40-90
Butyrophenone	3.75	0.999	4.68	1.000	-0.63	0.989	-10.94	1.000	50-90
Valerophenone	4.05	0.999	5.21	1.000	-0.86	0.989	-18.31	0.998	60-100
Nitrobenzene	3.04	1.000	2.77	1.000	-0.46	0.979	-8.47	0.999	40-90
m-Nitrotoluene	3.49	0.999	3.13	0.999	-0.58	0.982	-12.76	1.000	50-90
Toluene	3.64	0.997	2.00	0.999	-0.66	0.956	-19.48	0.993	50-100
Styrene	3.72	1.000	3.53	1.000	-0.71	0.995	-11.68	1.000	60-90
Ethylbenzene	4.12	0.996	0.92	0.999	-0.87	0.966	-31.83	0.993	60-100
Isopropylbenzene	4.60	0.996	0.56	1.000	-1.09	0.971	-58.15	0.995	70-100
Propylbenzene	4.57	0.999	1.85	1.000	-1.09	0.978	-46.96	0.993	70-100
Butylbenzene	4.98	1.000	3.24	1.000	-1.18	0.981	-45.71	0.993	70-100
Pentylbenzene	5.58	1.000	2.79	1.000	-1.45	0.969	-149.77	1.000	80-100
Hexylbenzene	6.04	1.000	3.55	1.000	-1.57	0.970	-159.76	1.000	80-100
Heptylbenzene	—	—	—	—	—	—	—	—	—
Octylbenzene	—	—	—	—	—	—	—	—	—

TABLE 3.14. Improvement in R^2 values from linear to quadratic fit for $\log k'$ vs. ϕ for solutes with linear correlation coefficients (R^2) < 0.990.

Column	Organic Solvent	Solute	Range (%)	R^2	
				Linear	Quadratic
Unisphere Al-PBD	MeCN	Nitrobenzene	0-30	0.980	0.999
		Propylbenzene	30-70	0.970	0.981
		Butylbenzene	40-70	0.988	0.996
	MeOH	2-Butanone	0-40	0.978	0.993
		3-Pentanone	0-40	0.974	0.991
		Acetophenone	0-50	0.985	0.990
		Nitrobenzene	0-50	0.985	0.986
Millipore Al-PBD	MeOH	m-Nitrotoluene	10-40	0.989	1.000
Unisphere Al-C ₁₈	MeOH	Nitrobenzene	0-60	0.985	0.999
	MeCN	2-Pentanone	0-30	0.978	0.999
		2-Hexanone	0-40	0.988	0.999
		Styrene	20-70	0.989	1.000
	MeOH	Isopropylbenzene	30-70	0.988	1.000
		Butylbenzene	40-80	0.988	0.999
		Pentylbenzene	40-80	0.987	0.999
		2-Pentanone	0-40	0.985	0.997
		2-Octanone	30-70	0.980	0.991
		2-Pentanone	0-30	0.783	0.999
		2-Hexanone	0-40	0.942	0.997
Unisphere Al-CN	MeCN	2-Heptanone	0-50	0.975	0.996
		Isopropylbenzene	30-80	0.987	1.000
		Propylbenzene	30-80	0.987	1.000
		2-Pentanone	0-40	0.968	0.983
		2-Hexanone	0-60	0.985	0.999
	MeOH	2-Heptanone	0-60	0.984	0.999
		Acetophenone	0-70	0.988	0.999
		Nitrobenzene	10-70	0.986	0.998
LiChrospher Si-C ₁₈	MeCN	2-Propanone	0-30	0.874	0.993
		2-Butanone	0-50	0.868	0.971
	MeOH	2-Propanone	0-50	0.941	0.994
		2-Butanone	0-70	0.969	0.991

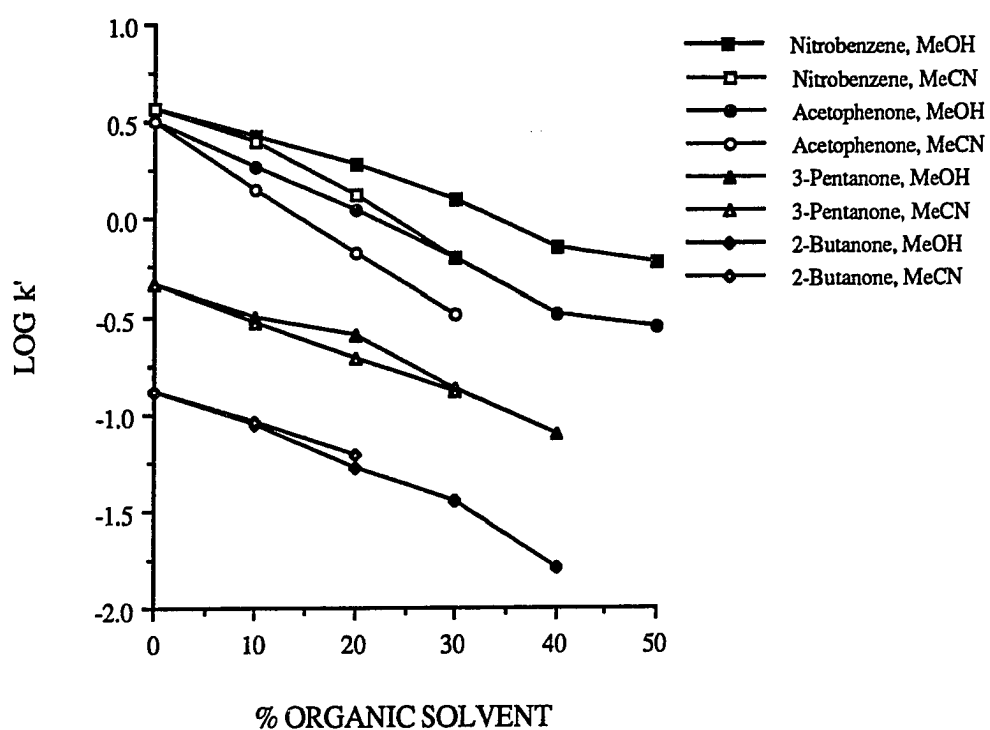


FIGURE 3.1. Characteristic curvature in plots of $\log k'$ vs. ϕ for solutes with retention data at 0% organic solvent for the Unisphere Al-PBD column.

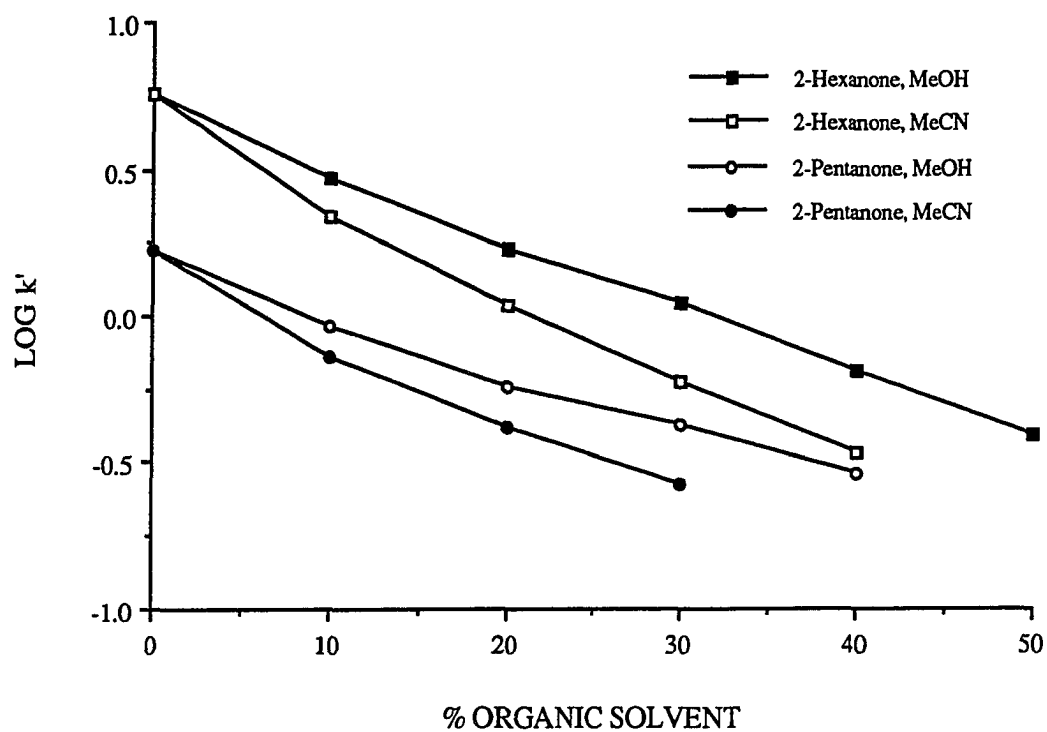


FIGURE 3.2. Characteristic curvature in plots of $\log k'$ vs. ϕ for solutes with retention data at 0% organic solvent for the Unisphere Al-C₁₈ column.

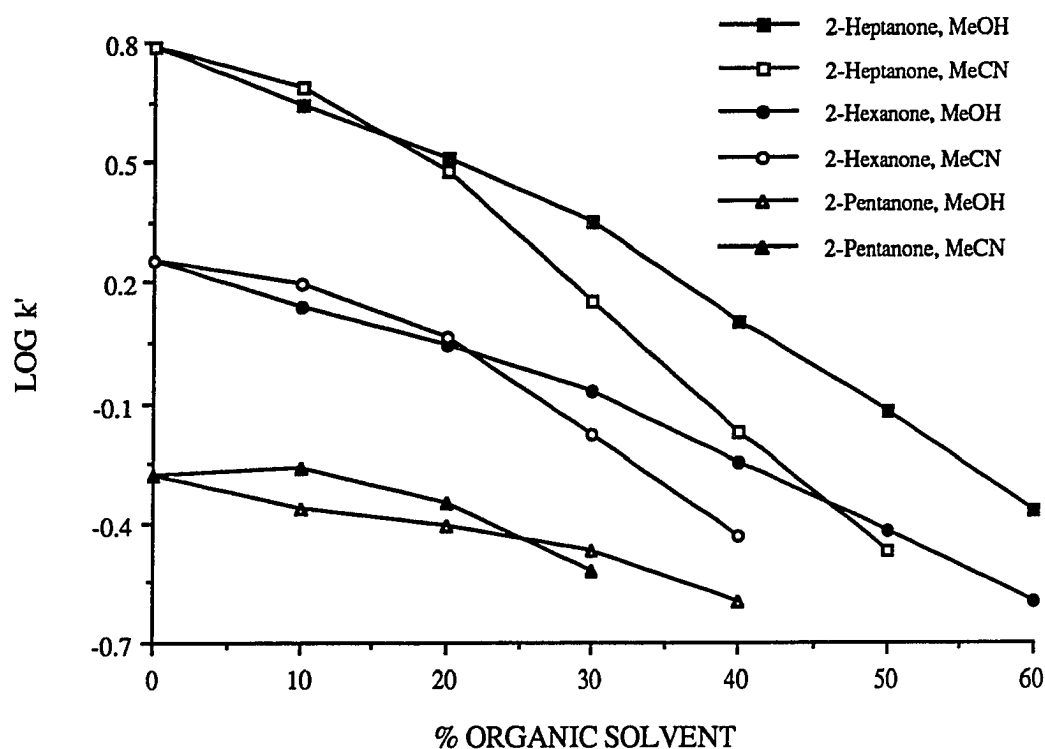


FIGURE 3.3. Characteristic curvature in plots of $\log k'$ vs. ϕ for solutes with retention data at 0% organic solvent for the Unisphere Al-CN column.

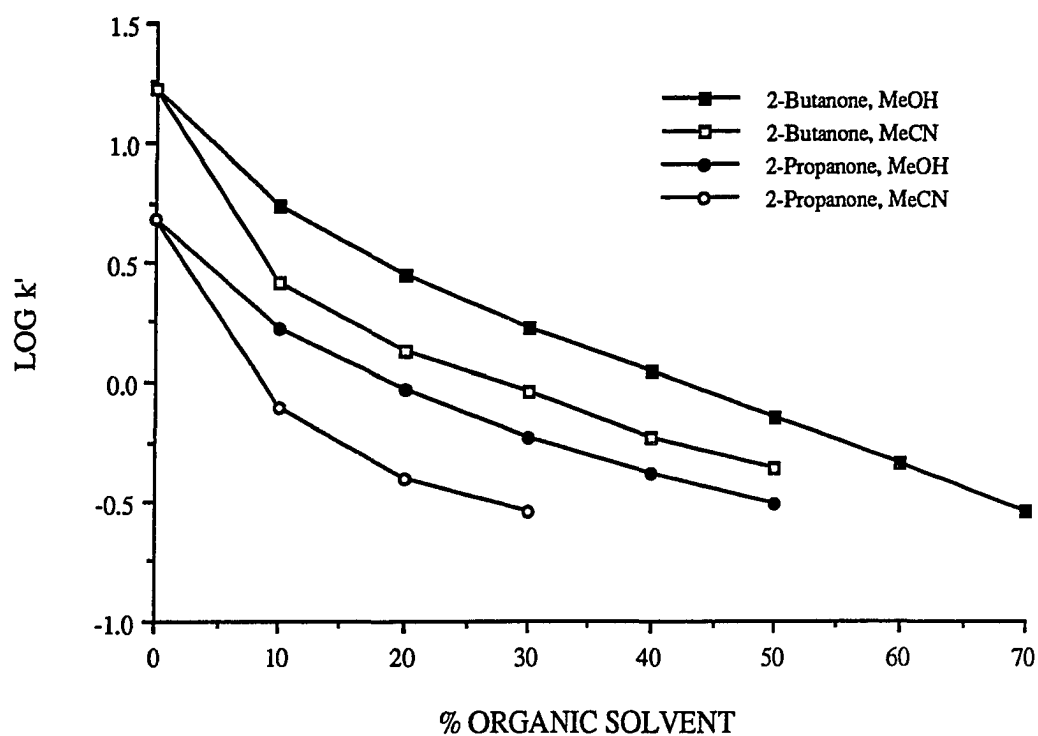


FIGURE 3.4. Characteristic curvature in plots of $\log k'$ vs. ϕ for solutes with retention data at 0% organic solvent for the LiChrospher Si-C₁₈ column.

Si-C₁₈ columns at the H₂O-rich mobile phases, especially for MeCN/H₂O (Figs. 3.3 and 3.4).

2. Using The $E_T(30)$ Solvent Polarity Scale

Retention in RPLC is expected to be proportional to the difference in polarity between the mobile and stationary phases. One of the most popular and convenient measure of mobile phase polarity is based on the widely employed $E_T(30)$ solvent polarity scale which is based on the charge transfer absorption of 2,6-diphenyl-4-(2,4,6-triphenyl-N-pyridinio)phenolate, also known as ET-30. This molecule is very sensitive to subtle changes in solvent polarity, exhibiting one of largest observed solvatochromic effects of any molecule. The charge transfer absorption maximum of ET-30 shifts from 453 nm in water (a very polar solvent) to 810 nm in diphenyl ether (a very nonpolar solvent) [13, 14]. According to Dorsey and Johnson [14], the major advantage of using this empirical scale is that the polarity values are determined independently of the stationary phase.

A study by Johnson *et al.* [13] of 332 sets of retention data showed that solute retention ($\log k'$) in RPLC generally correlates better with $E_T(30)$ polarity than with the volume fraction of MeCN or MeOH. They also observed a more significant improvement in linearity for the MeCN system where the average R^2 value was 0.9914 for plots of $\log k'$ vs. $E_T(30)$ polarity for 240 data sets, compared to 0.9733 for plots of $\log k'$ vs. ϕ . For MeOH/H₂O, the average R^2 value was 0.9907 and 0.9956, respectively, for 92 data sets. This improved linearity could presumably be used to obtain a better estimate of S for a given solute, if differences in the volume fraction and solvatochromic scales were taken into account.

Table 3.15 shows the $E_T(30)$ polarity scale for MeCN/H₂O and MeOH/H₂O used for plotting $\log k'$ vs. $E_T(30)$ polarity. These values were determined at 25.0° C. Polarity values at other mobile phase compositions can be calculated using Eqns. 3.3

TABLE 3.15. $E_T(30)$ polarity values at different concentrations of MeCN and MeOH for binary hydroorganic mobile phases [14].

% Organic Solvent	$E_T(30)$ polarity (kcal/mol)	
	MeCN	MeOH
0	63.11	63.11
10	61.43	62.15
20	59.81	60.94
30	58.44	59.78
40	57.46	59.17
50	56.82	58.30
60	56.19	57.46
70	55.71	56.84
80	55.09	56.37
90	53.80	55.89
100	45.97	55.62

and 3.4 below, which were obtained from a second degree polynomial fit of the experimental data as reported by Dorsey and Johnson [14]. Similar to the procedure used by Johnson *et al.* [13], retention factors at 90 and 100% MeCN were not included in plots of $\log k'$ vs. $E_T(30)$ polarity since a very rapid decrease in the measured polarity was observed at concentrations $> 80\%$ MeCN. The authors attributed this to the relatively weaker hydrogen-bonding characteristics of MeCN compared to either MeOH or H₂O.

For 0 - 80% MeCN [14]:

$$E_T(30) = 63.0412 - 0.1773(\% \text{ MeCN}) + 0.0010(\% \text{ MeCN})^2 \quad (3.3)$$

For 0 - 100% MeOH [14]:

$$E_T(30) = 63.1927 - 0.1222(\% \text{ MeOH}) + 0.0005(\% \text{ MeOH})^2 \quad (3.4)$$

The R^2 values for linear and quadratic fits of plots of $\log k'$ vs. $E_T(30)$ polarity for the retention factors in Tables 3.1A-3.6B are given in Tables 3.8A-3.13B. Similar to the results obtained for $\log k'$ vs. ϕ , in all cases a quadratic function provides a better description of the relationship between $\log k'$ and $E_T(30)$ polarity than does a linear function for both stationary phase types.

Unfortunately, in contrast to the results obtained previously for various alkylbonded, silica-based stationary phases [13], *a significantly poorer linear correlation was observed for majority of the solutes used in this study for all the alumina-based and silica-based columns.* This can clearly be seen in Fig. 3.5 which illustrates the distribution of R^2 values for linear fits of plots of $\log k'$ vs. ϕ , and $\log k'$ vs. $E_T(30)$ polarity. Overall, 172 data sets were investigated with 31 sets having R^2 values < 0.990 , and 141 sets having R^2 values ≥ 0.990 for $\log k'$ vs. ϕ . On the other hand, 79 sets had $R^2 < 0.990$, while only 93 sets had $R^2 \geq 0.990$ for plots of $\log k'$ vs. $E_T(30)$.

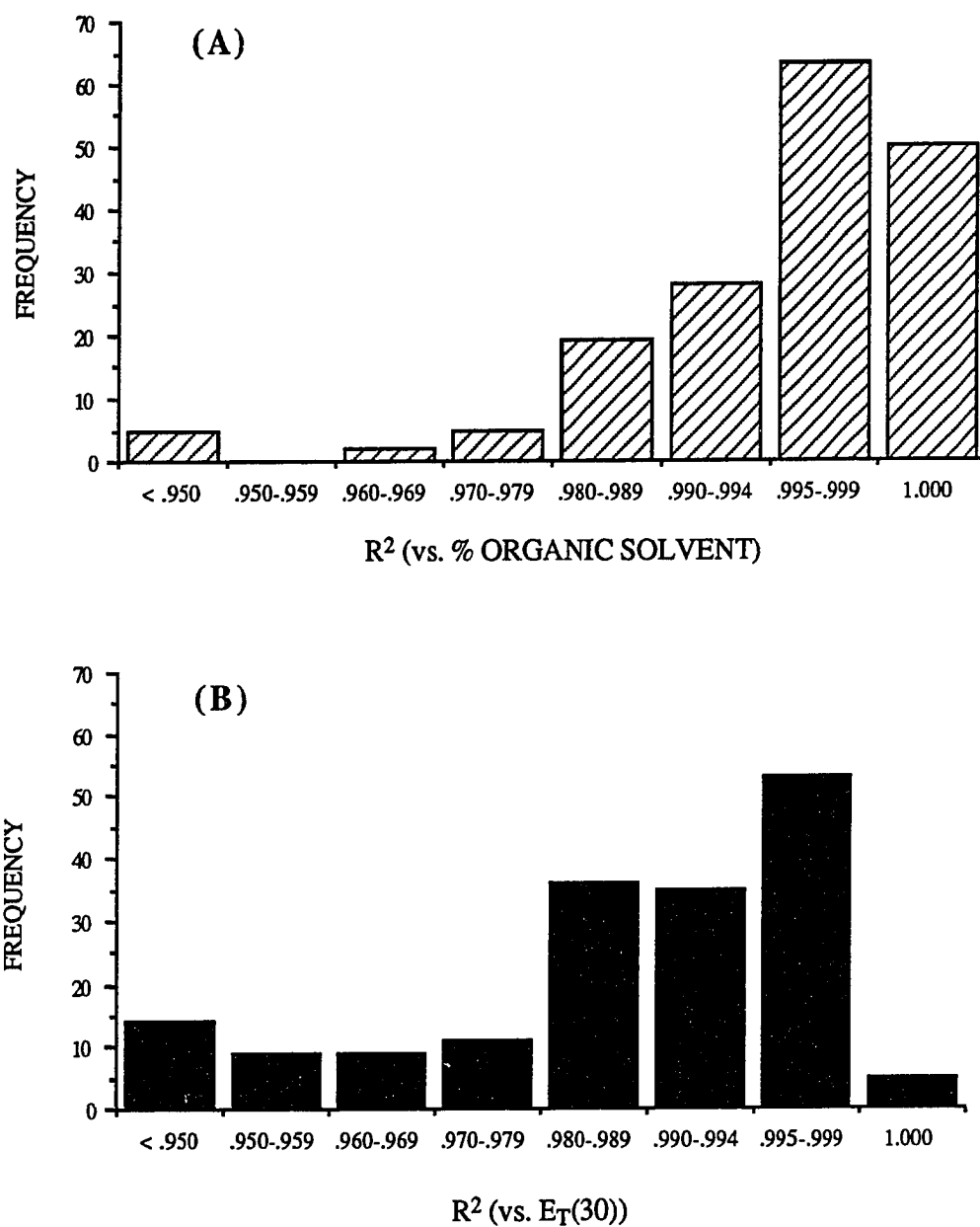


FIGURE 3.5. Frequency plots of R^2 for linear fits of (A) $\log k'$ vs. ϕ , and (B) $\log k'$ vs. $E_T(30)$.

The better linearity obtained for plots of k' vs. ϕ is even more obvious since 50 sets of data had $R^2 = 1.000$, 63 sets had R^2 within 0.995-0.999, while only 5 sets had $R^2 < 0.950$ (Fig. 3.5). For $\log k'$ vs. $E_T(30)$, the frequencies were 5, 53 and 14, respectively. To make matters worst, of the 141 data sets with $R^2 \geq 0.990$ for $\log k'$ vs. ϕ , 50 sets (Table 3.16) eventually had $R^2 < 0.990$ upon using the $E_T(30)$ polarity scale.

The overall average R^2 values obtained for linear fits of $\log k'$ vs. ϕ , and vs. $E_T(30)$ for 172 data sets were 0.992 and 0.981, respectively. Again, these values suggest better linearity for plots of $\log k'$ vs. ϕ . The average R^2 values for each column for either MeCN/H₂O or MeOH/H₂O can be seen in Table 3.17. As can be seen, except for the LiChrospher Si-C₁₈ with MeCN/H₂O as mobile phase, no improvement in linearity was obtained for all the other columns using the $E_T(30)$ polarity scale for both mobile phases. In terms of the two different solvent systems used, the average R^2 values for MeCN/H₂O were 0.988 and 0.983 using % organic solvent and $E_T(30)$ polarity, respectively. Similarly, for the MeOH/H₂O solvent system, the average R^2 values were 0.995 and 0.979, respectively. Again, even in terms of solvent, no improvement in linearity was obtained.

Initially, the main objective of using the $E_T(30)$ scale was to obtain a better linearity compared to those obtained from plots of $\log k'$ vs. ϕ , especially for solutes with $R^2 < 0.990$, eventually resulting in a better measure of $S_{E_T(30)}$ (equal to the negative of the slope from plots of $\log k'$ vs. $E_T(30)$ polarity) for Eqn. 3.2. However, as can be seen in Table 3.18, improvement in linearity was observed in only 13 cases out of a total of 31 data sets with $R^2 < 0.990$ for linear fits of $\log k'$ vs. ϕ . Thus, *the use of the $E_T(30)$ polarity scale appears to be futile, and apparently more reliable values of S (i.e., better linearity) can still be obtained from plots of $\log k'$ vs. ϕ .*

It is not known why the results of this study were significantly different from that obtained by Johnson *et al.* [13]. The $E_T(30)$ solvent polarity values reported by Dorsey

TABLE 3.16. List of solutes with R^2 values ≥ 0.990 for linear fits of plots of $\log k'$ vs. ϕ that decreased to < 0.990 with $\log k'$ vs. $E_T(30)$ polarity.

Column	Organic Solvent	Solute	Range (%)	R^2	
				vs. ϕ	vs. $E_T(30)$
Unisphere Al-PBD	MeCN	Heptane	60-80	0.998	0.987
	MeOH	Toluene	40-80	0.999	0.979
		Styrene	40-80	1.000	0.988
		Ethylbenzene	40-80	1.000	0.986
		Hexane	60-100	1.000	0.984
		Heptane	60-100	1.000	0.984
Millipore Al-PBD	MeCN	Acetophenone	0-60	0.990	0.925
		m-Nitrotoluene	20-60	1.000	0.969
Microsorb Si-C ₁₈	MeCN	Pentane	60-80	0.999	0.988
		Heptane	60-80	0.999	0.989
Microsorb Si-C ₁₈	MeOH	Toluene	50-100	0.998	0.958
		Styrene	50-100	0.991	0.939
		Ethylbenzene	50-100	0.991	0.940
		Pentane	60-100	0.999	0.977
		Hexane	70-100	0.999	0.942
		Heptane	70-100	1.000	0.881
Unisphere Al-C ₁₈	MeCN	2-Heptanone	10-50	0.998	0.975
		Nitrobenzene	10-50	0.998	0.980
		m-Nitrotoluene	20-60	0.994	0.989
		Toluene	20-70	0.993	0.986
	MeOH	2-Heptanone	10-60	0.997	0.974
		Acetophenone	10-60	1.000	0.989
		Nitrobenzene	10-70	0.994	0.966
		Toluene	40-80	0.999	0.982
		Styrene	40-80	1.000	0.988
	MeCN	2-Octanone	10-60	0.996	0.959
		Acetophenone	0-50	0.993	0.952
		Propiophenone	10-60	0.997	0.972
Unisphere Al-CN		Butyrophenone	20-60	0.994	0.989
		Nitrobenzene	10-60	0.998	0.961
		m-Nitrotoluene	20-70	0.992	0.987
		Toluene	20-70	0.993	0.985
	MeOH	2-Octanone	20-70	0.996	0.980
		Propiophenone	10-80	0.996	0.965
		Toluene	30-80	0.999	0.989
		Styrene	40-90	1.000	0.983
		Ethylbenzene	40-90	1.000	0.981
		Isopropylbenzene	50-90	1.000	0.986
		Propylbenzene	50-90	1.000	0.987
		Butylbenzene	50-90	1.000	0.987
	MeCN	2-Pentanone	10-70	0.990	0.980
		2-Hexanone	20-80	0.996	0.984
		Acetophenone	20-80	0.996	0.985

TABLE 3.16 (continued).

Column	Organic Solvent	Solute	Range (%)	R ²	
				vs. ϕ	vs. E _T (30)
	MeOH	2-Heptanone	40-90	1.000	0.984
		2-Octanone	50-90	0.999	0.988
		Butyrophenone	50-90	0.999	0.989
		Valerophenone	60-100	0.999	0.989
		Nitrobenzene	40-90	1.000	0.979
		m-Nitrotoluene	50-90	0.999	0.982
		Toluene	50-100	0.997	0.956
		Ethylbenzene	60-100	0.996	0.966
		Isopropylbenzene	70-100	0.996	0.971
		Propylbenzene	70-100	0.999	0.978
		Butylbenzene	70-100	1.000	0.981
		Pentylbenzene	80-100	1.000	0.969
		Hexylbenzene	80-100	1.000	0.970

TABLE 3.17. Average R^2 values for linear correlations in Tables 3.8A-3.13B. ^{a, b}

Column	n ^c	<u>MeCN/H₂O</u>		n ^c	<u>MeOH/H₂O</u>	
		vs. ϕ	vs. $E_T(30)$		vs. ϕ	vs. $E_T(30)$
Unisphere Al-PBD	13	0.993 ± 0.009	0.991 ± 0.010	13	0.993 ± 0.010	0.976 ± 0.019
Millipore Al-PBD	8	0.997 ± 0.005	0.982 ± 0.025	9	0.998 ± 0.005	0.989 ± 0.013
Unisphere Al-C ₁₈	22	0.992 ± 0.005	0.992 ± 0.006	18	0.997 ± 0.006	0.988 ± 0.009
Unisphere Al-CN	17	0.976 ± 0.051	0.961 ± 0.064	20	0.995 ± 0.009	0.978 ± 0.020
All Alumina-Based Columns	60	0.989 ± 0.028	0.982 ± 0.037	60	0.996 ± 0.008	0.983 ± 0.017
Microsorb Si-C ₁₈	6	0.998 ± 0.002	0.994 ± 0.005	6	0.996 ± 0.004	0.940 ± 0.032
LiChrospher Si-C ₁₈	19	0.983 ± 0.040	0.986 ± 0.026	21	0.995 ± 0.014	0.982 ± 0.012
All Si-C ₁₈ Columns	25	0.987 ± 0.035	0.988 ± 0.023	27	0.995 ± 0.012	0.972 ± 0.025
All Columns ^d	85	0.988 ± 0.030	0.983 ± 0.034	87	0.995 ± 0.009	0.979 ± 0.020

^a Reported as average $R^2 \pm$ standard deviation.

^b The overall average R^2 values \pm standard deviation are 0.992 ± 0.023 for $\log k'$ vs. % organic, and 0.981 ± 0.028 for $\log k'$ vs. $E_T(30)$ polarity.

^c n = number of data sets.

^d Includes all alumina-based and silica-based columns.

TABLE 3.18. Comparison of R^2 values for linear fits of $\log k'$ vs. ϕ or $E_T(30)$ polarity for solutes with R^2 values < 0.990 for linear fits of $\log k'$ vs. ϕ .^a

Column	Organic Solvent	Solute	Range (%)	R^2	
				vs. ϕ	vs. $E_T(30)$
Unisphere Al-PBD	MeCN	Nitrobenzene	0-30	0.980	0.966
		<i>Propylbenzene</i>	<i>30-70</i>	<i>0.970</i>	<i>0.990</i>
		Butylbenzene	40-70	0.988	0.976
	MeOH	2-Butanone	0-40	0.978	0.945
		3-Pentanone	0-40	0.974	0.946
		Acetophenone	0-50	0.985	0.984
		Nitrobenzene	0-50	0.985	0.968
		m-Nitrotoluene	10-40	0.989	0.942
		Nitrobenzene	0-60	0.985	0.955
		2-Pentanone	0-30	0.978	0.988
Millipore Al-PBD	MeOH				
Unisphere Al-C ₁₈	MeCN	2-Hexanone	0-40	0.988	0.997
		<i>Styrene</i>	<i>20-70</i>	<i>0.989</i>	<i>0.990</i>
		<i>Isopropylbenzene</i>	<i>30-70</i>	<i>0.988</i>	<i>0.999</i>
		Butylbenzene	40-80	0.988	0.993
		<i>Pentylbenzene</i>	<i>40-80</i>	<i>0.987</i>	<i>0.992</i>
		2-Pentanone	0-40	0.985	0.981
		2-Octanone	30-70	0.980	0.979
		2-Pentanone	0-30	0.783	0.746
		2-Hexanone	0-40	0.942	0.890
		2-Heptanone	0-50	0.975	0.911
Unisphere Al-CN	MeCN	<i>Isopropylbenzene</i>	<i>30-80</i>	<i>0.987</i>	<i>0.998</i>
		<i>Propylbenzene</i>	<i>30-80</i>	<i>0.987</i>	<i>0.998</i>
		2-Pentanone	0-40	0.968	0.924
		2-Hexanone	0-60	0.985	0.955
		2-Heptanone	0-60	0.984	0.955
		Acetophenone	0-70	0.988	0.958
		Nitrobenzene	10-70	0.986	0.950
		2-Propanone	0-30	0.874	0.899
		2-Butanone	0-50	0.868	0.932
		2-Propanone	0-50	0.941	0.960
LiChrospher Si-C ₁₈	MeOH	2-Butanone	0-70	0.969	0.985

^a Italicized entries were used for solutes whose R^2 values increased using the $E_T(30)$ solvent polarity scale.

and Johnson [14] were determined at 25° C, the same temperature used in this study, except for the Al-CN stationary phase. Anyway, no correction for temperature is necessary for the equations recommended by Dorsey and Johnson [14] for the calculation of $E_T(30)$ polarity values for hydroorganic mixtures of MeCN and MeOH (Eqns. 3.3 and 3.4, respectively). Johnson *et al.* [13] even employed a temperature of 40° C for their retention measurements. Thus, the discrepancies in the two studies are most likely due to other factors, namely: to differences in the measurement of t_m , and to a slight extent, maybe due to differences in the quality of HPLC-grade solvents used (MeCN, MeOH and H₂O), and/or differences in the *actual* composition (*i.e.*, volume proportions of aqueous and organic solvents) delivered by the HPLC units employed. It is assumed that the differences in stationary phases used in these studies would not be a factor since as stated earlier, solvatochromic polarity measurements are carried out independently of the stationary phase [14].

It should be noted that of the 332 data sets studied by Johnson *et al.* [13], only 11 data sets were actually experimentally determined by the authors. The other retention values used were obtained from the literature [15-19]. A closer look at the regression results obtained from the latter study [13] reveals that although (in general) better linearity were obtained for plots of $\log k'$ vs. $E_T(30)$ polarity, there were instances wherein trends similar to those obtained in this study were observed for some data sets. This can clearly be seen in Table 3.19 for the retention data of Woodburn [18] for the MeOH/H₂O system (and to limited extent for the MeCN/H₂O system), and those of Jandera [19] for the MeCN/H₂O system. Results similar to those obtained in this study were even obtained by Johnson *et al.* [13] for the MeOH/H₂O system, although only 5 data sets were reported (Table 3.19). Thus, it appears that *to really determine whether or not an improvement in linearity is obtained from plots of $\log k'$ vs. $E_T(30)$ polarity compared to $\log k'$ vs. ϕ , the $E_T(30)$ polarity values to be employed should be*

TABLE 3.19. Frequency of cases where R^2 actually decreased for linear fits of $\log k'$ vs. ϕ to $\log k'$ vs. $E_T(30)$ polarity from published results of Johnson *et al.* [13].

MeCN/H ₂ O	MeOH/H ₂ O	Column	Source of retention data used
2 of 12	5 of 5	Ultrasphere ODS	Johnson <i>et al.</i> [13]
0 of 69	—	Hypersil ODS	Hanai and Hubert [15]
1 of 2	—	Ultrasphere ODS	Lipford [16]
0 of 46	—	Unisil Q C18	Hanai and Hubert [17]
30 of 85	52 of 62	Sepralyte C2, C4, C8, C18	Woodburn [18]
22 of 26	2 of 25	Silasorb C8	Jandera [19]

determined experimentally for the actual solutions delivered by the HPLC unit to be used for the retention measurements, using at least the same brand(s) of HPLC solvents, and preferably the same temperature for both measurements. This assumes that an accurate measure of t_m is to be performed at each mobile phase composition.

C. Comparison Of The S Values For The Different Columns

Although the quadratic relationship in Eqn. 3.1 best describes solute retention over a wide range of mobile phase composition, to a first approximation, it is reasonable to assume a linear relationship, particularly for those compounds in this study for which S has been measured for a sufficiently large number of mobile and stationary phase combinations (Tables 3.20-3.22) to permit broad conclusions. According to Schoenmakers [9], the most useful range for k' is within 1-10, and within this range the relationship between $\log k'$ vs. ϕ is quite adequately defined by a linear relationship. Assuming a linear relationship for the retention data in Tables 3.1A-3.6B is justified since for all solutes k' values were determined only over a limited range of mobile phase composition so as to avoid very small or very large retention factors which can lead to either insufficient resolution or long analysis time, respectively [9]. Very small k' values are also more susceptible to errors in t_m . Examples of linear plots of $\log k'$ vs. ϕ for different solutes for the various columns used in this study are shown in Fig. 3.6.

As stated earlier, semiquantitative comparisons of solvent strength can easily be achieved using Snyder's S value, determined experimentally as the negative of the slope from linear plots of $\log k'$ vs. ϕ . From the preceding discussion, it was concluded that better linearity was obtained from plots of $\log k'$ vs. ϕ compared to $E_T(30)$ polarity. Thus, S values from $\log k'$ vs. ϕ were used.

TABLE 3.20. Comparison of S values for Unisphere Al-PBD, Millipore Al-PBD and Microsorb Si-C₁₈.

Solute	<u>Unisphere Al-PBD</u>		<u>Millipore Al-PBD</u>		<u>Microsorb Si-C₁₈</u>	
	MeCN	MeOH	MeCN	MeOH	MeCN	MeOH
Toluene	3.13	3.06	3.44	2.94	2.81	3.54
Styrene	3.38	3.36	3.63	3.35	2.99	4.04
Ethylbenzene	3.54	3.53	3.63	3.49	3.03	4.23
Pentane	2.77	3.84	2.75	3.79	2.70	4.18
Hexane	2.96	4.34	2.92	4.34	2.95	4.78
Heptane	3.13	4.77	3.07	4.82	3.16	5.20
Average ± S.D.	3.15 ± 0.28	3.82 ± 0.64	3.24 ± 0.38	3.79 ± 0.69	2.94 ± 0.16	4.33 ± 0.58

TABLE 3.21. Comparison of S values for Unisphere Al-C₁₈, Unisphere Al-CN and LiChrospher Si-C₁₈.

Solute	<u>Unisphere Al-C₁₈</u>		<u>Unisphere Al-CN</u>		<u>LiChrospher Si-C₁₈</u>	
	MeCN	MeOH	MeCN	MeOH	MeCN	MeOH
2-Heptanone	3.12	2.67	—	—	2.67	3.43
2-Octanone	—	—	3.52	2.92	2.76	3.92
2-Nonanone	3.84	3.92	3.93	3.63	2.77	4.31
Acetophenone	3.32	2.59	—	—	2.75	3.09
Propiophenone	3.60	2.98	3.25	2.50	2.89	3.36
Butyrophenone	3.69	3.56	3.75	3.13	2.87	3.75
Valerophenone	3.91	3.92	3.73	3.67	2.99	4.05
Nitrobenzene	3.17	2.31	—	—	2.92	3.04
m-Nitrotoluene	3.60	3.10	3.47	2.86	3.19	3.49
Toluene	3.28	3.13	3.29	2.92	2.83	3.64
Styrene	—	—	3.40	3.30	3.01	3.72
Ethylbenzene	3.50	3.59	3.56	3.47	2.96	4.12
Propylbenzene	3.32	4.14	—	—	3.07	4.57
Butylbenzene	—	—	3.72	4.51	3.24	4.98
Hexylbenzene	—	—	3.62	5.23	3.73	6.04
Average ± S.D.	3.49 ± 0.27	3.26 ± 0.61	3.57 ± 0.21	3.47 ± 0.79	2.98 ± 0.26	3.97 ± 0.78

TABLE 3.22. Comparison of S values for all alumina-based and silica-based columns.

Solute	<u>Unisphere Al-PBD</u>		<u>Millipore Al-PBD</u>		<u>Microsorb Si-C₁₈</u>		<u>Unisphere Al-C₁₈</u>		<u>Unisphere Al-CN</u>		<u>LiChrospher Si-C₁₈</u>	
	MeCN	MeOH	MeCN	MeOH	MeCN	MeOH	MeCN	MeOH	MeCN	MeOH	MeCN	MeOH
Toluene	3.13	3.06	3.44	2.94	2.81	3.54	3.28	3.13	3.29	2.92	2.83	3.64
Styrene	3.38	3.36	3.63	3.35	2.99	4.04	3.61	3.55	3.40	3.30	3.01	3.72
Ethylbenzene	3.54	3.53	3.63	3.49	3.03	4.23	3.50	3.59	3.56	3.47	2.96	4.12
Average	3.35	3.32	3.57	3.26	2.94	3.94	3.46	3.42	3.42	3.23	2.93	3.83

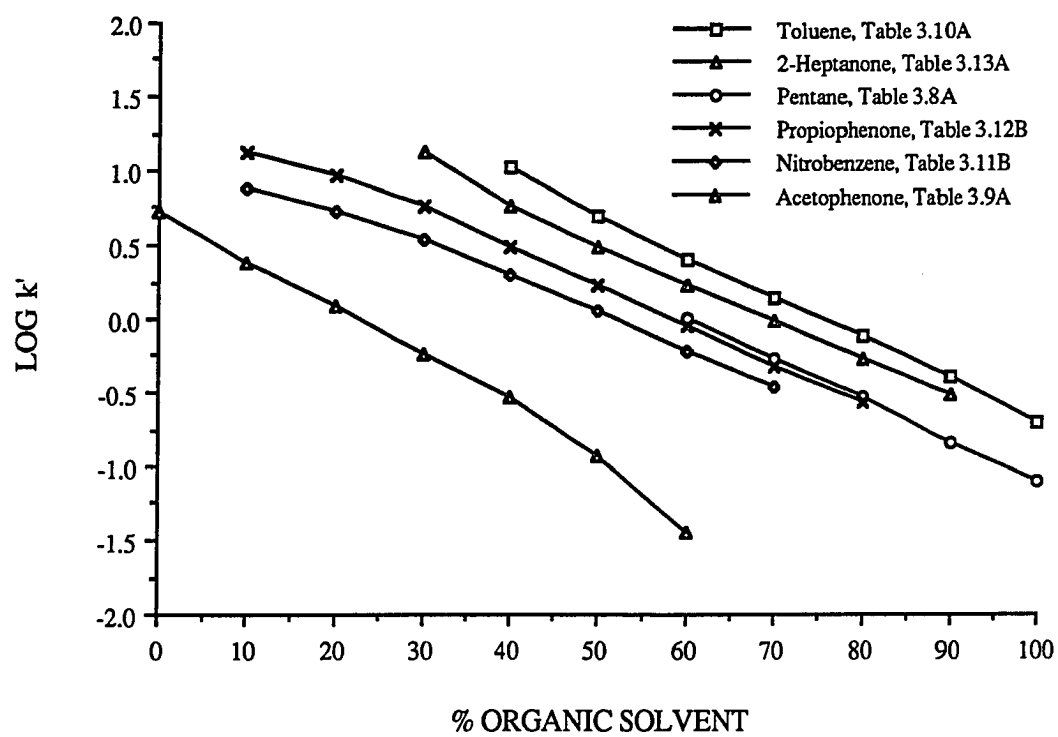


FIGURE 3.6. Examples of solutes that exhibit an approximately linear relationship for $\log k'$ vs. ϕ for the various stationary phases.

Limitations Of Using The S Value As A Measure Of Solvent Strength

It has been shown by different authors that the value of S systematically varies according to the retention behavior of the solute used to measure S [4, 20]. For MeOH/H₂O, S apparently increases with increasing solute retention. So as to get a good measure of S, only values from plots with linear correlation coefficients (R^2) ≥ 0.990 were considered.

The S values for the different alumina- and silica-based columns in Tables 3.8A-3.13B show that for the same column and organic solvent, the value of S generally increases with increasing solute molecular weight, or more specifically with increasing solute retention, for both MeCN/H₂O and MeOH/H₂O. This is easily observed for members of a homologous series. For example, for the Al-C₁₈ column with MeOH/H₂O as mobile phase (Table 3.11B), the value of S increased from 3.13 to 5.19 from toluene to pentylbenzene. With MeCN/H₂O, a good example is given in Table 3.13A for the LiChrospher Si-C₁₈ column, wherein S increases from 2.83 for toluene to 4.38 for octylbenzene. This suggests that *S should be used only for the comparison of organic solvent strength for the same solute.*

It is also seen that for the same solute and column, it is not always true that the S value for the weaker solvent is always less than that for the stronger solvent. Tables 3.1A-3.6B clearly show that for the same solute, column and % organic modifier, solute retention was always greater for the MeOH/H₂O system compared to the MeCN/H₂O system for both alumina-based and Si-C₁₈ columns. Thus, MeOH is a weaker solvent compared to MeCN for all the columns used. However, this trend was not always reflected in the values of S reported in Tables 3.8A-3.13B. Examples of this inconsistency, however, can be more easily seen in Tables 3.20-3.23, which list the values of S that were actually used in comparing the solvent strength of MeCN and MeOH for the various columns. For example, in Table 3.20, the S values for the n-

alkanes were all greater for MeOH than MeCN for all three columns. On the other hand, for toluene, styrene and ethylbenzene, S for MeOH was greater than that for MeCN only for the Si-C₁₈ column. A similar trend has also been reported in the literature [5] where the authors calculated the S values for MeCN and MeOH for a silica-based C₁₈ stationary phase from reference [8] and reported S values for MeCN and MeOH as 2.9 and 3.5, respectively. Therefore, *one should be cautious in determining solvent strength based on the S value alone for different organic modifiers even if the same test solute and column are used.*

Another difficulty involved in predicting solvent strength based on the S value is that it also *depends on the range of % organic solvent considered.* This is illustrated in Fig. 3.7 for the Unisphere Al-PBD column. It should be noted that the values of S employed for Fig. 3.7 for the different solutes were recalculated so as to correspond to the % organic solvent range indicated. As can be seen, if S is measured between 0 and 30% organic solvent, the S value of MeOH is less than that of MeCN, between 40 and 70% organic solvent, the S values of MeOH and MeCN are approximately equal, and between 60 and 100% organic solvent, the S value of MeCN is less than that of MeOH.

Despite the limitations of predicting solvent strength using the S value, *comparisons of S for the same solute, organic solvent and preferably similar % range of organic solvent for different columns appear to be reasonable.* As can be seen in Table 3.20, the S values for both types of PBD-coated alumina columns are almost equal except for a slight difference observed for toluene, ethylbenzene and styrene for the MeCN/H₂O solvent system. The significance of this slight difference will be discussed later. Thus, this strategy was used in analyzing the solvent strength difference between MeCN and MeOH among the various alumina- and silica-based columns, and to satisfy these requirements, and additionally that $R^2 \geq 0.990$, only the S values for the solutes given in Tables 3.20-3.23 were considered.

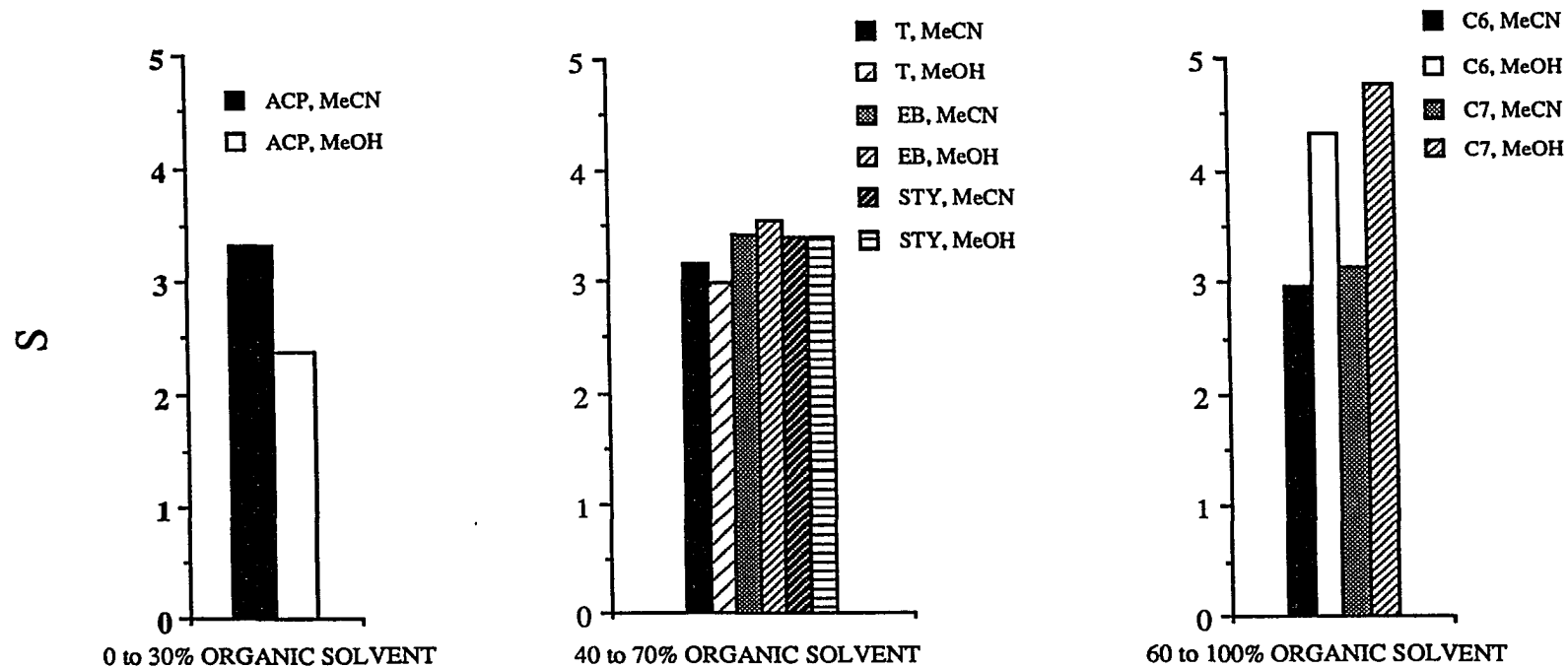


FIGURE 3.7. Dependence of S (Eqn. 3.2) on the mobile phase composition range over which it is measured for the Unisphere Al-PBD column. Solute identification: ACP, acetophenone; T, toluene; EB, ethylbenzene; STY, styrene; C6, hexane; C7, heptane.

**D. Comparison Of The Difference In Solvent Strength Between MeCN
And MeOH For The Polymer-Coated Aluminas And Si-C₁₈ Columns
Using The S Value**

1. Unisphere And Millipore Al-PBD vs. Microsorb Si-C₁₈

Based on the assumption that solute retention proceeds via displacement from the stationary phase surface of adsorbed solvent species upon adsorption of the solute, it has been proposed that solute retention can be described by the equation [21]

$$k' = \frac{I}{[D_O]^z} \quad (3.5)$$

where k' is the solute retention factor, I is a constant which is a function of the partition coefficient, the phase ratio and the adsorbed organic displacing agent, $[D_O]$ is the concentration of the organic solvent in the mobile phase, and z is the number of solvent molecules displaced. Writing Eqn. 3.5 in logarithmic form, it can be seen that Eqn. 3.6

$$\log k' = \log I - z \log [D_O] \quad (3.6)$$

is very similar to Eqn. 3.2, differing only in how the coefficients are interpreted.

The polymer-coated alumina surface can be visualized as consisting of porous alumina coated with the polymer. Assuming that complete coverage of the porous surface is achieved during the coating process, it is reasonable to assume that solute retention will occur predominantly via solute adsorption for the Al-PBD stationary phase, and that for solute adsorption to occur, the solute molecule should be able to displace the solvent species adsorbed on the stationary phase surface. Thus, either Eqn. 3.2 or 3.6 can be used to describe solute retention for the Al-PBD columns. In the discussion that follows, the negative of the slope obtained from linear plots of $\log k'$ vs. ϕ will be designated by S (Eqn. 3.2), which is numerically equal to z in Eqn. 3.6. The

S values to be used for comparing the solvent strengths of MeCN and MeOH for the Unisphere and Millipore Al-PBD columns to that of the Microsorb Si-C₁₈ column are listed in Table 3.20. Values of S for the LiChrospher Si-C₁₈ stationary phase were not employed in this part of the study since (the S values for) only 3 data sets (toluene, styrene and ethylbenzene) can be used for this column.

For the MeOH/H₂O solvent system in Table 3.20, we can see that for the same solute the values of S are approximately equal for both brands of Al-PBD columns. Thus, the average S values for MeOH are 3.82 and 3.79 for the Unisphere and Millipore columns, respectively. The S values for MeOH are, however, always smaller for the Al-PBD columns compared to the Si-C₁₈ column. This trend suggests that the solvent strength of MeOH for the two types of PBD-coated alumina columns is approximately equal, and that *the solvent strength of MeOH is weaker for the Al-PBD columns than that for the Si-C₁₈ column (i.e., for an equal change in % MeOH, solute retention is affected to a greater extent for the silica-based C₁₈ stationary phase)*. It should be noted that the weaker solvent strength of MeOH for the PBD-coated alumina columns does not imply that solute retention is expected to be greater for these columns than for the Si-C₁₈ column (Tables 3.1, 3.2 and 3.5 clearly show that this is not the case) since their column strengths are not equal. The Si-C₁₈ phase is a stronger column (more retentive) than either Al-PBD stationary phases in RPLC. Similarly, the smaller S value for the Al-PBD columns also suggests that for solute retention to occur, more of the MeOH solvent species adsorbed on the Si-C₁₈ stationary phase must be displaced compared to the number of adsorbed solvent species that must be displaced from the PBD-coated alumina stationary phase. Thus, the weaker solvent strength of MeOH observed for the Al-PBD stationary phase implies that *the solvent species in the MeOH/H₂O solvent system have a lesser affinity for the Al-PBD stationary phase than the Si-C₁₈ stationary phase*.

For the MeCN/H₂O solvent system in Table 3.20, we can see that for the same non-UV absorbing compound (n-alkanes), the values of S are approximately equal for both PBD-coated alumina and Si-C₁₈ stationary phases. This suggests that the solvent strength of MeCN is approximately equal for both types of stationary phases. For UV-absorbing compounds, the values of S are greater for the Al-PBD phase than the Si-C₁₈ phase, suggesting that *MeCN is a stronger solvent for the Al-PBD columns*, or that for solute retention to occur, more adsorbed solvent species in the MeCN/H₂O solvent system must be displaced from the PBD-coated alumina surface compared to the number of adsorbed solvent species that must be displaced from the silica-based stationary phase. The stronger solvent strength of MeCN for the Al-PBD surface implies that *the solvent species in the MeCN/H₂O solvent system have a greater affinity for the PBD-coated alumina stationary phase than the Si-C₁₈ stationary phase*. It is hypothesized that the greater affinity of MeCN for the PBD surface is due primarily to the presence of residual C=C bonds (from the incomplete crosslinking of polybutadienes [22, 23]) on the Al-PBD surface, which will interact more with the π electrons of MeCN via π - π interaction. (This phenomenon is very similar to that observed for PS-DVB in RPLC [24].) According to Kevin Holland of Biotage [22], only about 30-35% of the PBD unsaturation is actually used in the crosslinking process for the synthesis of the Unisphere Al-PBD stationary phase employed in the study.

The results obtained for the non-UV absorbing compounds contradict the results obtained for the UV absorbing compounds for the MeCN/H₂O solvent system. A possible explanation for this discrepancy is that upon solute adsorption on the stationary phase surface, the UV absorbing compounds (which all possess one benzene ring) occupies a larger surface area compared to the non-UV absorbing compounds (all n-alkanes, C₅ to C₇). The stationary phase surface area interacting with the n-alkanes is small enough that even though more MeCN molecules are adsorbed on the stationary

phase surface of the PBD-coated alumina, an approximately equal number of adsorbed MeCN molecules are being displaced from the Al-PBD and Si-C₁₈ surface upon solute adsorption. Therefore, the correct conclusion is that MeCN is really a stronger solvent for the Al-PBD stationary phase compared to the Si-C₁₈ stationary phase. The use of bulkier molecules (*e.g.*, polyaromatic hydrocarbons and longer chain n-alkanes) is expected to magnify the difference in solvent strength for MeCN between these two materials.

As stated earlier in the text, the S values for toluene, ethylbenzene and styrene are slightly greater for the Millipore than the Unisphere Al-PBD columns for the MeCN/H₂O solvent system. For example, for toluene the S values are 3.44 and 3.13 for the Millipore and Unisphere columns, respectively (Table 3.20). This implies that the solvent strength of MeCN is greater for the Millipore column than it is for the Unisphere column. Hence, based on the proposed displacement mechanism for solute retention for the PBD-coated alumina columns, more residual C=C bonds are expected to be present in the PBD surface of the Millipore column.

It should be noted that the analysis of the solvent strength difference between MeCN and MeOH for the two Al-PBD and Si-C₁₈ columns would have been easier if the average S values indicated in Table 3.20 were used. However, discrepancies for the UV and non-UV absorbing compounds for the MeCN/H₂O solvent system would not have been reflected in these values.

2. *Unisphere Al-C₁₈ And Unisphere Al-CN vs. LiChrospher Si-C₁₈*

The S values to be used for comparing the solvent strengths of MeCN and MeOH for the Unisphere Al-C₁₈ and Al-CN columns to that of the LiChrospher Si-C₁₈ column are listed in Table 3.21. As can be seen, trends similar to that for the Al-PBD and Microsorb Si-C₁₈ were obtained. That is, *MeCN is a stronger solvent for both Al-C₁₈ and Al-CN stationary phases compared to the Si-C₁₈ phase*, and conversely, that *MeOH*

is a weaker solvent for both Al-C₁₈ and Al-CN stationary phases compared to the Si-C₁₈ phase. For the MeCN/H₂O system, this trend is evident from the larger average S values for both Al-C₁₈ and Al-CN, 3.49 and 3.57, respectively, relative to an S value of 2.98 for the Si-C₁₈ column. On the other hand, for the MeOH/H₂O system, the average S values for Al-C₁₈ and Al-CN, 3.26 and 3.47, respectively, are both smaller than the corresponding values for the LiChrospher Si-C₁₈ column, 3.97. It should be noted that the use of the average value of S from Tables 3.21 and 3.22 is justified, since no retention data were measured for the n-alkanes (C₅-C₇) for these phases.

Similar to the conclusions drawn for the Al-PBD columns, the weaker solvent strength of MeOH for the Al-C₁₈ and Al-CN stationary phases implies that the solvent species in the MeOH/H₂O solvent system have a lesser affinity for the Al-C₁₈ and Al-CN phases than the Si-C₁₈ phase. Similarly, the stronger solvent strength of MeCN for the Al-C₁₈ and Al-CN stationary phases implies that the solvent species in the MeCN/H₂O solvent system have a greater affinity for these stationary phases than the Si-C₁₈ phase. It is also hypothesized that the greater affinity of MeCN for either Al-C₁₈ or Al-CN surface is due primarily to the presence of residual C=C bonds on both materials, which will interact more with the π electrons of MeCN. However, these residual C=C bonds can arise from either incomplete crosslinking of the respective polymer coating, or from incomplete derivatization of the C=C bonds (present in the "starting" polybutadienes used for the synthesis of either 2-octadecyl-1,3-butadiene or the cyano copolymer) with the reagent necessary to provide either the -C₁₈ or -CN functionality. For the Al-CN column, additional π electrons are present in the -CN group, which could possibly explain why the average S value for the MeCN/H₂O system is larger for the Al-CN phase compare to the Al-C₁₈ phase (3.57 and 3.49, respectively).

Comparison of the average S values for all polymer-coated aluminas (including Al-PBD) and Si-C₁₈ columns can be seen in Table 3.22. As can be seen, similar average S values were obtained for both Microsorb and LiChrospher Si-C₁₈ columns (2.94 and 2.93 for MeCN/H₂O and 3.94 and 3.83 for MeOH/H₂O, respectively). More importantly, however, is that in all cases the average S values for all polymer-coated aluminas were larger with MeCN/H₂O and smaller for MeOH/H₂O compared to similar values for either Microsorb or LiChrospher Si-C₁₈. Additionally, the average S values for MeCN for the polymer-coated aluminas were all larger than that for MeOH, consistent with the expected trend. However, an inverse relationship for both Si-C₁₈ columns was observed, at least for toluene, styrene and ethylbenzene. No explanation is provided for these trends, except that it could be a manifestation of the greater solvent strength difference between MeCN and MeOH for the polymer-coated aluminas.

E. Comparison Of The Solvent Strengths Of MeCN And MeOH Using ϵ

The combination of the two observations discussed earlier, that (i) MeCN is a stronger solvent on the polymer-coated aluminas than on the Si-C₁₈ columns, and conversely that (ii) MeOH is a weaker solvent on the polymer-coated aluminas than on the Si-C₁₈ columns, implies that *the difference in solvent strength between MeCN and MeOH will be much greater on the polymer-coated alumina columns than on the Si-C₁₈ columns*. In this study, a parameter designated as ϵ is defined so as to be able to determine how the difference in solvent strength between MeCN and MeOH varies with mobile phase composition. The parameter ϵ is defined for a given column as the ratio of retention factors for a solute in MeOH/H₂O and MeCN/H₂O at the same temperature and volume fraction of organic modifier (Eqn. 3.7). For any given temperature and

$$\epsilon = \frac{k'_{\text{MeOH/H}_2\text{O}}}{k'_{\text{MeCN/H}_2\text{O}}} \quad (3.7)$$

volume fraction of organic solvent, ϵ is always greater than 1 as MeCN is a stronger solvent than MeOH. Obviously, the larger the value of ϵ , the greater is the difference in solvent strength between MeCN and MeOH. For quantitative purposes, it is also useful to employ the logarithm of ϵ .

There are three important characteristics of ϵ . First, as it is based on the ratio of k' values, it is a valid thermodynamic measure of differences in solvent strength. Second, ϵ is also independent of the phase ratio of the column. Finally, $\log \epsilon$ is directly proportional to the difference in the free energies of transfer of a given solute for the two different mobile phases:

$$\log \epsilon = \Delta\Delta G = \Delta G_{\text{tr}} (\text{MeCN/H}_2\text{O}) - \Delta G_{\text{tr}} (\text{MeOH/H}_2\text{O}) \quad (3.8)$$

A recent study by Arenas and Foley [25] has shown that ϵ does indeed reflect the difference in solvent strength between MeCN and MeOH. Using selected values from the retention data in Tables 3.1A-3.2B, 3.5A, and 3.5B, it was shown that the values of ϵ for the Al-PBD columns were always larger than those for the Si-C₁₈ column, confirming the greater difference in solvent strength between MeCN and MeOH as determined earlier using Snyder's S value for the Al-PBD stationary phase. For example, the values of ϵ for toluene using a hydroorganic mobile phase containing 50% organic solvent are 4.05, 4.64 and 2.80 for the Unisphere Al-PBD, Millipore Al-PBD and Si-C₁₈ columns, respectively. Between the two types of PBD-coated alumina columns, the difference in solvent strength between MeCN and MeOH was greater for the Millipore column. This is further evidence of the presence of more residual C=C bonds on the Millipore Al-PBD surface.

Relationship Between Log ϵ And Volume Fraction Of Organic Solvent

Instead of just comparing numerical values (or magnitudes) of ϵ for a specific solute at a given % organic solvent, a more important use of ϵ is that it can illustrate how the difference in solvent strength between MeCN and MeOH varies with mobile phase composition. This can be seen from plots of log ϵ vs. % organic solvent for different solutes as illustrated in Figs. 3.8-3.11 for the various polymer-coated aluminas, and in Figs. 3.12-3.14 for three Si-C₁₈ columns.

From Figs. 3.8-3.11, one can clearly see that for all polymer-coated alumina columns, log ϵ increases steadily from pure water (*i.e.*, 0% organic solvent) to ca. 40-50% organic solvent, reaches a plateau between ca. 50 and 70% organic solvent, and then decreases with higher percentages of organic solvent. Hence, the difference in solvent strength between MeCN and MeOH is largest at ca. 50-70% organic modifier for the alumina-based columns.

The relationship between log ϵ and mobile phase composition for the polymer-coated alumina columns can be very well explained by the relative proportions of solvent species actually present in solution for the so-called "binary" MeOH/H₂O and MeCN/H₂O mobile phases. According to Katz and co-workers [26, 27], the supposedly "binary" MeOH/H₂O solvent mixture is in fact "ternary" in nature, consisting of free MeOH, free H₂O and associated MeOH·H₂O. Between 0 and 40% MeOH, the mixture consists primarily of free H₂O and associated MeOH·H₂O with very little free MeOH. Between 40 and 80% MeOH, the MeOH/H₂O mixture is substantially "ternary" in nature, consisting of significant amounts of all three species: free H₂O, associated MeOH·H₂O and free MeOH, with the associated MeOH·H₂O species accounting for ca. 45-60% of the total. Finally, between 80 and 100% MeOH, the MeOH/H₂O mixture consists primarily of free MeOH and associated MeOH·H₂O.

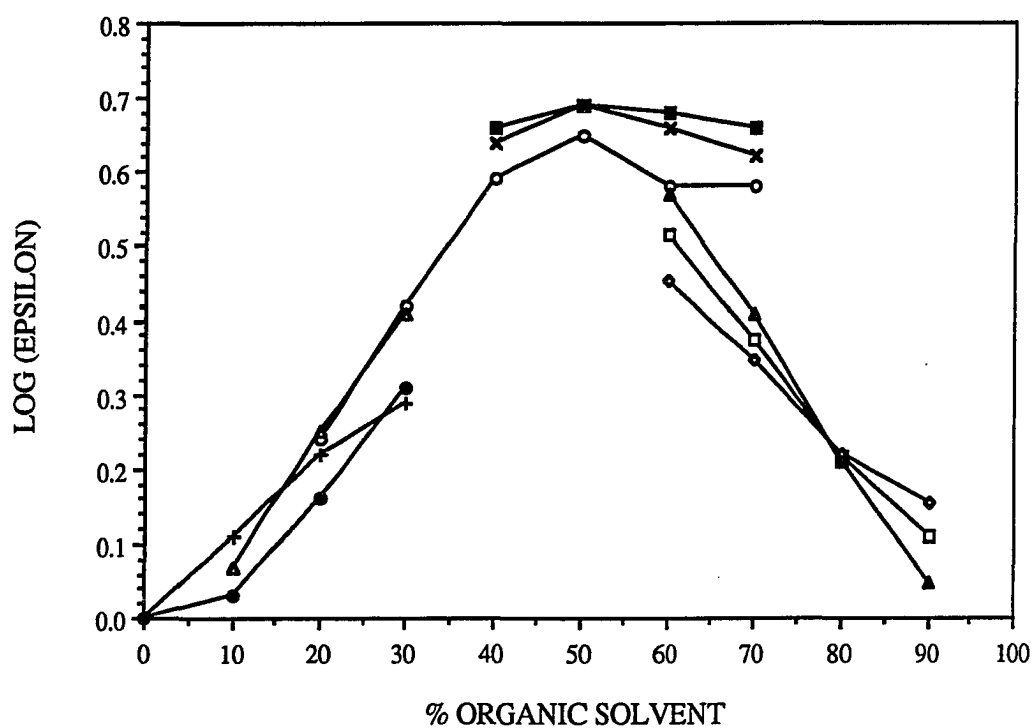


FIGURE 3.8. Difference in solvent strength between MeCN and MeOH as a function of mobile phase composition for the Unisphere A1-PBD column.

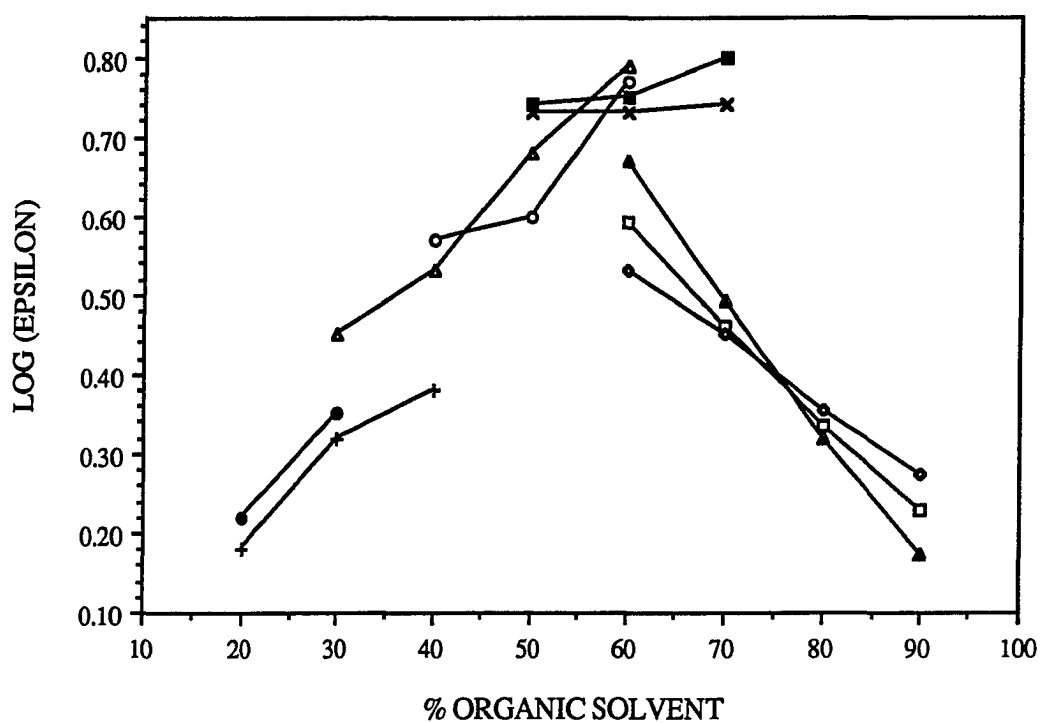


FIGURE 3.9. Difference in solvent strength between MeCN and MeOH as a function of mobile phase composition for the Millipore Al-PBD column.

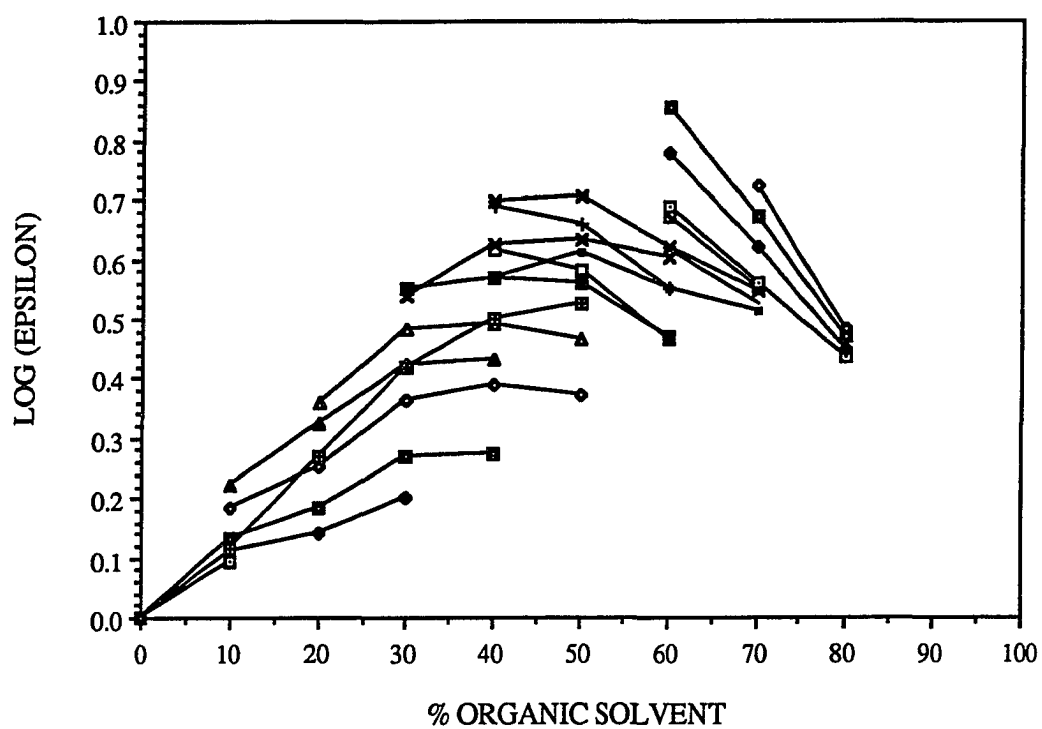


FIGURE 3.10. Difference in solvent strength between MeCN and MeOH as a function of mobile phase composition for the Unisphere Al-C₁₈ column.

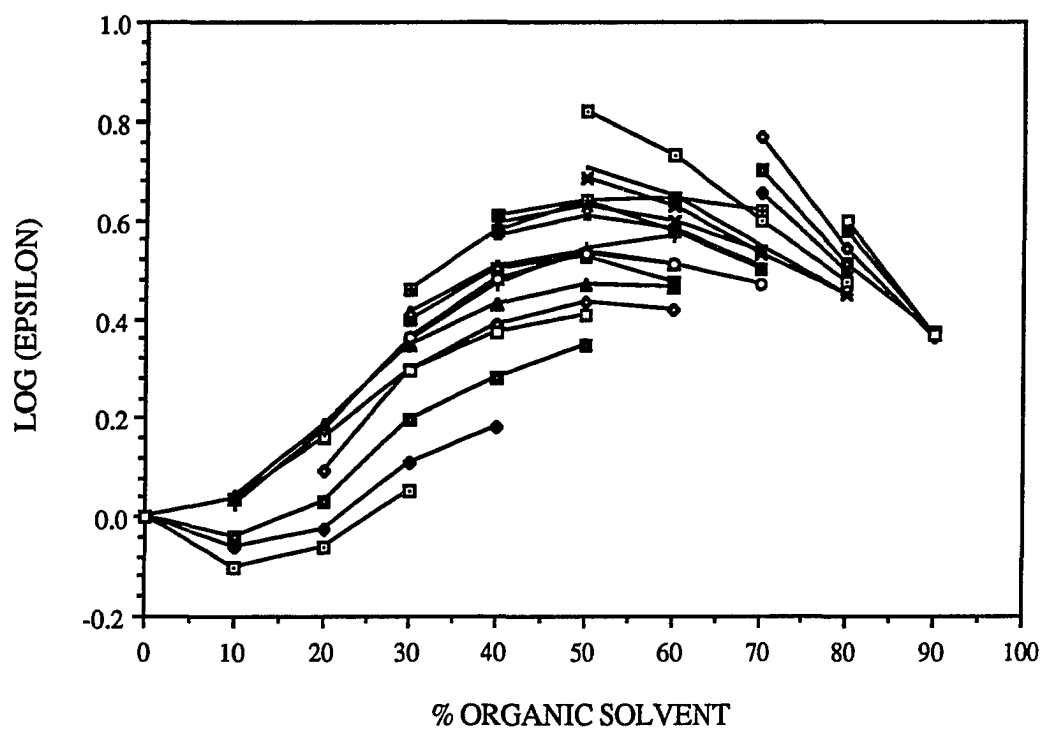


FIGURE 3.11. Difference in solvent strength between MeCN and MeOH as a function of mobile phase composition for the Unisphere Al-CN column.

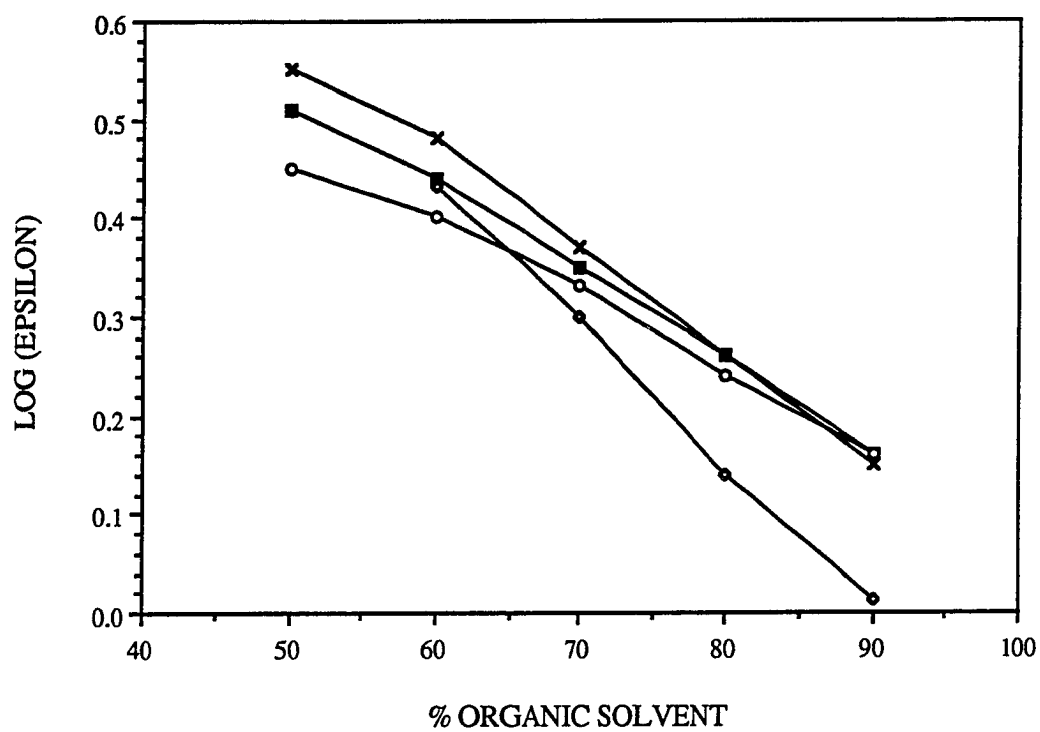


FIGURE 3.12. Difference in solvent strength between MeCN and MeOH as a function of mobile phase composition for the Microsorb Si-C₁₈ column.

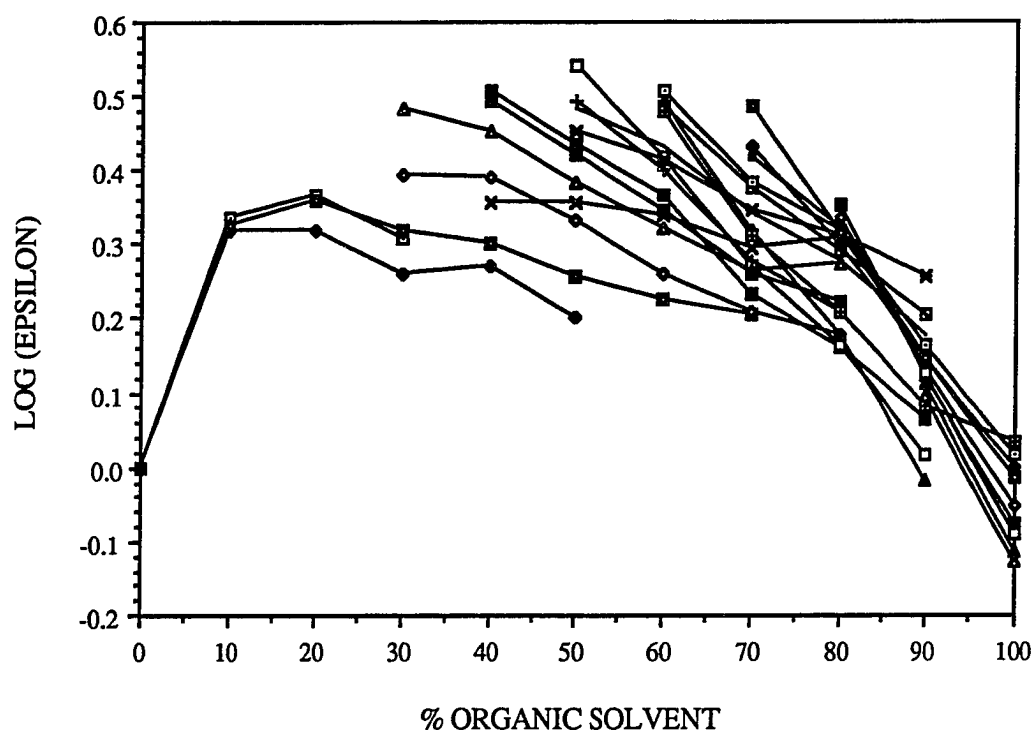


FIGURE 3.13. Difference in solvent strength between MeCN and MeOH as a function of mobile phase composition for the LiChrospher Si-C₁₈ column.

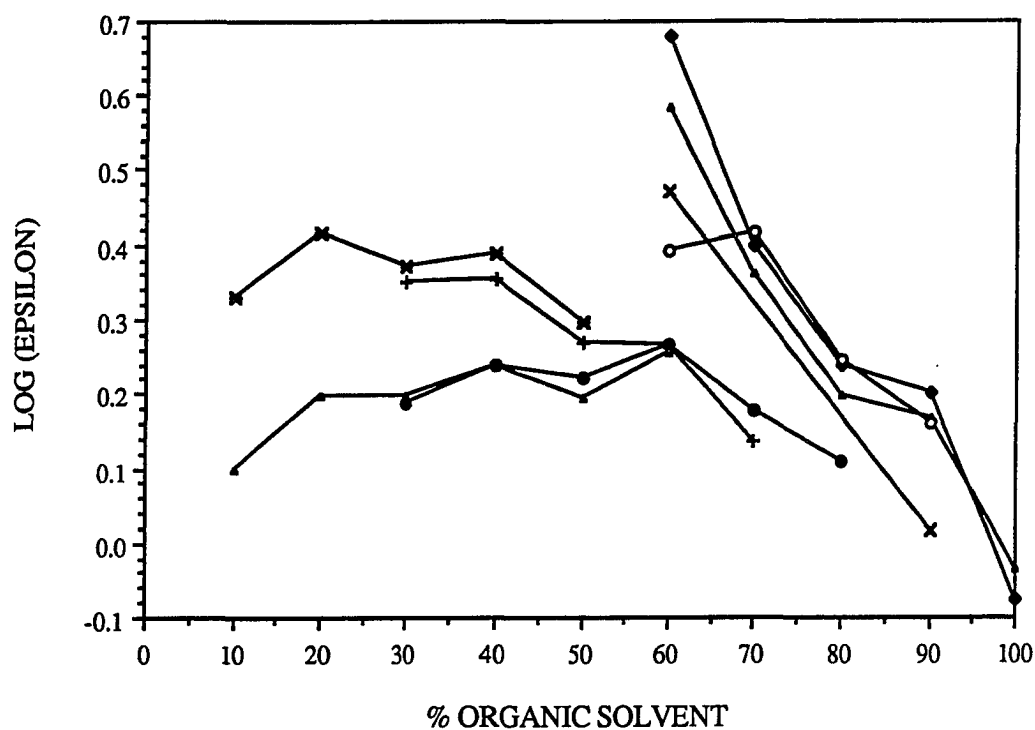


FIGURE 3.14. Difference in solvent strength between MeCN and MeOH as a function of mobile phase composition for the Nucleosil 10-RP18 (silica-based) column. Data obtained from Schoenmakers *et al.* [1].

A similar association of MeCN and H₂O was also observed by Katz *et al.* [26], but to a much lesser extent. For the MeCN-H₂O solvent mixture, the associated MeCN·H₂O species accounts for at most only 5% of the total fractional volume of the mixture. The MeCN/H₂O solvent system is therefore essentially binary in nature, with the volume fraction of free MeCN and free H₂O increasing and decreasing linearly, respectively, as the nominal volume fraction of MeCN increases.

The solvent strengths of the different species present in the MeOH/H₂O and MeCN/H₂O solvent systems can be ranked as follows: H₂O < associated MeOH·H₂O < MeOH < MeCN. Hence, the interaction between the solute and free organic solvent (either free MeCN or free MeOH) is much greater than that between the solute and free H₂O or associated MeOH·H₂O.

For the MeOH/H₂O system, it has been shown that for solutes distributed largely in the aqueous phase, solute elution is controlled almost exclusively by the concentration of the free MeOH [27]. Unfortunately, no similar report has been published for the MeCN/H₂O solvent system. It is believed, however, that the stronger interactions between polar solvent molecules compared to the weaker interactions of solvent or solute molecules with the nonpolar stationary phase is the driving force for solute retention in RPLC. Thus, solute retention occurs because the less polar solute molecule is effectively "squeezed out" of the mobile phase by the free energy advantage of increased solvent-solvent interaction [28]. Assuming solute retention to be controlled predominantly by the volume fraction of free MeCN and free MeOH for both MeCN/H₂O and MeOH/H₂O, it is then expected that the difference in solvent strength between MeCN and MeOH ($\log \epsilon$) will follow the difference in the concentrations of free MeCN and free MeOH (at the same mobile phase composition). Using the data of Katz *et al.* [26], the concentrations of free MeCN and free MeOH at various mobile phase compositions are illustrated in Fig. 3.15. As shown, the proportion of free

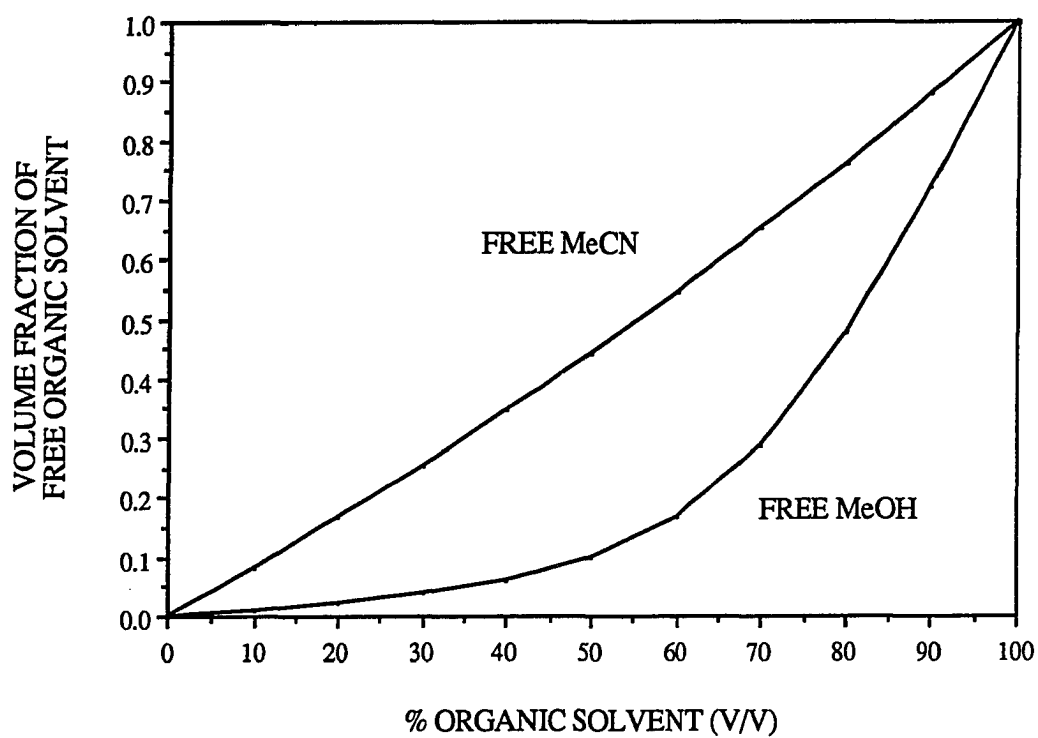


FIGURE 3.15. Relative proportion of free MeCN and free MeOH as a function of mobile phase composition. Data obtained from Katz *et al.* [25].

MeCN increases almost linearly over the entire range of mobile phase composition whereas that of free MeOH rises slowly but linearly at first, then faster in an exponential fashion from 40% to 70% organic solvent, and finally increases very quickly and linearly beginning at about 75% organic solvent. Hence the difference in concentration of free MeCN and free MeOH is largest between 50 and 70% organic solvent, which coincides almost exactly with the range (in Figs. 3.8-3.11) where the largest difference in solvent strength between MeCN and MeOH for the various polymer-coated alumina columns were observed.

Figures 3.12 to 3.14 show the dependence of $\log \epsilon$ on mobile phase composition for three silica-based C_{18} columns. Figures 3.12 and 3.13 are for the Microsorb and LiChrospher Si- C_{18} columns, respectively. The data in Fig. 3.14, which is for a Nucleosil 10 RP-18 stationary phase, were obtained from the work of Schoenmakers *et al.* [1].

From Fig. 3.12, it is seen that the largest difference in solvent strength between MeCN and MeOH is at 0.45-0.55 $\log \epsilon$ units and occurs at ca. 50% organic modifier. The trend appears to be similar to that observed for the various polymer-coated aluminas, although not as dramatic (smaller $\log \epsilon$). Unfortunately, no retention data were collected at less than 50% organic modifier for the Microsorb Si- C_{18} column.

Figures 3.13 and 3.14 show that for the LiChrospher and Nucleosil Si- C_{18} stationary phases, the observed trends, if any, are different from the clear trends observed for the polymer-coated aluminas in Figs. 3.8-3.11 and to a lesser extent for the Microsorb Si- C_{18} column in Fig. 3.12. $\log \epsilon$ for the different solutes in Figs. 3.13 and 3.14 decreases from 70-100% organic solvent, similar to the trend observed for similar solutes in the same mobile phase range in Figs. 3.8-3.11 for the polymer-coated aluminas and in Fig. 3.12 for the other Si- C_{18} column. However, $\log \epsilon$ values for the other solutes in Figs. 3.13 and 3.14 do not show a common, clear maximum value

between 10 and 80% organic solvent. It is hypothesized that the smaller systematic trend (or lack of a trend) for the Si-C₁₈ columns in Figs. 3.12-3.14 is due in part to the smaller difference in solvent strength between MeCN and MeOH for these columns compared with the polymer-coated alumina columns.

CONCLUSIONS

The larger difference in solvent strength between MeCN and MeOH on the polymer-coated aluminas implies that a wider polarity range of solutes can be eluted on these columns than on the Si-C₁₈ stationary phases. This could be done using a two-stage gradient consisting of water to MeOH in the first stage, and MeOH to MeCN in the second stage. Such a gradient represents a significantly larger change in mobile phase strength for the polymer-coated aluminas than for the Si-C₁₈ columns, on which MeCN and MeOH have been shown to be of very similar solvent strength. Note that the dramatic change in mobile phase strength during this two-stage gradient is further amplified, because, as discussed earlier, the difference in solvent strength between MeCN and MeOH will be particularly large for large molecules that would be expected to elute during the final stage.

REFERENCES FOR CHAPTER III

1. Schoenmakers, P.J.; Billiet, H.A.H.; de Galan, L. *J. Chromatogr.* **1981**, *218*, 261-284.
2. Schoenmakers, P.J.; Billiet, H.A.H.; Tijssen, R.; de Galan, L. *J. Chromatogr.* **1978**, *149*, 519-537.
3. Schoenmakers, P.J.; Billiet, H.A.H.; de Galan, L. *J. Chromatogr.* **1979**, *185*, 179-195.
4. Schoenmakers, P.J.; Billiet, H.A.H.; de Galan, L. *J. Chromatogr.* **1983**, *282*, 107-121.
5. Snyder, L.R.; Dolan, J.W.; Gant, J.R. *J. Chromatogr.* **1979**, *165*, 3-30.
6. Berendsen, G.E.; de Galan, L. *J. Chromatogr.* **1980**, *196*, 21-37.
7. Werkhoven-Goewie, C.E.; Brinkman, U.A.Th.; Frei, R.W. *Anal. Chem.* **1981**, *53*, 2072-2080.
8. Dolan, J.W.; Gant, J.R.; Snyder, L.R. *J. Chromatogr.* **1979**, *165*, 31-58.
9. Schoenmakers, P.J. *Optimization of Chromatographic Selectivity - A Guide to Method Development*; Elsevier Science Publishers B.V.: The Netherlands, 1986; Chapter 3.
10. Ahuja, S. *Selectivity and Detectability Optimizations in HPLC*; John Wiley & Sons, Inc.: New York, 1989; Chapter 6.
11. Karger, B.L.; Gant, J.R.; Hartkopf, A.; Weiner, P.H. *J. Chromatogr.* **1976**, *128*, 65-78.
12. Abbott, S.R.; Berg, J.R.; Achener, P.; Stevenson, R.L. *J. Chromatogr.* **1976**, *126*, 421-437.
13. Johnson, B.P.; Khaledi, M.G.; Dorsey, J.G. *Anal. Chem.* **1986**, *58*, 2354-2365.
14. Dorsey, J.G.; Johnson, B.P. *J. Liquid Chromatogr.* **1987**, *10*, 2695-2706.
15. Hanai, T.; Hubert, J. *J. High Res. Chromatogr., Chromatogr. Commun.* **1983**, *6*, 20-26.
16. Lipford, L.C. M.S. Thesis, University of Florida, 1985.
17. Hanai, T.; Hubert, J. *J. Liquid Chromatogr.* **1985**, *8*, 2463-2473.
18. Woodburn, K.B. Doctoral Thesis, University of Florida, 1985.
19. Jandera, P. *Chromatographia* **1985**, *19*, 101-112.

20. Hafkenscheid, T.L.; Tomlinson, E. *J. Chromatogr.* **1983**, *264*, 47-62.
21. Geng, X.; Regnier, F.E. *J. Chromatogr.* **1985**, *332*, 147-168.
22. Holland, K.B., Biotage, Inc., personal communication by R.V. Arenas and J.P. Foley.
23. Hamilton, R.A., Millipore, Inc., personal communication by J.P. Foley.
24. Tanaka, N.; Araki, M. In *Advances in Chromatography - Selectivity and Retention in Chromatography*; Giddings, J.C.; Grushka, E.; Brown, P.R., Eds.; Marcel Dekker, Inc.: New York, 1989; Vol. 30, Chapter 2.
25. Arenas, R.V.; Foley, J.P. *Anal. Chim. Acta* **1991**, *246*, 113-130.
26. Katz, E.D.; Ogan, K.; Scott, R.P.W. *J. Chromatogr.* **1986**, *352*, 67-90.
27. Katz, E.D.; Lochmüller, C.H.; Scott, R.P.W. *Anal. Chem.* **1989**, *61*, 349-355.
28. Snyder, L.R. *Physicochemical Basis of Retention in Selectivity and Detectability Optimizations in HPLC* by Ahuja, S.; John Wiley & Sons, Inc.: New York, 1989; Chapter 2.

CHAPTER IV

EFFECT OF BINARY MOBILE PHASE COMPOSITION AND STATIONARY PHASE TYPE ON METHYLENE SELECTIVITY

INTRODUCTION

Group selectivity refers to the retention of a compound with a chemical group of interest relative to that of an otherwise identical compound without that group [1]. Thus, methylene group selectivity (α_{CH_2}) refers to the relative retention of two solutes differing only by one methylene unit. Mathematically, selectivity (α) or relative retention can be defined as

$$\alpha = \frac{k'_2}{k'_1} \quad (4.1)$$

where k'_1 is the retention factor of the earlier eluting peak. Equation 4.2 shows the relationship between k' and the solute distribution coefficient (K)

$$k' = K \left(\frac{V_S}{V_M} \right) = K\phi \quad (4.2)$$

where V_S is the stationary phase volume, V_M is the mobile phase volume, and ϕ is the phase ratio (equal to V_S/V_M). Combining Eqns. 4.1 and 4.2 yields Eqn. 4.3 which

$$\alpha = \frac{K_2}{K_1} \quad (4.3)$$

relates α to K .

As can be seen in Eqn. 4.3, α is independent of the phase ratio of the column, and is determined only by thermodynamic parameters. Thus, α_{CH_2} is independent of the

factors which affect the phase ratio (*e.g.* surface area, porosity, degree of surface coverage and chain length [2]), and is affected only by variables which affect the distribution coefficient, namely: solute, mobile phase composition, stationary phase type, temperature and pressure [3]. However, the effect of pressure on retention in liquid chromatography is normally negligible. Hence, if the solute, mobile phase composition and temperature are kept constant, any differences observed for α_{CH_2} will be due to differences in the stationary phase. Similarly, if the solute, temperature and stationary phase are kept constant, any differences observed for α_{CH_2} will be due to differences in the mobile phase.

$\log \alpha_{CH_2}$ is also related to the difference in the change in free energy of transfer due to the extra methylene group (Eqn. 4.4). Finally, methylene selectivity is not

$$\log \alpha_{CH_2} = -\Delta\Delta G \quad (4.4)$$

affected much by the presence of surface hydroxyl groups.

RESULTS AND DISCUSSION

Tables 4.1-4.6 compare the methylene group selectivities (α_{CH_2}) measured using *n*-alkylbenzenes, *n*-alkanes, 2-ketones, and alkylphenones for the different polymer-coated aluminas and Si-C₁₈ columns. Methylene group selectivity was determined either from the slope of a $\log k'$ vs. carbon number plot (homologous series) or from the ratio of k' values for two homologues differing only by one methylene unit (as in Eqn. 4.1). Unless indicated otherwise, the α_{CH_2} values in Tables 4.1-4.6 were determined using the slope method. For almost all data sets, the linear correlation coefficient for plots of $\log k'$ vs. carbon number was ≥ 0.999 . From Table 4.1 it is seen that although α_{CH_2} values determined using the slope and ratio methods for the *n*-alkylbenzenes with

TABLE 4.1. Effect of binary mobile phase composition on methylene group selectivity of n-alkylbenzenes and n-alkanes for the Unisphere Al-PBD column. ^a

% Organic Solvent	<u>Methylene Group Selectivity (α_{CH_2})</u>		
	<u>n-Alkylbenzenes</u>		<u>n-Alkanes</u>
	Slope ^b	k'_{EB}/k'_T ^c	
I. MeCN/H ₂ O:			
0	—	—	—
10	—	—	—
20	—	—	—
30	2.12	2.09	—
40	1.76	1.80	—
50	1.69	1.62	—
60	1.58	1.52	1.63
70	1.58	—	1.55
80	—	—	1.51
90	—	—	1.51
100	—	—	1.33
II. MeOH/H ₂ O:			
0	—	—	—
10	—	—	—
20	—	—	—
30	—	—	—
40	—	2.22	—
50	2.06	1.94	—
60	1.86	1.69	1.86
70	1.66	1.51	1.67
80	1.50	1.48	1.49
90	—	—	1.35
100	—	—	1.20

^a n-Alkylbenzenes: toluene, ethylbenzene, propylbenzene and butylbenzene.

n-Alkanes: pentane, hexane and heptane.

^b k' values used for toluene and ethylbenzene were from the first set of data in Table 3.1.

^c EB = ethylbenzene; T = toluene.

TABLE 4.2. Effect of binary mobile phase composition on methylene group selectivity of n-alkylbenzenes and n-alkanes for the Millipore Al-PBD column. ^a

% Organic Solvent	<u>Methylene Group Selectivity (α_{CH_2})</u>	
	n-Alkylbenzenes (k'_{EB}/k'_T ^b)	n-Alkanes
I. MeCN/H ₂ O:		
0	—	—
10	—	—
20	—	—
30	—	—
40	1.67	—
50	1.55	—
60	1.43	1.61
70	—	1.57
80	—	1.55
90	—	1.48
100	—	1.38
II. MeOH/H ₂ O:		
0	—	—
10	—	—
20	—	—
30	—	—
40	—	—
50	1.77	—
60	1.55	1.88
70	1.36	1.65
80	—	1.48
90	—	1.32
100	—	—

^a n-Alkylbenzenes: toluene, ethylbenzene.

n-Alkanes: pentane, hexane and heptane.

Two different Millipore Al-PBD columns were used: n-alkylbenzenes data: SN B00221C1; n-alkanes data: SN B90441D2.

^b EB = ethylbenzene; T = toluene.

TABLE 4.3. Effect of binary mobile phase composition on methylene group selectivity of *n*-alkylbenzenes and *n*-alkanes for the Microsorb Si-C₁₈ column. ^a

% Organic Solvent	<u>Methylene Group Selectivity (α_{CH_2})</u>	
	<i>n</i> -Alkylbenzenes (k'_{EB}/k'_T ^b)	<i>n</i> -Alkanes
I. MeCN/H ₂ O:		
0	—	—
10	—	—
20	—	—
30	—	—
40	1.82	—
50	1.61	—
60	1.48	1.64
70	1.43	1.56
80	1.37	1.49
90	1.35	1.45
100	—	1.30
II. MeOH/H ₂ O:		
0	—	—
10	—	—
20	—	—
30	—	—
40	—	—
50	2.03	—
60	1.78	—
70	1.56	—
80	1.44	1.56
90	1.31	1.40
100	—	1.27

^a *n*-Alkylbenzenes: toluene, ethylbenzene.

n-Alkanes: pentane, hexane and heptane.

^b EB = ethylbenzene; T = toluene.

TABLE 4.4. Effect of binary mobile phase composition on methylene group selectivity of 2-ketones, alkylphenones and n-alkylbenzenes for the Unisphere Al-C₁₈ column. ^a

% Organic Solvent	<u>Methylene Group Selectivity (α_{CH_2})</u> ^b		
	2-Ketones	Alkylphenones	n-Alkylbenzenes
I. MeCN/H ₂ O:			
0	3.29	—	—
10	2.84	2.89*	—
20	2.69	2.49	—
30	2.22	2.14	2.02*
40	1.87	1.85	1.84
50	1.68	1.59	1.65
60	1.59*	1.48*	1.54
70	—	—	1.47
80	—	—	1.41
90	—	—	—
100	—	—	—
II. MeOH/H ₂ O:			
0	3.29	—	—
10	3.05	—	—
20	3.04	2.80*	—
30	2.72	2.51	—
40	2.38	2.26	—
50	2.11	2.00	—
60	1.79	1.75	1.81
70	1.55*	1.53	1.60
80	—	—	1.46
90	—	—	—
100	—	—	1.18*

^a 2-Ketones: 2-butanone to 2-nonanone.

Alkylphenones: acetophenone to valerophenone.

n-Alkylbenzenes: toluene to nonylbenzene.

^b Selectivity values ending with "*" were determined using the ratio method.

TABLE 4.5. Effect of binary mobile phase composition on methylene group selectivity of 2-ketones, alkylphenones and n-alkylbenzenes for the Unisphere Al-CN column. ^a

% Organic Solvent	<u>Methylene Group Selectivity (α_{CH_2})</u> ^b		
	2-Ketones	Alkylphenones	n-Alkylbenzenes
I. MeCN/H ₂ O:			
0	3.41	—	—
10	2.95	3.14*	—
20	2.58	2.54	—
30	2.14	2.12	1.96
40	1.79	1.84	1.70
50	1.61	1.64	1.52
60	1.48*	1.46	1.41
70	—	—	1.34
80	—	—	1.29
90	—	—	1.24
100	—	—	—
II. MeOH/H ₂ O:			
0	3.41	—	—
10	3.16	3.19*	—
20	2.90	2.94*	—
30	2.62	2.48	—
40	2.28	2.21	2.00*
50	1.98	1.96	1.90
60	1.71	1.73	1.66
70	1.51*	1.54	1.50
80	—	1.37	1.36
90	—	—	1.23
100	—	—	—

^a 2-Ketones: 2-pentanone to 2-nonanone.

Alkylphenones: acetophenone to valerophenone.

n-Alkylbenzenes: toluene to nonylbenzene.

^b Selectivity values ending with "*" were determined using the ratio method.

TABLE 4.6. Effect of binary mobile phase composition on methylene group selectivity of 2-ketones, alkylphenones and n-alkylbenzenes for the LiChrospher Si-C₁₈ column. ^a

% Organic Solvent	<u>Methylene Group Selectivity (α_{CH_2})</u> ^b		
	2-Ketones	Alkylphenones	n-Alkylbenzenes
I. MeCN/H ₂ O:			
0	3.43*	—	—
10	3.36	—	—
20	3.04	—	—
30	2.58	2.44*	—
40	2.10	2.01	—
50	1.84	1.77	1.59*
60	1.68	1.65	1.57
70	1.62	1.60	1.51
80	1.56	1.58	1.45
90	1.53	1.35*	1.40
100	—	—	1.33
II. MeOH/H ₂ O:			
0	3.43*	—	—
10	3.33	—	—
20	3.09	—	—
30	2.86	—	—
40	2.58	2.34*	—
50	2.27	2.06	—
60	1.98	1.87	1.78*
70	1.75	1.66	1.66
80	1.56	1.50	1.49
90	1.38	1.32	1.37
100	—	—	1.26

^a 2-Ketones: 2-propanone to 2-nonanone.
 Alkylphenones: acetophenone to valerophenone.
 n-Alkylbenzenes: toluene to nonylbenzene.

^b Selectivity values ending with "*" were determined using the ratio method.

the Unisphere Al-PBD column are similar, the slope method gives slightly higher results, indicating better selectivity for higher homologues. For example, using 60% MeOH results in α_{CH_2} values of 1.86 and 1.69 for the slope and ratio methods, respectively. Similar trends are expected for the α_{CH_2} values reported in Tables 4.2-4.6 wherein both slope and ratio methods were employed.

A. Effect Of Mobile Phase Composition On Methylene Group Selectivity

The dependence of methylene group selectivity on binary mobile phase composition was about the same for all polymer-coated aluminas and Si-C₁₈ columns. *As the volume fraction of organic solvent increased, α_{CH_2} values decreased* for both MeCN/H₂O and MeOH/H₂O for all solute groups. This can be seen in Tables 4.1-4.6 and Figs. 4.1A-4.4B. For example, α_{CH_2} values for the 2-ketones decreased from 3.41 to 1.51 from 0 to 70% MeOH for the Unisphere Al-C₁₈ stationary phase (in Table 4.5).

Another look at Figs. 4.1A-4.4B reveals that in general, better linearity was obtained from plots of α_{CH_2} vs. % MeOH compared to α_{CH_2} vs. % MeCN. This is very obvious in Figs. 4.1A and 4.1B for the n-alkylbenzenes with MeCN/H₂O and MeOH/H₂O as mobile phases, respectively.

Several authors [4, 5] have reported better linearity for plots of $\log \alpha_{CH_2}$ vs. %MeOH compared to those obtained with MeCN/H₂O. It should be noted, however, that these studies were carried out over a wide range of mobile phase composition (*i.e.*, from 0 to 100% organic solvent). Unfortunately, such broad conclusions cannot be made in this study except for the LiChrospher Si-C₁₈ where α_{CH_2} values for the 2-ketones were determined from 10-90% organic solvent (Fig. 4.5). Similar to the results reported by Karger *et al.* [4], and Colin *et al.* [5], better linearity was observed for the MeOH/H₂O solvent system. The R² values obtained for the curves in Fig. 4.5 were 0.993 and 0.919 for MeOH/H₂O and MeCN/H₂O, respectively. For the other columns in the study, α_{CH_2} values were determined only over a limited range of mobile

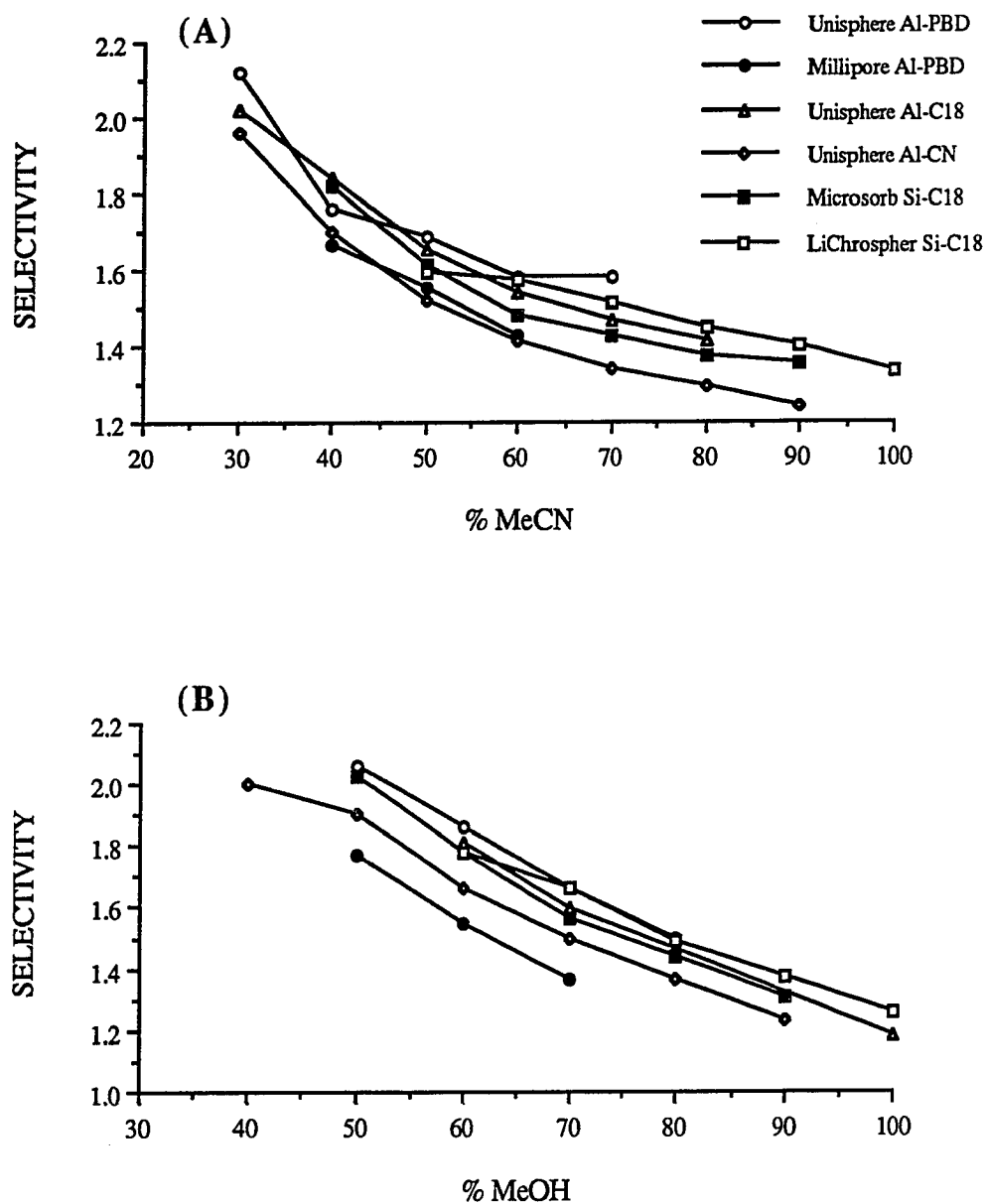


FIGURE 4.1. Effect of the binary mobile phase composition of (A) MeCN/H₂O, and (B) MeOH/H₂O on the methylene group selectivity of *n*-alkylbenzenes for the various polymer-coated aluminas and Si-C₁₈ columns.

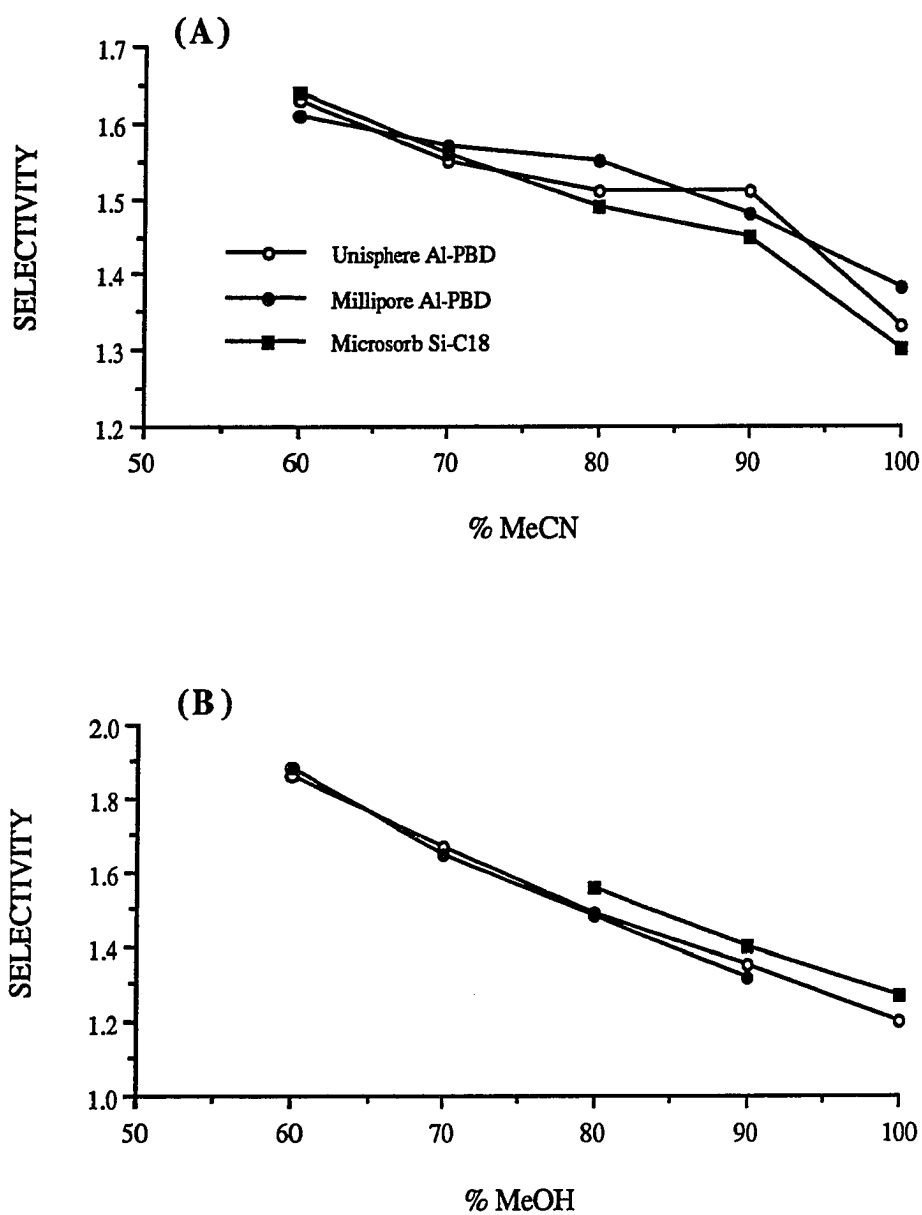


FIGURE 4.2. Effect of the binary mobile phase composition of (A) MeCN/H₂O, and (B) MeOH/H₂O on the methylene group selectivity of n-alkanes for the various polymer-coated aluminas and Si-C₁₈ columns.

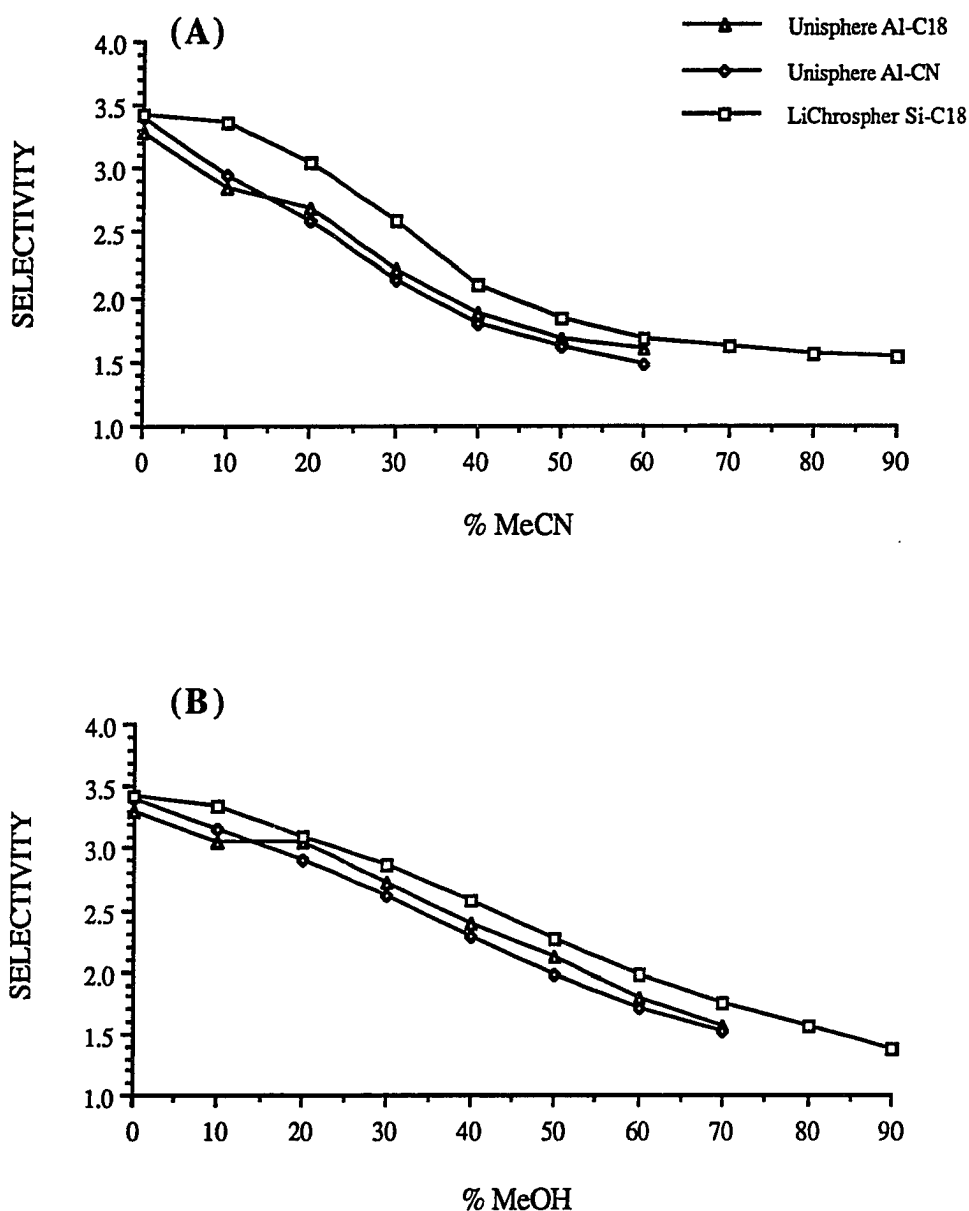


FIGURE 4.3. Effect of the binary mobile phase composition of (A) MeCN/H₂O, and (B) MeOH/H₂O on the methylene group selectivity of 2-ketones for the various polymer-coated aluminas and Si-C₁₈ columns.

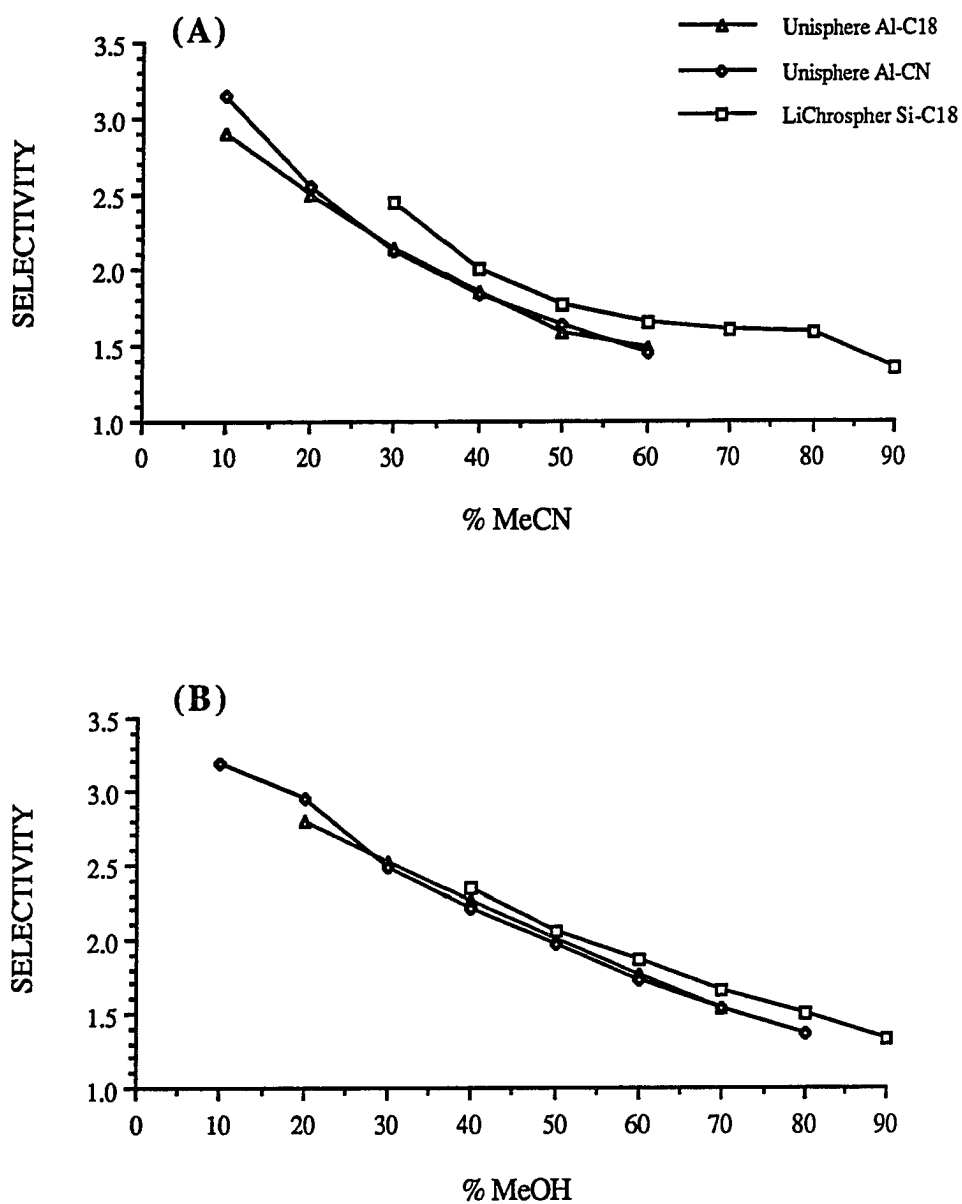


FIGURE 4.4. Effect of the binary mobile phase composition of (A) MeCN/H₂O, and (B) MeOH/H₂O on the methylene group selectivity of alkylphenones for the various polymer-coated aluminas and Si-C₁₈ columns.

phase composition. An example is given in Fig. 4.6 for the Unisphere Al-C₁₈ column. For this particular plot, the R^2 values obtained were 0.938 and 0.984 for MeOH/H₂O and MeCN/H₂O, respectively, indicating better linearity for the MeCN/H₂O system.

In a previous study of Si-C₁₈ columns, it was reported that at equal organic modifier concentrations for binary hydroorganic solvents, increasing α_{CH_2} values are obtained according to the sequence: tetrahydrofuran < isopropanol < dioxane < acetonitrile < ethanol < methanol [6]. A similar trend was observed in this study for all polymer-coated aluminas and Si-C₁₈ columns. That is, for the same stationary phase and solute class at the same temperature and % organic modifier, α_{CH_2} values for MeOH/H₂O were generally greater than that for MeCN/H₂O. For example, for the Unisphere Al-C₁₈ column at 30% organic solvent (Table 4.4), α_{CH_2} values for the 2-ketones were 2.72 and 2.22 for MeOH/H₂O and MeCN/H₂O, respectively. However, the latter trend was not observed for predominantly organic mobile phases (*i.e.*, with \geq 80-90% organic solvent), especially for the n-alkanes in Tables 4.1-4.3.

B. Effect Of Stationary Phase Type On Methylene Group Selectivity

To demonstrate the effect of stationary phase type on methylene selectivity, other variables such as solute type, temperature and mobile phase composition must be kept constant. As stated earlier, α_{CH_2} values determined using the slope method results in slightly higher values compared to those obtained using the ratio method. Thus, to eliminate this factor, α_{CH_2} values using the ratio method for the same solute pair were evaluated. The results from such calculations are presented in Figs. 4.7-4.10 for the different columns.

1. Toluene And Ethylbenzene

A comparison of the α_{CH_2} values obtained using toluene and ethylbenzene is illustrated in Fig. 4.7. Among the polymer-coated aluminas, α_{CH_2} values were slightly greater for the Unisphere Al-PBD phase for both solvent systems. For example, α_{CH_2}

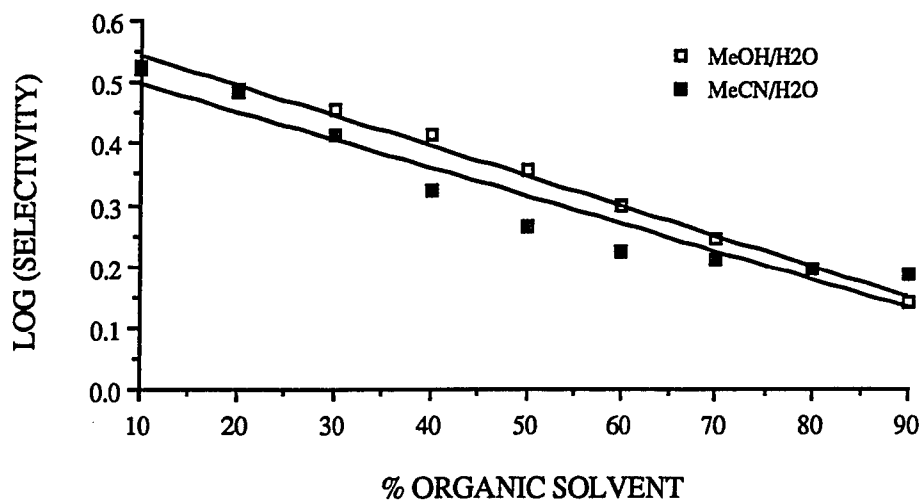


FIGURE 4.5. Linearity of plots of $\log (\alpha_{\text{CH}_2})$ vs. % organic solvent for the 2-ketones for the LiChrospher Si-C₁₈ column.

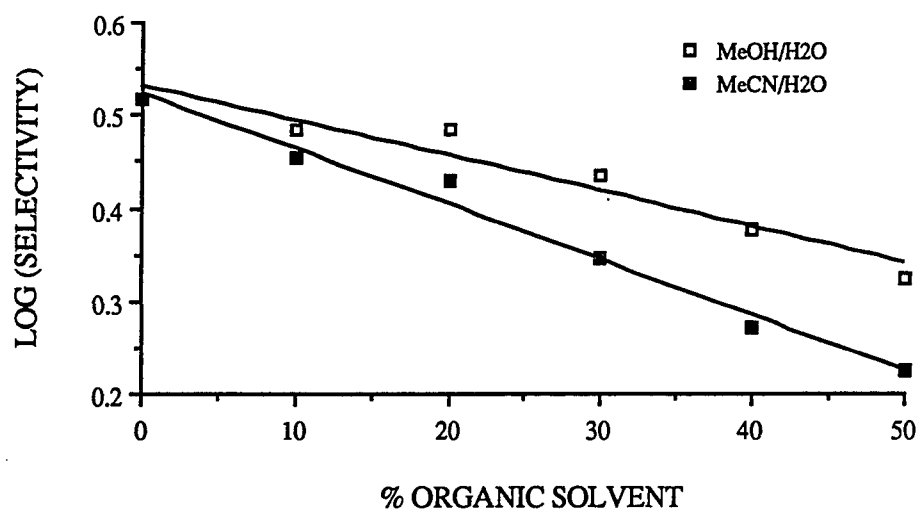


FIGURE 4.6. Linearity of plots of $\log (\alpha_{\text{CH}_2})$ vs. % organic solvent for the 2-ketones for the Unisphere Al-C₁₈ column.

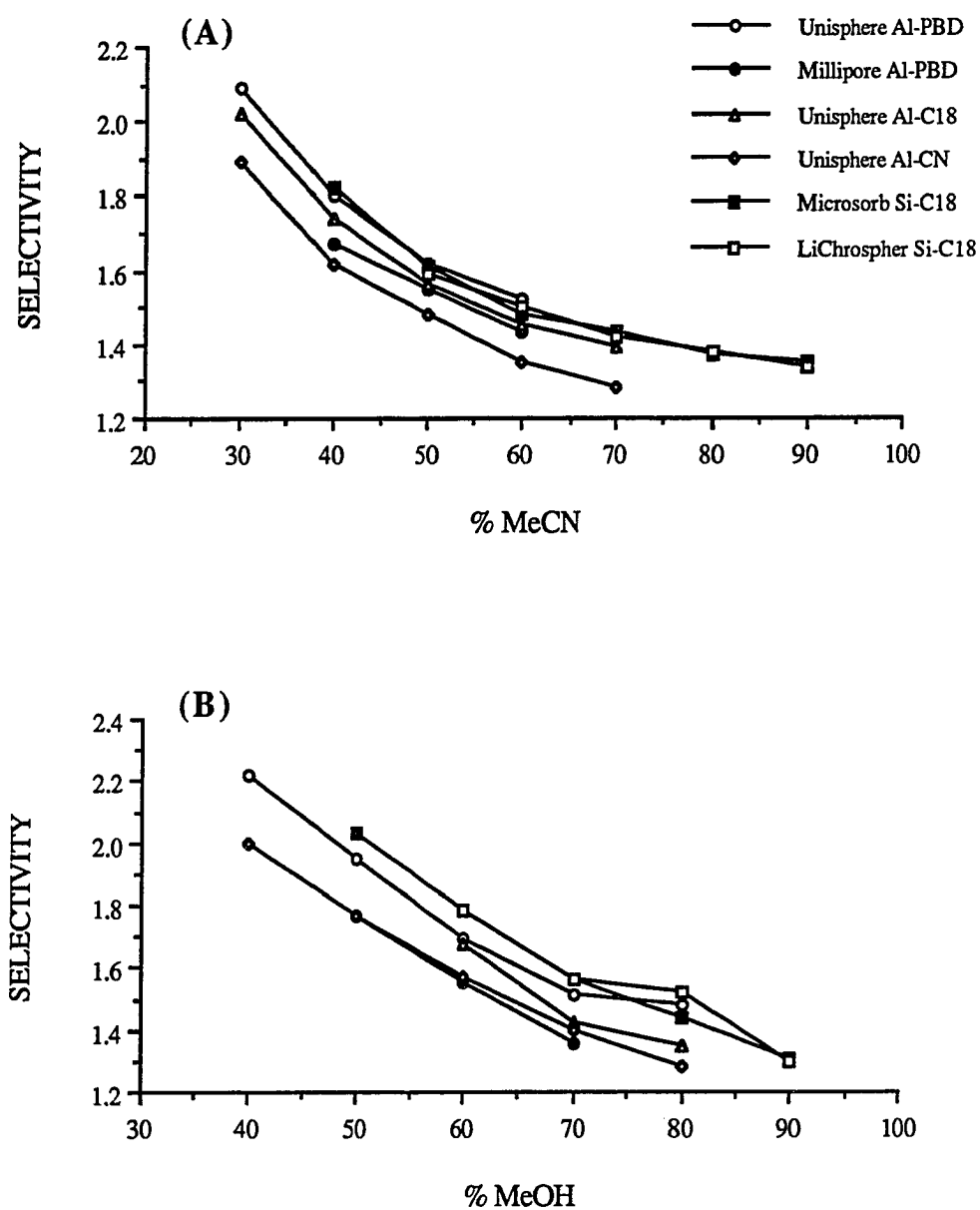


FIGURE 4.7. Comparison of the α_{CH_2} values for the n-alkylbenzenes (toluene and ethylbenzene) using the ratio method with (A) MeCN/H₂O, and (B) MeOH/H₂O as mobile phases.

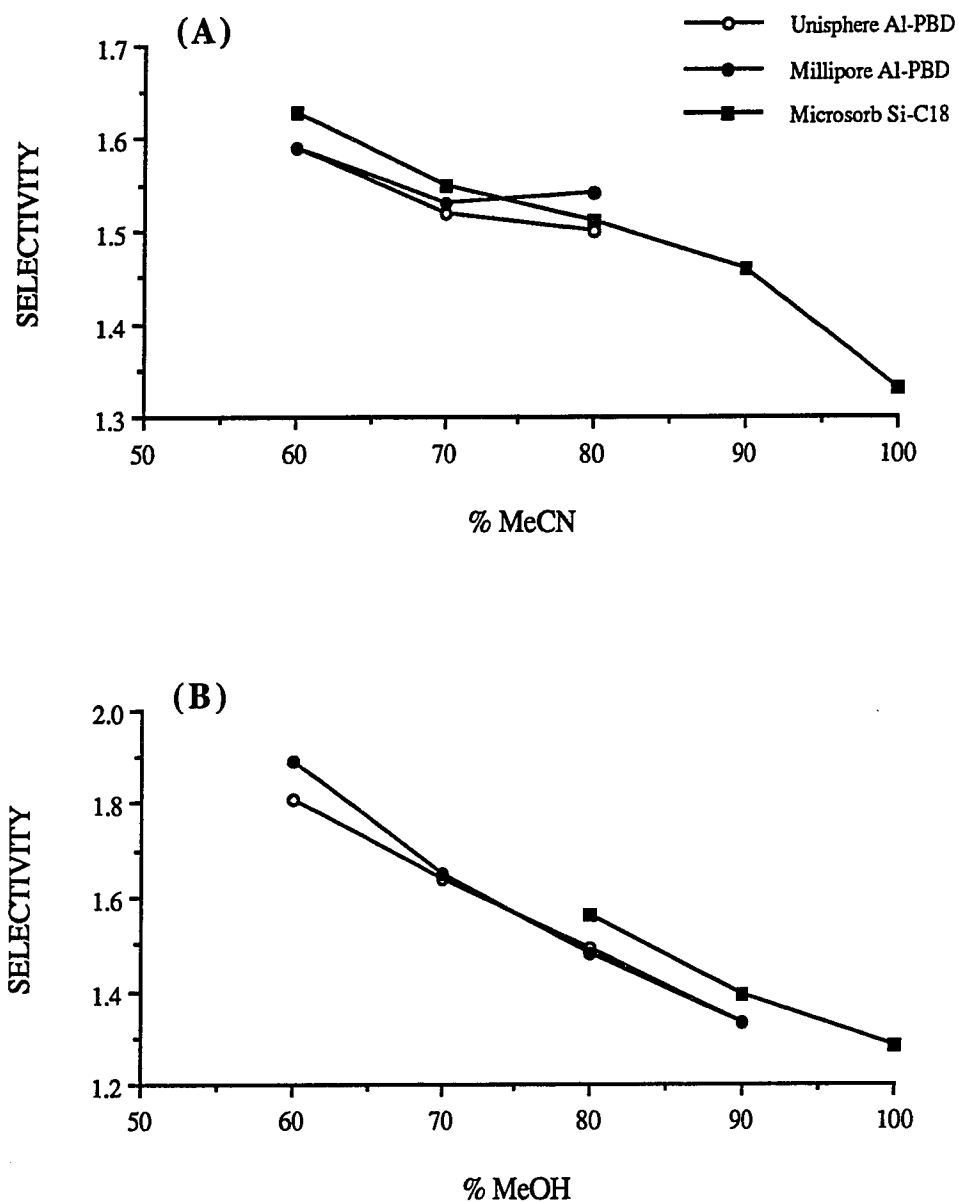


FIGURE 4.8. Comparison of the α_{CH_2} values for the n-alkanes (hexane and heptane) using the ratio method with (A) MeCN/H₂O, and (B) MeOH/H₂O as mobile phases.

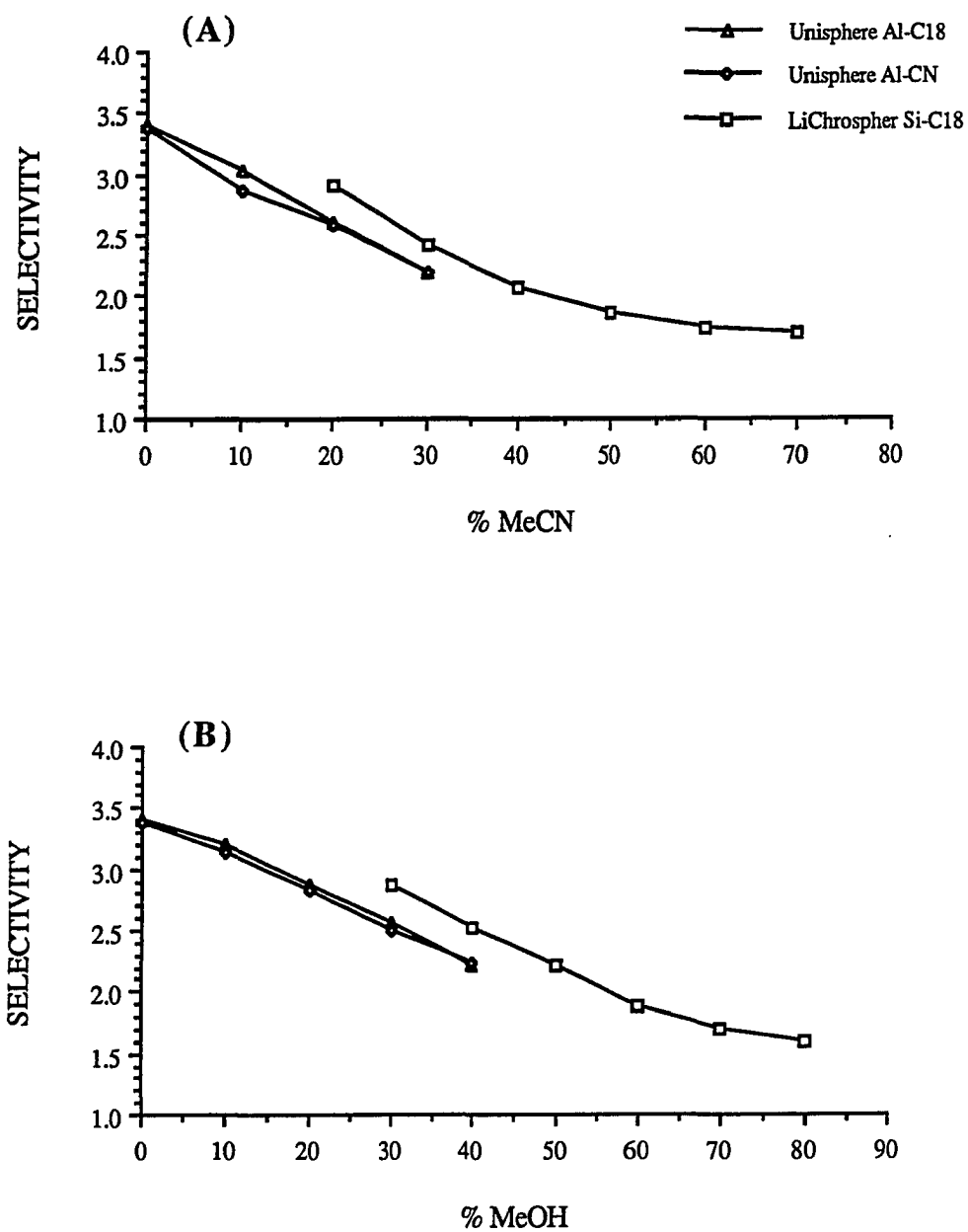


FIGURE 4.9. Comparison of the α_{CH_2} values for the 2-ketones (2-pentanone and 2-hexanone) using the ratio method with (A) MeCN/H₂O, and (B) MeOH/H₂O as mobile phases.

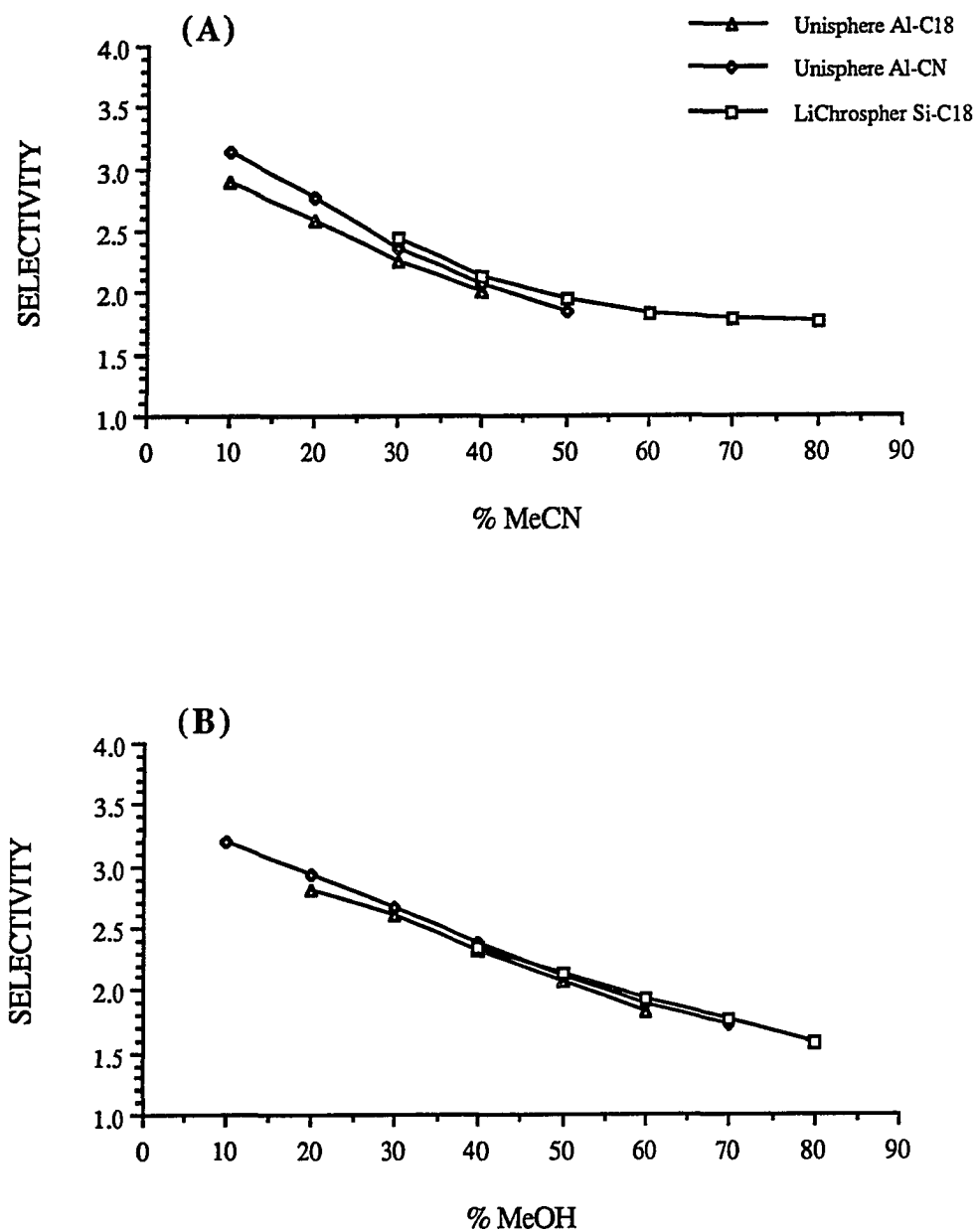


FIGURE 4.10. Comparison of the α_{CH_2} values for the alkylphenones (acetophenone and propiophenone) using the ratio method with (A) MeCN/H₂O, and (B) MeOH/H₂O as mobile phases.

values at 50% MeCN were 1.62, 1.55, 1.56 and 1.48 for the Unisphere Al-PBD, Millipore Al-PBD, Al-C₁₈ and Al-CN columns, respectively. However, it should be noted that the α_{CH_2} for the Al-CN column may be slightly understated since k' values for this stationary phase were determined at 31.0° C, while those for the other columns were all determined at 25.0° C (see Chapter V). This was also the case for the plots shown in Figs. 4.8-4.10. On the other hand, the α_{CH_2} values for both Si-C₁₈ columns were almost equal at each mobile phase composition for both MeCN and MeOH, and are comparable to values reported elsewhere by other investigators for Si-C₁₈ columns [7, 8].

Overall, the α_{CH_2} values for all columns are approximately equal in magnitude at a given mobile phase composition, although the values for the Si-C₁₈ are slightly higher than those of the Millipore Al-PBD, Al-C₁₈ and Al-CN columns. For example, α_{CH_2} values at 70% MeOH were 1.56 for both Si-C₁₈ columns, 1.51 for the Unisphere Al-PBD, and 1.36, 1.42 and 1.40 for the Millipore Al-PBD, Al-C₁₈ and Al-CN columns, respectively.

2. *Hexane And Heptane*

A comparison of the methylene group selectivity values for the n-alkanes can be seen in Fig. 4.8. Similar to the results obtained for toluene and ethylbenzene, the α_{CH_2} values were approximately equal for both brands of Al-PBD, and Si-C₁₈ columns with either MeCN/H₂O or MeOH/H₂O as mobile phase. At 80% MeCN, α_{CH_2} values were 1.50, 1.54 and 1.51 for the Unisphere and Millipore Al-PBD, and Si-C₁₈ columns, respectively. Unfortunately, no selectivity data were determined for the other alumina columns.

3. *2-Pentanone And 2-Hexanone*

The effect of stationary phase type on α_{CH_2} for this solute pair is illustrated in Fig. 4.9. As can be seen, α_{CH_2} values are reported only for the Al-C₁₈, Al-CN and

LiChrospher Si-C₁₈ columns, similar to that in Fig. 4.10 for the alkylphenones. Overall, for both solvent systems, α_{CH_2} values were slightly higher for the Si-C₁₈ column, while for both Al-C₁₈ and Al-CN, α_{CH_2} values were in general approximately equal. For example, at 30% MeOH the observed α_{CH_2} values are 2.56, 2.50 and 2.87 for the Al-C₁₈, Al-CN and Si-C₁₈ columns, respectively.

4. *Acetophenone And Propiophenone*

The effect of stationary phase type on α_{CH_2} for acetophenone and propiophenone can be seen in Fig. 4.10. For the MeCN/H₂O system, α_{CH_2} values for Si-C₁₈ were slightly higher than those for Al-C₁₈ and Al-CN. At 30% MeCN, α_{CH_2} values for the Al-C₁₈, Al-CN and Si-C₁₈ columns were 2.26, 2.36 and 2.43, respectively. On the other hand, approximately equal α_{CH_2} values were obtained for the alkylphenones with MeOH/H₂O as mobile phase. For example, at 40% MeOH the α_{CH_2} values were 2.31, 2.38 and 2.34, respectively. Another trend observed in Fig. 4.10 was that the α_{CH_2} values for the Al-CN columns were slightly higher than those for the Al-C₁₈ column for both solvent systems. For example, the α_{CH_2} values were 2.89 and 3.14 for the Al-C₁₈ and Al-CN columns, respectively, at 10% MeCN. As stated earlier, an even greater difference in α_{CH_2} might have been observed for these two columns if the retention data were collected at the same temperature.

CONCLUSIONS

In general, for similar solutes at the same temperature and mobile phase composition, α_{CH_2} values obtained for all polymer-coated aluminas and Si-C₁₈ stationary phases were approximately equal, although in certain solute types the α_{CH_2} values for the Si-C₁₈ columns were slightly higher. This trend, coupled with the less retentive nature of the various alumina-based columns discussed in Chapter 3, suggest a

potentially important advantage of polymer-coated aluminas, namely that for a given homologous series it should be possible to employ a weaker mobile phase on the polymer-coated columns, thereby achieving higher methylene selectivity with equivalent retention, particularly when MeCN is used as the organic modifier. Assuming the efficiency of the alumina-based columns is comparable to that of silica-based C₁₈ columns, the greater methylene selectivity achieved via a more aqueous mobile phase is a significant advantage, as the polymer-coated columns would thereby provide better resolution of a homologous series. A detailed examination of the combined effects of α_{CH_2} , k' and column efficiency on resolution is discussed in Chapter VII. Similarly, using polymer-coated aluminas is advantageous over Si-C₁₈ columns since at equal methylene selectivities, shorter analysis time will be involved for the alumina-based columns.

REFERENCES FOR CHAPTER IV

1. Melander, W.R.; Horváth, C. *Reversed-Phase Chromatography In High-Performance Liquid Chromatography-Advances and Perspectives*, Horváth, C., Ed.; Academic Press: New York, 1980; Vol. 2.
2. Johnson, B.P.; Khaledi, M.G.; Dorsey, J.G. *J. Chromatogr.* **1987**, *384*, 221-230.
3. Schoenmakers, P.J. *Optimization of Chromatographic Selectivity - A Guide to Method Development*; Elsevier Science Publishers B.V.: The Netherlands, 1986; Chapter 1.
4. Karger, B.L.; Gant, J.R.; Hartkopf, A.; Weiner, P.H. *J. Chromatogr.* **1976**, *128*, 65-78.
5. Colin, H.; Guiochon, G.; Yun, Z.; Diez-Masa, J.C.; Jandera, J. *J. Chromatogr. Sci.* **1983**, *21*, 179-184.
6. Hoffman, N.E.; Liao, J.C. *Anal. Lett.* **1978**, *A11*, 287-306.
7. Schoenmakers, P.J.; Billiet, H.A.H.; de Galan, L. *J. Chromatogr.* **1981**, *218*, 261-284.
8. Khaledi, M.G. *Anal. Chem.* **1988**, *60*, 876-887.

CHAPTER V

EFFECT OF TEMPERATURE ON RETENTION AND METHYLENE SELECTIVITY

INTRODUCTION

The dependence of the change in free energy (ΔG°) on the solute distribution coefficient (K) for chromatographic retention is given in Eqn. 5.1. Equation 5.2 relates ΔG° to the solute retention factor (from Eqns. 4.2 and 5.1). Assuming the column phase ratio (ϕ) to be independent of temperature, and substituting Eqn. 5.2 to Eqn. 5.3 (Gibb's relationship for free energy change) yields Eqn. 5.4 which relates k' to the standard enthalpy (ΔH°) and entropy (ΔS°) of solute transfer from the mobile phase to the stationary phase in liquid chromatography

$$\Delta G^\circ = -RT \ln K \quad (5.1)$$

$$\Delta G^\circ = -RT \ln \left(\frac{k'}{\phi} \right) \quad (5.2)$$

$$\Delta G^\circ = \Delta H^\circ - T \Delta S^\circ \quad (5.3)$$

$$\ln k' = - \frac{\Delta H^\circ}{RT} + \frac{\Delta S^\circ}{R} + \ln \phi \quad (5.4)$$

where R is the universal gas constant.

According to Melander *et al.* [1], the relationship between $\ln k'$ and $1/T$ (Eqn. 5.4) will be linear provided the retention mechanism involved does not change within the temperature range considered, and the value of ΔH° is constant. Thus, values of ΔH° and ΔS° can be determined from the slope and y-intercept, respectively, from linear plots of $\ln k'$ vs. $1/T$ (commonly called van't Hoff plots). Unfortunately, evaluation of ΔS° from the y-intercept is not straightforward due to the difficulties in the calculation of the

phase ratio (or more specifically the volume of the stationary phase). This is especially true in RPLC using bonded or polymer-coated phases wherein the stationary phase volume cannot be exactly determined. Sentell and Dorsey [2] have reviewed the various methods that have been employed for the estimation of ϕ . It should be noted that a good estimate of ΔS° is essential in getting an accurate value of ΔG° for the separation process.

EXPERIMENTAL

Retention factors (k') were obtained at 15.0, 25.0, 35.0, 45.0 and 55.0° C for the various polymer-coated aluminas and LiChrospher Si-C₁₈ column, unless indicated otherwise. Although a limited number of k' values were measured using binary hydroorganic mobile phases containing 60% organic solvent (Unisphere Al-PBD (SN: 593ATC) and Millipore Al-PBD (SN: B90441D2)), majority of the retention data (for the other Unisphere Al-PBD (SN: 003-0253), Al-C₁₈, Al-CN (SN: 262ATC) and LiChrospher Si-C₁₈) were obtained using mobile phases containing 30% organic solvent. This occurred because retention data at the different temperatures were experimentally determined after a particular column re-equilibration experiment has been completed (see Chapter VIII). This was done to minimize the additional time and solvent necessary for equilibrating the column at the desired mobile phase composition and temperature prior to solute injection. Initially, a 100 to 60% organic solvent reversed step gradient was employed to monitor the effect of temperature on the column re-equilibration process after gradient elution. However, after it was determined that the re-equilibration column volume was greater for gradients started with H₂O-rich mobile phases, reversed step gradients corresponding to 100 to 30% organic modifier were being used to monitor the column re-equilibration process, thus the two sets of data.

RESULTS AND DISCUSSION

For all polymer-coated alumina and Si-C₁₈ columns, solute retention decreased with increasing temperature, a trend commonly observed in RPLC. However, the effect of temperature on k' is not very large, especially when compared to the effect of binary mobile phase composition. For example, for the Al-C₁₈ column with nitrobenzene as solute, the k' value decreased from 3.42 to 0.59 from 30 to 60% MeOH (Table 3.3), which represents approximately a 6-fold decrease in retention. On the other hand, the k' value of nitrobenzene decreased from 3.42 to 1.68 with a corresponding increase in temperature from 25.0 to 55.0° C, respectively. According to Kevin Holland of Biotage [3], the various Unisphere polymer-coated aluminas can be subjected to temperatures as high as 60° C, the same recommended maximum temperature for the Si-C₁₈ stationary phases [4]. The rate of decrease of k' with temperature observed in this study for the different alumina-based columns was consistent with the observations of Majors [5], and Snyder and Kirkland [4], wherein they indicated that an increase in temperature of *ca.* 30-35° C results in a 2-fold decrease in k' .

A. Effect Of Temperature On Methylene Selectivity

The effect of temperature on methylene selectivity (α_{CH_2}) for the polymer-coated aluminas and Si-C₁₈ stationary phase are given in Tables 5.1-5.3 for the 2-ketones, n-alkylphenones and n-alkylbenzenes, using either 30% MeCN or 30% MeOH as mobile phase. These selectivity values were determined using the slope method (as in Chapter IV), unless indicated otherwise, where linear correlation coefficients (R^2 values) ≥ 0.996 were obtained for all plots. In general, R^2 values for majority of the plots were ≥ 0.999 . The selectivity values listed in Table 5.4 for the Unisphere and Millipore Al-PBD columns were obtained from reference [6].

As can be seen from Tables 5.1-5.4, α_{CH_2} *decreases slightly with an increase in temperature for all alumina-based and silica-based columns*, except at 45.0° C with

TABLE 5.1. Effect of temperature on the methylene group selectivity for the 2-ketones.

Column ^a	Methylene group selectivity (α_{CH_2})				
	Temperature (° C)				
	15.0	25.0	35.0	45.0	55.0
A. 30/70 MeCN/H ₂ O:					
Unisphere Al-PBD (3)	2.27	2.19	2.13	2.05	1.98
Unisphere Al-C ₁₈ (5)	2.32	2.22	2.13	2.06	2.00
LiChrospher Si-C ₁₈ (4)	2.51	2.46	2.34	2.31	2.24
Unisphere Al-CN (4)	2.24	2.17	2.10	2.02	1.98
B. 30/70 MeOH/H ₂ O:					
Unisphere Al-PBD (4)	2.84	2.72	2.59	2.45	2.34
Unisphere Al-C ₁₈ (4)	2.82	2.72	2.57	2.50	2.36
LiChrospher Si-C ₁₈ (3)	2.83	2.77	2.72	2.66	2.60
Unisphere Al-CN (4)	2.74	2.64	2.55	2.40	2.32

^a Numbers in parentheses correspond to the number of compounds used for the plot of log k' vs. carbon number.

TABLE 5.2. Effect of temperature on the methylene group selectivity for the n-alkylphenones.

Column ^a		Methylene group selectivity (α_{CH_2})				
		Temperature (° C)				
		15.0	25.0	35.0	45.0	55.0
A. 30/70 MeCN/H ₂ O:						
Unisphere Al-PBD	(4)	2.20	2.14	2.10	2.02	1.97
Unisphere Al-C ₁₈	(4)	2.20	2.14	2.09	2.04	1.98
LiChrospher Si-C ₁₈	^b	2.47	2.43	2.35	2.32	2.26
Unisphere Al-CN	(3)	2.19	2.17	2.12	2.09	2.04
B. 30/70 MeOH/H ₂ O:						
Unisphere Al-PBD	(4)	2.56	2.50	2.43	2.35	2.28
Unisphere Al-C ₁₈	(4)	2.71	2.51	2.44	2.37	2.26
LiChrospher Si-C ₁₈		—	—	—	—	—
Unisphere Al-CN	(3)	2.56	2.50	2.43	2.37	2.31

^a Numbers in parentheses correspond to the number of compounds used for the plot of log k' vs. carbon number.

^b α_{CH_2} was calculated using the equation $k'_{\text{Propiophenone}}/k'_{\text{Acetophenone}}$.

TABLE 5.3. Effect of temperature on the methylene group selectivity for the n-alkylbenzenes.

Column	Methylene group selectivity (α_{CH_2}) ^a				
	Temperature (° C)				
	15.0	25.0	35.0	45.0	55.0
A. 30/70 MeCN/H ₂ O:					
Unisphere Al-PBD	2.06	2.02	1.98	1.93	1.90
Unisphere Al-C ₁₈	2.05	2.02	1.98	1.95	1.88
B. 30/70 MeOH/H ₂ O:					
Unisphere Al-PBD	—	2.41	2.35	2.26	2.19
Unisphere Al-C ₁₈	—	—	—	—	—

^a α_{CH_2} was calculated using the equation $k'_{\text{Ethylbenzene}}/k'_{\text{Toluene}}$.

TABLE 5.4. Effect of temperature on the methylene group selectivity for the n-alkylbenzenes for the Unisphere and Millipore Al-PBD columns (from reference [6]).

Column	Methylene group selectivity (α_{CH_2}) ^a			
	Temperature (° C)			
	15.0	25.0	35.0	45.0
A. 60/40 MeCN/H ₂ O:				
Unisphere Al-PBD	1.60	1.58	1.55	1.55
Millipore Al-PBD	1.72	1.67	1.65	1.65
B. 60/40 MeOH/H ₂ O:				
Unisphere Al-PBD	1.92	1.86	1.81	1.74
Millipore Al-PBD	1.82	1.77	1.73	1.69

^a α_{CH_2} corresponds to the antilogarithm of the slope of the plot of log k' vs. carbon number, wherein the smallest R^2 value obtained was 0.998 ($n = 4$).

60/40 MeCN/H₂O as mobile phase for the Unisphere and Millipore Al-PBD columns in Table 5.4. The discrepancy observed at 45.0° C was probably due to errors in t_m , which becomes more significant for lower values of k' . Similar to the effect of temperature on retention, changes in temperature exhibited a smaller effect on α_{CH_2} than changes in mobile phase composition. For example, for the Al-C₁₈ column for the 2-ketones with 30% MeOH as mobile phase (Table 5.1), α_{CH_2} decreased only from 2.72 at 25.0° C to 2.36 at 55.0° C, or a 13% decrease in selectivity value. On the other hand, a similar % decrease in α_{CH_2} was obtained by increasing %MeOH from 30 to 40%, corresponding to α_{CH_2} values of 2.72 and 2.38, respectively, at 25.0° C (Table 4.4). In general, for all solute groups and column types in Tables 5.1-5.4, α_{CH_2} decreased by less than 18% with an increase in temperature from 15.0 to 55.0° C for both solvent systems. Finally, a detailed examination of the plots of the data given in Tables 5.1-5.4 revealed no significant relationship other than those mentioned earlier. An example of such a plot is shown in Fig. 5.1 for the 2-ketones. Similar plots of the data in Tables 5.2-5.4 can be seen in Appendix A (Figs. A.1-A.3).

Although beyond the scope of this study, it is noteworthy to mention that at least for MeOH/H₂O, resolution is generally improved at higher temperature and lower concentration of organic solvent in the mobile phase [7]. This improvement in resolution is mainly due to an increase in selectivity, since although k' decreases with an increase in temperature, retention is kept constant due to the simultaneous increase in the water content of the mobile phase. It is also worth noting that an increase in temperature not only results in a decrease in k' and α_{CH_2} , but also results in lowering the viscosity of the mobile phase, improving the solute diffusion coefficient and mass transfer, which according to some researchers [7-9] generally leads to an improvement of column efficiency. The lower viscosity also results in lower backpressure which allows the use of more polar mobile phases and higher flow rates. An increase in temperature also

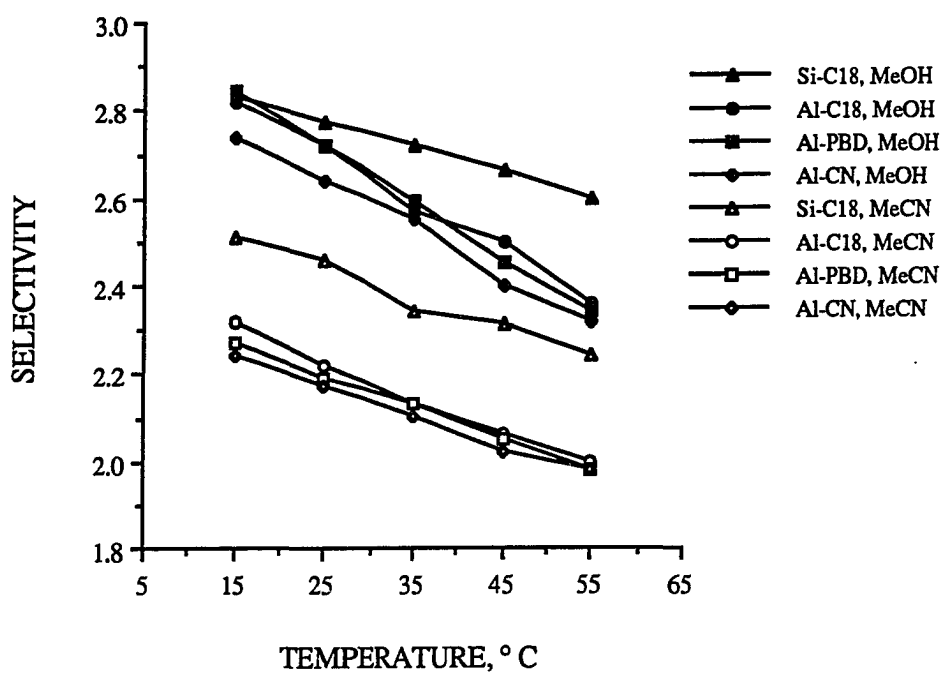


FIGURE 5.1. Effect of temperature on methylene selectivity for the 2-ketones for the various polymer-coated aluminas and Si-C₁₈ column (same data as in Table 5.1).

improves the solubility of sparingly soluble solutes [4]. From the personal experience of the author, it was observed that controlling the temperature of the column is essential for obtaining reproducible retention data.

B. Comparison Of ΔH° Values

Tables 5.5-5.9 give the values of ΔH° and $(\Delta S^\circ/R + \ln \phi)$, including the R^2 values from the corresponding van't Hoff plots, for the various polymer-coated aluminas and Si-C₁₈ column. Entropies of transfer (ΔS°) were not evaluated due to the difficulty of obtaining an accurate estimate of the phase ratio for these columns. An estimate of ΔS° is however not as important as an estimate of ΔH° , since as indicated by Melander and Horváth [10], ΔH° largely determines the effect of temperature on solute retention in RPLC.

A linear relationship was generally observed for $\ln k'$ vs. $1/T$ (Fig. 5.2), indicating an invariant retention mechanism and constant enthalpy of retention over the temperature range studied. Deviations from linearity were generally observed in cases where solute retention was extremely small, wherein errors in t_m are expected to result in large errors in k' . The worst case was observed for 2-pentanone in Table 5.8 with 30% MeCN, where the reported R^2 value was 0.142. For this solute, the apparent k' value at all temperatures remained constant at 0.29, except at 45.0° C wherein k' was 0.30. With 30% MeOH as mobile phase, the R^2 value for 2-pentanone for the same column was 0.217. In the latter case the k' value decreased only from 0.32 to 0.30 from 15.0 to 55.0° C.

As can be seen in Fig. 5.2, the enthalpies of transfer for closely related compounds (in this case a series of 2-ketones) do not differ greatly. Quantitatively, this can be seen in Tables 5.5-5.9. For a homologous series, succeeding members differ in ΔH° values by less than 1 kcal/mol.

TABLE 5.5. Thermodynamic parameters for the Unisphere Al-PBD column. ^a

Compound	$-\Delta H^\circ$ (kcal·mol ⁻¹)	$-(\Delta S^\circ/R + \ln \phi)$	R ²
A. 30/70 MeCN/H ₂ O:			
2-Heptanone	0.89	2.19	0.975
2-Octanone	1.59	2.60	0.994
2-Nonanone	2.20	2.84	0.995
Acetophenone	0.96	2.86	0.943
Propiophenone	1.55	3.00	0.989
Butyrophenone	2.05	3.14	0.997
Valerophenone	2.55	3.23	0.997
Nitrobenzene	1.95	3.82	0.996
m-Nitrotoluene	2.41	3.84	0.997
Styrene	2.76	3.55	0.997
Toluene	2.45	3.30	0.996
Ethylbenzene	2.85	3.26	0.997
Isopropylbenzene	3.16	3.23	0.997
B. 30/70 MeOH/H ₂ O:			
2-Hexanone	0.79	2.38	0.978
2-Heptanone	1.64	2.85	0.983
2-Octanone	2.57	3.42	0.993
2-Nonanone	3.49	3.95	0.995
Acetophenone	2.69	4.96	0.996
Propiophenone	3.21	4.87	0.997
Butyrophenone	3.73	4.91	0.997
Valerophenone	4.44	5.16	0.997
Nitrobenzene	3.28	5.22	0.998
m-Nitrotoluene	4.12	5.64	0.998
Styrene	4.51	5.27	0.998
Toluene	3.59	4.23	0.997
Ethylbenzene ^b	4.37	4.66	0.997

^a Temperatures used: 15.0, 25.0, 35.0, 45.0 and 55.0° C.^b No retention data collected at 15.0° C.

TABLE 5.6. Thermodynamic parameters for the Unisphere Al-C₁₈ column. ^a

Compound	$-\Delta H^\circ$ (kcal·mol ⁻¹)	$-(\Delta S^\circ/R + \ln \phi)$	R ²
A. 30/70 MeCN/H ₂ O:			
2-Pentanone	0.15	1.56	0.462
2-Hexanone	0.89	2.03	0.997
2-Heptanone	1.59	2.42	0.998
2-Octanone	2.23	2.70	0.999
2-Nonanone ^b	2.97	3.12	0.998
Acetophenone	1.69	3.21	0.998
Propiophenone	2.27	3.37	0.999
Butyrophenone	2.68	3.36	0.999
Valerophenone	3.23	3.52	0.999
Nitrobenzene	2.69	4.26	0.995
m-Nitrotoluene	3.15	4.29	0.999
Styrene	3.32	3.79	0.999
Toluene	2.89	3.36	0.999
Ethylbenzene	3.28	3.31	0.998
B. 30/70 MeOH/H ₂ O:			
2-Pentanone	1.53	3.44	0.974
2-Hexanone	2.20	3.62	0.998
2-Heptanone	3.10	4.13	0.998
2-Octanone	4.01	4.64	0.995
Acetophenone	4.25	6.57	1.000
Propiophenone	4.88	6.67	1.000
Butyrophenone ^c	5.45	6.75	1.000
Nitrobenzene	4.85	6.93	0.999
m-Nitrotoluene ^c	5.67	7.30	1.000

^a Temperatures used: 15.0, 25.0, 35.0, 45.0 and 55.0° C.

^b No retention data collected at 35.0° C.

^c No retention data collected at 15.0° C.

TABLE 5.7. Thermodynamic parameters for the LiChrospher Si-C₁₈ column. ^a

Compound	$-\Delta H^\circ$ (kcal·mol ⁻¹)	$-(\Delta S^\circ/R + \ln \phi)$	R ²
A. 30/70 MeCN/H ₂ O:			
2-Butanone	-0.15	-0.14	0.313
2-Pentanone	0.44	-0.05	0.930
2-Hexanone	0.96	-0.04	0.986
2-Heptanone	1.54	0.05	0.991
Acetophenone	1.89	1.51	0.997
Propiophenone	2.31	1.35	0.997
Nitrobenzene	2.88	2.61	0.997
B. 30/70 MeOH/H ₂ O:			
2-Propanone	0.93	2.06	0.965
2-Butanone	1.23	1.57	0.988
2-Pentanone	1.73	1.37	0.995

^a Temperatures used: 15.0, 25.0, 35.0, 45.0 and 55.0° C.

TABLE 5.8. Thermodynamic parameters for the Unisphere Al-CN column. ^a

Compound	$-\Delta H^\circ$ (kcal·mol ⁻¹)	$-(\Delta S^\circ/R + \ln \phi)$	R ²
A. 30/70 MeCN/H ₂ O:			
2-Pentanone	-0.08	1.10	0.142
2-Hexanone	0.62	1.51	0.977
2-Heptanone	1.22	1.75	0.987
2-Octanone	1.76	1.90	0.995
Acetophenone	1.85	3.02	0.992
Propiophenone	2.25	2.84	0.996
Butyrophenone	2.55	2.67	0.998
Nitrobenzene	2.82	3.76	0.998
m-Nitrotoluene	3.07	3.47	0.998
Toluene	2.72	2.80	1.000
B. 30/70 MeOH/H ₂ O:			
2-Pentanone	0.17	1.44	0.217
2-Hexanone	0.98	1.86	0.975
2-Heptanone	1.70	2.12	0.989
2-Octanone	2.62	2.68	0.992
Acetophenone	3.31	4.78	0.997
Propiophenone	3.77	4.56	0.998
Butyrophenone	4.29	4.60	0.998
Nitrobenzene	4.14	5.12	0.998
m-Nitrotoluene	4.82	5.33	0.998
Toluene	3.86	3.87	0.998

^a Temperatures used: 15.0, 25.0, 35.0, 45.0 and 55.0° C.

TABLE 5.9. Thermodynamic parameters for the Unisphere and Millipore Al-PBD columns (from reference [6]). ^a

Compound	$-\Delta H^\circ$ (kcal·mol ⁻¹)	$-(\Delta S^\circ/R + \ln \phi)$	R ²
I. Unisphere Al-PBD:			
A. 60/40 MeCN/H ₂ O:			
Toluene	0.62	2.06	0.929
Ethylbenzene	0.70	1.77	0.986
Propylbenzene	0.97	1.78	1.000
Butylbenzene	1.22	1.71	0.999
B. 60/40 MeOH/H ₂ O:			
Toluene	2.70	4.24	0.997
Ethylbenzene	3.19	4.50	0.996
Propylbenzene	3.85	4.99	0.998
Butylbenzene	4.41	5.27	0.999
II. Millipore Al-PBD:			
A. 60/40 MeCN/H ₂ O:			
Toluene	1.25	3.28	0.859
Ethylbenzene	1.32	2.85	0.976
Propylbenzene	1.52	2.67	0.996
Butylbenzene	1.65	2.40	0.998
B. 60/40 MeOH/H ₂ O:			
Toluene	2.86	4.19	0.996
Ethylbenzene	3.22	4.27	0.998
Propylbenzene	3.59	4.33	0.998
Butylbenzene	4.21	4.76	0.998

^a Temperatures used: 15.0, 25.0, 35.0 and 45.0° C.

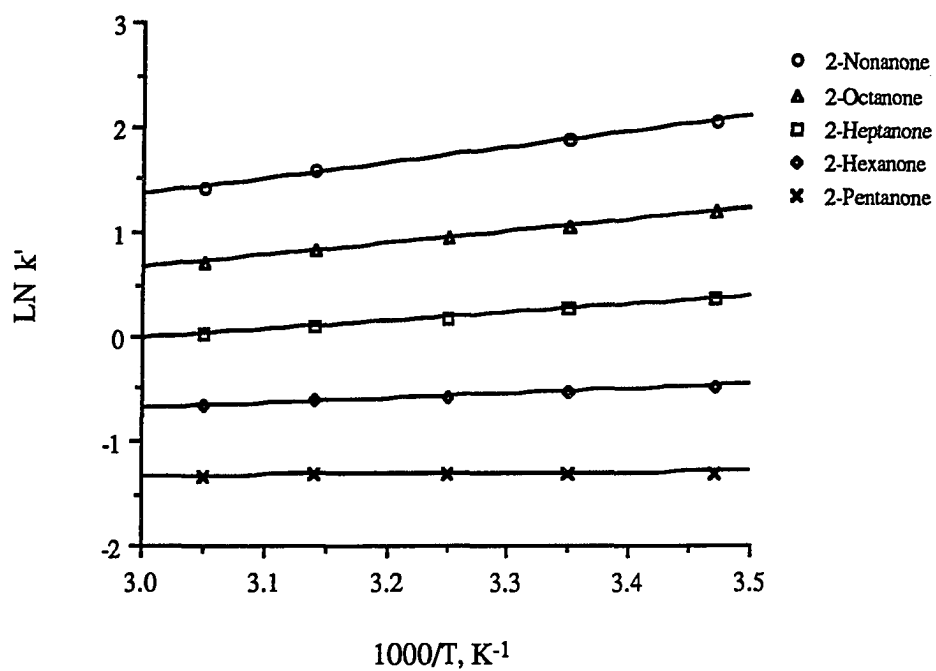


FIGURE 5.2. Van't Hoff plots for the retention of the 2-ketones for the Unisphere Al- C_{18} stationary phase using 30/70 MeCN/ H_2O as mobile phase.

In general, values of $-\Delta H^\circ$ for the test solutes considered were observed to be directly related to solute retention. That is, *values of $-\Delta H^\circ$ increase with increasing retention*. This trend can more easily be seen for a homologous series. For example, for the n-alkylphenones in Table 5.6 with 30% MeCN as mobile phase (Al-C₁₈ column), $-\Delta H^\circ$ increased from 1.69 kcal/mol for acetophenone to 3.23 kcal/mol for valerophenone. This trend is also consistent with the type of stationary phase or organic solvent used. In terms of stationary phase type, it has been shown in Chapter III that the LiChrospher Si-C₁₈ column is more retentive than the polymer-coated aluminas. This trend was also reflected in the $-\Delta H^\circ$ values, in general, although to a lesser degree. For example, $-\Delta H^\circ$ values for nitrobenzene with 30% MeCN as mobile phase are equal to 2.88 and 2.69 kcal/mol for the LiChrospher Si-C₁₈ and Al-C₁₈ columns, respectively. In terms of solvent type, the $-\Delta H^\circ$ values associated with the MeOH/H₂O system are much larger than those for the MeCN/H₂O system, a trend consistent with that observed on other silica-based C₁₈ columns by other investigators [11]. For example, for the Unisphere Al-PBD column in Table 5.5, observed $-\Delta H^\circ$ values for toluene were 2.45 kcal/mol with 30% MeCN and 3.59 kcal/mol with 30% MeOH.

Overall, the data for $-\Delta H^\circ$ in Tables 5.5-5.9 were comparable to values reported in the literature for other reversed-phase stationary phases [10]. For benzene derivatives, $-\Delta H^\circ$ values ranged from 2.9 to 5.8 kcal/mol using Permaphase ODS as stationary phase and 60/40 MeOH/H₂O as mobile phase. For alkylbenzenes and phenols, $-\Delta H^\circ$ values ranged from 3.5 to 6.5 kcal/mol using pyrocarbon as stationary phase and 80/20 MeOH/H₂O as mobile phase.

REFERENCES FOR CHAPTER V

1. Melander, W.; Campbell, D.E.; Horváth, C. *J. Chromatogr.*, **1978**, *158*, 215-225.
2. Sentell, K.B.; Dorsey, J.G. *J. Liq. Chromatogr.* **1988**, *11*, 1875-1885.
3. Kevin B. Holland, Biotage, Inc., personal communication by R.V. Arenas.
4. Snyder, L.R.; Kirkland, J.J. *Introduction to Modern Liquid Chromatography*, 2nd ed.; John Wiley & Sons, Inc.: New York, 1979; Chapter 7.
5. Majors, R.E. *Analysis*, **1975**, *10*, 549-550.
6. Arenas, R.V.; Foley, J.P. *Anal. Chim. Acta* **1991**, *246*, 113-130.
7. Gant, J.R.; Dolan, J.W.; Snyder, L.R. *J. Chromatogr.* **1979**, *185*, 153-177.
8. Knox, J.H.; Vasvari, G. *J. Chromatogr.* **1973**, *83*, 181-194.
9. Colin, H.; Diez-Masa, J.C.; Guiochon, G.; Czajkowska, T.; Miedziak, I. *J. Chromatogr.* **1978**, *167*, 41-65.
10. Melander, W.R.; Horváth, C. *Reversed-Phase Chromatography In High-Performance Liquid Chromatography-Advances and Perspectives*, Horváth, C., Ed.; Academic Press: New York, 1980; Vol. 2.
11. Stalcup, A.M.; Martire, D.E.; Wise, S.A. *J. Chromatogr.* **1988**, *442*, 1-14.

CHAPTER VI

POLAR GROUP SELECTIVITY OF POLYMER-COATED ALUMINAS

INTRODUCTION

As defined in the introduction section of Chapter IV, group selectivity (α) is based on the relative retention of two compounds differing only by the presence or absence of a particular group. Thus, nitro group selectivity (α_{NO_2}) can be determined from the relative retention of nitrobenzene and benzene (Eqn. 6.1), and similarly, hydroxyl group selectivity from the retention data of phenol and benzene (Eqn. 6.2).

$$\alpha_{\text{NO}_2} = \frac{k'_{\text{Nitrobenzene}}}{k'_{\text{Benzene}}} \quad (6.1)$$

$$\alpha_{\text{OH}} = \frac{k'_{\text{Phenol}}}{k'_{\text{Benzene}}} \quad (6.2)$$

Group selectivity values are important, because compared to other chromatographic parameters, α is the most directly related to the chemical nature of the stationary phase. The main objective of this part of the study is to determine unique retention characteristics and selectivities of the various Unisphere polymer-coated aluminas in comparison with conventional Si-C₁₈ columns from two manufacturers.

RESULTS AND DISCUSSION

Group selectivity values were evaluated for several aromatic compounds relative to the retention of benzene. The retention factors (k') used for calculating α for the different Unisphere polymer-coated aluminas and Si-C₁₈ columns are given in Tables 6.1-6.3. The retention data reported in Table 6.1 were obtained using 50/50 MeOH/H₂O as mobile phase, while k' values in Tables 6.2 and 6.3 are for the Al-PBD

TABLE 6.1. Retention factors of selected compounds for the various Unisphere polymer-coated aluminas and Si-C₁₈ columns with 50/50 MeOH/H₂O as mobile phase.

Compound	Al-PBD	Al-CN	Al-C ₁₈	Si-C ₁₈ (Microsorb, SN 10412)	Si-C ₁₈ (Microsorb, SN10788)	Si-C ₁₈ (LiChrospher)
Aniline	0.14	0.45	0.30	2.88	2.48	3.13
Phenol	0.15	0.61	0.36	1.29	1.00	1.41
Acetophenone	0.27	0.86	0.54	2.94	2.23	3.52
N-Methylaniline	0.35	1.44	0.72	9.72	5.00	8.64
Nitrobenzene	0.55	2.40	1.11	4.12	2.97	5.09
Methylbenzoate	0.61	1.84	1.21	6.26	4.52	7.72
Anisole	0.83	2.45	1.57	5.91	4.04	7.57
Benzene	0.95	2.21	1.75	6.13	4.07	7.83
Toluene	1.94	4.27	3.68	13.53	8.63	17.42

TABLE 6.2. Retention factors of selected compounds for the Al-PBD column at different MeOH/H₂O concentrations.

Compound	<u>% MeOH</u>					
	0	10	20	30	40	50
Aniline	0.53	0.42	0.31	0.25	(0.19)	(0.14)
Phenol	0.94	0.70	0.53	0.39	(0.24)	(0.15)
Acetophenone	2.29	1.54	1.04	0.68	0.42	0.27
N-Methylaniline	1.70	1.31	1.01	0.75	0.51	0.35
Nitrobenzene	3.19	2.53	1.96	1.41	0.90	0.55
Methylbenzoate	6.29	4.48	3.12	1.96	1.11	0.61
Anisole	5.54	4.33	3.31	2.29	1.42	0.83
Benzene	4.78	3.97	3.25	2.41	1.59	0.95
Toluene	—	12.23	9.24	6.21	3.65	1.94

TABLE 6.3. Retention factors of selected compounds for the Al-C₁₈ column at different MeOH/H₂O concentrations.

Compound	<u>% MeOH</u>					
	0	10	20	30	40	50
Aniline	2.18	1.27	0.84	0.68	0.42	0.30
Phenol	3.86	2.20	1.54	1.03	0.63	0.36
Acetophenone	—	5.99	3.16	1.82	0.97	0.54
N-Methylaniline	—	4.10	2.60	2.02	1.15	0.72
Nitrobenzene	—	7.69	5.33	3.42	1.97	1.11
Methylbenzoate	—	—	—	4.94	2.41	1.21
Anisole	—	—	—	5.17	2.85	1.57
Benzene	—	—	—	4.95	3.02	1.75
Toluene	—	—	—	—	7.04	3.68

and Al-C₁₈ columns, respectively, at different MeOH/H₂O concentrations. It should be noted that all k' data were obtained at 25.0° C. The corresponding group selectivity values calculated from these retention data are listed in Tables 6.4-6.6.

A. Hydrophobic Selectivity

Hydrophobic selectivity for the different stationary phases was determined from the relative retention of toluene and benzene ($R = -CH_3$ in Tables 6.4-6.6), which is numerically equal to the methylene group selectivity (α_{CH_2}) since toluene and benzene differ by only one methylene unit. Similar to the results discussed earlier in Chapter IV, the α_{CH_2} values given in Table 6.4 were approximately equal for all alumina- and silica-based columns, although in general, α_{CH_2} values were slightly higher for the Si-C₁₈ phases. More specifically, α_{CH_2} values for the aluminas are ≤ 2.10 , while those for the Si-C₁₈ columns are > 2.10 (Table 6.4). This implies that *the various polymer-coated aluminas employed in the study are slightly less hydrophobic than the Si-C₁₈ phases*, consistent with the more retentive nature (Chapter III) and higher $-\Delta H^\circ$ values (Chapter V) observed for the Si-C₁₈ phases.

B. Polar Group Selectivity

All of the group selectivity data in Table 6.4, except for $-CH_3$ (*i.e.*, α_{CH_2}), can be classified as polar group selectivity values. A very obvious trend in Table 6.4 is the large difference in magnitude between α_{CH_2} and the different polar selectivities. As can be seen in the table, α_{CH_2} values for all alumina- and silica-based phases are ≈ 2 , while most polar selectivity values (with a few exceptions the significance of which will be discussed later) are ≤ 1 . This trend can more easily be seen in Fig. 6.1, which shows the plots of the data in Table 6.4. The latter trend reinforces the conclusions made in Chapter IV regarding the advantage of using polymer-coated aluminas for the separation of homologs, and reflects the highly hydrophobic nature of these phases.

TABLE 6.4. Group selectivity values for the various Unisphere polymer-coated aluminas and Si-C₁₈ phases with 50/50 MeOH/H₂O as mobile phase. ^a

R Group ^b	Al-PBD	Al-CN	Al-C ₁₈	Si-C ₁₈ (Microsorb, SN 10412)	Si-C ₁₈ (Microsorb, SN 10788)	Si-C ₁₈ (LiChrospher)
-CH ₃	2.04	1.93	2.10	2.21	2.12	2.22
-COCH ₃	0.28	0.39	0.31	0.48	0.55	0.45
-COOCH ₃	0.64	0.83	0.69	1.02	1.11	0.99
-NH ₂	0.15	0.20	0.17	0.47	0.61	0.40
-NHCH ₃	0.37	0.65	0.41	1.59	1.23	1.10
-NO ₂	0.58	1.09	0.63	0.67	0.73	0.65
-OH	0.16	0.28	0.21	0.21	0.25	0.18
-OCH ₃	0.87	1.11	0.90	0.96	0.99	0.97

^a Group selectivity (α) = $k'_{\text{solute}}/k'_{\text{benzene}}$.

^b R represents the additional group attached to the benzene ring.

TABLE 6.5. Group selectivity values for the Al-PBD column at different MeOH/H₂O concentrations. ^a

R Group ^b	<u>% MeOH</u>					
	0	10	20	30	40	50
-CH ₃	—	3.08	2.84	2.58	2.30	2.04
-COCH ₃	0.48	0.39	0.32	0.28	0.26	0.28
-COOCH ₃	1.32	1.13	0.96	0.81	0.70	0.64
-NH ₂	0.11	0.11	0.10	0.10	0.12	0.15
-NHCH ₃	0.36	0.33	0.31	0.31	0.32	0.37
-NO ₂	0.67	0.64	0.60	0.59	0.57	0.58
-OH	0.20	0.18	0.16	0.16	0.15	0.16
-OCH ₃	1.16	1.09	1.02	0.95	0.89	0.87

^a Group selectivity (α) = $k'_{\text{solute}}/k'_{\text{benzene}}$.^b R represents the additional group attached to the benzene ring.TABLE 6.6. Group selectivity values for the Al-C₁₈ column at different MeOH/H₂O concentrations. ^a

R Group ^b	<u>% MeOH</u>		
	30	40	50
-CH ₃	—	2.33	2.10
-COCH ₃	0.37	0.32	0.31
-COOCH ₃	1.00	0.80	0.69
-NH ₂	0.14	0.14	0.17
-NHCH ₃	0.41	0.38	0.41
-NO ₂	0.69	0.65	0.63
-OH	0.21	0.21	0.21
-OCH ₃	1.04	0.94	0.90

^a Group selectivity (α) = $k'_{\text{solute}}/k'_{\text{benzene}}$.^b R represents the additional group attached to the benzene ring.

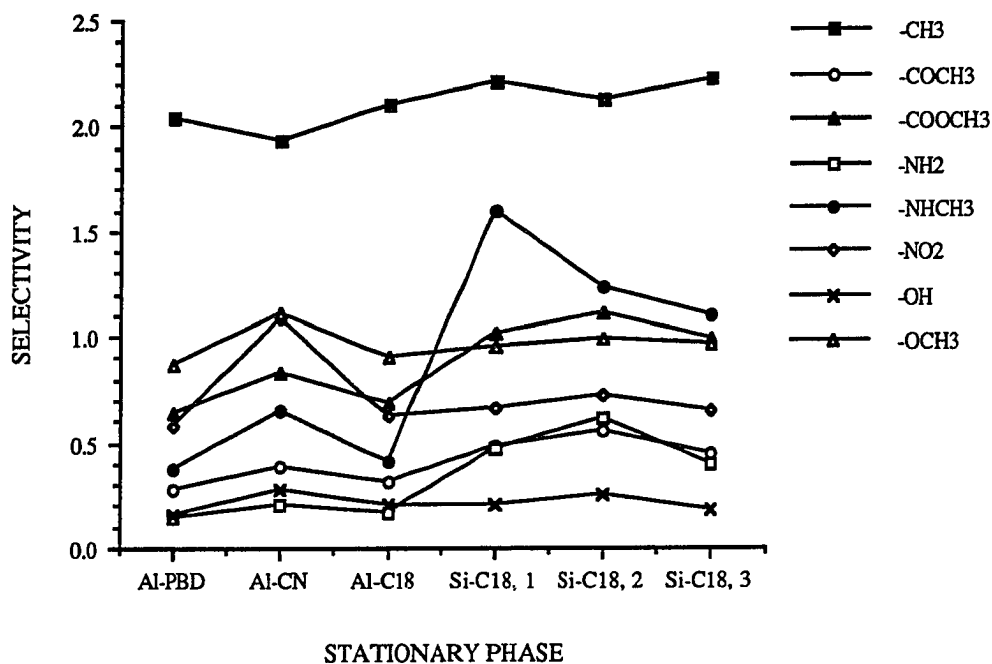


FIGURE 6.1. Group selectivity for the various Unisphere polymer-coated aluminas and Si-C₁₈ columns (Si-C18, 1 = Microsorb Si-C₁₈, SN 10788; Si-C18, 2 = Microsorb Si-C₁₈, SN 10412; Si-C18, 3 = LiChrospher Si-C₁₈) with 50/50 MeOH/H₂O as mobile phase at 25.0° C. (Same data as in Table 6.4.)

Among the Si-C₁₈ columns, group selectivity values were approximately equal except for a slightly greater difference in magnitude observed for -NH₂ and -NHCH₃ (the importance of which is discussed later in the text). For example, α values for -OCH₃ are 0.96, 0.99 and 0.97 for the two Microsorb and LiChrospher Si-C₁₈ columns, respectively. This is to be expected since all three stationary phases consist of -C₁₈ groups covalently bonded to the silica support.

Although it has been shown in Chapter IV and also in Part A of this section that the Al-PBD, Al-CN and Al-C₁₈ phases are similar in terms of hydrophobic selectivity, differences exist among these columns in terms of polar group selectivity. *Between Al-PBD and Al-C₁₈, polar group selectivities are approximately equal.* This is not surprising since both stationary phases have similar carbonaceous coatings on the alumina support, although the Al-C₁₈ phase possess -C₁₈ groups covalently bonded to the polymer. However, the presence of the -C₁₈ groups apparently does not make any difference in terms of polar group selectivities. For example, α values for -OCH₃ were 0.87 and 0.90 for the Al-PBD and Al-C₁₈, respectively. On the other hand, *higher polar group selectivity values were obtained for the Al-CN phase relative to those obtained for the Al-PBD and Al-C₁₈ phases*, with the greatest difference observed for the -NO₂ group. For example, α_{NO_2} values were 0.58, 0.63 and 1.09 for the Al-PBD, Al-C₁₈ and Al-CN columns, respectively. The higher polar group selectivity values obtained for the Al-CN stationary phase is most likely due to the more polar nature of the coating due to the presence of -CN groups on the stationary phase surface, which apparently interacts more with the polar groups of the test probes used, especially -NO₂. The concentration of these cyano groups, however, seems to be just enough to manifest the higher polar group selectivities for the Al-CN column, and still maintain a hydrophobicity similar to that of Al-PBD and Al-C₁₈.

It can be seen from Table 6.4 that $-\text{NO}_2$, $-\text{OH}$ and $-\text{OCH}_3$ selectivity values are approximately equal for the different polymer-coated aluminas and Si- C_{18} columns, except for the larger nitro group selectivity of Al-CN. At 50% MeOH, α_{NO_2} for Al-CN was 1.09 while those for the other columns (alumina- and silica-based) were all < 0.75 . Thus, nitrobenzene is retained more than benzene on the Al-CN column, although the reversed situation is true for the other columns (see k' values in Table 6.1). The higher retentivity of the Al-CN phase for compounds with an additional nitro group was also observed from the relative retentions of *m*-nitrotoluene and toluene, as can be seen from the k' values given in Tables 3.1A-3.4B, 3.6A and 3.6B. The k' values of *m*-nitrotoluene and toluene are almost equal for the Al-CN phase, while for the other columns the k' data of toluene is almost double that of *m*-nitrotoluene. For example, at 20% MeCN the k' of toluene and *m*-nitrotoluene are 11.16 and 7.41 for the Al- C_{18} column (Table 3.3A) while that for the Al-CN column are 13.74 and 13.96 (Table 3.6A), respectively. A similar relationship was also observed using MeOH/ H_2O as mobile phase, although this time the k' values for *m*-nitrotoluene were greater for the Al-CN column (Table 3.6B). The k' for *m*-nitrotoluene was 15.23 while that for toluene was 13.19 with 30% MeOH. Thus, α_{NO_2} will be > 1 for the Al-CN stationary phase with MeOH/ H_2O as mobile phase.

For $-\text{COCH}_3$, $-\text{COOCH}_3$, $-\text{NH}_2$ and $-\text{NHCH}_3$, the group selectivity values for the three Si- C_{18} columns were all larger than those of the polymer-coated aluminas. For example, $-\text{COOCH}_3$ selectivities for the LiChrospher Si- C_{18} was 0.99 while that of Al-PBD, Al- C_{18} and Al-CN were 0.64, 0.69 and 0.83, respectively (Table 6.4 and Fig. 6.1).

1. Surface Hydroxyl Group Participation In Solute Retention

Although polar group selectivity values for the Si- C_{18} columns were found to be (in general) larger than those of the aluminas, it is also important to compare the asymmetry

factors for these columns since resolution (R_s) depends not only on selectivity, but also on column efficiency (N) and k' as shown in Eqn. 6.3.

$$R_s = \frac{\sqrt{N}}{4} \left(\frac{\alpha-1}{\alpha} \right) \frac{k'_2}{1+k'_2} \quad (6.3)$$

Evaluation of peak asymmetry is essential especially for basic compounds (*e.g.* aniline and N-methylaniline) which exhibit severe band tailing on conventional Si-C₁₈ columns due to silanophilic interactions (*i.e.*, interactions with accessible hydroxyl groups on the stationary phase). It should be noted that severe band tailing and band broadening result in lower plate counts.

Peak asymmetry was calculated using Eqn. 6.4

$$As_{0.1} = \frac{b}{a} \quad (6.4)$$

where $As_{0.1}$ is the peak asymmetry value at 10% of peak height, and a and b are as defined in Fig. 6.2. According to Dolan and Snyder [1], excellent peak shapes are characterized by asymmetry factors of 1.00-1.05, while $As_{0.1} \geq 2.0$ is unacceptable.

The asymmetry factors obtained for the different columns are listed in Table 6.7. It can be seen that $As_{0.1}$ values for aniline and N-methylaniline are larger for the Si-C₁₈ columns compared to those obtained for the different polymer-coated aluminas, indicating a higher degree of interaction between these basic solutes and the free hydroxyl groups of the Si-C₁₈ phases. This is very obvious for the Si-C₁₈ phases since $As_{0.1}$ for the anilines are significantly larger than those of other compounds. For example, for the Rainin Microsorb column (SN 10788), $As_{0.1}$ for aniline and N-methylaniline are 2.1 and 2.4, respectively, while those for the other solutes are either

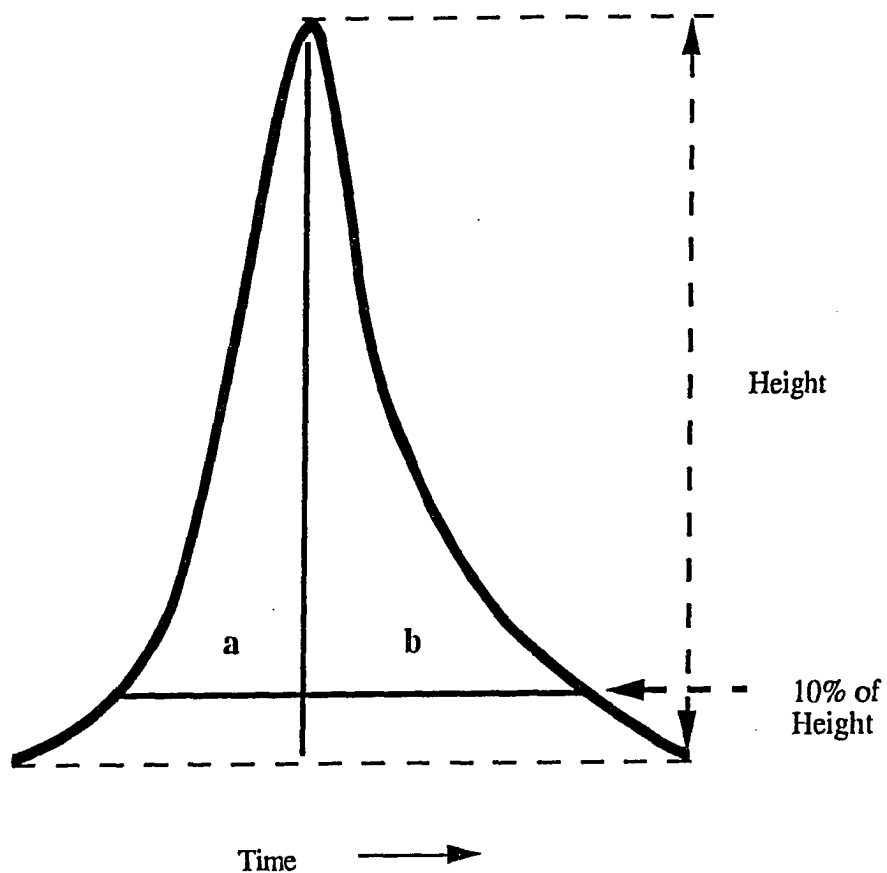


FIGURE 6.2. Calculation of peak asymmetry.

TABLE 6.7. Peak asymmetry factors for the different columns with 50/50 MeOH/H₂O as mobile phase. ^a

Compound	Al-PBD	Al-CN	Al-C ₁₈	Si-C ₁₈ (Microsorb, SN 10412)	Si-C ₁₈ (Microsorb, SN 10788)	Si-C ₁₈ (LiChrospher)
Benzene	1.4	1.7	1.6	1.9	1.2	1.6
Toluene	1.3	1.4	1.4	1.7	1.2	1.2
Acetophenone	1.9	1.9	1.6	1.8	1.2	1.6
Methylbenzoate	1.6	1.6	1.7	1.8	1.2	1.5
Aniline	2.0	2.3	1.9	2.7	2.1	4.6
N-Methylaniline	1.8	1.7	1.7	2.4	2.4	4.2
Nitrobenzene	1.7	1.7	1.7	1.8	1.2	1.7
Phenol	1.9	2.2	1.4	2.1	1.4	1.7
Anisole	1.6	1.6	1.7	1.7	1.4	1.4
$As_{0.1, \text{ aniline}}/As_{0.1, \text{ phenol}}$	1.1	1.1	1.4	1.3	1.5	2.7

^a Based on the average of three measurements.

1.2 or 1.4. This is not surprising since another study [2] has classified the Rainin column as unsuitable for separating basic samples. The situation is even worse for the LiChrospher Si-C₁₈ phase wherein $As_{0.1}$ for aniline and N-methylaniline are 4.6 and 4.2, respectively, while those for the other solutes are all < 2.0. It should be noted that the asymmetry values for the anilines for the Unisphere aluminas are also not outstanding, ranging from 1.7 to 2.3 (unacceptable by Dolan and Snyder's standard [1]). Unfortunately, it is difficult to conclude based on these values alone whether or not surface hydroxyl groups on the alumina support are accessible or are involved in solute retention since $As_{0.1}$ for the other solutes are of similar value, if not larger. A good example is the $As_{0.1}$ values for acetophenone and N-methylaniline for the Al-CN column, 1.9 and 1.7, respectively. For Al-C₁₈, $As_{0.1}$ was 1.7 for N-methylaniline, nitrobenzene, methylbenzoate and anisole.

Several other chromatographic test methods have been employed by other researchers to evaluate surface hydroxyl group participation in solute retention in RPLC (reviewed in references [3-5]), the simplest of which is the qualitative method of Rabel [3, 4] utilizing a mixture of aniline and phenol. According to Rabel [3, 4], aniline should elute before phenol for well deactivated phases, while aniline elutes after phenol for phases that have accessible -OH groups. However, unlike Rabel's method which employs 60/40 MeOH/H₂O as mobile phase, a 50/50 MeOH/H₂O mixture was used in this study to obtain higher k' values for the polymer-coated aluminas (Table 6.1). The mobile phase used in this study also satisfies the recommendations of Engelhardt *et al.* [5], that for the evaluation of the silanophilic properties of Si-C₈ and Si-C₁₈ columns, the mobile phase should contain < 60% H₂O to adequately wet the stationary phase. The usefulness of using the elution order of aniline and phenol to predict the presence of accessible -OH groups has been demonstrated by Lay *et al.* [6], and Engelhardt and Jungheim [7].

Table 6.1 shows that aniline elutes before phenol for all the polymer-coated aluminas, while as expected, the reverse situation is true for the Si-C₁₈ columns. For example, k' values for aniline and phenol are 0.45 and 0.61, respectively, for the Al-CN column. The same results are shown graphically in Fig. 6.3 wherein α values ($k'_{\text{phenol}}/k'_{\text{aniline}}$) for the aluminas are > 1 , while those for the Si-C₁₈ are < 1 . This implies that *the polymer-coating process utilized for the synthesis of the alumina-based stationary phases effectively shields the -OH groups of the alumina support, rendering these groups inaccessible for the solutes during the chromatographic separation.*

Although the use of aniline and phenol as test solutes to determine the suitability of a given column for separating basic samples seems to be appropriate for the Si-C₁₈ phases based on the retention data listed in Table 6.1, it appears to be somewhat inadequate for the less retentive polymer-coated aluminas, especially for the Al-PBD phase wherein the k' data are too small (0.14 and 0.15, respectively), and thus are more subject to errors in t_m . Although this can be easily remedied by using a weaker mobile phase, another set of test solutes can also be used (*e.g.* N-methylaniline and methylbenzoate). As seen in Fig. 6.3, N-methylaniline elutes before methylbenzoate for well deactivated phases (*i.e.*, for the polymer-coated aluminas), while for the Si-C₁₈ columns which have been shown to exhibit severe silanophilic interactions with basic solutes, N-methylaniline elutes after methylbenzoate. Similar results can also be obtained using nitrobenzene, anisole or benzene instead of methylbenzoate. It should be noted that unlike the retention data obtained for aniline and phenol, higher k' values were obtained for these test solutes with 50% MeOH. However, use of these alternative solute pairs still need further chromatographic testing.

According to Engelhardt and Jungheim [7], columns suitable for the separation of basic samples should satisfy the following: (1) aniline should elute before phenol, and the asymmetry ratio of aniline and phenol ≤ 1.3 ; and (2) o-, m- and p-toluidines should

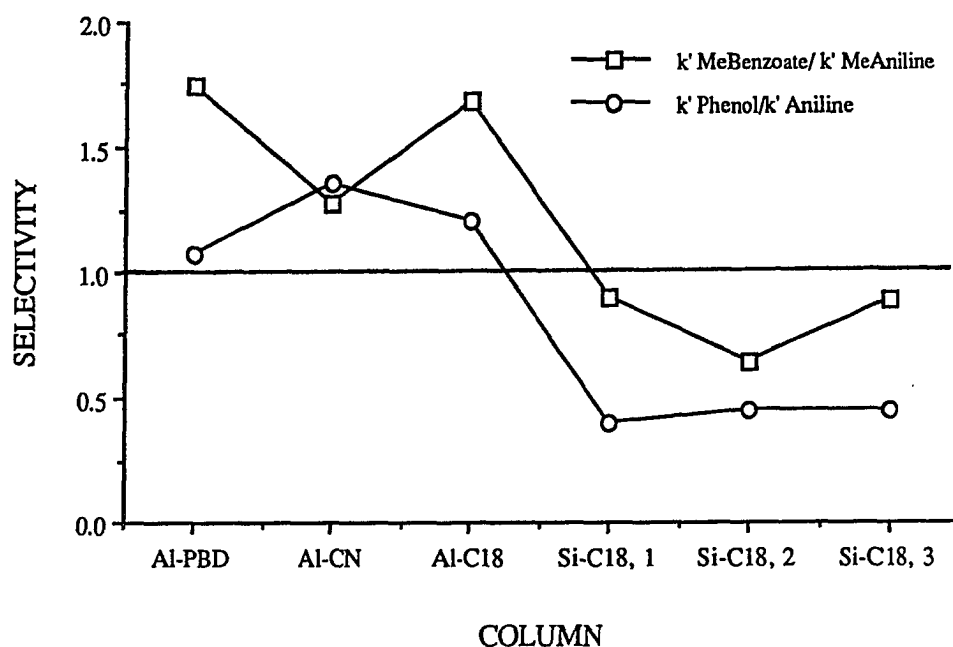


FIGURE 6.3. Surface hydroxyl group participation in solute retention as reflected by the selectivity values for phenol-aniline and methylbenzoate (MeBenzoate)-methylaniline (MeAniline) for the Unisphere polymer-coated aluminas and Si-C₁₈ columns (Si-C18, 1 = Microsorb Si-C₁₈, SN 10788; Si-C18, 2 = Microsorb Si-C₁₈, SN 10412; Si-C18, 3 = LiChrospher Si-C₁₈) with 50/50 MeOH/H₂O as mobile phase at 25.0° C.

coelute, or their k' ratios < 1.3 . From Tables 6.1 and 6.7, it is seen that both Al-PBD and Al-CN satisfy the first condition, and although the other requirement (2) has not been evaluated for the different columns used, it is apparent that *the polymer-coated Unisphere aluminas appear to be more suitable for the separation of basic samples compared to the Si-C₁₈ columns used in the study.*

2. Effect Of Mobile Phase Composition On Polar Group Selectivity

The dependence of polar group selectivity on mobile phase composition was similar to those obtained for methylene group selectivity (see related text in Chapter IV, and α_{CH_3} values in Tables 6.5 and 6.6). As seen in Tables 6.5 and 6.6, in general *polar group selectivity decreases with increasing % organic solvent*, at least with MeOH/H₂O as mobile phase for the Al-PBD and Al-CN columns. This trend can more easily be seen in Figs. A.4 and A.5 (in Appendix A), which illustrates the plots of the data given in Tables 6.5 and 6.6, respectively. For example, α_{COOCH_3} decreased from 1.32 to 0.64 from 0 to 50% MeOH for the Al-PBD column (Table 6.5). However, values for α_{NH_2} , α_{NHCH_3} and α_{OH} in both Tables 6.5 and 6.6 appear to remain approximately constant within the % MeOH range studied. For the Al-CN phase, α_{OH} remained at 0.21 from 30 to 50% MeOH as shown in Table 6.6. Another trend that can be observed from Figs. A.4 and A.5 (Appendix A) is that in general the rate of decrease of α_{CH_2} with increasing %MeOH is greater than those obtained for the various polar group selectivities.

Unfortunately, no polar group selectivity values were evaluated using MeCN/H₂O as mobile phase. However, α_{NO_2} values can be calculated from the retention data of m-nitrotoluene and toluene (Tables 3.1A-3.6B). A comparison of the nitro group selectivity obtained from such an approach is shown in Fig. 6.4 using 50% organic solvent (MeCN and MeOH) as mobile phase. As can be seen from the figure, in general larger nitro group selectivity values were obtained using 50% MeOH as mobile phase

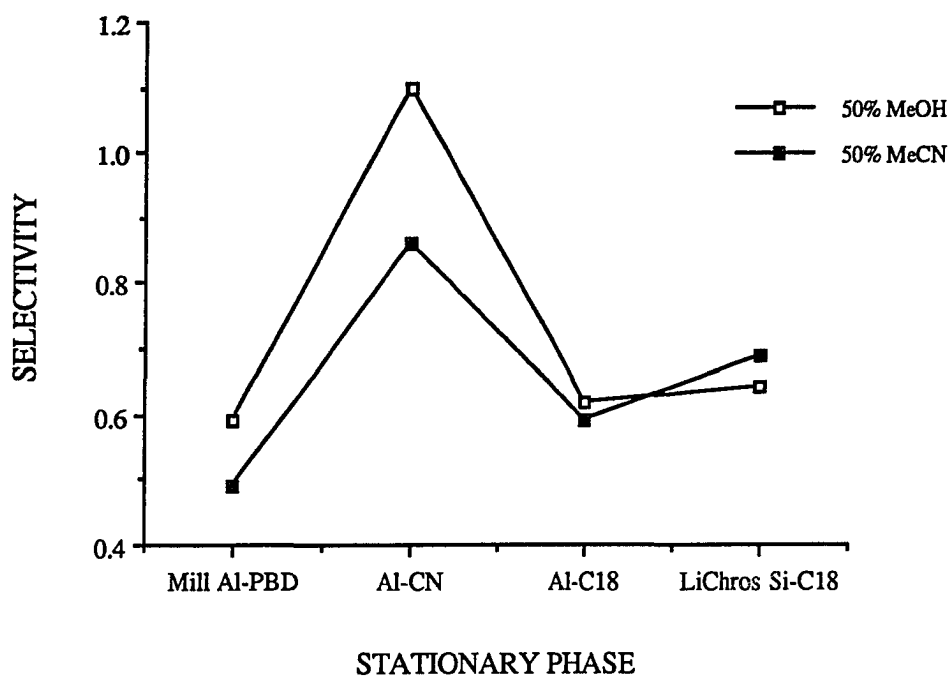


FIGURE 6.4. Comparison of the nitro group selectivity for the various polymer-coated aluminas and Si-C₁₈ column using 50% MeCN and 50% MeOH as mobile phases. Column identification: Mill Al-PBD = Millipore Al-PBD; LiChros Si-C18 = LiChrospher Si-C₁₈.

compared to those obtained with 50% MeCN, at least for the different polymer-coated aluminas used. It should be noted that the α_{NO_2} values obtained using the retention data of m-nitrotoluene and toluene were similar to those given in Table 6.4.

CONCLUSIONS

Although Si-C₁₈ polar group selectivity values are in general slightly higher than those obtained for the different polymer-coated aluminas, use of a weaker mobile phase on the aluminas will result in similar if not larger group selectivity values with equivalent or even smaller retention due to the less retentive nature of these columns. Thus, the use of polymer-coated alumina stationary phases may result in better separation resolution assuming the column efficiencies of the alumina- and silica-based columns are comparable (Eqn. 6.3). These conclusions are similar to those made in Chapter IV regarding methylene selectivity. Again, a detailed examination of the combined effects of α_{CH_2} , k' and N on resolution is discussed in Chapter VII of this dissertation.

REFERENCES FOR CHAPTER VI

1. Dolan, J.W.; Snyder, L.R. *Troubleshooting LC Systems*, The Humana Press Inc.: New Jersey, 1989; Chapter 14.
2. Stadalius, M.A.; Berus, J.S.; Snyder, L.R. *LC-GC* 1988, 6, 494-500.
3. Sander, L.C.; Wise, S.A. *CRC Crit. Rev. Anal. Chem.* 1987, 18, 299-415.
4. Sander, L.C. *J. Chromatogr. Sci.* 1988, 26, 380-387.
5. Engelhardt, H.; Löw, H.; Götzinger, W. *J. Chromatogr.* 1991, 544, 371-379.
6. Lay, B.M.; Ryall, R.R.; Lane, P.A. Presented at the 14th International Symposium on Column Liquid Chromatography, Boston, May 22, 1990; Paper P431.
7. Engelhardt, H.; Jungheim, M. *Chromatographia* 1990, 29, 59-68.

CHAPTER VII

KINETIC PERFORMANCE OF POLYMER-COATED ALUMINAS

INTRODUCTION

Evaluation of the kinetic performance of a column is important since this provides information related to the mass transfer characteristics of the stationary phase and packing efficiency (*i.e.*, how well the column was packed), allowing a fair comparison of columns manufactured using different technologies. As indicated by Bristow and Knox [1], identifying what types of mixtures are best resolved by a particular column is not of major importance in assessing kinetic performance, hence the test probes to be used should show the column at its best. In general, kinetic performance determines to what extent high plate count (N), short analysis time (t_R) and low pressure drop (ΔP) can be achieved simultaneously. The advantages and disadvantages of the different parameters related to kinetic performance are reviewed elsewhere [1-4].

The most popular measure of column efficiency is the plate number (N), which represents the extent of band broadening as a function of retention, the basic definition of which is given in Eqn. 7.1, where σ^2 is the peak variance. For symmetrical peaks

$$N = \frac{t_R^2}{\sigma^2} \quad (7.1)$$

with a Gaussian peak profile, N is most commonly evaluated using the half-height method (Eqn. 7.2), where $N_{0.5}$ is the plate count using the half-height method and $W_{0.5}$

$$N_{0.5} = 5.54 \left(\frac{t_R}{W_{0.5}} \right)^2 \quad (7.2)$$

is the peak width at half height. Typical values of N for 250 mm Si-C₁₈ columns packed with 5 μm particles are within 20,000 to 25,000 [3, 5]. However, for skewed or tailed peaks (*i.e.*, nonsymmetric peaks), use of Eqn 7.2 tends to overestimate N [6-8], and for these situations column efficiency is best measured using the Foley-Dorsey Equation, which is based on an exponentially modified Gaussian peak profile and is accurate to within $\pm 1.5\%$ [6,7].

$$N_{\text{Foley-Dorsey}} = \frac{41.7 \left(\frac{t_R}{W_{0.1}} \right)^2}{A_{S0.1} + 1.25} \quad (7.3)$$

Reduced Parameters

Although N is easily measurable and is proportional to resolution (Eqn. 6.3), comparison of N values for different columns is difficult since N depends on column length (L), particle diameter (d_p), flow rate (F), and other experimental (*i.e.*, operational) variables, the most important of which are mobile phase composition and temperature. On the other hand, the use of reduced parameters allows ready comparison of column performance with set standards. The recommended reduced variables useful for the evaluation of kinetic performance as suggested by Bristow and Knox [1] for liquid chromatographic columns are: (a) reduced plate height, h ; (b) reduced velocity, v ; (c) column resistance factor, ϕ ; and (d) separation impedance, E , mathematically defined in Eqns. 7.4-7.7, where H is the plate height which measures efficiency per unit length,

$$h = \frac{L}{Nd_p} = \frac{H}{d_p} \quad (7.4)$$

$$v = \frac{Ld_p}{t_m D_m} = \frac{u d_p}{D_m} \quad (7.5)$$

$$\phi = \left(\frac{d_p}{L} \right)^2 \frac{\Delta P t_m}{\eta} = \frac{d_p^2}{\kappa} \quad (7.6)$$

$$E = h^2\phi \quad (7.7)$$

D_m is the diffusion coefficient of the solute, ΔP is the pressure drop, η is the mobile phase viscosity, and K is the column permeability. Solute diffusion coefficients can be estimated using the Wilke-Chang Equation [9], where ψ_2 is the solvent association

$$D_m = \frac{7.4 \times 10^{-8}(\psi_2 M_2)^{0.5} T}{\eta V_1^{0.6}} \quad (7.8)$$

constant, which is 2.6 for H_2O and 1.9 for $MeOH$, M_2 is the solvent molecular weight, and V_1 is the molar volume of the solute. It should be noted that values of D_m estimated using the Wilke-Chang Equation is accurate only to *ca.* $\pm 20\%$. Note that reduced variables are independent of column length and particle diameter, and the lower the value of h , ϕ and E , the better the chromatographic quality of the column.

As indicated in Eqn. 7.4, the reduced plate height corresponds to the number of particles per plate. Reduced velocity (Eqn. 7.5) is the rate of flow relative to the rate of diffusion of solute over one particle diameter. Column resistance factor (Eqn. 7.6) is a function of column length, particle diameter and mobile phase viscosity. The parameter ϕ represents resistance to flow, evident from the pressure drop of the chromatographic system, with higher values resulting from either partial blockage (low K) or larger than actual particle diameter. Finally, separation impedance (Eqn. 7.7) is a parameter used to represent the optimum combination of plate height and permeability to flow. Large E values can result from either large h values (for inefficient columns) or excessive pressure drop. Characteristic values of h , v , ϕ , and E for excellent chromatographic columns are listed in Table 7.1. *Assuming that the column efficiencies of the polymer-coated aluminas are comparable to that of conventional Si-C₁₈ columns, lower ϕ and E*

TABLE 7.1. Limiting values of reduced parameters for excellent columns. ^a

Parameter	Values for well-packed columns	Source
h	2-4 ^b	[3]
	2-6	[4]
	2-10	[1]
ϕ	ca. 1500 ^c	[4]
	500-750 ^d	[1]
E	ca. 2000 ^e	[1]
	3000-5000	[5]

^a Recommended range for ν is within 3-20 for 5 and 10 μm particles [1, 4].

^b According to Pauls and McCoy [3], reduced plate heights < 10 are acceptable.

^c For porous spheres [4].

^d For slurry-packed, porous spheres [1].

^e Based on $h = 2$ and $\phi = 500$ [1].

values are expected for the aluminas if it is true that comparatively lower backpressures are obtained for these phases under identical separation conditions. The main objectives of this part of the study are (i) to evaluate at optimum and practical linear velocities the kinetic performance of the different Unisphere polymer-coated aluminas by comparing the measured parameters to recommended values and to values measured for two commercially available Si-C₁₈ columns; (ii) to evaluate and compare the normalized pressure drops (in terms of column length and particle diameter) obtained for the Unisphere aluminas to that of a Si-C₁₈ column, (iii) to determine the column stability of Al-CN and Al-C₁₈, and (iv) to determine and compare the combined effects of k' , α and N on resolution for certain test solutes. It should be noted that k' and α are thermodynamic factors that affect resolution.

RESULTS AND DISCUSSION

A. Comparison Of Pertinent Kinetic Parameters At Optimum Flow Rates

The dependence of column efficiency on mobile phase volumetric flow rate is commonly evaluated from plots of plate height vs. linear velocity, u , calculated using Eqn. 7.9. From plots of H vs. u (commonly called van Deemter plots) one can

$$u = \frac{L}{t_m} \quad (7.9)$$

determine what value of u provides maximum column efficiency (termed optimum linear velocity, u_{opt} , which corresponds to the lowest value of H), and the rate at which H increases with linear velocity.

Van Deemter plots for the three types of polymer-coated aluminas and a Si-C₁₈ column were constructed for different solutes (one unretained and the others with k' values between 1-3) using 60/40 MeOH/H₂O as mobile phase at 25.0° C. Plate height

values were determined based on N values using the half-height method (*i.e.*, $N_{0.5}$), and using flow rates ranging from 0.05 to 4.99 mL/min. Premixed mobile phases were employed in the study to eliminate volume changes and flow rate variations due to the mixing of MeOH and H₂O.

The van Deemter plots obtained for the polymer-coated aluminas and Microsorb Si-C₁₈ column are shown in Figs. 7.1-7.4. The kinetic parameters at optimum linear velocity are listed in Table 7.2, which also shows kinetic values for an Ultrasphere ODS column (considered representative of conventional reversed-phase columns by the authors) obtained from reference [5].

A closer look at the van Deemter plots for the aluminas (Figs. 7.1-7.3) reveals a broader minimum for the unretained solute (acetone), while the retained solutes displayed a more rapid loss in efficiency (increase in plate height) with increasing linear velocities, which is almost linear. Note that for the unretained solute, the increase in H with u is minimal (*i.e.*, less steep), especially up to 3 mm/s, and H remains almost constant for the Al-C₁₈ column (Fig. 7.3). On the other hand, the shape of the van Deemter curves were similar for the retained and unretained solutes for the Microsorb Si-C₁₈ column (Fig. 7.4), although the minimum for acetone is slightly broader. It should be noted that a completely opposite trend compared to that of the aluminas was observed for the Ultrasphere ODS packing [5] wherein the minimum of the van Deemter plot was broader for anisole and toluene while a more rapid decrease in column efficiency was observed for acetone.

From Table 7.2 it can be seen that for both stationary phase types (alumina- and silica-based), u_{opt} was within 0.12-0.67 mm/s which corresponds to flow rates ranging from 0.10 to 0.50 mL/min, and to reduced velocities ranging from 1.5 to 5.5 (which are acceptable according to the criteria listed in Table 7.1). However, in general u_{opt} for the aluminas are slightly lower ranging from 0.12 to 0.31 mm/s (0.10 to 0.25 mL/min). An

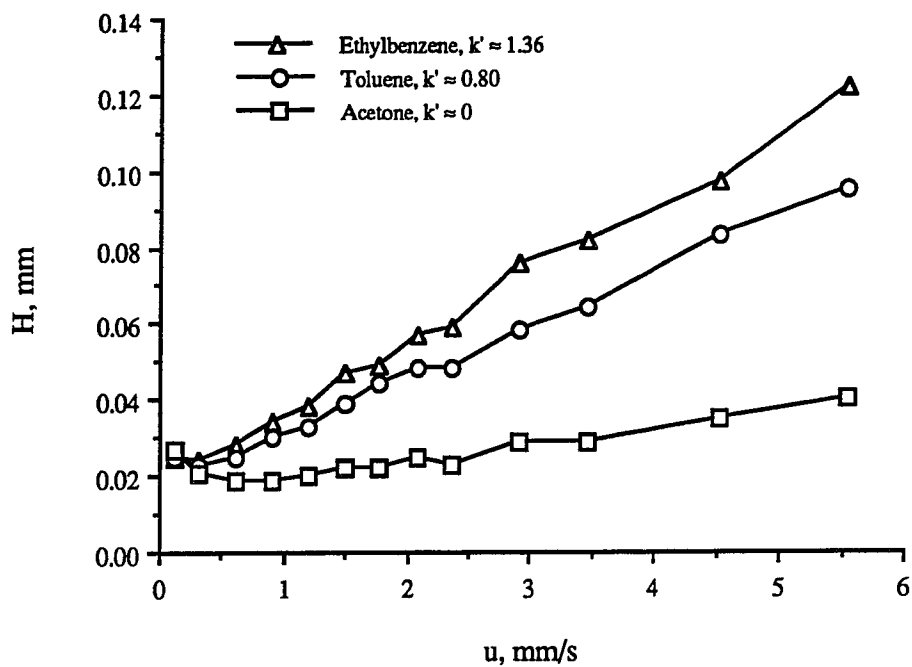


FIGURE 7.1. Van Deemter plot for the Unisphere Al-PBD column.

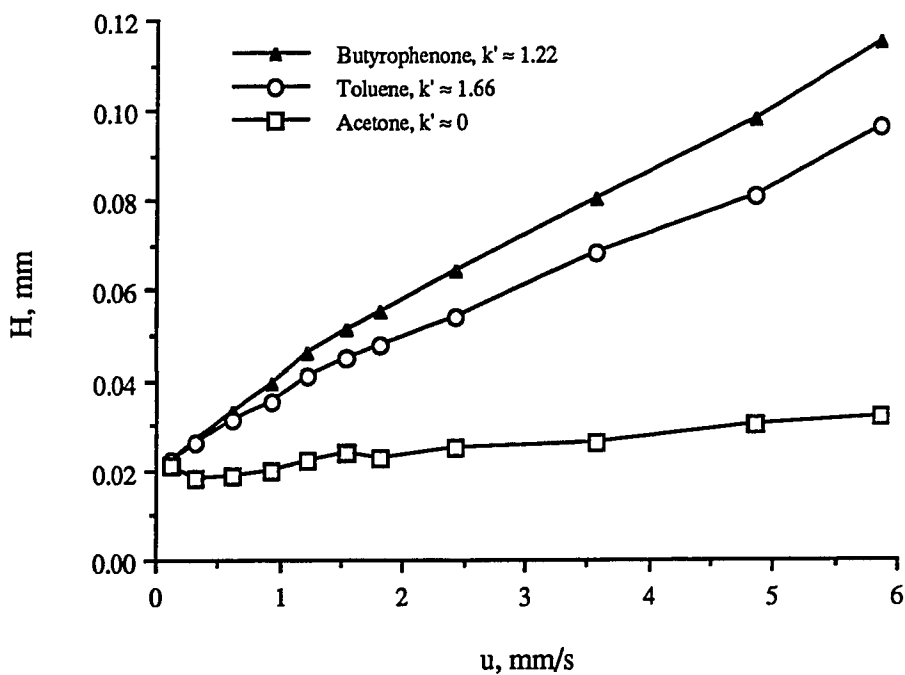


FIGURE 7.2. Van Deemter plot for the Unisphere Al-CN column.

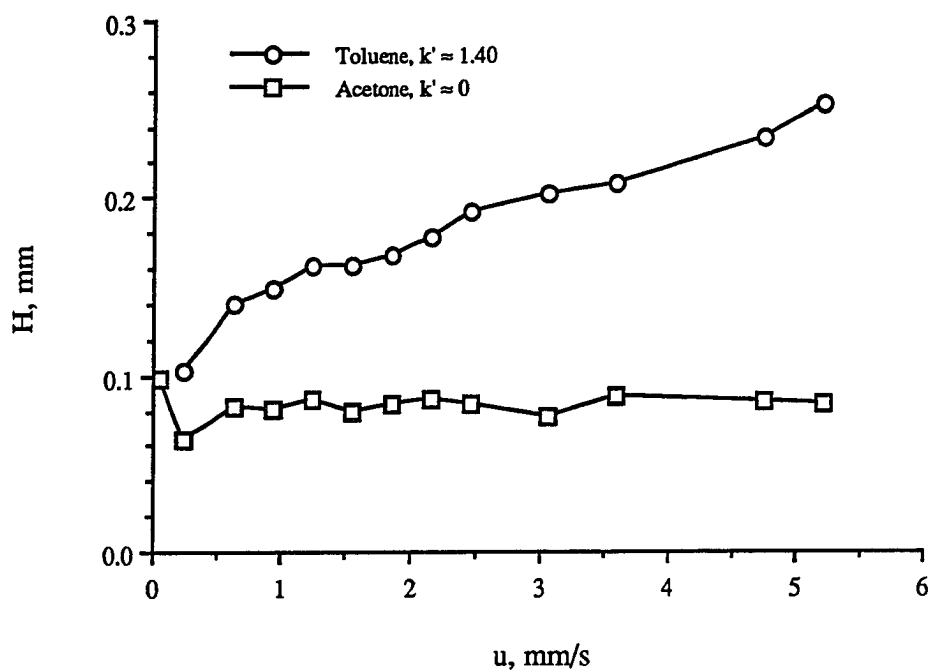


FIGURE 7.3. Van Deemter plot for the Unisphere Al-C₁₈ column.

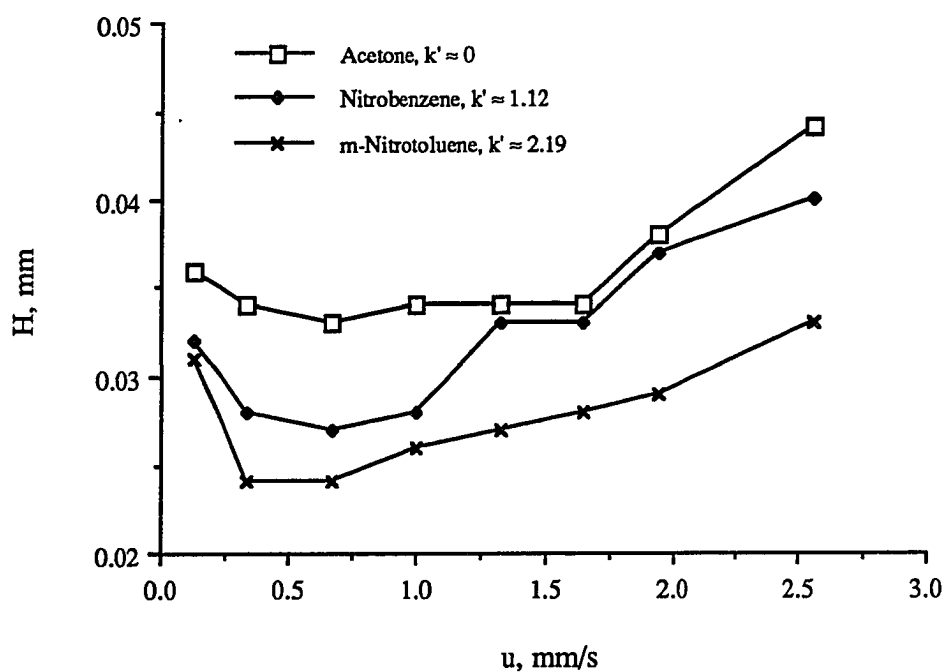


FIGURE 7.4. Van Deemter plot for the Microsorb Si-C₁₈ column (SN 10788).

TABLE 7.2. Comparison of pertinent kinetic parameters at optimum linear velocity. ^a

Column ^b	Solute	t _R (s)	k'	u _{opt} ^c (mm/s)	F (mL/min)	v	ΔP (bar)	H (mm)	N _{0.5}	N _{0.5} /s	N _{0.5} /bar	h	φ	E
Al-PBD	Acetone	413	0.00	0.61	0.50	5.5	66.7	0.019	13200	32.0	198	2.4	1860	10700
	Toluene	1480	0.80	0.30	0.25	3.7	36.0	0.023	10900	7.36	303	2.9	1000	8410
	Ethylbenzene	1933	1.36	0.30	0.25	4.0	36.0	0.024	10400	5.38	289	3.0	1000	9000
Al-CN	Acetone	802.8	0.00	0.31	0.25	2.8	45.6	0.018	13900	17.3	305	2.2	2470	12000
	Butyrophenone	4432	1.22	0.12	0.10	1.9	6.80	0.022 ^d	11400	2.57	1680	2.8	368	2880
	Toluene	5329	1.66	0.12	0.10	1.5	6.80	0.022 ^d	11400	2.14	1680	2.8	368	2880
Al-C ₁₈	Acetone	985.8	0.00	0.25	0.20	2.3	20.4	0.064	3910	3.97	192	8.0	1360	87000
	Toluene	2358	1.40	0.25	0.20	3.1	20.4	0.102 ^d	2450	1.04	120	12.8	1360	223000
Si-C ₁₈ (Microsorb)	Acetone	223	0.00	0.67	0.50	3.8	85.71	0.033	4540	20.4	53.0	6.6	1400	61000
	Nitrobenzene	471	1.12	0.67	0.50	5.0	85.71	0.027	5560	11.8	64.9	5.4	1400	40800
	m-Nitrotoluene	1400	2.19	0.34	0.25	2.8	44.9	0.024	6250	4.46	139	4.8	732	16900
Si-C ₁₈ ^e (Ultrasphere)	Toluene	592	2.50	1.48	1.0	5.7	119	0.011	21800	36.8	183	2.3	1070	5650

^a Mobile Phase: 60/40 MeOH/H₂O; Temperature: 25.0° C.^b For Unisphere polymer-coated aluminas: L = 250 mm; d_p = 8 μm.
For Si-C₁₈ (Microsorb, SN 10788): L = 150 mm; d_p = 5 μm.^c Determined by inspection of Figs. 7.1-7.4.^d It is possible that the minimum H values for these systems occurs at lower linear velocities, which unfortunately were not evaluated.^e Data obtained from reference [5] wherein a conventional 250 x 4.6 mm RPLC column (Ultrasphere ODS; d_p = 5 μm) was used with 60/40 MeCN/H₂O as mobile phase.

exception was observed for acetone for the Al-PBD phase wherein u_{opt} was 0.61 mm/s corresponding to an F value of 0.50 mL/min. The optimum linear velocity was slightly higher for the Microsorb Si-C₁₈ ranging from 0.34-0.67 mm/s, equivalent to flows of 0.25-0.50 mL/min. Even larger u_{opt} values were observed by McCoy and Pauls [5], corresponding to flow rates of 1.0 and 2.0 mL/min for the Ultrasphere 5 μ m Si-C₁₈ and Perkin-Elmer 3 μ m Si-C₁₈ columns, respectively.

In the succeeding discussion the values of the different kinetic parameters at optimum linear velocity for the polymer-coated aluminas will be compared to those obtained by McCoy and Pauls [5] for the Ultrasphere Si-C₁₈ column as given in Table 7.2. In terms of column efficiency, the Microsorb Si-C₁₈ columns used in the study unfortunately are not representative of highly efficient Si-C₁₈ columns commercially available since as noted in Chapter 3, the Microsorb columns employed have already been used extensively, thus the high reduced plate heights in Table 7.2, ranging from 4.8 to 6.6.

At optimum linear velocity, comparable reduced plate heights were obtained for the Al-PBD, Al-CN and Ultrasphere Si-C₁₈ columns, although h values for the retained solutes are slightly better for the silica-based column (Table 7.2). Reduced plate height for the Si-C₁₈ was 2.3 while those for the aluminas were between 2.8 and 3.0. However, the minimum h values obtained for the Al-C₁₈ were unacceptable, 8.0 and 12.8 for acetone and toluene, respectively. Similar unacceptable h values were obtained for another brand-new Al-C₁₈ column (SN B-0013), which implies that a definite improvement in the mass transfer characteristics is needed for this stationary phase for improved column efficiency. This recommendation, however, assumes that both Al-C₁₈ columns were packed properly, using particles with a narrow PSD. The poor column efficiency of the Al-C₁₈ relative to the other columns used can also be seen in Figs. 7.5

and 7.6 wherein van Deemter plots are shown for retained ($k' = 1.12$ to 1.22) and unretained solutes, respectively.

The reduced plate height for the same Al-PBD column used as determined by Biotage was 3.172 ($N = 9852$; $H = 0.02538$ mm) for *o*-xylene ($t_R = 9.291$ min) with 55/45 MeCN/H₂O at 0.5 mL/min at ambient temperature [10]. This is close to the h values determined in this study at 0.25 mL/min (at u_{opt}) for toluene and ethylbenzene, 2.9 and 3.0 (Table 7.2), respectively, using 60% MeOH. At 0.50 mL/min, h values determined for the same solutes and mobile phase were 3.1 and 3.4, respectively.

The poor column efficiency of the Al-C₁₈ phase may be due to the inherent difficulty involved in obtaining a thin, uniform coating for this stationary phase. It should be noted the mechanical and chemical stability of the coating depends on the degree of polymerization and crosslinking of the parent polymer, and that among the different polymer-coated aluminas employed (Al-PBD, Al-CN and Al-C₁₈), only the Al-C₁₈ coating possess bulky (-C₁₈) groups on the support surface, which can extend in all directions during the synthesis of the stationary phase. Unfortunately, no direct evidence is provided for this hypothesis.

Although the ϕ and E values for the Al-PBD, Al-CN and Ultrasphere Si-C₁₈ (Table 7.2) are in general within the range for excellent columns as prescribed in Table 7.1, especially for the retained solutes, a valid comparison of these parameters at optimum conditions is not possible since u_{opt} is different for the different solute-column combinations (ranging from 0.12 to 1.48 mm/s), and mobile phases differing significantly in viscosity were employed (60/40 MeOH/H₂O in this study and 60/40 MeCN/H₂O by McCoy and Pauls [5]). Higher ϕ and E values are expected for higher u_{opt} values and more viscous solvents. However, unacceptable E values were still obtained for the Al-C₁₈ and Microsorb Si-C₁₈ columns due to large h values for these columns. Similar arguments can also be made regarding the comparison of the number

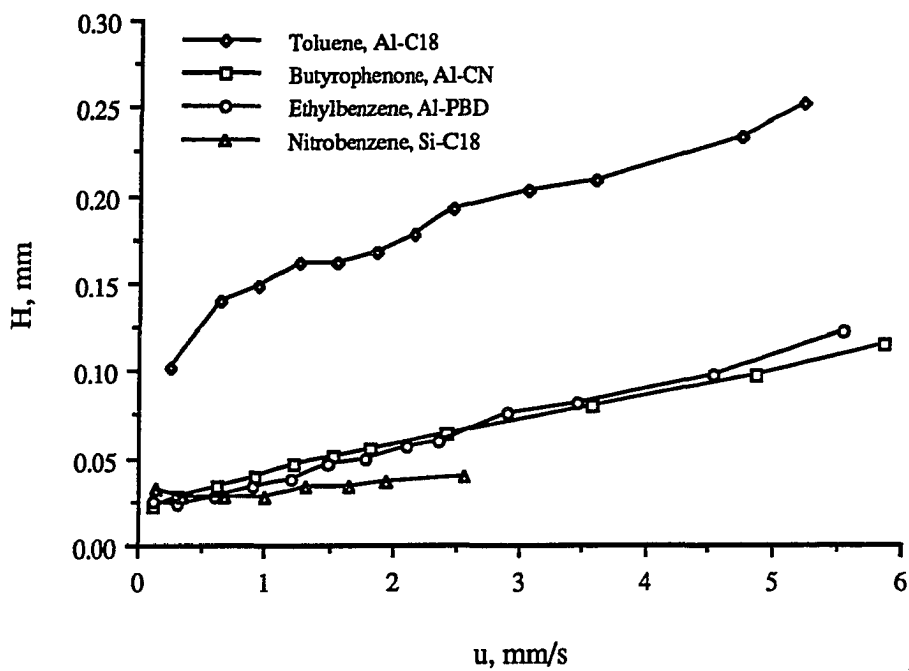


FIGURE 7.5. Van Deemter plots for retained solutes for all columns.

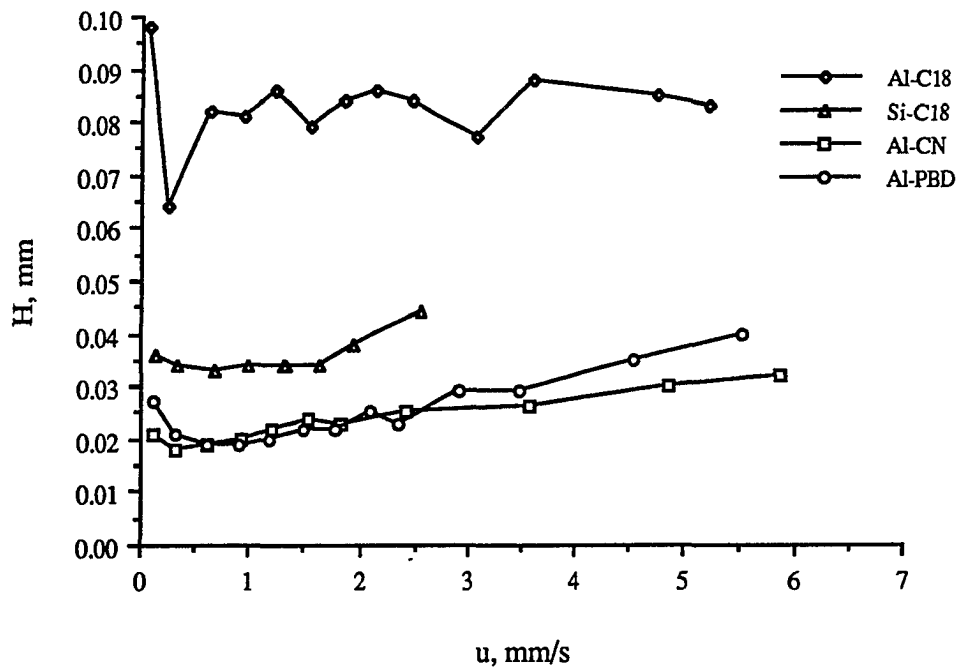


FIGURE 7.6. Van Deemter plots for acetone for all columns.

of plates generated per unit time ($N_{0.5}/s$) and per unit pressure drop ($N_{0.5}/bar$), hence valid comparisons of these values for the different columns are also not possible.

B. Comparison Of Pertinent Kinetic Parameters At Practical Flow Rates

The lower u_{opt} values, slightly larger h values at u_{opt} , and the more rapid decrease in column efficiency with increasing linear velocity observed for the polymer-coated aluminas versus the Si-C₁₈ columns impose a very serious drawback in utilizing these columns for rapid chromatographic analysis which is most commonly and easily accomplished by increasing the mobile phase flow rate. It should be noted that in actual runs, use of u_{opt} to achieve the highest separation efficiency possible is impractical because of the long analysis times involved. This is especially true for the aluminas since they have much lower u_{opt} values. For example, elution of toluene at u_{opt} takes 592, 1480, 2358 and 5329 seconds for the Ultrasphere Si-C₁₈, Al-PBD, Al-C₁₈ and Al-CN columns, respectively, even though k' is largest for the Si-C₁₈ column (2.50, 0.80, 1.40 and 1.66, respectively; see Table 7.2).

Higher flow rates (than u_{opt}) are employed to achieve shorter run times, but often result in a significant decrease in column efficiency, the exact magnitude of which depends on the steepness of the curves (Figs. 7.1-7.6). To demonstrate the effect of higher flow rates on column efficiency and other pertinent kinetic parameters, the corresponding values for these parameters were evaluated at 2.0 mL/min for the Unisphere aluminas, and at 1.0 mL/min for the silicas for nitrobenzene and toluene. The flow rate employed for the 25 cm Unisphere columns was double that of the 15 cm Si-C₁₈ columns since it was observed that approximately equal elution times were obtained for solutes with similar k' values using these flow rates. Note that in actual analysis, it is elution time and not k' which determines how long the last analyte will come out of the column.

The kinetic values at elevated flow rates for the alumina- and silica-based columns are given in Tables 7.3 and 7.4 for nitrobenzene and toluene, respectively. In contrast to Table 7.2, N , h and E were also calculated using the Foley-Dorsey method.

As stated earlier, acceptable h values were obtained at optimum linear velocities for retained solutes for the Al-PBD and Al-CN columns, ranging from 2.8 to 3.0 using the half-height method. However, significantly larger h values were obtained for all the polymer-coated aluminas at 2.0 mL/min, while the decrease in efficiency was much less for the Microsorb Si-C₁₈ (SN 10788). Note that for the Si-C₁₈, column data for comparing kinetic values at optimum and practical velocities are available only for the Microsorb column with serial number 10788 (Tables 7.2-7.4). The corresponding decrease in efficiencies for the aluminas was within 50 to 80%, while that for the Si-C₁₈ was only approximately 10%. Even lower h values were obtained using the Foley-Dorsey Equation. As can be seen in Fig. 7.5, this larger reduction in efficiency observed for the Unisphere columns is mainly due to the steeper van Deemter curves for these columns compared to that of the Si-C₁₈. The slope of the curves were approximately equal for the aluminas, but larger than that for the Si-C₁₈.

Among the polymer-coated aluminas, the lowest h values at practical flow rates were observed for Al-PBD, 5.73 and 7.23 for nitrobenzene and toluene, respectively, using half-height (Tables 7.3 and 7.4). However, these values are still larger than those for the three Si-C₁₈, ranging from 3.00 to 5.42. The worst reduced plate heights were obtained for Al-C₁₈, 30.3 and 26.7 for nitrobenzene and toluene, respectively, which are unacceptable by any standard. For the Al-CN column, reduced plate heights were 11.5 and 10.8, respectively.

Flow resistance (ϕ) was within acceptable limits for good quality columns, ranging from 812 to 1300 for all the aluminas and silicas. Hence, reasonable backpressures were obtained for all columns used. However, very large E values were observed for

TABLE 7.3. Comparison of pertinent kinetic parameters for the different polymer-coated aluminas and Si-C₁₈ columns for nitrobenzene at practical flow rates. ^a

Parameter	Al-PBD	Al-CN	Al-C ₁₈	Si-C ₁₈ (Microsorb, #10412)	Si-C ₁₈ (Microsorb, #10788)	Si-C ₁₈ (LiChrospher)
L, mm	250	250	250	150	150	125
t _m , s	104.9	103.9	101.2	92.88	101.0	69.00
d _p , μm	8	8	8	5	5	5
F, cm ² /min	2.00	2.00	2.00	1.00	1.00	1.00
υ	30.3	30.6	31.4	12.8	11.8	14.4
ΔP, bar	178.9	191.2	200.0	157.8	146.3	117.7
ε _{Total} ^b	0.84	0.83	0.81	0.62	0.68	0.73
k'	0.55	2.40	1.11	4.12	2.97	5.09
φ	1200	1270	1300	1020	1030	812
A. Using the half-height equation (Eqn. 7.2) for N:						
N _{0.5}	5450	2710	1030	7540	5540	6080
H, mm	0.0459	0.0922	0.243	0.0199	0.0271	0.0206
h	5.73	11.5	30.3	3.98	5.42	4.11
E	39400	168000	1190000	16200	30300	13700
B. Using the Foley-Dorsey equation (Eqn. 7.3) for N:						
As _{0.1}	1.7	1.7	1.7	1.8	1.2	1.7
N _{Foley-Dorsey}	2930	1660	681	3820	4870	3800
H, mm	0.0853	0.151	0.367	0.0393	0.0308	0.0329
h	10.7	18.8	45.9	7.85	6.16	6.58
E	137000	449000	2740000	62900	39100	35200

^a MP: 50/50 MeOH/H₂O at 2.0 mL/min for the polymer-coated aluminas and 1.0 mL/min for the Si-C₁₈ columns; T: 25.0° C. Note here that analysis time are comparable at these flow rates.

^b $\epsilon_{\text{Total}} = \frac{4F}{\pi D_c^2 u}$ where ϵ_{Total} is the total column porosity and D_c is the column inner diameter. Note that $\epsilon_{\text{Total}} = \epsilon_e + \epsilon_i$ where ϵ_e is the interstitial (or external) porosity and ϵ_i is the intraparticle (or internal) porosity.

TABLE 7.4. Comparison of pertinent kinetic parameters for the different polymer-coated aluminas and Si-C₁₈ columns for toluene at practical flow rates. ^a

Parameter	Al-PBD	Al-CN	Al-C18	Si-C ₁₈ (Microsorb, #10412)	Si-C ₁₈ (Microsorb, #10788)	Si-C ₁₈ (LiChrospher)
L, mm	250	250	250	150	150	125
t _m , s	104.9	103.9	101.2	92.88	101.0	69.00
d _p , μm	8	8	8	5	5	5
F, cm ² /min	2.00	2.00	2.00	1.00	1.00	1.00
υ	31.1	31.4	32.2	13.2	12.1	14.8
ΔP, bar	178.9	191.2	200.0	157.8	146.3	117.7
ε _{Total} ^b	0.84	0.83	0.81	0.62	0.68	0.73
k'	1.94	4.27	3.68	13.53	8.63	17.42
φ	1200	1270	1300	1020	1030	812
A. Using the half-height equation (Eqn. 7.2) for N:						
N _{0.5}	4320	2900	1170	7850	5950	8340
H, mm	0.0579	0.0862	0.214	0.0191	0.0252	0.0150
h	7.23	10.8	26.7	3.82	5.04	3.00
E	62700	148000	927000	14900	26200	7310
B. Using the Foley-Dorsey equation (Eqn. 7.3) for N:						
As _{0.1}	1.3	1.4	1.4	1.7	1.2	1.2
N _{Foley-Dorsey}	3420	2200	999	4490	5470	7850
H, mm	0.0731	0.114	0.250	0.0334	0.0274	0.0159
h	9.14	14.2	31.3	6.68	5.48	3.19
E	100000	256000	1270000	45500	30900	8260

^a MP: 50/50 MeOH/H₂O at 2.0 mL/min for the polymer-coated aluminas and 1.0 mL/min for the Si-C₁₈ columns; T: 25.0° C. Note here that analysis time are comparable at these flow rates.

^b $\epsilon_{\text{Total}} = \frac{4F}{\pi D_c^2 u}$ where ϵ_{Total} is the total column porosity and D_c is the column inner diameter. Note that $\epsilon_{\text{Total}} = \epsilon_e + \epsilon_i$ where ϵ_e is the interstitial (or external) porosity and ϵ_i is the intraparticle (or internal) porosity.

both column types, due mainly to the large h values for the corresponding columns. Consistent with the h values, significantly larger E values were observed for the polymer-coated aluminas versus the Si-C₁₈ columns, ranging from 39,400 to 1,190,000 for the aluminas, and 7,310 to 30,300 for the Si-C₁₈ columns for toluene and nitrobenzene based on the half-height method.

C. Comparison Of Pressure Drops Over A Range Of Flow Rates

As indicated in Chapter I, the unique morphology of the Unisphere alumina backbone *supposedly* allows the use of packed columns at higher flow rates with relatively lower back pressures (*i.e.*, compared to conventional RPLC columns) [11-14]. This, in turn, should allow (i) the use of longer columns for higher plate counts, (ii) the employment of higher flow rates for shorter analysis time, and (iii) the use of higher viscosity solvents, if necessary. If lower system backpressures are *truly* attainable with the Unisphere columns, then combining the use of longer columns with higher mobile phase flow rate resulting in equivalent analysis time versus Si-C₁₈ columns may offset the lower efficiency observed for the aluminas relative to conventional 150 mm or shorter Si-C₁₈ columns. If the efficiency of the polymer-coated aluminas can be improved, and the van Deemter curves made less steep than those shown in Figs. 7.1-7.3, the lower backpressures claimed for these columns would lead to a definite decrease in analysis time if higher flow rates are employed. For the 8 μ m particles, the prescribed maximum operating pressure for the Al-PBD is 6000 psi (408 bars), while the recommended maximum flow rate is between 10 to 12 mL/min, depending on the mobile phase [10]. Similar recommendations are anticipated for the Al-CN and Al-C₁₈ columns. It should be noted that the major objective in synthesizing alumina-based stationary phases is to take advantage of its inherently wider pH stability.

The mobile velocity along the column in LC is related to the column parameters d_p and L by Darcy's Law (Eqn. 7.10). The term κ_o is the specific permeability coefficient, calculated using Eqn. 7.11, where ϵ_e is the interparticle (or external) porosity, defined as the fraction of column volume available to the flowing solvent. Equation 7.12 (obtained from Eqn. 7.10) relates ΔP to column length and packing particle diameter. According

$$u = \frac{\Delta P \kappa}{\eta L} = \frac{\Delta P d_p^2}{\phi \eta L} = \frac{\Delta P \kappa_o}{\epsilon_e \eta L} \quad (7.10)$$

$$\kappa_o = \frac{\epsilon_e^3}{180(1-\epsilon_e)^2} \quad (7.11)$$

$$\Delta P = \frac{u \eta \phi L}{d_p^2} \quad (7.12)$$

to Eqn. 7.12, at a given mobile phase velocity ΔP is expected to increase with increasing column length and with decreasing particle diameter (or more correctly with decreasing d_p^2). More importantly, Eqn. 7.12 indicates that a valid comparison of column pressure drop can be achieved by comparing values of $(\Delta P d_p^2/L)$ using the same mobile phase at equal velocity.

Differing conclusions have been reported regarding the comparison of pressure drop for the Unisphere alumina-based columns and other packing materials. Reports by researchers from Alcoa [11, 12, 15] show that the backpressures obtained (i) for 10 μm Unisphere alumina (*i.e.*, unmodified alumina) were less than that for similarly-sized irregularly-shaped alumina and spherical microporous aluminas with 85/15 Isooctane/MeOH as mobile phase; and (ii) for an 8 μm Unisphere C-18 were less than those for a 10 μm Alcobond C-18 with 30/30/40 MeOH/MeCN/H₂O as mobile phase. Note that for both the latter Unisphere C-18 and Alcobond C-18 columns, the C₁₈ group is covalently bonded to the alumina support. Note also that in both studies the columns employed were of the same dimensions (*i.e.*, column length and inner diameter),

although the difference in d_p was not considered in the latter comparison. Nevertheless, the difference in ΔP for the C_{18} bonded aluminas will increase when normalized for d_p , favoring the Unisphere C-18 column.

Surprisingly, comparison of the pressure drops obtained for a 250 x 4.6 mm Unisphere Al-PBD ($d_p = 8 \mu\text{m}$) and a 150 x 4.6 mm Vydac ODS ($d_p = 5 \mu\text{m}$) at the same flow rates with 15/85 MeCN/0.1% aqueous TFA solution as mobile phase reveals that ΔP is actually lower for the Vydac ODS material, when normalized for both column length and particle diameter [16]. To normalize the backpressures for column length, Haky *et al.* [16] simply divided ΔP by L . However, to correct for discrepancies due to difference in particle size, they multiplied $\Delta P/L$ for the ODS phase by the factor 25/64, which corresponds to the ratio of the squares of the particle diameters of the Si- C_{18} and Al-PBD columns. Such an approach is valid since as can be seen in Eqn. 7.12, $\Delta P \propto 1/d_p^2$.

In a very similar study, Haky *et al.* [17] compared the ΔP values obtained at different flow rates for a 250 x 4.6 mm Unisphere ODA column ($d_p = 8 \mu\text{m}$) to that of a 150 x 4.6 mm Vydac ODS column ($d_p = 5 \mu\text{m}$). However, in contrast to the results of the previous study [16], they observed that the backpressures obtained at any given flow rate for the Unisphere ODA was substantially lower than that of the ODS column. Unfortunately, unlike the previous report [16], both ODA and ODS columns were normalized for differences in column length by dividing ΔP by the square of the column length. It should be noted that such an approach is not valid since according to Eqn. 7.12, ΔP is proportional to L , and not to L^2 .

Figure 7.7 shows a comparison of normalized pressure drops (*i.e.*, $\Delta P d_p^2/L$ values) obtained for three Unisphere polymer-coated aluminas and two Si- C_{18} columns. The backpressure values were obtained simultaneously with the determination of the van Deemter plots, with 60/40 MeOH/H₂O as mobile phase at room temperature. No ΔP

values were obtained for the Si-C₁₈ columns at flow rates greater than 2.50 mL/min since at such settings ΔP exceeded 6000 psi, the maximum recommended operating pressure. For the Unisphere aluminas, the maximum flow rate used was 4.99 mL/min, which corresponds to the maximum flow rate of the HPLC employed.

At first glance it appears as though the normalized backpressures obtained for the Unisphere aluminas and the Si-C₁₈ columns in Fig. 7.7 are almost equal, especially at lower flow rates (0.5 to around 2.0 mL/min). At 1.00 mL/min, the observed normalized pressure drops were within 4.07×10^4 to 4.71×10^4 psi-mm for both types of column. However, assuming ΔP values varies linearly with flow rate (Table 7.5), it can be seen from Fig. 7.7 that the difference in backpressures between these two stationary phase types is greater at higher flow rates. At 5.00 mL/min, the expected normalized backpressure values ($\times 10^4$) for the Al-C₁₈, Al-PBD and Al-CN are 15.5, 13.6 and 12.6 psi-mm, respectively, while the corresponding values for the Microsorb and LiChrospher Si-C₁₈ are 19.1 and 17.3 psi-mm, respectively.

The difference in backpressures at elevated flow rates become more significant when the ΔP values for the Si-C₁₈ columns are adjusted so as to correspond to that of a 250 mm column with 8 μ m packings. This trend can more easily be seen in Fig. 7.8, wherein ΔP values for the Si-C₁₈ columns were calculated using a procedure similar to that employed by Haky *et al.* [16]. Again, similar to the trend observed in Fig. 7.7, very minimal difference in ΔP was observed at low flow rates. However, a greater difference in ΔP values are expected at 5.00 mL/min, corresponding to ΔP values of *ca.* 7460 and 6770 psi for the Microsorb and LiChrospher Si-C₁₈ columns, respectively, and 6140, 5300 and 4920 psi for the Al-C₁₈, Al-PBD and Al-CN, respectively. More significantly, at 5.00 mL/min anticipated ΔP values for both Si-C₁₈ columns exceeded the set HPLC pressure limit (6000 psi), although ΔP for the Al-C₁₈ column is also expected to exceed 6000 psi. Also, the largest difference in ΔP between the alumina-

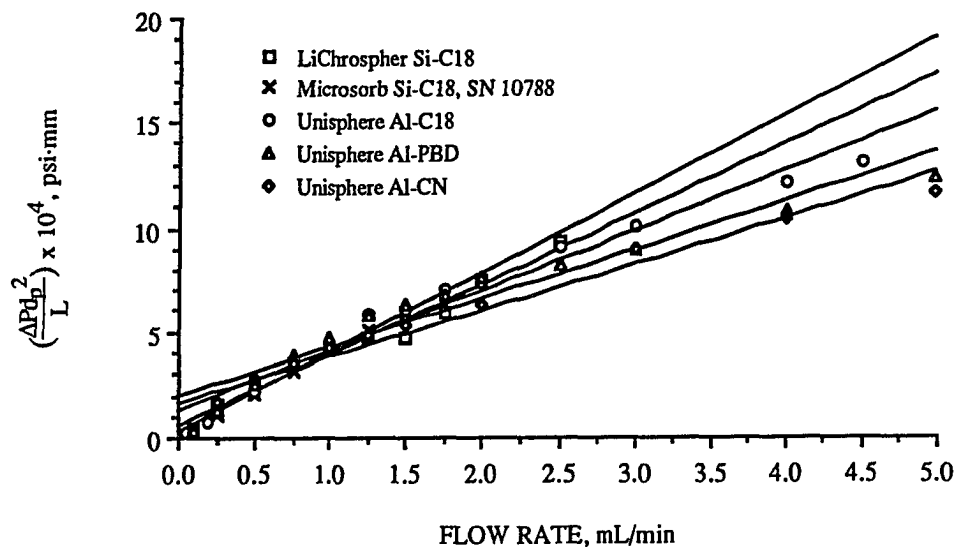


FIGURE 7.7. Comparison of normalized pressure drops ($\Delta P_{d_p}^2/L$) for two porous Si-C₁₈ and three Unisphere polymer-coated aluminas.

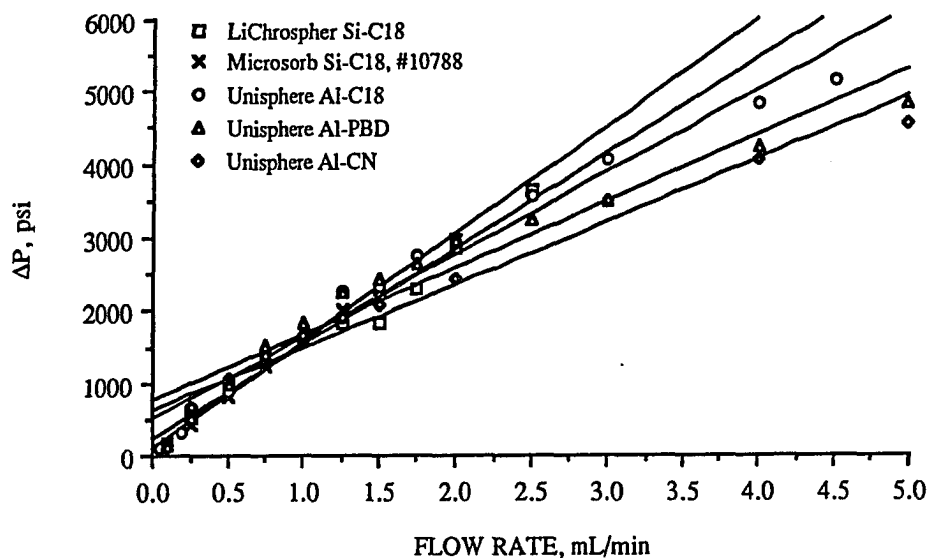


FIGURE 7.8. Comparison of backpressures for hypothetical columns of equal column length (250 mm) and particle diameter (8 μ m) for various silica- and alumina-based reversed-phase packings.

TABLE 7.5. Linear regression results for the curves in Figs. 7.7-7.8.

Column	Slope	Intercept	R ²
A. For Fig. 7.7 ^a			
Microsorb Si-C ₁₈ (SN 10788)	3.78	0.211	0.997
LiChrospher Si-C18	3.36	0.500	0.971
Al-C ₁₈	2.86	1.23	0.967
Al-PBD	2.34	1.89	0.932
Al-CN	2.21	1.56	0.963
B. For Fig. 7.8			
Microsorb Si-C ₁₈ (SN 10788)	1480	82.7	0.997
LiChrospher Si-C18	1310	195	0.971
Al-C ₁₈	1130	484	0.968
Al-PBD	912	738	0.932
Al-CN	863	609	0.963

^a Linear regression results listed are from a plot of $(\Delta P \cdot d_p^2 / L) \times 10^4$ vs. F.

and silica-based columns was 2540 psi at 5.00 mL/min, which corresponds to that for the Microsorb Si-C₁₈ and Al-CN columns.

It is not known why the trend observed by Haky *et al.* [16] on the comparison of ΔP values for a Unisphere Al-PBD and a Vydac Si-C₁₈ at different flow rates (2-5 mL/min) is inconsistent with the results obtained in this study. The results in Figs. 7.7-7.8 clearly indicate the superiority of the Unisphere polymer-coated aluminas over standard/conventional Si-C₁₈ columns (Microsorb and LiChrospher) in terms of lower backpressures, especially at higher flow rates. On the other hand, Haky *et al.* [16] observed lower normalized backpressures for the Vydac Si-C₁₈ at all flow rates. Their plot even showed a greater difference in normalized ΔP at higher flow settings, favoring the Si-C₁₈. The only explanation provided by the authors was that the Vydac column used consisted of highly porous, spherical silica support with a nominal pore size of 300 Å. However, unless the morphology of the Vydac silica is unique compared to common spherical silicas used in RPLC, and possess something like the *megapores* of the Unisphere aluminas (see Chapter I) or other proprietary features which would provide greater permeability, the highly porous nature of the Vydac silica fails to explain satisfactorily why ΔP for the Vydac column was less than that for the Unisphere Al-PBD, since the solvent will not flow through the 300 Å pores [18].

D. Column Stability Of Al-CN And Al-C₁₈

During the course of the study, deterioration of column performance with time for the Al-C₁₈ and Al-CN phases was monitored by following the change in k' and N (using the half-height method) for toluene with 50/50 MeOH/H₂O as mobile phase. Column stability was evaluated only for these two stationary phases since the Si-C₁₈ columns employed have been used extensively prior to the study, while no single Al-PBD column was used extensively during the research. Also, column deterioration as a result of exposure to different (i) mobile phase compositions of MeOH/H₂O and MeCN/H₂O,

(ii) temperatures (15.0-55.0° C), and (iii) flow rates (0.05-4.99 mL/min) were the only factors examined. The effect of subjecting the columns to acidic or basic conditions was not determined. The effects of these latter factors have, however, already been documented by other researchers [19-21].

Figures 7.9 and 7.10 show the change in column performance with time obtained for the Al-C₁₈ and Al-CN columns, respectively. Only a 2.4% decrease in k' value was observed for the Al-C₁₈ column after approximately 17.4 L of solvent have been used, while a 6.5% decrease in k' was obtained for the Al-CN phase after approximately 16.2 L of mobile phase. Hence, *both Al-C₁₈ and Al-CN exhibited very minimal loss of stationary phase (i.e., polymer-coating) with column use.* More significantly, however, these results indicate that the polymer-coating process employed by Biotage does not only render the surface hydroxyl groups of the alumina support inaccessible for polar solutes (see Chapter VI), but also results in *mechanically stable* stationary phases, which can withstand not only sudden changes in mobile phase composition (*e.g.*, 100 to 0% MeOH or MeCN as carried out in Chapter VIII), but also high flow rates (up to 4.99 mL/min) and elevated temperatures (up to 55.0° C).

In terms of column efficiency, a more significant loss in N was obtained for the Al-CN column, decreasing from 4820 to 2960, which corresponds to a 38.6% decrease in column efficiency. For the Al-C₁₈, an almost constant value of N was observed throughout the study, with N values ranging from 1170 to 1520. It is hypothesized that the significant decrease in column efficiency for the Al-CN was most probably due to the formation of voids within the column which occurred later when it was subjected to changes in flow rate from both the determination of van Deemter plots and the effect of mobile phase flow rate on column re-equilibration (see Chapter VIII). Formation of empty spaces within the Al-CN column is evident from changes in $As_{0.1}$ with time as seen in Fig. 7.11, wherein $As_{0.1}$ remained approximately constant at 1.3 for almost the

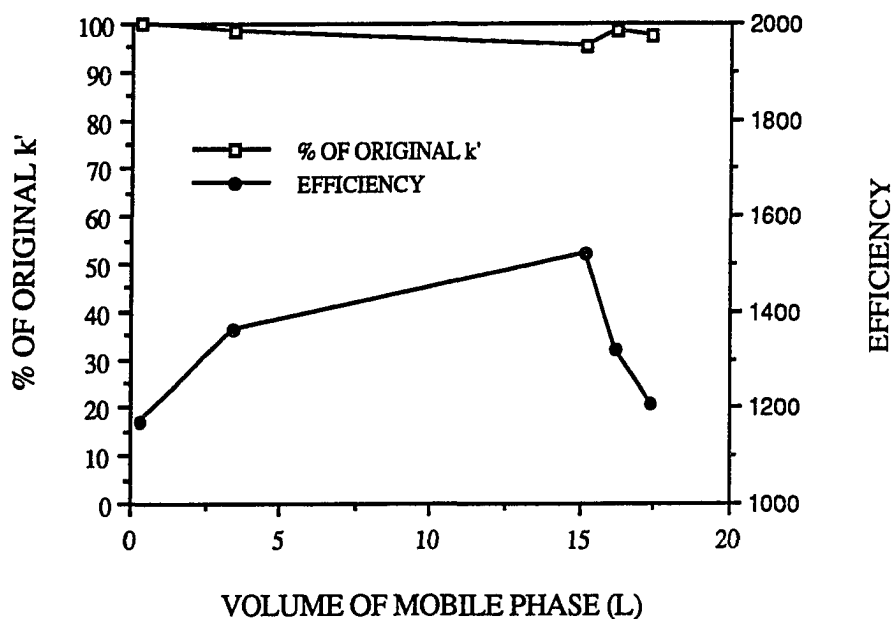


FIGURE 7.9. Loss of stationary phase and change in column efficiency with time for the Unisphere Al-C₁₈.

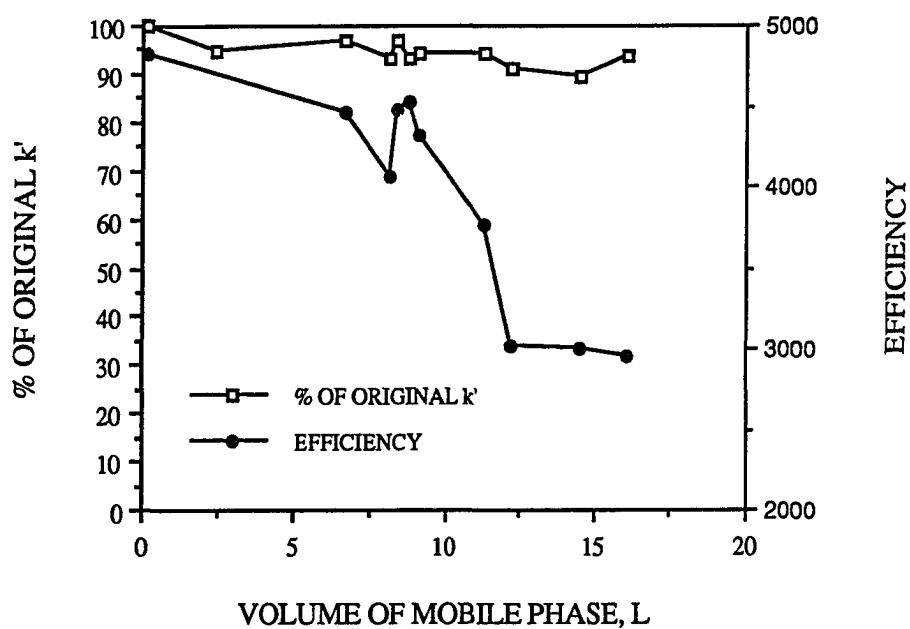


FIGURE 7.10. Loss of stationary phase and change in column efficiency with time for the Unisphere Al-CN.

entire life of the column, increasing to 1.7 only after around 11.5 L of mobile phase have been used, which coincides almost exactly with the time when the column was subjected to higher flow rates. Decrease in N due to mechanical crushing of the Al-CN particles (which will result in a wider particle size distribution (PSD), hence, lower plate count) is highly improbable since as can be seen in Fig. 7.11, the maximum system backpressure obtained was less than 2600 psi. Collapse of the alumina support upon exposure to high flow rates would have resulted in higher backpressures than obtained, most likely exceeding 6000 psi. The constant increase in ΔP in Fig. 7.11 was most likely a result of the gradual accumulation of particulate matter by the column inlet frit.

On the other hand, development of voids occurred much sooner for the Al-C₁₈ as shown in Fig. 7.12 for the asymmetry plot. The Al-C₁₈ column was subjected to elevated flow rates after around 15 L of mobile phase have been used, however, the peak asymmetry factor was already unacceptably high (> 2.0) after only 3.5 L. This implies that the adsorbent material was not tightly packed during column manufacture, hence the formation of empty spaces even at a flow rate setting of only 2.0 mL/min. It should be noted that during the initial stages of column use, $As_{0.1}$ was 1.3 while N was 2940. Thus, the low N value for the Al-C₁₈ is most likely due to the poor mass transfer properties of the stationary phase.

E. Combined Effects Of k' , α And $N_{0.5}$ On Resolution

Equation 6.3 describes how resolution varies with N , α and k' ; to a first approximation the effect of these three variables can be considered independently for easier optimization of R_s . Improving column efficiency leads to narrower bands, hence higher R_s . However, R_s increases only with the square root of the N . Thus, L must be quadrupled to double R_s , which has the disadvantage of resulting in longer analysis time. Improving selectivity increases the distance between the band centers, and is considered to be the most powerful technique for improving R_s [22]. Finally,

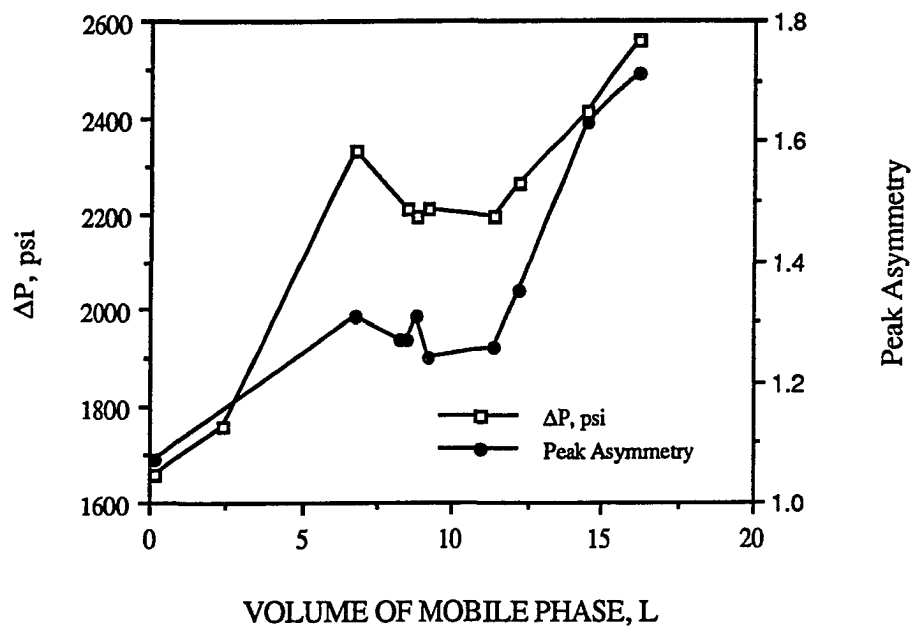


FIGURE 7.11. Changes in ΔP and $As_{0.1}$ with time for the Unisphere Al-CN.

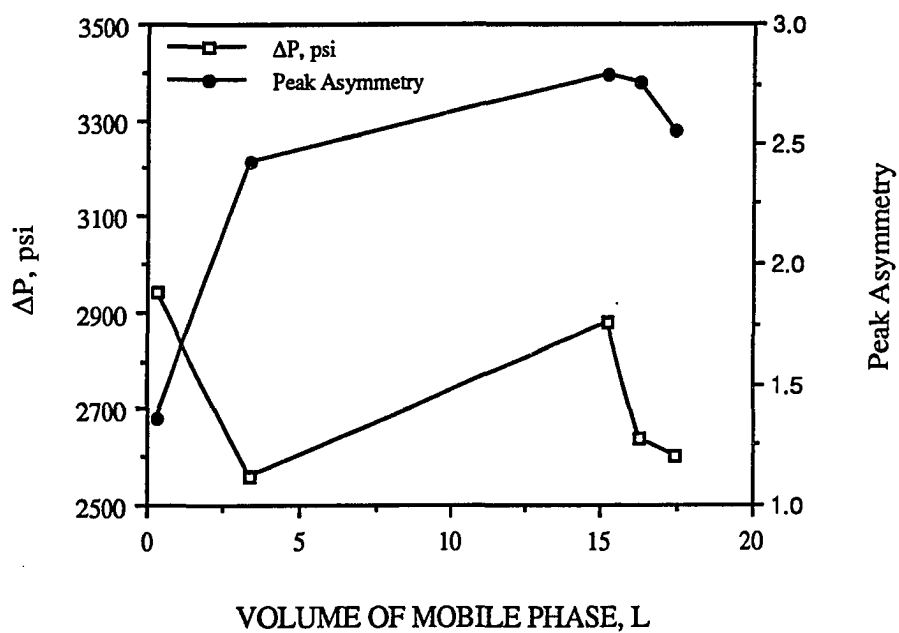


FIGURE 7.12. Changes in ΔP and $As_{0.1}$ with time for the Unisphere Al-C₁₈.

increasing k' results in a rapid improvement of R_s only when k' is small. The optimum range for k' is between 1 and 10, with a minimal increase in R_s accompanied by long separation times with k' values > 10 . It should be noted that an R_s value of 1.0 is generally considered adequate for optimized separation with only 2% of one band overlapping with another. Baseline resolution corresponds to an R_s value of 1.5.

In the comparison of R_s values at different mobile phase compositions that follows, a constant value of N was assumed for each column based on a measurement for toluene using 50% MeOH as mobile phase and flow rates of 2.0 mL/min for the Unisphere aluminas, and 1.0 mL/min for the Si-C₁₈ columns and Millipore Al-PBD. The measured efficiencies (N) of the different columns are listed in Table 7.6.

Toluene And Ethylbenzene

Table 7.7 shows the R_s values obtained for toluene and ethylbenzene at different mobile phase compositions. As can be seen, for either types of mobile phase the R_s at a given % organic solvent is significantly larger for the Si-C₁₈ columns than the polymer-coated aluminas. At 60% MeOH, R_s values for the Microsorb and LiChrospher Si-C₁₈ are 6.86 and 9.34, respectively, while those for the aluminas range from 2.47 to 4.71. The relatively larger R_s values obtained for the silica-based columns at a given mobile phase composition are mainly due to the higher N and k' values for these phases (Tables 7.6 and 3.1A-3.6B), and in general, slightly higher α_{CH_2} values (Fig. 4.7).

For optimum separation, both short analysis time and minimum baseline resolution ($R_s = 1.5$) are desired. Hence, an effective strategy that can be employed to obtain a fair evaluation of R_s values for the different columns is to compare these values at mobile phase compositions that provide fairly equal retentions for ethylbenzene. It should be noted that analysis time is determined by the last eluting band (ethylbenzene in this case), and that the k' values for ethylbenzene can be directly related to analysis time since as indicated earlier in the text, the flow rates used for the different columns were

TABLE 7.6. N values used for calculating R_s for the different columns.

Column	Serial Number	N
Unisphere Al-PBD	593ATC	3130
Millipore Al-PBD	B00221C1	1460
Unisphere Al-C ₁₈	B-0014	1520
Unisphere Al-CN	262ATC	4820
Microsorb Si-C ₁₈	10412	4660
LiChrospher Si-C ₁₈	86484701 8340	

TABLE 7.7. R_s values for toluene and ethylbenzene at different mobile phase compositions for the various columns.

% Organic	Unis Al-PBD	Mill Al-PBD	Al-C ₁₈	Al-CN ^a	Micro Si-C ₁₈	LiChro Si-C ₁₈
I. MeCN/H ₂ O						
30	6.38	—	4.44	7.49	—	—
40	4.44	2.81	3.18	5.30	7.30	—
50	2.70	1.80	2.04	3.50	5.73	7.66
60	1.53	0.96	1.22	1.97	4.35	6.19
70	—	—	0.72	1.10	3.39	4.72
80	—	—	—	—	2.34	3.47
90	—	—	—	—	1.55	2.24
II. MeOH/H ₂ O						
30	—	—	—	—	—	—
40	7.04	—	—	8.12	—	—
50	5.67	3.56	—	6.57	8.36	—
60	3.89	2.47	2.91	4.71	6.86	9.34
70	2.30	1.38	1.58	2.82	5.02	6.96
80	1.36	—	0.89	1.42	3.40	5.62
90	—	—	—	—	1.74	2.52

^a R_s values for the Unisphere Al-CN column were determined at 31.0° C.

such that retention times would be approximately equal for solutes with similar k' values.

Tables 7.8A and 7.8B show the R_s values for the different columns at equivalent retention for MeCN/H₂O and MeOH/H₂O, respectively. As can be seen, R_s for all column types are > 1.5 , except at 60% MeCN and 70% MeOH for the Millipore Al-PBD, and at 60% MeCN for the Al-C₁₈. Among the polymer-coated aluminas for both mobile phase types, the trend obtained for the R_s values was: Al-CN $>$ Unisphere Al-PBD \gg Al-C₁₈ $>$ Millipore Al-PBD. For example, at 70% MeOH, the observed R_s for the aluminas are 2.82, 2.30, 1.58 and 1.38, respectively (Table 7.8B). This trend is mainly due to differences in column efficiency (Table 7.6), although at all mobile phase compositions considered, k' for ethylbenzene is always slightly larger for Al-CN, while α_{CH_2} was always slightly greater for the Unisphere Al-PBD. In general, since k' and α_{CH_2} are of similar values at a given mobile phase composition, R_s values for the solute pair can be made approximately equal for the different polymer-coated aluminas if N for these columns are made similar (*i.e.*, all equal to 4820, the N value for Al-CN). Improving column efficiency is especially important for the Millipore Al-PBD and Unisphere Al-C₁₈ columns, which both have N values less than 2000 (Table 7.6).

Between the Si-C₁₈ columns used, Tables 7.8A and 7.8B show that R_s was always greater for the LiChrospher column at a given mobile phase composition. This is mainly a result of the larger k' and N values used for calculating R_s for the LiChrospher column, since similar α_{CH_2} were observed for both Si-C₁₈ columns at the same % organic solvent. At 70% MeCN (Tables 7.6 and 7.8A), k' , α_{CH_2} and N values were 1.94, 1.43 and 4660 for the Microsorb, and 2.32, 1.42 and 8340 for the LiChrospher columns, respectively.

A more important comparison is that between the different polymer-coated aluminas and Si-C₁₈ columns, especially with the LiChrospher Si-C₁₈ for which the highest

TABLE 7.8A. Relevant parameters for the comparison of R_s values for toluene and ethylbenzene at equivalent retention for ethylbenzene with MeCN/H₂O as mobile phase. ^a

Parameter	Unis Al-PBD	Mill Al-PBD	Al-C ₁₈	Al-CN ^b	Micro Si-C ₁₈	LiChro Si-C ₁₈
% Organic	60	60	60	60	90	90
$k'_{\text{Ethylbenzene}}$	0.47	0.50	0.68	0.78	0.54	0.63
α_{CH_2}	1.52	1.43	1.45	1.35	1.35	1.34
R_s	1.53	0.96	1.22	1.97	1.55	2.24
$N_{\text{Req'd}}^c$	6710	7990	5090	6220	N.A.	N.A.
% Organic	50	50	50	50	80	80
$k'_{\text{Ethylbenzene}}$	1.02	1.13	1.40	1.64	1.03	1.23
α_{CH_2}	1.62	1.55	1.56	1.48	1.37	1.38
R_s	2.70	1.80	2.04	3.50	2.34	3.47
$N_{\text{Req'd}}^c$	5160	5440	4390	4750	N.A.	N.A.
% Organic	40	40	—	—	70	70
$k'_{\text{Ethylbenzene}}$	2.49	2.76	—	—	1.94	2.32
α_{CH_2}	1.80	1.67	—	—	1.43	1.42
R_s	4.44	2.81	—	—	3.39	4.72
$N_{\text{Req'd}}^c$	3540	4110	—	—	N.A.	N.A.

^a Column identification: Unis = Unisphere; Mill = Millipore; Micro = Microsorb; LiChro = LiChrospher.

^b R_s values for the Unisphere Al-CN column were determined at 31.0° C.

^c N.A. = Not Applicable.

TABLE 7.8B. Relevant parameters for the comparison of R_s values for toluene and ethylbenzene at equivalent retention for ethylbenzene with MeOH/H₂O as mobile phase. ^a

Parameter	Unis Al-PBD	Mill Al-PBD	Al-C ₁₈	Al-CN ^b	Micro Si-C ₁₈	LiChro Si-C ₁₈
% Organic	70	70	70	70	90	90
$k'_{\text{Ethylbenzene}}$	0.95	1.20	1.21	1.32	0.76	0.92
α_{CH_2}	1.51	1.36	1.42	1.40	1.31	1.30
R_s	2.30	1.38	1.58	2.82	1.74	2.52
$N_{\text{Req'd}}^c$	3750	4870	3870	3840	N.A.	N.A.
% Organic	60	60	60	60	80	80
$k'_{\text{Ethylbenzene}}$	2.13	2.67	2.80	2.97	1.88	2.57
α_{CH_2}	1.69	1.55	1.68	1.57	1.44	1.52
R_s	3.89	2.47	2.91	4.71	3.40	5.62
$N_{\text{Req'd}}^c$	6550	7580	5680	6850	N.A.	N.A.
% Organic	50	—	—	—	70	—
$k'_{\text{Ethylbenzene}}$	4.96	—	—	—	4.54	—
α_{CH_2}	1.95	—	—	—	1.56	—
R_s	5.67	—	—	—	5.02	—
$N_{\text{Req'd}}^c$	N.A.	—	—	—	N.A.	N.A.

^a Column identification: Unis = Unisphere; Mill = Millipore; Micro = Microsorb; LiChro = LiChrospher.

^b R_s values for the Unisphere Al-CN column were determined at 31.0° C.

^c N.A. = Not Applicable.

column efficiency was obtained. As can be seen in Tables 7.8A and 7.8B, at equivalent retention for ethylbenzene, methylene selectivity values for the polymer-coated aluminas are always greater than those for the corresponding Si-C₁₈ columns used. Hence, in cases wherein k' are approximately equal, differences in column efficiency between the two column types will determine if R_s for the aluminas will be higher or lower than those for the corresponding Si-C₁₈ columns.

In general, both Unisphere Al-PBD and Al-CN exhibited better R_s values than the Microsorb Si-C₁₈ for both mobile phase types. However, k' , N and α_{CH_2} values for the Al-CN column were all greater than corresponding values for the Microsorb column at any given mobile phase composition considered in Tables 7.8A and 7.8B. The k' and α_{CH_2} values used for the Unisphere Al-PBD were also in general greater than those for the Microsorb Si-C₁₈, except at 50 and 60% MeCN for the Al-PBD phase, although column efficiency for the Al-PBD was less than that for the Si-C₁₈ (3130 and 4660, respectively). Thus, even though higher R_s values were obtained in these cases for the two polymer-coated aluminas, the elution time for ethylbenzene were also longer for both Al-PBD and Al-CN columns compared to the Microsorb Si-C₁₈.

The best example which clearly illustrates the potential advantage of using polymer-coated aluminas over conventional Si-C₁₈ stationary phases as suggested in Chapter 4 is apparent from the comparison of R_s values obtained for the Unisphere Al-PBD and Microsorb Si-C₁₈ at 50 and 60% MeCN for the Al-PBD phase. In this situation, k' values for both columns are approximately equal (e.g., 1.02 at 50% MeCN for the Al-PBD, and 1.03 at 80% MeCN for the Si-C₁₈ from Table 7.8A), and although N for the Microsorb column is greater than that for the Al-PBD (4660 and 3130 for the Si-C₁₈ and Al-PBD, respectively), the larger α_{CH_2} values for the Al-PBD (e.g., 1.62 and 1.37 for the Al-PBD and Si-C₁₈ at 50% MeCN for the Al-PBD phase, respectively) still resulted in greater R_s values for the Unisphere Al-PBD (2.70 and 2.34, in favor of the Al-PBD

column). More importantly, with the Unisphere Al-PBD column, it is even possible to achieve R_s values similar to that of the Microsorb Si-C₁₈ by using a stronger solvent resulting in shorter analysis time. Finally, use of the Al-PBD phase in this case is more attractive from the environmental point of view since less organic solvent is consumed to achieve similar or even better resolution.

Unfortunately, except for Unisphere Al-PBD and Al-CN versus Microsorb Si-C₁₈, and Al-CN versus LiChrospher Si-C₁₈ at 50% MeCN and 70% MeOH for the Al-CN, R_s values at equivalent retention for the Si-C₁₈ are significantly greater than those of the polymer-coated aluminas, due primarily to the very low N values for the alumina-based columns. The difference in magnitude of the R_s values for both column types is even greater when compared to the more efficient LiChrospher Si-C₁₈ phase. For example, R_s at 60% MeOH for the Millipore Al-PBD (Table 7.8B) was 2.47 while that for the corresponding LiChrospher Si-C₁₈ was 5.62. Hence, it is apparent that for the conclusions made in Chapter 4 to be a reality, N values for the polymer-coated aluminas have to be drastically improved.

Tables 7.8A and 7.8B also list the required number of theoretical plates ($N_{\text{Req'd}}$, calculated using Eqn. 7.11) for the polymer-coated aluminas necessary to obtain R_s values equal to that of the LiChrospher Si-C₁₈. The maximum $N_{\text{Req'd}}$ values (in bold

$$N_{\text{Req'd}} = 16R_s^2 \left(\frac{\alpha}{\alpha-1} \right)^2 \left(\frac{1+k'_2}{k'_2} \right)^2 \quad (7.11)$$

type) were 6710, 7990, 5680 and 6850 for the Unisphere and Millipore Al-PBD, Al-C₁₈ and Al-CN, respectively, equivalent to reduced plate heights of 3.7, 3.8, 5.5 and 4.6, respectively. Thus, it appears necessary to improve the column efficiencies of the different polymer-coated aluminas by a factor of almost 6.

CONCLUSIONS

The lower u_{opt} values, larger h values at u_{opt} , and the more rapid loss in column efficiency with increasing mobile phase flow rate observed for the polymer-coated aluminas compared to the Si-C₁₈ columns impose a very serious drawback in the possibility of utilizing the alumina-based columns for rapid chromatographic analysis. At practical flow rates (2.00 mL/min for the polymer-coated aluminas and 1.0 mL/min for the Si-C₁₈), h values ranged from 5.7 to 11.5 for Al-PBD and Al-CN, 26.7 to 30.3 for Al-C₁₈, and 3.0 to 5.4 for the Si-C₁₈ columns. Hence, although methylene selectivity values were larger for the polymer-coated aluminas compared to the Si-C₁₈ columns at equivalent retention (*i.e.*, analysis time), the difference in α_{CH_2} seems to be inadequate to provide better R_s values for the polymer-coated aluminas at practical flow rates. Therefore, for the Unisphere columns to be advantageous over conventional Si-C₁₈ in terms of analysis time, the van Deemter minimum for the aluminas should be made broader, and the column efficiencies improved by at least a factor of 6.

It should be noted that if the Unisphere columns are made more efficient than its silica-based counterpart, better R_s values, and shorter analysis time (achieved by using higher flow rates) are easily attainable for the aluminas since ΔP values for the Unisphere phases were observed to be less than that of the Si-C₁₈ phases at the same flow rate and mobile phase composition, with the difference in magnitude greater at elevated flow rates. Utilization of the polymer-coated aluminas would also result in lesser consumption of organic solvent while at the same time resulting in better, if not similar, R_s values relative to the Si-C₁₈ phase. Making these apparent advantages a reality would render the Unisphere polymer-coated aluminas more attractive to use in RPLC, especially in preparative LC.

REFERENCES FOR CHAPTER VII

1. Bristow, P.A.; Knox, J.H. *Chromatographia* **1977**, *10*, 279-289.
2. Knox, J.H. *J. Chromatogr. Sci.* **1980**, *18*, 453-461.
3. Pauls, R.E.; McCoy, R.W. *J. Chromatogr. Sci.* **1986**, *24*, 66-69.
4. Landy, J.S.; Ward, J.L.; Dorsey, J.G. *J. Chromatogr. Sci.* **1983**, *21*, 49-56.
5. McCoy, R.W.; Pauls, R.E. *J. Liq. Chromatogr.* **1982**, *5*, 1869-1897.
6. Bidlingmeyer, B.A.; Warren, F.V. *Anal. Chem.* **1984**, *56*, 1583A-1596A.
7. Foley, J.P.; Dorsey, J.G. *Anal. Chem.* **1983**, *55*, 730-737.
8. Kirkland, J.J.; Yau, W.W.; Stoklosa, H.J.; Dilks, C.H. *J. Chromatogr. Sci.* **1977**, *15*, 303-316.
9. Wilke, C.R.; Chang, P. *Am. Inst. Chem. Eng J.* **1955**, *1*, 264-270.
10. Unisphere Al-PBD (#003-0253) column literature provided by Biotage, Inc.
11. Wilhelmy, R.B. Presented at the 1988 Pittsburgh Conference and Exposition on Analytical Chemistry and Applied Spectroscopy, New Orleans, February 23, 1988; Paper 390.
12. Wieserman, L.F.; Martin, E.S.; Cross, K. Presented at the 1988 Pittsburgh Conference and Exposition on Analytical Chemistry and Applied Spectroscopy, New Orleans, February 23, 1988; Paper 391.
13. Wieserman, L.F.; Burr, R.R.; Cross, K.; Simpson, Jr., F. Presented at the 1988 Pittsburgh Conference and Exposition on Analytical Chemistry and Applied Spectroscopy, New Orleans, February 23, 1988; Paper 393.
14. Biotage, Inc. *Unisphere-PBD Alumina*, 1990.
15. Alcoa, *Unisphere - Controlled Morphology Alumina*, Chromatography Product Data, 1(4).
16. Haky, J.E.; Raghani, A.; Dunn, B.M. *J. Chromatogr.* **1991**, *541*, 303-315.
17. Haky, J.E.; Raghani, A.R.; Dunn, B.M.; Wieserman, L.F. *Chromatographia* **1991**, *32*, 49-55.
18. Guiochon, G. *Optimization in Liquid Chromatography In High-Performance Liquid Chromatography-Advances and Perspectives*, Horváth, C., Ed.; Academic Press: New York, 1980; Vol. 2.
19. Bien-Vogelsang, U.; Deege, A.; Figge, H.; Köhler, J.; Schomburg, G.

20. Conroy, C.M.; Washington, J.M.; Holland, K.B.; Zeller, K.; Burke, D.; Moe, D.C. Presented at the 1991 Pittsburgh Conference and Exposition on Analytical Chemistry and Applied Spectroscopy, Chicago, March 3, 1991; Paper 028P.
21. Holland, K.B.; Washington, J.M.; Zeller, K.; Burke, D.; Conroy, C.M.; Moe, D.C. Presented at the 1991 Pittsburgh Conference and Exposition on Analytical Chemistry and Applied Spectroscopy, Chicago, March 5, 1991, 1991; Paper 340P.
22. Snyder, L.R.; Kirkland, J.J. *Introduction to Modern Liquid Chromatography*, 2nd ed.; John Wiley & Sons, Inc.: New York, 1979; Chapter 2.

CHAPTER VIII

COLUMN RE-EQUILIBRATION AFTER GRADIENT ELUTION

INTRODUCTION

A. Gradient Elution In RPLC

Gradient elution is a very popular technique for overcoming the so-called *general elution problem* in liquid chromatography. Using this strategy, it is feasible to separate a mixture of compounds with a very wide range of polarities within a reasonable amount of time, resulting in even spacing of the peaks, better resolution, and narrower bands that are more easy to detect. Separation of the same compounds by isocratic elution (*i.e.*, with the same mobile phase composition throughout the run) would have resulted in poorly resolved early eluting bands with retention times near t_m , and tailed, broad, and hard-to-detect late eluting bands. Excellent reviews about gradient elution have been published elsewhere [1-3].

In practice, gradient elution is normally carried out using two solvents: A (the weak solvent, *e.g.* H₂O) and B (the strong solvent, *e.g.* MeCN or MeOH). During the gradient run, the mobile phase composition is changed by increasing the concentration of solvent B in the mobile phase. Thus, the strength of the mobile phase increases during the analysis. Typical changes in the concentration of solvent B during the gradient is within 5 to 100% B. Thus, as Dolan [4] puts it, the weakly retained compounds elute from the column first, in a weak mobile phase, while the strongly retained compounds elute last, in a strong mobile phase.

Dolan and Snyder [5] have identified three obstacles to the wider application of gradient elution in liquid chromatography, namely: (i) the need for method development; (ii) the use of more complex samples; and (iii) the longer analysis times involved, compared to isocratic elution. In reality, an even "longer" run time is necessary when

one considers the re-equilibration step that is required after each gradient run. Hence, one can assume that the "total" run time for gradient elution is actually the sum of the time required for the actual gradient plus the additional time necessary for column re-equilibration (CR) between runs. According to Snyder *et al.* [3], the additional time required for CR is generally approximately equal to the gradient time.

B. Column Re-equilibration After Gradient Elution In RPLC

In this study, CR after gradient elution refers to the return of the column to initial equilibrium conditions required for the analysis, which can most easily be achieved by flushing the column with the starting mobile phase. It is emphasized that the CR process being investigated is limited to stationary phases for RPLC.

Column re-equilibration is essential in gradient elution since insufficient equilibration of the stationary phase with the starting mobile phase leads to variations in both retention and resolution, especially for early eluting peaks [3, 6]. Unfortunately, this additional step adds considerable time and expense to the analysis without contributing any additional information. Although not commonly practiced, it is also possible to inject the sample prior to complete equilibration in gradient elution. However, this is not recommended, and reproducible results can only be obtained if an exact protocol for CR is followed, and if sample injection is carried out at exactly the same time interval between runs so as to maintain the same degree of equilibration for each analysis. This approach will most likely necessitate the use of an autosampler [2, 3]. Equilibration of the stationary phase is also essential in isocratic elution whenever a new mobile phase is required, or whenever the column is flushed with 100% organic solvent to quickly remove strongly retained compounds from the column between runs.

C. Literature Survey On Column Re-equilibration

Except for the recent report of Cole and Dorsey [7], and to a limited extent the study of Engelhardt *et al.* [8], there has been no definitive study about the column re-

equilibration process in RPLC. Simple guidelines have, however, been published by Snyder's group regarding this subject matter (mainly as part of the text on gradient elution), unfortunately with no experimental data to support their claim [1-3, 5, 6, 9].

1. Recommendations By Snyder's Group

Various recommendations have been published regarding the volume of mobile phase necessary to completely equilibrate the stationary phase with the new mobile phase in RPLC. In general, flushing the column with 15 column volumes of new mobile phase is sufficient [6], although other reports suggest 15-20 [3], and 10-20 [9] column volumes. They did indicate, however, that it is necessary to experimentally verify whether or not the column has been fully equilibrated with the new mobile phase by repeated injection of a standard sample or mixture every 10-20 minutes [1, 3, 9].

For gradient elution, a simple equation has been proposed by Dolan and Snyder [5] to estimate equilibration time (Eqn. 8.1) or volume (Eqn. 8.2):

$$\text{Equilibration time} = 0.15 \times t_m \times \Delta\%B \quad (8.1)$$

$$\text{Equilibration volume} = 0.15 \times V_m \times \Delta\%B \quad (8.2)$$

where $\Delta\%B$ is the change in % organic solvent during the gradient (*e.g.*, for a 5-100% B gradient, $\Delta\%B$ is 95), and V_m is the column void volume. The most significant feature of Eqns. 8.1 and 8.2 is that it takes into account the effect of the magnitude of the gradient step ($\Delta\%B$). In relation to this, Snyder's group also recommends starting gradient runs in RPLC with at least 5% organic solvent, since use of a mobile phase with < 5% organic solvent will result in long equilibration times between runs, due primarily to the poor wettability of the stationary phase [1, 3, 5].

The major contention of Snyder's group is that *column equilibration is mainly dependent on the total volume of mobile phase passed through the column, and not the*

time for equilibration. Hence, the most effective strategy in decreasing equilibration time is to use the highest flow rate possible [1, 3, 6]. Snyder's group also advocates that excessively long equilibration times indicate slow equilibration of the column, most likely due to some components of the mobile phase being strongly retained by the stationary phase. Thus, decreasing equilibration time may require either (i) adding the strongly retained component to both solvents A and B, or (ii) totally removing the strongly retained component altogether, if applicable [3, 9]. Common examples of these strongly retained components are additives such as amine modifiers (*e.g.* triethylamine) which are added to reduce silanol activity, and ion-pairing reagents (*e.g.* tributyl ammonium ion).

2. Research Results Of Other Investigators

Column re-equilibration after gradient elution can be achieved either (i) by carrying out a reverse gradient from solvents B to A, or (ii) by flushing the column with pure solvent A (*i.e.*, a reverse step gradient from 100% B to 100% A). Unlike in normal-phase LC where reverse gradients have been reported to result in shorter equilibration times [10, 11], no similar advantage has been observed in RPLC. On the contrary, a step gradient to 100% A has been reported to decrease re-equilibration time in RPLC, at least when the mixing volume between the pump and column is small [1].

To the best of the author's knowledge, Engelhardt *et al.* [8] was first to show experimental evidence on the long equilibration times involved in using 100% water as mobile phase for silica-based bonded phases (C₁₈) for RPLC. Their results indicate that in general, equilibrating the column with any combination of MeOH/H₂O mixture required a maximum of about 20 empty column volumes for complete equilibration, whereas about 250 empty column volumes were required to equilibrate the same system with pure H₂O. Using 100% H₂O as mobile phase, the reported *k'* values of the test solute was 23% lower than the actual value when only 20 column volumes of pure H₂O

have been passed through the column. No definite explanation was given for these observations, except that these long equilibration times were related to the change in total porosity as measured with D₂O. At MeOH concentrations $\leq 40\%$, an 11% decrease in total porosity was observed. It was hypothesized that in a MeOH-rich environment, the MeOH molecules penetrate the space between the alkyl chains. Upon subjecting the stationary phase to a H₂O-rich environment ($\leq 40\%$ MeOH), the methanol molecules located within these groups are extracted, resulting in a collapse of the alkyl chains, and eventually a decrease in porosity. Apparently, replacement of the MeOH molecules (within the alkyl chains) with pure water takes longer than with a MeOH/H₂O mixture.

Based on the preferential solvation of the stationary phase by the organic solvent as has been reported by several investigators (see introduction section of reference [7]), Cole and Dorsey [7] propose that maintaining a constant volume of 3% 1-propanol (1-PrOH) in the mobile phase throughout the gradient run provides consistent solvation of the Si-C₁₈ phase, resulting in reduction of CR time. Using this simple strategy, they were able to significantly reduce CR time, obtaining reductions as high as 78% for gradients from 3/97 1-PrOH/H₂O to 3/97 1-PrOH/solvent B compared to separation gradients from 0 to 100% B, for both MeCN/H₂O and MeOH/H₂O solvent systems. Unfortunately, use of 3% 1-PrOH results in a significant decrease in retention for the test solute used (acetone). For example, t_R for acetone was 13.0 min with 100% H₂O, while t_R for the same solute was only 4.6 min with 3/97 1-PrOH/H₂O, which represents a 65% decrease in solute retention. Smaller reductions in retention are, however, expected for gradients started with stronger mobile phases. Cole and Dorsey [7] also observed that for 0 to 100% organic solvent gradients, CR time (without the use of 3% 1-PrOH) was greater with MeCN as organic solvent compared to MeOH. This was attributed to the less polar nature of MeCN, resulting in greater affinity for the stationary phase. Hence, it will be more difficult for water to replace MeCN than for water to

replace MeOH in the stationary phase. Finally, Cole and Dorsey [7] demonstrated the importance of alkyl chain ordering in CR by using Si-C₁₈ columns of different bonding densities ranging from 1.60 to 4.07 $\mu\text{mol}/\text{m}^2$. Using gradients from 0 to 100% organic solvent, they showed that re-equilibration column volume reaches a maximum value at bonding densities of about 2.9 $\mu\text{mol}/\text{m}^2$ (close to the critical alkyl chain bonding density of approximately 2.7 $\mu\text{mol}/\text{m}^2$). At bonding densities greater than 2.9 $\mu\text{mol}/\text{m}^2$, the volume of mobile phase required for re-equilibration decreases with increasing bonding density. It should be noted that above the critical alkyl chain bonding density, chain ordering increases while partitioning decreases with increasing bonding density, and since the stationary phase exhibits limited changes in conformation at higher bonding densities, re-equilibration column volume is expected to decrease for these columns.

Finally, unpublished results by Payne *et al.* [12] on column re-equilibration after gradient elution for Si-C₁₈ stationary phases suggest that diffusion in the mobile phase stagnant zone (within the pores) and mass transfer between the flowing and stagnant zones are the rate limiting step(s), and that an increase in flow rate may not facilitate efficient re-equilibration. Less mobile phase were required to fully re-equilibrate the column when lower flow rates, higher temperatures, or less viscous solvents were employed.

The objectives of this part of the study are to determine the effects of the magnitude of the gradient step, flow rate and temperature on column re-equilibration after gradient elution for the various Unisphere polymer-coated aluminas and Si-C₁₈ columns. It is emphasized that no attempt was made to identify the mechanism(s) and rate limiting step(s) involved in the CR process investigated. Based on the author's experience, the limited results obtained from the study do not provide sufficient evidence to allow such broad conclusions to be made.

EXPERIMENTAL

Column re-equilibration was monitored by carrying out a reverse step gradient from 100% B (MeCN or MeOH). Initially, the column is equilibrated with 100% organic solvent. Then a reverse step gradient is performed to a finally weaker mobile phase (consisting of a mixture of organic solvent and water, or pure water). During the reverse step gradient, a test solute is injected periodically at intervals of either 0.5 or 1.0 min. The test solute used was chosen so as to provide a retention factor of approximately unity at equilibrium conditions. It was expected that such a test solute will be more sensitive to slight changes in the mobile phase solvation of the stationary phase, and more convenient to use in terms of analysis time. Re-equilibration experiments performed in our laboratory exclusively on Si-C₁₈ stationary phases using two test solutes with k' values of 1.1 (acetophenone) and 15.1 (propylbenzene) showed that re-equilibration column volume is independent of solute retention with either MeCN/H₂O or MeOH/H₂O as mobile phase [12].

Column re-equilibration was considered to be complete when the calculated retention factor for the test solute is within 1% (99 - 101%) of its steady state value (k'_{ss}), which was taken as the average retention factor measured after at least 15 column volumes (usually > 20 column volumes, depending on the step gradient involved) of the weaker mobile phase have been used. A typical plot of k'/k'_{ss} versus re-equilibration column volume is shown in Fig. 8.1.

All equilibration experiments were performed at 25.0° C, except for the temperature dependent studies, using 4.6 x 150 mm Si-C₁₈ and 4.6 x 250 mm Unisphere columns, unless stated otherwise. However, experiments for the effect of the magnitude of the gradient step for the Unisphere Al-CN column were performed at 31.0° C. Also, unless indicated otherwise, a flow rate of 2.0 and 1.0 mL/min was used for all Unisphere and Si-C₁₈ columns, respectively. A higher flow rate was used for the 250 mm Unisphere

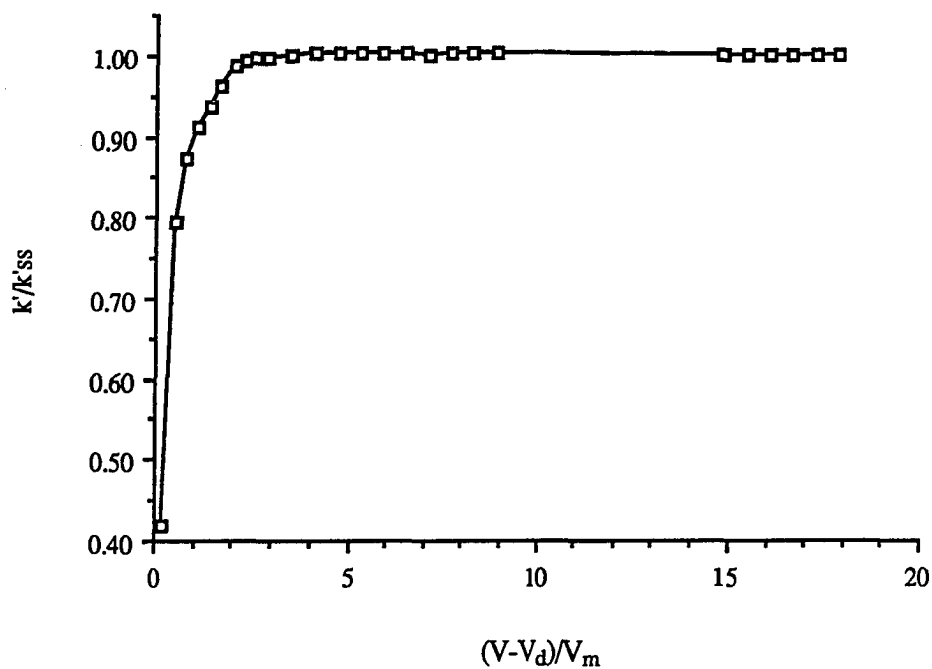


FIGURE 8.1. Typical plot of k'/k'_{ss} vs. $(V-V_d)/V_m$. Example given is that for 100 to 60% MeCN for the Unisphere Al-CN column with n-propylbenzene as test solute ($k'_{ss} = 1.114 \pm 0.001$).

columns compared to the shorter Si-C₁₈ columns to reduce analysis time. Finally, a 100-30% organic modifier step gradient was used to monitor the effects of temperature and flow rate on re-equilibration. Due to the relatively higher column backpressures obtained for the Si-C₁₈, a 4.6 x 50 mm Si-C₁₈ column (SN 10053) was used to monitor the effect of flow rate on column equilibration.

Re-equilibration column volume (RCV) was calculated using Eqn. 8.3

$$RCV = \frac{(V_t - V_d)}{V_m} \quad (8.3)$$

where V_t is the total volume of mobile phase that has passed through the column during the reverse step gradient, V_d is the delay volume of the HPLC, and V_m is the column void volume. Delay volume was determined by carrying out a step gradient from 100% organic modifier to 100% organic modifier spiked with acetone. The difference between the void volume and the volume of mobile phase required to reach the point just before the baseline drift was taken as the delay volume. The void volume was taken as the volume required to elute acetone using 100% organic solvent.

Majority of the column re-equilibration experiments were carried out only once due to the long analysis time involved for each run. However, for some runs performed more than once, the RSD obtained ranged from 7.1 to 19.5%. For example, for the Microsorb Si-C₁₈ (SN 10788) for the 100-0% MeCN reversed step gradient at 1.0 mL/min, RCV values obtained were 51.3 and 46.4 for acetone ($k'_{ss} = 3.12 \pm 0.02$). For the Al-CN column for the 100-30% MeOH reversed step gradient at 2.0 mL/min, RCV values obtained were 7.49 and 8.94 for 2-hexanone ($k'_{ss} = 0.79 \pm 0.02$).

RESULTS AND DISCUSSION

A. Effect Of The Magnitude Of The Gradient Step ($\Delta\%B$)

Although Dolan and Snyder [5] did recognize the significance of $\Delta\%B$ on column re-equilibration after gradient elution, Dolan-Snyder's approximation as mathematically given in Eqns. 8.1 and 8.2 is applicable only at initial gradient compositions $> 0\%$ organic solvent as can be seen in Figs. 8.2 to 8.5 for the Microsorb Si-C₁₈ and the various Unisphere polymer-coated aluminas. Predicted RCV values at a given initial % organic solvent calculated using Eqn. 8.2 are represented by broken lines in the latter figures. For both stationary phase types and organic modifiers, RCV was largest at 0% organic solvent, and in general, RCV increases with decreasing initial % organic modifier (or with increasing $\Delta\%B$). Both Al-C₁₈ and Al-CN exhibited trends similar to those predicted by Dolan and Snyder [5] as shown in Figs. 8.4 and 8.5. However, an abrupt increase in RCV was observed from 10 to 0% MeCN for both Si-C₁₈ and Al-PBD columns (Figs. 8.2 and 8.3).

Except for gradient runs started with 100% H₂O, Figs. 8.2-8.5 clearly provide concrete evidence to support the general rule of thumb that *flushing the column with at least 20 column volumes of starting mobile phase is enough to fully equilibrate any reversed-phase liquid chromatographic stationary phase* (at least for the Si-C₁₈ and polymer-coated aluminas employed in the study). About 3.8 to 10.2 column volumes were required to bring the retention factors of the test solutes to within 1% of the steady state value using the Si-C₁₈ column for gradients started with at least 5% organic modifier. Similar values for the different polymer-coated aluminas ranged from 2.5 to 19.6 column volumes when equilibrated with mobile phases containing at least 10% organic solvent. More importantly, to the best of the author's knowledge, this is the

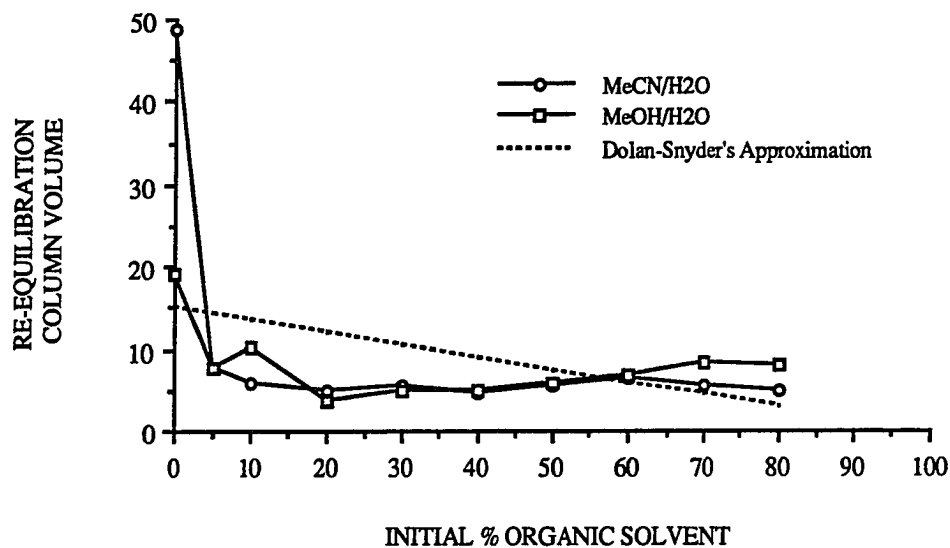


FIGURE 8.2. Effect of initial mobile phase composition of the gradient run on column re-equilibration after gradient elution for the Microsorb Si-C₁₈.

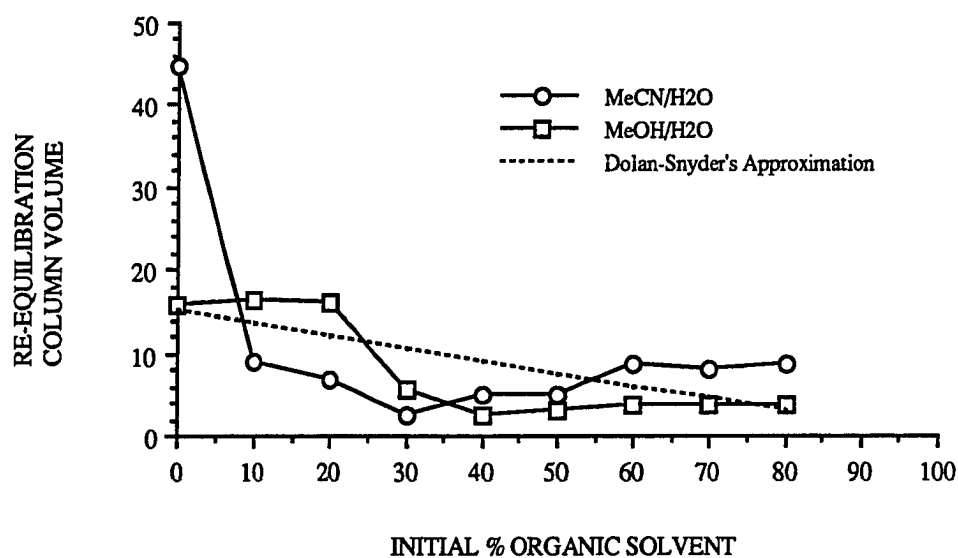


FIGURE 8.3. Effect of initial mobile phase composition of the gradient run on column re-equilibration after gradient elution for the Unisphere Al-PBD.

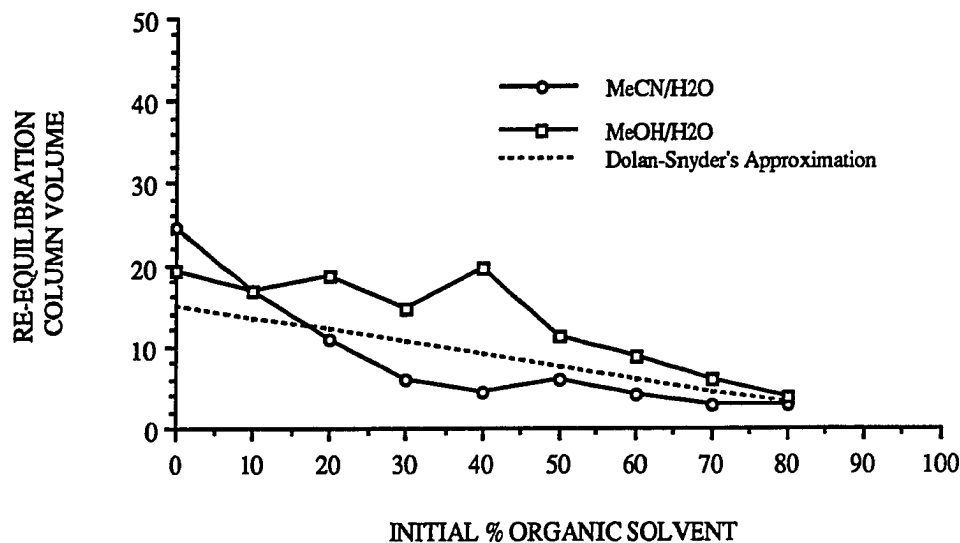


FIGURE 8.4. Effect of initial mobile phase composition of the gradient run on column re-equilibration after gradient elution for the Unisphere Al-C₁₈.

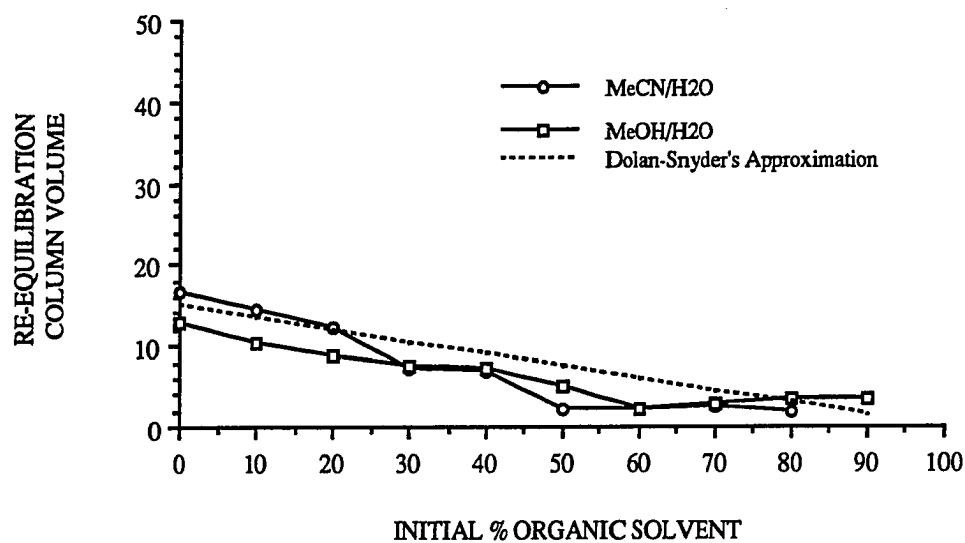


FIGURE 8.5. Effect of initial mobile phase composition of the gradient run on column re-equilibration after gradient elution for the Unisphere Al-CN.

first time that such experimental evidence have been reported to support the previous recommendation.

For Si-C₁₈ columns, it is well known that long re-equilibration times (and therefore more mobile phase) are required if a gradient is started with 100% water [1, 3, 5, 7, 8]. This was also the case for the Microsorb Si-C₁₈ used in the study (Fig. 8.2). A very abrupt increase in RCV was observed from 5 to 0% organic solvent for the Si-C₁₈, especially with MeCN/H₂O corresponding to values of 7.7 and 48.8, respectively. With MeOH/H₂O as mobile phase, the change in RCV was from 7.9 with 5% MeOH to 19.0 with 0% MeOH. This sudden increase in RCV occurred since complete removal or replacement of the partitioned organic solvent (*i.e.*, organic solvent within the stationary phase) is very difficult for the 100% organic solvent to 100% H₂O reverse step gradient, due mainly to the polarity difference of the latter two solvents. This is a result of the poor water wettability of the Si-C₁₈ chains, hence, the alkyl groups tend to resist replacement of the partitioned organic solvent with water.

It is hypothesized that column re-equilibration for the Si-C₁₈ for the 100 to 0% organic modifier reverse step gradient proceeds not via the partitioning of H₂O into the Si-C₁₈, but via the extraction of the partitioned organic solvent by H₂O, accompanied by the clumping together and collapse of the C₁₈ chains as most of the organic solvents are extracted out. With further collapse of the alkyl chains as the extraction of the organic solvent progresses, the remaining partitioned organic solvent are effectively "squeezed out", and with time are completely extracted from the stationary phase. Note that theoretically the stationary phase is considered fully equilibrated with pure water only when all the partitioned organic solvent has been removed from the column. This hypothesis is supported by the very gradual increase in k'/k'_{ss} with mobile phase volume, especially near the limiting value of 1.00 as shown in Fig. 8.6 for the 100%

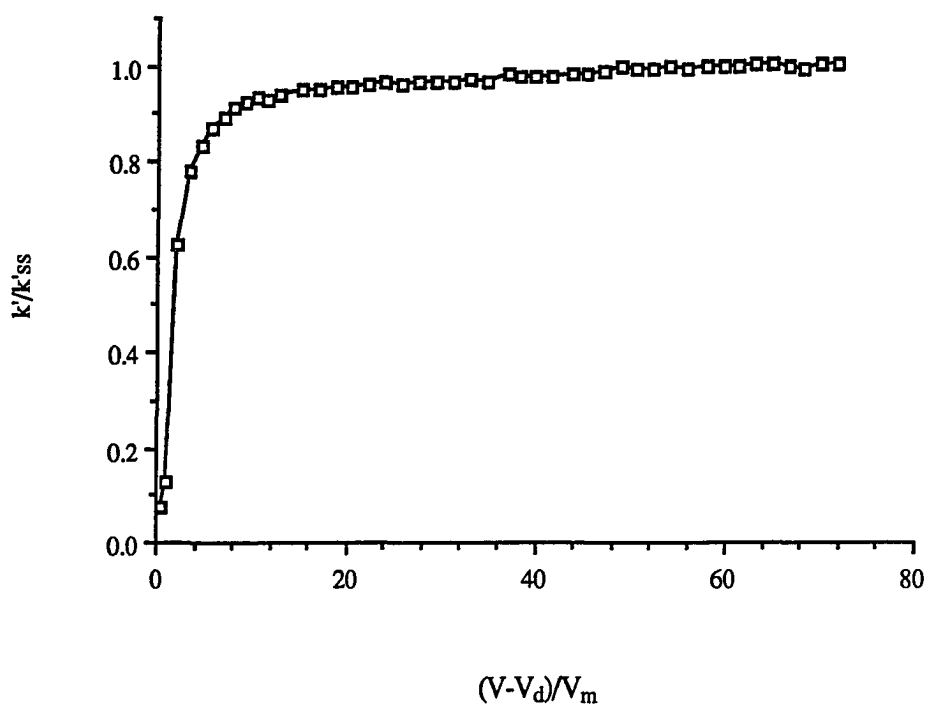


FIGURE 8.6. Plot of k'/k'_{ss} vs. $(V-V_d)/V_m$. Example given is that for 100% MeCN to 100% H₂O for the Microsorb Si-C₁₈ column with acetone as test solute ($k'_{ss} = 3.133 \pm 0.011$).

MeCN to 100% H₂O reversed step gradient, as compared to that of Fig. 8.1 for a 100 to 60% MeCN gradient.

Similar arguments can also be used to explain why a sudden increase in RCV was observed from 10 to 0% MeCN for the Al-PBD phase as illustrated in Fig. 8.3. It should be noted that hydrocarbon groups (or chains) with a minimum chain length corresponding to that of a vinyl group are known to exist on the surface of Al-PBD phases [13].

No definite conclusions can be made regarding the effect of solvent type on column re-equilibration. In general, approximately equal numbers of column volume were necessary to fully equilibrate the stationary phase with the desired mobile phase at all initial gradient compositions studied except for those started with 100% H₂O. This was especially true for the Si-C₁₈ and Al-CN columns as shown in Figs. 8.2 and 8.5, respectively. However, for all columns equilibrated with 100% H₂O, RCV values were always greater when MeCN was used as organic modifier compared to MeOH. As seen in Figs. 8.2-8.5, the difference in RCV at 0% organic for both solvent systems was greatest for the Si-C₁₈ and Al-PBD columns. These results were similar to those obtained by Cole and Dorsey [7] for several Si-C₁₈ columns, and can be attributed to the less polar nature of MeCN relative to MeOH. Hence, MeCN will exhibit greater affinity for the nonpolar stationary phase compared to MeOH, making it more difficult for water to completely replace MeCN than for water to completely replace MeOH.

B. Effect Of Flow Rate

The effect of flow rate on column re-equilibration after gradient elution was monitored using a 100 to 30% organic solvent reversed step gradient, employing flow rates in the range of 0.5 to 3.0 mL/min for the Si-C₁₈, and 1.0 to 4.0 mL/min for the Unisphere polymer-coated aluminas. Lower maximum flow rates were used for the Si-C₁₈ column since ΔP was already equal to 4780 psi at 2.5 mL/min with MeOH/H₂O as

mobile phase, while ΔP was 4350 psi at 3.0 mL/min with MeCN/H₂O. At 4.0 mL/min, maximum ΔP values observed for the Unisphere columns were 3270 and 4440 psi for MeCN/H₂O and MeOH/H₂O, respectively.

To a first approximation, it appears that *the volume of mobile phase needed to equilibrate the stationary phase was independent of flow rate*. This can be seen from Fig. 8.7 for the Si-C₁₈, and from Figs. 8.8 to 8.10 for the Unisphere polymer-coated aluminas. As shown in these figures, RCV for all the curves were less than 20. In general, although some plots do indicate that more mobile phase was required for re-equilibration at higher flow rates, the observed increase in mobile phase volume was insignificant, fluctuating only within 5 column volumes and up to a maximum range of about 7 column volumes in three instances.

Figures 8.11 to 8.14 illustrate the effect of mobile phase flow rate on column re-equilibration time (using the same sets of data in Figs. 8.7 to 8.10). As can be seen, *increasing the flow rate results in a significant decrease in re-equilibration time*, which translates to a significant reduction of the "total" run time for each gradient run ("total" run time = time for actual gradient separation + time for column re-equilibration). However, in general, the corresponding reductions obtained were greater at lower flow rate values. For the Si-C₁₈ column with MeCN as organic modifier, increasing the flow rate from 0.5 to 1.0 to 3.0 mL/min decreased re-equilibration time from 16.6 to 7.2 to 3.1 min, respectively (Fig. 8.11). Similarly, increasing flow rate from 1.0 to 2.0 to 4.0 mL/min for the Al-C₁₈ stationary phase with MeOH as organic solvent resulted in a shortening of column re-equilibration time from 31.3 to 24.0 to 13.8 min, respectively (Fig. 8.13). Overall, for both solvent systems, increasing mobile phase flow rate from 1.0 to 4.0 mL/min resulted in a 65% reduction in column re-equilibration time for the polymer-coated aluminas, while increasing flow rate from 0.5 to 2.5 (or 3.0) mL/min

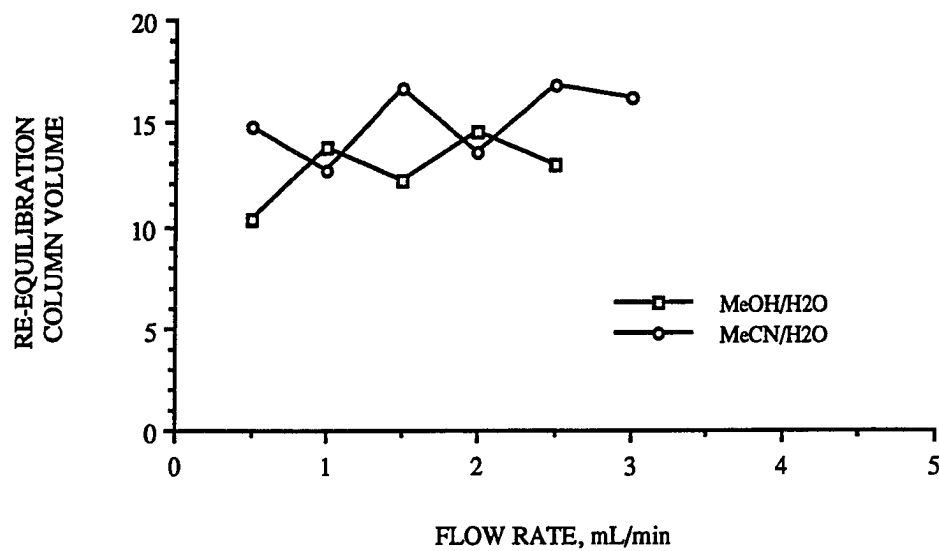


FIGURE 8.7. Effect of flow rate on column re-equilibration volume after gradient elution for the Microsorb Si-C₁₈.

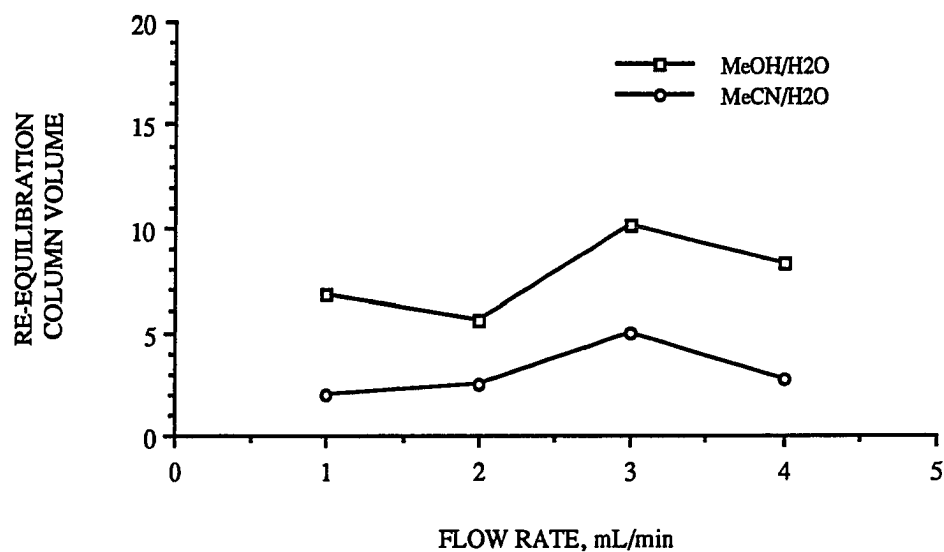


FIGURE 8.8. Effect of flow rate on column re-equilibration volume after gradient elution for the Unisphere Al-PBD.

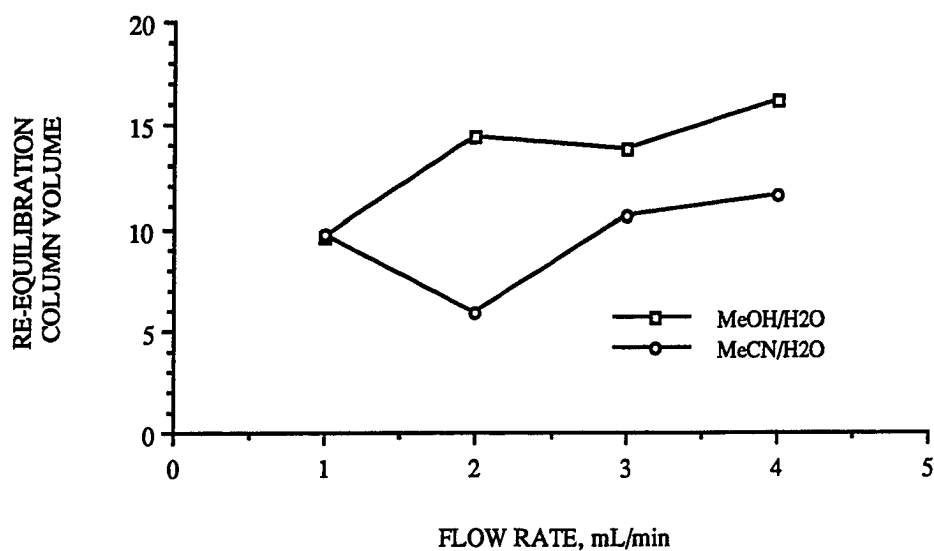


FIGURE 8.9. Effect of flow rate on column re-equilibration volume after gradient elution for the Unisphere Al-C₁₈.

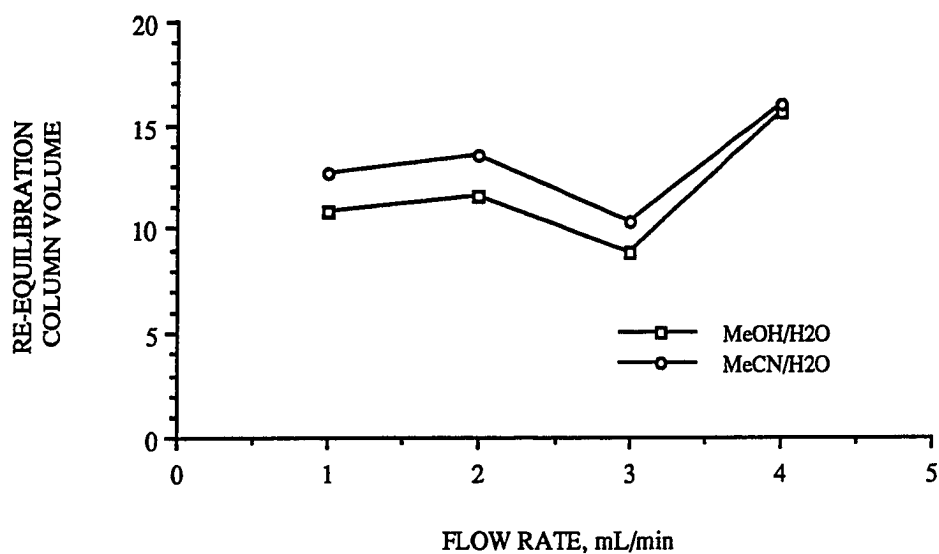


FIGURE 8.10. Effect of flow rate on column re-equilibration volume after gradient elution for the Unisphere Al-CN.

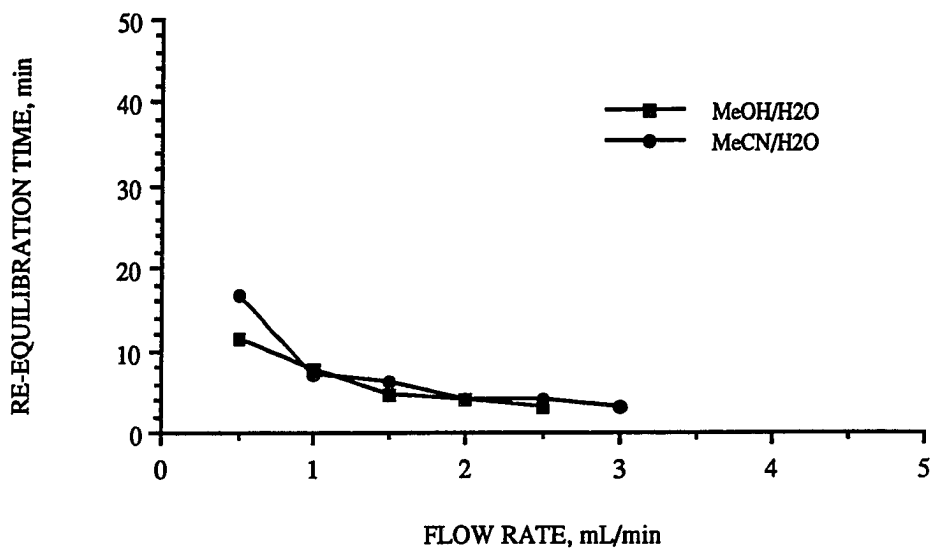


FIGURE 8.11. Effect of flow rate on column re-equilibration time after gradient elution for the Microsorb Si-C₁₈.

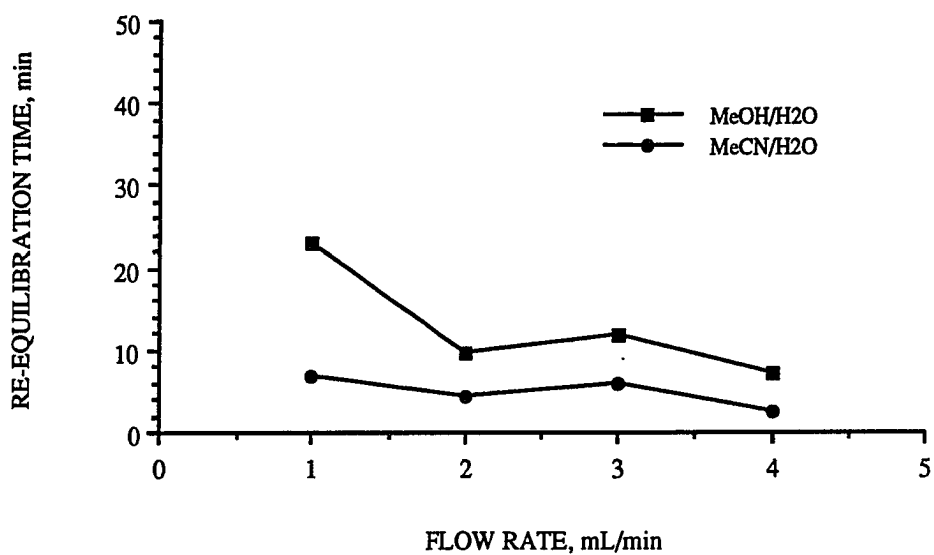


FIGURE 8.12. Effect of flow rate on column re-equilibration time after gradient elution for the Unisphere Al-PBD.

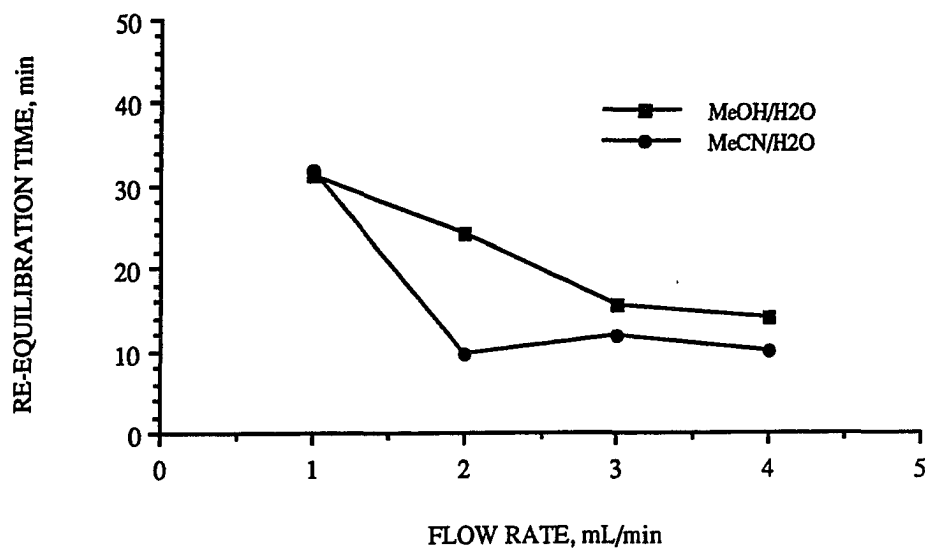


FIGURE 8.13. Effect of flow rate on column re-equilibration time after gradient elution for the Unisphere Al-C₁₈.

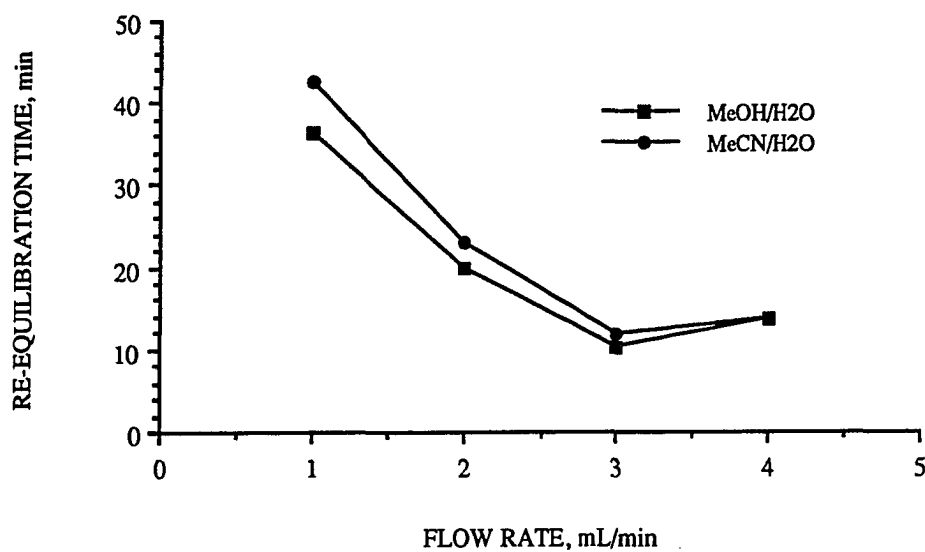


FIGURE 8.14. Effect of flow rate on column re-equilibration time after gradient elution for the Unisphere Al-CN.

decreased column re-equilibration time by almost 80% for the Microsorb Si-C₁₈ column.

The results obtained regarding the effect of mobile phase flow rate on column re-equilibration for both silica- and alumina-based columns are consistent with the claims of Snyder's group [1, 3, 6] that *column re-equilibration is determined primarily by the total volume of mobile phase pumped through the column, and not by the total time employed for equilibration*. Therefore, it is recommended that the stationary phase be flushed with the new mobile phase using the highest flow rate allowable. This will lead to more efficient re-equilibration due primarily to the significant reduction in equilibration time while still consuming approximately the same volume of new mobile phase. Hence, the only limiting factor to the use of high flow rates will be the corresponding column backpressure which is an inherent property of the stationary phase. Since relatively lower column backpressures are obtained for the Unisphere reversed-phase columns compared to conventional Si-C₁₈ (see Chapter VII), column equilibration can be carried out using higher flow rates for the aluminas, resulting in shorter "total" analysis time.

C. Effect Of Temperature

Figures 8.15 to 8.18 illustrate the effect of temperature on column re-equilibration. These experiments were carried out using column temperatures ranging from 15.0 to 55.0° C. Similar to the results obtained from the previous section, no definite conclusions can be made as a result of increasing temperature since the RCV values obtained fluctuated over an average range of only about 5 column volumes for both Si-C₁₈ and polymer-coated aluminas. However, comparison of the mobile phase volumes necessary to equilibrate the different stationary phases at 15.0 and 55.0° C reveals a general decrease in re-equilibration volumes. For the 4.0 x 125 mm LiChrospher Si-C₁₈ with MeCN as organic modifier, increasing the temperature from 15.0 to 55.0° C

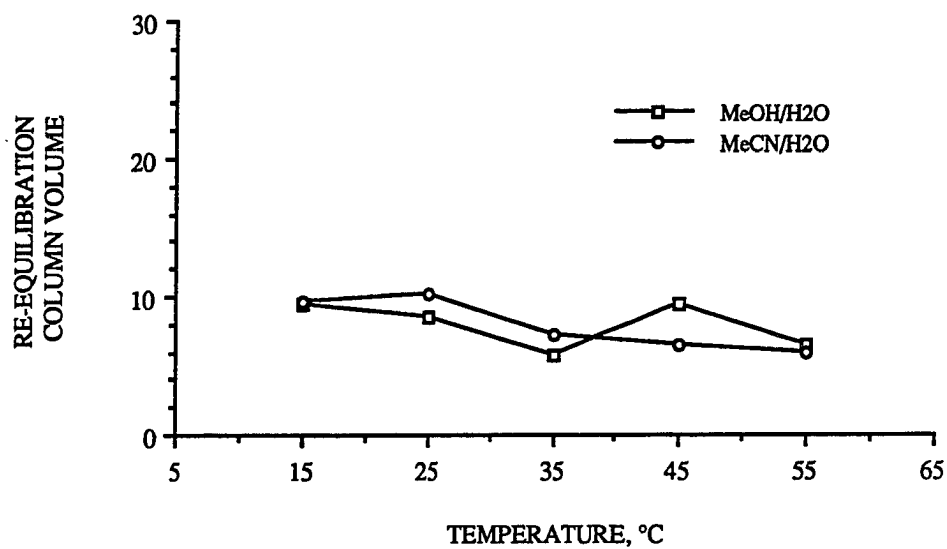


FIGURE 8.15. Effect of temperature on column re-equilibration after gradient elution for the LiChrospher Si-C₁₈.

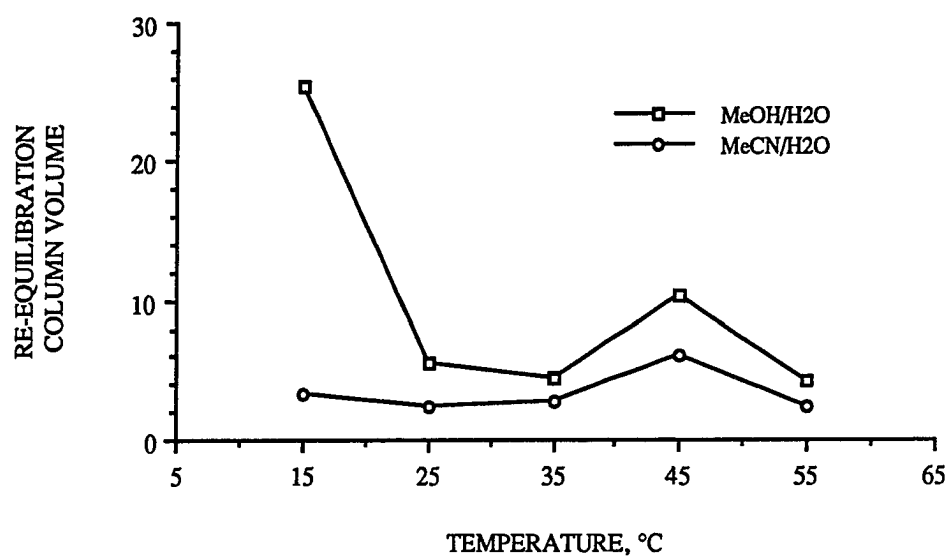


FIGURE 8.16. Effect of temperature on column re-equilibration after gradient elution for the Unisphere Al-PBD.

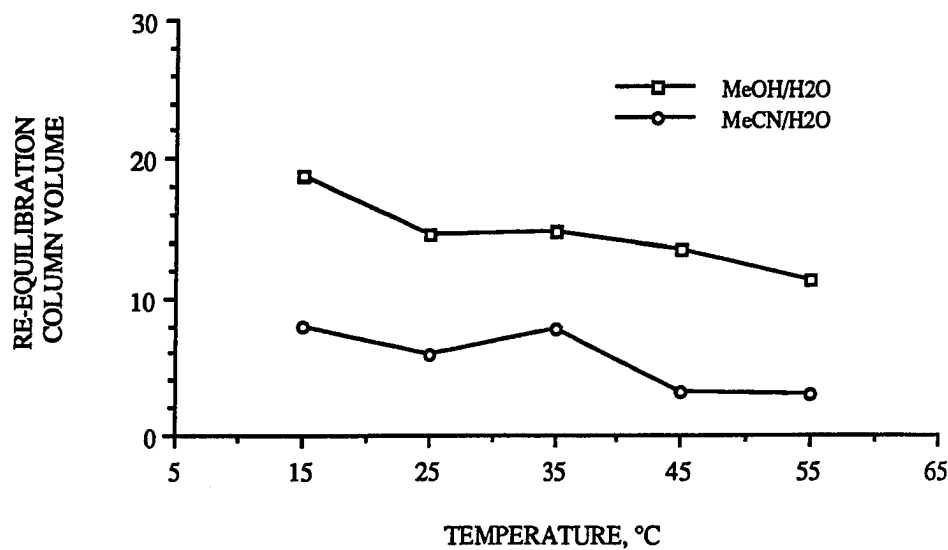


FIGURE 8.17. Effect of temperature on column re-equilibration after gradient elution for the Unisphere Al-C₁₈.

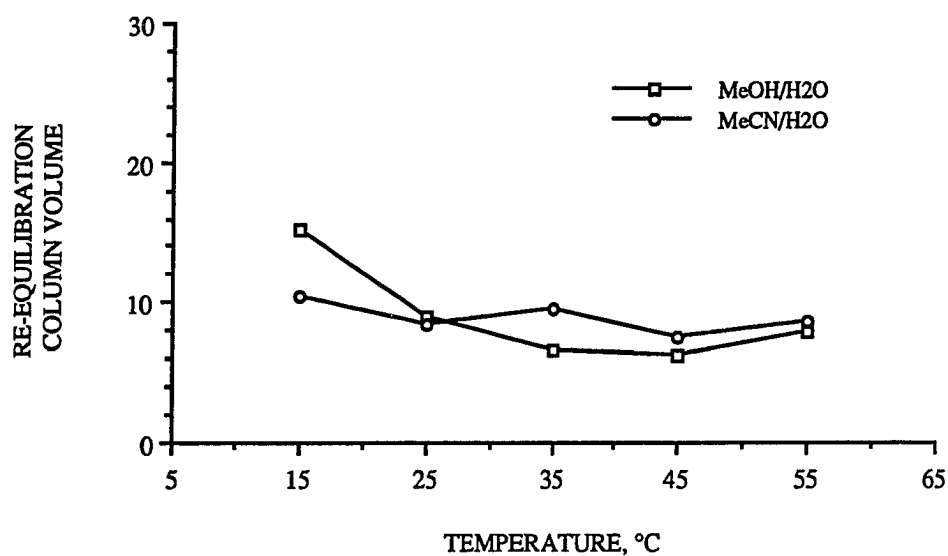


FIGURE 8.18. Effect of temperature on column re-equilibration after gradient elution for the Unisphere Al-CN.

resulted in a decrease in RCV from 9.6 to 5.9 column volumes, respectively. Similar results were obtained for the polymer-coated aluminas, decreasing from 7.9 to 2.9 column volumes for the Al-C₁₈ phase. Overall, increasing temperature from 15.0 to 55.0° C resulted in an average reduction of re-equilibration volume of 35% for the Si-C₁₈, and 40% for the various Unisphere aluminas, for both solvent systems.

As indicated in the previous section, an effective strategy to use in reducing column re-equilibration time is to employ the highest flow rate possible. Such an approach reduces re-equilibration time by almost 80%. In relation to this, although increasing temperature during column re-equilibration may not definitely lead to a significant reduction in RCV, increasing temperature will reduce the viscosity of the mobile phase allowing the use of even higher flow rates for column re-equilibration relative to that obtained at room temperature. According to Melander and Horváth [14], increasing the temperature from 15 to 55° C decreases mobile phase viscosity by approximately 50% for both MeOH/H₂O and MeCN/H₂O. Based on Eqn. 7.12, a 50% reduction in solvent viscosity should result in a 50% decrease in system backpressure. For example, using 30/70 MeOH/H₂O as mobile phase, observed reductions in ΔP values resulting from a temperature increase from 15.0 to 55.0° C for the Si-C₁₈ column ranged from 2790 to 1790 psi, while similar values for the Al-PBD, Al-C₁₈ and Al-CN columns ranged from 2800 to 1740, 3220 to 1970 and 2530 to 1640 psi, respectively.

Reductions in mobile phase viscosity as a result of increasing temperature become more significant for gradient methods started with hydroorganic mobile phases containing between 20 to 60% MeOH. This can clearly be seen from Fig. 8.19, which illustrates how solvent viscosity varies with mobile phase composition for both solvents used. Figure 8.19 also indicates that for mobile phases containing the organic solvent, viscosity values for MeOH/H₂O are larger than corresponding values for MeCN/H₂O at equal organic modifier concentrations. Hence, higher flow rate settings can be used to

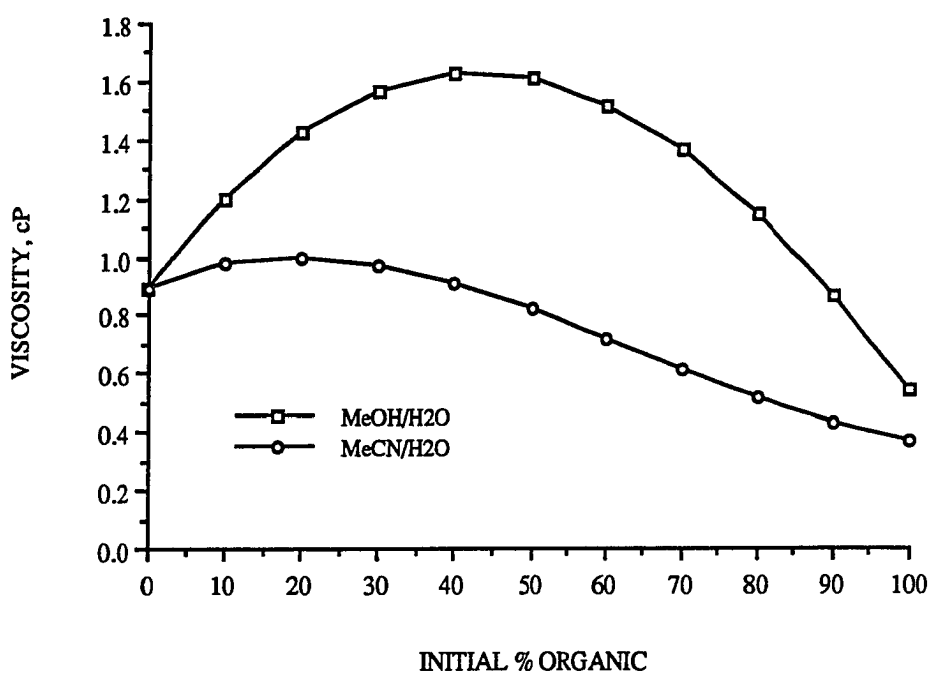


FIGURE 8.19. Mobile phase viscosity at different compositions for hydroorganic mixtures of MeCN and MeOH [15].

equilibrate a given stationary phase with 30/70 MeCN/H₂O than with 30/70 MeOH/H₂O. Finally, the easiest strategy to use to lower column backpressure would be to increase column temperature, which would allow the use of higher mobile phase flow rate, resulting in shorter equilibration time. Therefore, it is reasonable to conclude that *employing both high flow rate and high temperature will facilitate faster column re-equilibration after gradient elution*. It should be noted, however, that the latter recommendation assumes minimal temperature effects on the selectivity of the stationary phase.

REFERENCES FOR CHAPTER VIII

1. Snyder, L.R.; Kirkland, J.J. *Introduction to Modern Liquid Chromatography*, 2nd ed.; John Wiley & Sons, Inc.: New York, 1979; Chapter 16.
2. Snyder, L.R. *Gradient Elution In High-Performance Liquid Chromatography-Advances and Perspectives*, Horváth, C., Ed.; Academic Press: New York, 1980; Vol. 1.
3. Snyder, L.R.; Glajch, J.L.; Kirkland, J.J. *Practical HPLC Method Development*; John Wiley & Sons, Inc.: New York, 1988; Chapter 6.
4. Dolan, J.W. *LC-GC* 1987, 5, 384-390.
5. Dolan, J.W.; Snyder, L.R. *LC-GC* 1987, 5, 970-976.
6. Dolan, J.W. *LC-GC* 1987, 5, 466-470.
7. Cole, L.A.; Dorsey, J.G. *Anal. Chem.* 1990, 62, 16-21.
8. Engelhardt, H.; Dreyer, B.; Schmidt, H. *Chromatographia* 1982, 16, 11-17.
9. Dolan, J.W.; Snyder, L.R. *Troubleshooting LC Systems*, The Humana Press Inc.: New Jersey, 1989; Chapter 15.
10. Majors, R.E. *Anal. Chem.* 1973, 45, 755-762.
11. Engelhardt, H. *Z. Anal. Chem.* 1975, 277, 267-274.
12. Payne, L.D.; Arenas, R.V.; Little, E.L.; Foley, J.P. Presented at the 197th ACS National Meeting, Dallas, April 10, 1989, Paper ANYL6.
13. Holland, K.B., Biotage Inc., Personal correspondence by R.V. Arenas.
14. Melander, W.R.; Horváth, C. *Reversed-Phase Chromatography In High-Performance Liquid Chromatography-Advances and Perspectives*, Horváth, C., Ed.; Academic Press: New York, 1980; Vol. 2.
15. Foley, J.P.; Crow, J.A.; Thomas, B.A.; Zamora, M. *J. Chromatogr.* 1989, 478, 287-309.

PART B

VERSAL ALUMINAS FOR NORMAL-PHASE LIQUID CHROMATOGRAPHY

CHAPTER IX

GENERAL INTRODUCTION

A. γ -Alumina For Normal-Phase Liquid Chromatography

The major component of porous, chromatographic-grade alumina (collectively known as transition alumina) is crystalline γ -alumina, produced by controlled thermal decomposition of gibbsite, bayerite or boehmite [1].

Chromatographic γ -aluminas have surface areas between 50-200 m²/g. Although large pore diameter aluminas can be synthesized, most commercially-available chromatographic aluminas have maximum pore diameters of *ca.* 100 Å. Most γ -aluminas also have a large number of micropores, with pore diameters < 20 Å [2].

Alumina is amphoteric in nature, and five distinct acid-base sites have already been identified on the alumina surface [1]. γ -Alumina is stable over a pH range of 2-13 [3-5]. The isoelectric point of alumina is at *ca.* pH 7.5. However, this value shifts depending on the buffer used. Commercial γ -alumina is available either as neutral, acidic or basic alumina. These forms are, however, interconvertible by addition of either acid or base. Acidic alumina can be used as an anion exchanger, while basic alumina can be used as a cation exchanger. Snyder [6] gives a good review on the differences in selectivity of alumina and silica.

The surface activity of alumina for use in normal-phase liquid chromatography with nonpolar mobile phases is usually adjusted by controlling the water content of both the adsorbent and the mobile phase. This not only controls the selectivity and retention characteristics of the stationary phase, but also results in faster equilibration of the adsorbent with the mobile phase. Engelhardt [7] reviews the importance and different moderators that can be used for normal-phase liquid chromatography.

Versal GL And Versal GH Aluminas

The information contained here were obtained from Kaiser Aluminum Chemical Corporation [8] and LaRoche Chemicals, Inc. [9].

Versal GL and Versal GH are high purity, high performance catalytic-grade γ -aluminas manufactured by LaRoche Chemicals, Inc. in Baton Rouge, primarily for use as catalytic supports and ceramic raw material. Versal GL is a low density material with a very high macroporosity (*i.e.*, with pore diameters $> 350 \text{ \AA}$), while Versal GH is a high-density material. The surface areas (calcined at 600°C) of Versal GL and GH are 200-300 and 150-290 m^2/g , respectively, while the loose bulk densities of Versal GL and GH are 0.21 and 0.64 g/m^3 , respectively.

Unfortunately, LaRoche Chemicals, Inc. does not produce chromatographic-grade aluminas. Thus, the γ -alumina samples provided by LaRoche were prepared from bulk Versal GL and Versal GH by mechanically crushing the adsorbent, and then classifying by size.

The primary objectives of this part of the research are to optimize the slurry-packing procedure for Versal GL and GH aluminas for applications in normal-phase liquid chromatography, and to determine and compare the chromatographic properties of the packed Versal aluminas.

B. Packing Of HPLC Columns

HPLC columns are packed using either (i) the dry-fill packing procedure [10, 11] or (ii) the high-pressure slurry-packing procedure (*i.e.*, wet-fill packing) which can be operated either in the down-flow or up-flow modes [10, 12-15]. The dry-fill process is recommended for particles with $d_p > 20 \text{ }\mu\text{m}$ [10, 16]. However, according to Snyder and Kirkland [10], totally porous particles with $d_p < 30 \text{ }\mu\text{m}$ should not be dry-packed

unless they possess a narrow particle size distribution (*i.e.*, $\leq 2d_p$). Efficient HPLC columns of particles with $d_p < 20\ \mu\text{m}$ are difficult to dry-pack.

Modern HPLC columns are packed with particles with d_p in the range 3 - 20 μm , the most popular having diameters between 3 - 10 μm [16]. However, columns introduced at the 1991 Pittsburgh Conference showed a trend toward the use of 3 and 5 μm particles, and away from particles with $d_p \geq 10\ \mu\text{m}$ [17]. Thus, most HPLC columns at present are packed using the slurry method.

1. High-Pressure Slurry-Packing Of HPLC Columns

The main objective in packing HPLC columns is to prepare a column characterized by (i) a tightly-packed, homogeneous bed of uniform packing density, and (ii) high efficiency. Listed below are the requirements necessary to achieve a tightly-packed, homogeneous bed prepared by the high-pressure slurry-packing procedure according to Knox [16]. These conditions are particularly important when slurry packing is done using the down-flow mode, the method used in this study.

1. The particles must not sediment too fast during the procedure.
2. The particles must not agglomerate.
3. The particles must hit the accumulating bed at a high impact velocity.
4. Each particle should have time to settle in before it is buried by other particles landing on top.
5. The liquid used to support the slurry must be easily washed out of the packing and must not react with it.

Sedimentation (1), which leads to particle sizing and differences in packing density along the column, is easily prevented by using the balanced-density technique. This is normally achieved by employing a mixture of polar solvent (*e.g.* methanol or ethanol) and high-density, nonpolar halogenated alkane (*e.g.* diiodomethane which has a density of 3.3 g/mL). Unfortunately, high-density halogenated hydrocarbons are very

expensive (*e.g.* 100 grams of diiodomethane from Aldrich Chemicals Company, Inc. cost \$25.30), corrosive to stainless steel and other parts of the HPLC, and most are toxic (*e.g.* tetrabromoethane).

Particle agglomeration (2) causes non-uniform packing compaction, which results in non-uniform mobile phase velocities within the column. This is prevented by (i) using a slurry liquid that will effectively wet the adsorbent, and (ii) sonicating the slurry for a good amount of time immediately prior to packing.

Requirement (3) is achieved by slurry-packing the material at a high packing pressure (*e.g.* > 6000 psi), although one will be limited by the pressure stability of the material being used. Using too high a pressure for a particular adsorbent may cause it to collapse and produce smaller diameter particles which would lead to a wide PSD and may produce fines which could plug the column.

To allow the particles to have enough time to settle (4), and thus be able to reorient in a position that allows the tightest possible packing before being topped by other particles, a dilute slurry should be employed. As defined by Knox [16], dilute slurries consist of 1-10% (v/v) solid, while concentrated slurries should contain 10-50% (v/v) solid. Satisfying requirement (5) in some cases would limit what substances can be used as slurry liquids to satisfy requirements (1) - (3).

The major difficulty involved when optimizing a column packing procedure for a particular material is that there is no generalized procedure which is applicable for all stationary phases. Even for the "same" material but from different manufacturers, subtle differences in packing procedures are typically necessary for optimum performance. To complicate matters further, a lot of variables (which can interact with each other) are known to affect column packing. Some of the variables involved which are expected to affect the column packing properties of normal-phase aluminas are given below [15]:

1. Quality of absorbent.
 - a. Particle size.
 - b. Particle size distribution.
 - c. Pore size.
 - d. Pore size distribution.
 - e. Particle density.
 - f. Particle shape (spherical or irregular).
2. Slurry preparation.
 - a. Solvent (balanced-density or nonbalanced-density).
 - b. Solvent quality.
 - c. Slurry concentration.
 - d. Slurry temperature.
3. Packing procedure.
 - a. Pressure.
 - b. Upward versus downward packing.
 - c. Packing vessel geometry.
 - d. Geometry of packing vessel outlet.
4. Column characteristics.
 - a. Internal diameter.
 - b. Length.
 - c. Wall smoothness.
 - d. Frit porosity and thickness.
 - e. Distributor plates (if any).

Other variables which Verzele and Dewaele [15] did not identify but which we consider important for the packing procedure includes deciding (i) whether or not to pressurize and release, (ii) whether to depressurize slowly or abruptly, and (iii) the volume of push liquid to be used. With all these difficulties involved, variable results are to be expected, and to be able to apply statistics to the results, a large number of columns has to be packed (maybe at least ten columns at exactly the same conditions).

As such, slurry-packing HPLC columns is a procedure that is very involved, time consuming and very operator-dependent. Every operator has his own strategy and

"magic" formula for achieving a highly efficient column. This is especially true when a relatively unsophisticated apparatus (*e.g.* a column packer that only operates in the down-flow mode) is employed as in the present study. Despite such limitations inherent with basic column packing equipment, it is still possible in most cases, however, to evaluate the packing characteristics (limitations) of a particular adsorbent. The resulting information can then be incorporated into methodologies for packing highly efficient HPLC columns based on more sophisticated and expensive slurry-packing devices (*e.g.* multi-column packers which operate in the up-flow mode).

Slurry packers which operate in the up-flow mode can readily eliminate or minimize particle sedimentation and agglomeration since they are equipped with a mechanical stirrer in the slurry reservoir. However, they are more costly (\$4000 vs \$2000). For more information about the up-flow method for slurry-packing HPLC columns, the reader should refer to the following references [13-15].

2. Dry-Packing Of HPLC Columns

Dry-packing can be performed using either (i) the "rotate, bounce and tap" method or "tap-fill" method [10] widely used for particles with $d_p \geq 40 \mu\text{m}$, or (ii) the "lateral tapping" method [11]. The first method involves both vertical and lateral tapping of the column after each incremental addition of packing material. The second method utilizes only lateral tapping, which according to Davies [11] eliminates the rebounding of packed adsorbent (which loosens the packed bed) that occurs during the vertical bouncing of the column on a hard surface. It should be noted, however, that exposing the column to too much lateral and vertical vibrations can lead to sizing effects for materials with a very wide PSD.

REFERENCES FOR CHAPTER IX

1. Unger, K.K.; Trüdinger, U. In *High Performance Liquid Chromatography*; Brown, P.R.; Hartwick, R.A., Eds.; John Wiley & Sons, Inc.: New York, 1989; Chapter 3.
2. Unger, K.K. In *Packings and Stationary Phases in Chromatographic Techniques*; Unger, K.K., Ed.; Marcel Dekker, Inc.: New York, 1990; Chapter 6.
3. Billiet, H.; Laurent, C.; de Galan, L. *Tr. Anal. Chem.* **1985**, *4*, 100-103.
4. Schomburg, G. *LC-GC* **1988**, *6*, 36-50.
5. Majors, R.E. *LC-GC* **1990**, *8*, 198-210.
6. Snyder, L.R. *Principles of Adsorption Chromatography*; Marcel Dekker, Inc.: New York, 1968.
7. Engelhardt, H. *J. Chromatogr. Sci.* **1977**, *15*, 380-384.
8. Kaiser Aluminum Chemical Corporation, *Versal - A Family of High-Performance, Catalytic-Grade Aluminas*, 1987.
9. LaRoche Chemicals, *Alumina Products And Technology*, 1988.
10. Snyder, L.R.; Kirkland, J.J. *Introduction to Modern Liquid Chromatography*, 2nd ed.; John Wiley & Sons, Inc.: New York, 1979; Chapter 7.
11. Davies, R.D. *J. High Res. Chromatogr., Chromatogr. Commun.* **1981**, *4*, 270-275.
12. Melander, W.R.; Horváth, C. *Reversed-Phase Chromatography In High-Performance Liquid Chromatography-Advances and Perspectives*, Horváth, C., Ed.; Academic Press: New York, 1980; Vol. 2.
13. Linder, H.R.; Keller, H.P.; Frei, R.W. *J. Chromatogr. Sci.* **1976**, *14*, 234-239.
14. Bristow, P.A.; Brittain, P.N.; Riley, C.M.; Williamson, B.F. *J. Chromatogr.* **1977**, *131*, 56-64.
15. Verzele, M.; Dewaele, C. *LC-GC* **1986**, *4*, 614-618.
16. Knox, J.H. *J. Chromatogr. Sci.* **1977**, *15*, 352-364.
17. Majors, R.E. *LC-GC* **1991**, *9*, 192-203.

CHAPTER X

EXPERIMENTAL

A. Preparation Of Adsorbent And HPLC Column Blanks

The procedure suggested by Snyder and Kirkland [1] was employed. To remove the fines, the adsorbent was slurried in excess methanol, then sonicated for at least 15 minutes to break up aggregates and ensure complete wetting of the particles. The main fraction of the mixture was allowed to settle (usually less than one minute for 15 μm Versal GH alumina), after which the supernatant (which contains the fines) was discarded. Removal of fines was repeated at least twice, although it was recognized that additional material will be lost by doing so. After discarding the supernatant from the last sonication of the slurry, the residue is air-dried (which requires at least 3-5 hours and normally done overnight), and then the resulting cake (air-dried residue) is pulverized by scraping the surface with a glass rod, then mixed.

Empty HPLC column blanks of various lengths (5, 10, 15 and 25 cm) and with an internal diameter of 4.6 mm were obtained from Alltech Associates, Inc. (Deerfield, IL). These stainless steel tubes had a highly-polished, mirror-finished inner wall to eliminate friction between the column wall and adsorbent during packing. The interior of the tubes was cleaned by rinsing successively with dichloromethane (to remove any residual oil/grease left after manufacture), acetone, and water, followed by scrubbing with a warm detergent solution using a pipe cleaner (to ensure a smooth surface free from particulates). The tubes were then rinsed with water, methanol, and finally air-dried. The 2 μm 316 stainless steel frits that accompanied the blanks were cleaned by sonicating in methanol for at least 10 minutes, rinsing with methanol, and air-drying.

B. High-Pressure, Slurry-Packing Procedure

Figure 10.1 shows a diagram of the HPLC slurry packer (Alltech Associates, Inc., Deerfield, IL) used. It consists of (i) an air-driven constant-pressure pump (Haskel Inc., Burbank, CA) with a maximum pressure rating of 15000 psi, an amplification ratio (practical work ratio) of 122:1, and a liquid displacement capacity of 11 mL/stroke; and (ii) a 40 mL slurry reservoir (Scientific Systems, Inc., State College, PA) equipped with hand-operated, knurled closure nuts which allows quick connection of the slurry reservoir to the pump and precolumn/empty HPLC column assembly prior to pressurization. This HPLC slurry packer operates in the down-flow mode, and thus would necessitate a balanced-density packing technique (where the density of the slurry solvent is adjusted so as to be equal to the density of the adsorbent) for materials that are characterized by (i) a wide PSD, (ii) $d_p \geq 10 \mu\text{m}$ [1], and (iii) a relatively high density.

The procedure used for slurry-packing empty HPLC columns is outlined below. The different steps listed were as suggested by Snyder and Kirkland [1], and Melander and Horváth [2]. However, several modifications were included whenever practical.

1. Place frits and end-fitting assemblies at column inlet and outlet. Make sure that the ferrule is compressed very well on stainless steel tube. Disconnect end-fitting body and frit from one end. This will serve as the column inlet. The empty HPLC columns used come with $2 \mu\text{m}$ frits. If $d_p < 5 \mu\text{m}$, use $0.5 \mu\text{m}$ frits.
2. Fill solvent reservoir (1 L capacity) with displacement or push solvent. This should be filtered and degassed before use.
3. Prime the pump by allowing enough solvent to pass through for 1-2 minutes, with the pump pressure set at ≥ 30 psi (Note: The Haskel pump has an amplification ratio of 122:1, thus a pump inlet pressure of 30 psi corresponds to an outlet pressure of 3660 psi). This was accomplished by installing a high-

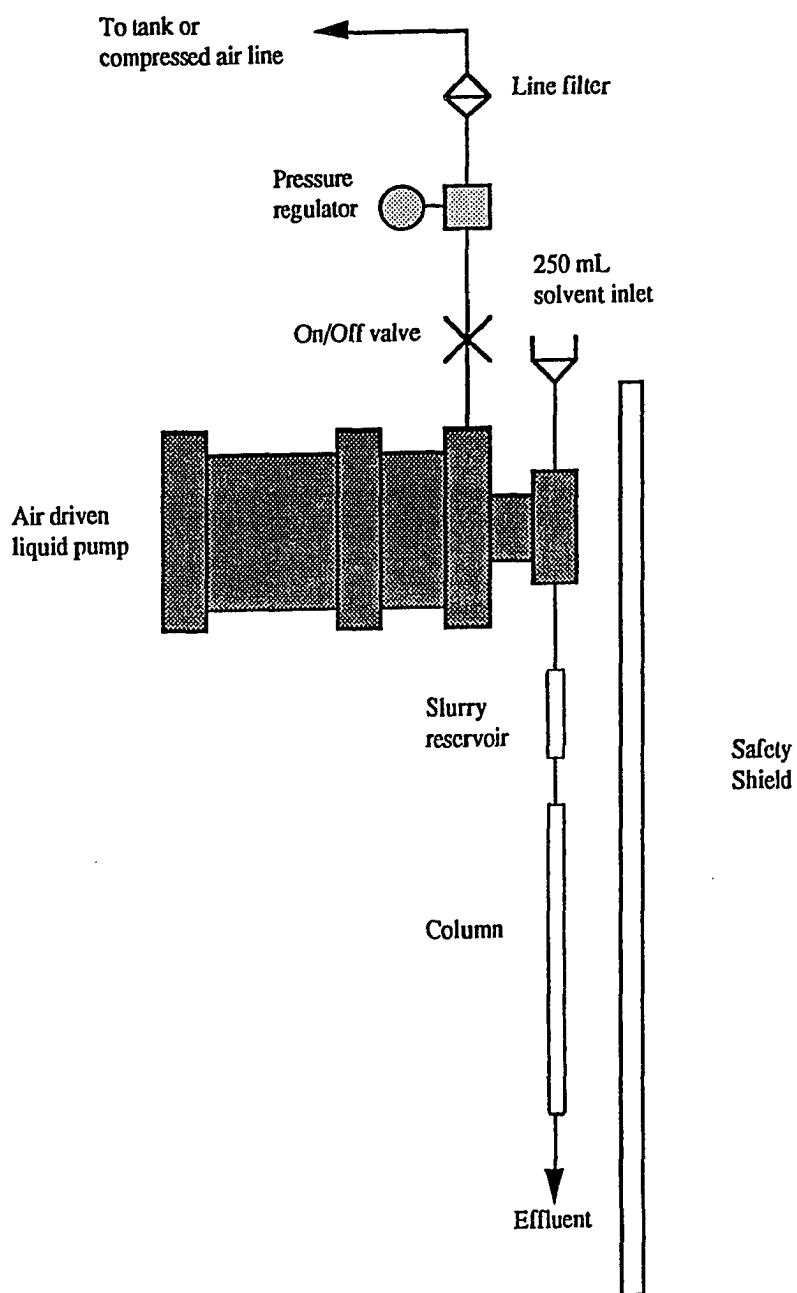


FIGURE 10.1. Diagram illustrating Alltech's high-pressure slurry packing apparatus (Alltech Associates, Inc., Product Data 29426-122-1). For the actual packer employed, a 5 cm precolumn (internal diameter = 4.6 mm) was used to connect the slurry reservoir and the empty HPLC column.

pressure fitting at the liquid outlet (*e.g.* connecting a packed HPLC column with end-fittings fixed at the outlet) prior to priming.

4. After priming, allow the system to depressurize. Then disconnect the high-pressure fitting at the outlet.
5. Connect empty HPLC column to slurry reservoir/precolumn assembly and fill the empty column with the same solvent to be used for preparing the slurry. Rap the sides of the HPLC column to dislodge any air trapped along the inner wall.
6. Prepare the slurry to be used by adding enough packing material to the slurry solvent and placing the mixture in an ultrasonic bath for at least 15 minutes to degas and prevent particle agglomeration.
7. Remove the slurry from the sonicator and shake for at least 10 seconds. Then carefully pour the slurry into the slurry reservoir/precolumn/empty column assembly and immediately fill the remaining volume with displacement solvent without disturbing the slurry. Be careful not to trap air within the reservoir.
8. Connect slurry reservoir/precolumn/empty column assembly to the pump.
9. Pack the empty HPLC column by pressurizing the pump. This can be done either (i) by pressurizing and releasing (*i.e.*, pressurizing the pump with the on/off valve of the packer closed, then immediately opening the valve during the packing process, thus subjecting the packing material to a sudden increase in pressure) or (ii) by pressuring the pump (within 15 seconds) with the on/off valve of the packer open thus exposing the packing material to a more gradual increase in pressure. The packing pressure to be used should be significantly higher than the highest pressure the column is expected to be subjected to.

10. Continue pumping until the displacement solvent elutes from the end of the column, and enough solvent has passed through the column to ensure a stable, tightly-packed bed.
11. Wait for the pump to cycle and turn off the pressure. Again, this can be done gradually or by immediately turning off the pump pressure using the on/off valve of the column packer.
12. Allow the system to depressurize naturally on the pump (15-30 minutes).
13. Disconnect the column, dry the top of the packing bed with a laboratory paper wipe, and carefully scrape away excess packing with a sharp razor blade. Then gently place frit and end-fitting body at column inlet without disturbing the packed bed.
14. Label the column.
15. Condition the column with the desired HPLC solvent to be used.

C. Dry-Packing Procedure

1. "Tap-Fill" Method

The procedure used is outlined below, and was based on the methodology of Snyder and Kirkland [1] with minor modifications.

1. Place frit and end-fitting assembly at column outlet.
2. With the column held vertically, add adsorbent slowly to fill 3 - 5 mm of column.
3. Bounce the column up and down on a hard surface, 2 - 3 times per minute, for 100 times, while gently rapping the side of the tube at approximately the point where the adsorbent is settling.
4. Repeat steps 2 and 3 until column is full.

5. When full, bounce the column for 5 minutes more, adding more packing if necessary. Remove excess material if needed.
6. Place frit and end-fitting assembly at column inlet.
7. Label the column.
8. Condition the column with the desired HPLC solvent to be used.

2. "Lateral Tapping" Method

The procedure employed was a modified version of the methodology of Davies [3]. The same steps as in the "tap-fill" method was used, except for the vertical tapping (or bouncing) part. Instead, for each incremental addition of adsorbent, the column was tapped laterally 40 times (at a rate of 2 taps per second) at approximately the point where the particles are settling. This is repeated until the column is full.

D. Conditioning The Column

Column conditioning is the process whereby the stationary phase is equilibrated with the mobile phase to be used. Since the packed Versal alumina columns are to be used in normal-phase liquid chromatography, the stationary phase has to be equilibrated with nonpolar solvents (*e.g.* (i) hexane/0.05% acetonitrile, or (ii) 85% isooctane, 15% (premixed 99.7% ethanol/0.3% water)).

After slurry packing, the polar alumina particles will be highly solvated with methanol (the push liquid). Column conditioning will take a very long time if carried out simply by flushing the column with the final (nonpolar) mobile phase to be used. A better alternative is to flush the adsorbent with a series of solvents of decreasing polarity, each of which is completely miscible with the immediately prior and successive solvents. To minimize solvent consumption and the total time required for conditioning, a maximum of six columns were connected end-to-end in series and flushed simultaneously at a flow rate of 1.0 mL/min. Conditioning was normally performed

overnight. Outlined below are the procedures for each of the two mobile phases employed.

a. Mobile phase: Hexane/0.05% Acetonitrile

Columns were conditioned by using in series 60 mL acetone, 120 mL dichloromethane, 60 mL toluene, and 120 mL hexane/0.05% acetonitrile.

b. Mobile phase: 85% Isooctane, 15% (premixed 99.7% ethanol/0.3% water)

Columns were conditioned by using in series 120 mL dichloromethane, then 120 mL 85% isooctane, 15% (premixed 99.7% ethanol/0.3% water).

For dry-packed columns, an additional step was necessary which involved flushing the column initially with 60 mL methanol.

An easy way to check whether or not a column has been fully equilibrated with the mobile phase is to repetitively measure the retention time for a retained solute. Any systematic trends or random imprecision in these data would imply that the stationary phase is not yet in equilibrium with the mobile phase.

E. Evaluation Of Column Performance

1. Instrumentation

All chromatographic runs were carried out using (i) either a Series 400 Liquid Chromatograph equipped with an OMEGA-4 data collection and integration system (Perkin-Elmer, Norwalk, CT), or a Rainin Model HP Liquid Chromatograph controlled by an Apple Macintosh personal computer with the Dynamax HPLC method manager (Rainin Instrument Co., Woburn, MA); (ii) a Model 7125-075 six-port injection valve (Rheodyne Inc., Cotati, CA) with 6 μ L loop; and (iii) a model V⁴ variable wavelength absorbance detector (ISCO, Lincoln, NE) set at 254 nm. For temperature control, the columns were kept in glass water jackets connected to a model RMS-6 circulating bath

(Brinkmann Instruments, Inc., Westbury, NY). Except for temperature dependent studies, all chromatographic experiments were conducted at 25.0° C.

2. Solvents And Solutes

HPLC grade methanol, acetonitrile, ethanol, dichloromethane, chloroform, toluene, hexane, isooctane, and water were filtered using 0.45 μm Nylon-66 membranes and degassed before use. The solvents were kept at room temperature during the analysis. All test solutes (toluene, nitrobenzene, o-, m- and p-nitroaniline) were dissolved in solvents that were weaker or equal in strength to the mobile phase in order to minimize sample solvent artifacts. Sample solutions were filtered through 0.2 μm Nylon-66 membranes prior to injection. Retention measurements were not made until the column was fully equilibrated with the mobile phase.

3. "Reference" Stationary Phases

A 250 x 4.6 mm Unisphere neutral alumina column (Biotage, Inc., Charlottesville, VA, SN 580ATC) packed with 10 μm spherical particles was used as one control. Another control employed was an in-house slurry-packed column of a granular chromatographic grade silica (IMPAQ RG2010Si, The PQ Corporation, Conshohocken, PA), with a mean particle diameter of 8.8 μm .

4. Chromatographic Parameters

To determine column performance, peak asymmetry (Eqn. 6.4), column efficiency (Eqns. 7.2 and 7.3), and reduced plate height (Eqn. 7.4) were determined for each column packed. And unless indicated otherwise, N was determined manually using the Foley-Dorsey Equation [4].

5. Column Test Mixture

According to Saunders [5], the chromatographic test mixture to be used should contain at least three test solutes to be able to evaluate both the packing quality of the column and its corresponding mass transfer characteristics. One of the test solute

should be a compound which is unretained, and the other two should have a retention factor (k') < 10. Solute retention factor was calculated using Eqn. 2.1. These three components should be well resolved so as not to overlap when column efficiency decreases (*e.g.* as the column ages). We employed a five-component test mixture consisting of toluene, nitrobenzene, o-nitroaniline, m-nitroaniline and p-nitroaniline. The reduced plate height obtained for the unretained solute (toluene) will give an indication as to how well the column was packed, since it will experience very little mass transfer contribution from the stationary phase. On the other hand, the reduced plate height of a retained solute will reflect both the packing quality and mass transfer characteristics of the stationary phase.

6. Alternative To Complete Column Conditioning For Evaluation Of Column Packing Efficiency

Due to the time- and solvent-consuming nature of the conditioning procedures described above (even with the simultaneous conditioning of up to 6 columns), a much faster, alternative procedure was developed for the measurement of column packing efficiency. This procedure utilizes the push liquid (methanol) of the slurry-packing procedure as the mobile phase. Since the column has already been exposed to significant amounts of methanol during the packing process, it is only necessary to pass a small additional amount of methanol before the column is fully equilibrated under these conditions and a dilute test solution of toluene in methanol can then be injected. As described above, the toluene peak, although unretained using methanol as a mobile phase, will nevertheless provide a good estimate of packing efficiency. In the tabulated results in Chapter XI, *data obtained via this faster procedure are denoted by the addition of an asterisk (*) to the column numbers of various tables, e.g. "15A*" in Table 11.4A.*

REFERENCES FOR CHAPTER X

1. Snyder, L.R.; Kirkland, J.J. *Introduction to Modern Liquid Chromatography*, 2nd ed.; John Wiley & Sons, Inc.: New York, 1979; Chapter 5.
2. Melander, W.R.; Horváth, C. *Reversed-Phase Chromatography In High-Performance Liquid Chromatography-Advances and Perspectives*, Horváth, C., Ed.; Academic Press: New York, 1980; Vol. 2.
3. Davies, R.D. *J. High Res. Chromatogr., Chromatogr. Commun.* **1981**, *4*, 270-275.
4. Foley, J.P.; Dorsey, J.G. *Anal. Chem.* **1983**, *55*, 730-737.
5. Saunders, D.L. *J. Chromatogr. Sci.* **1977**, *15*, 372-379.

CHAPTER XI

OPTIMIZATION OF HPLC COLUMN PACKING PROCEDURE

A. γ -Alumina Samples Received From LaRoche Chemicals, Inc.

Table 11.1 gives a list of γ -Al₂O₃ samples received from LaRoche Chemicals. It should be noted that except for the 15 μ m Versal GH alumina, all other samples were sized by sieving which as can be seen from the scanning electron micrographs (SEM) in Figs. 11.1-11.3, fails to remove the fines and gives a very wide particle size distribution. The detrimental consequences of these two properties of adsorbents sized by the sieving method on the chromatographic characteristics of the corresponding packed HPLC columns are discussed later in the text.

The 15 μ m Versal GH was sized via "air classification", in a third-party laboratory (*i.e.*, not at LSU or LaRoche Chemicals, Inc.). As can be seen from the corresponding SEM (Figs. 11.4 and 11.5), this method gives a much narrower PSD, but still fails to remove the fines. Another important observation made was that the "air-classified" alumina was grayish in color, compared to the alumina samples prepared at LaRoche by sieving which were white. It is not known what caused this grayish color to develop, or whether this could have detrimental effects on the mass transfer characteristics of the corresponding packed columns. However, it was observed that during the removal of the fines, carried out by slurring the alumina in methanol and decanting the supernatant containing the fines, this grayish material is less dense than the bulk alumina and thus can be poured off with the supernatant liquid. Unfortunately, complete removal of the grayish particles was not achieved.

Typical amounts of adsorbent materials required to slurry pack 15 cm HPLC columns are given in Table 11.2. These values correspond to the amount needed to fill the 15 cm tube plus approximately half of the 5 cm precolumn (used to connect the

TABLE 11.1. γ -Al₂O₃ samples received from LaRoche Chemicals, Inc.

γ -Al ₂ O ₃	d _p (μm)
Versal GL	37-44
Versal GL	10-15
Versal GH	37-44
Versal GH	10-15
Versal GH	5-10
Versal GH ^a	15

^a This sample was "air-classified". The particles received had a grayish color, unlike the other samples received which were white and prepared by sieving.

TABLE 11.2. Typical amount of adsorbent needed to slurry-pack 15 cm HPLC columns.

Adsorbent	d _p (μm)	Amount of adsorbent needed (g)
Versal GH	15	3.7
Versal GL	10-15	2.4
IMPAQ RG2010Si	8.8	2.5

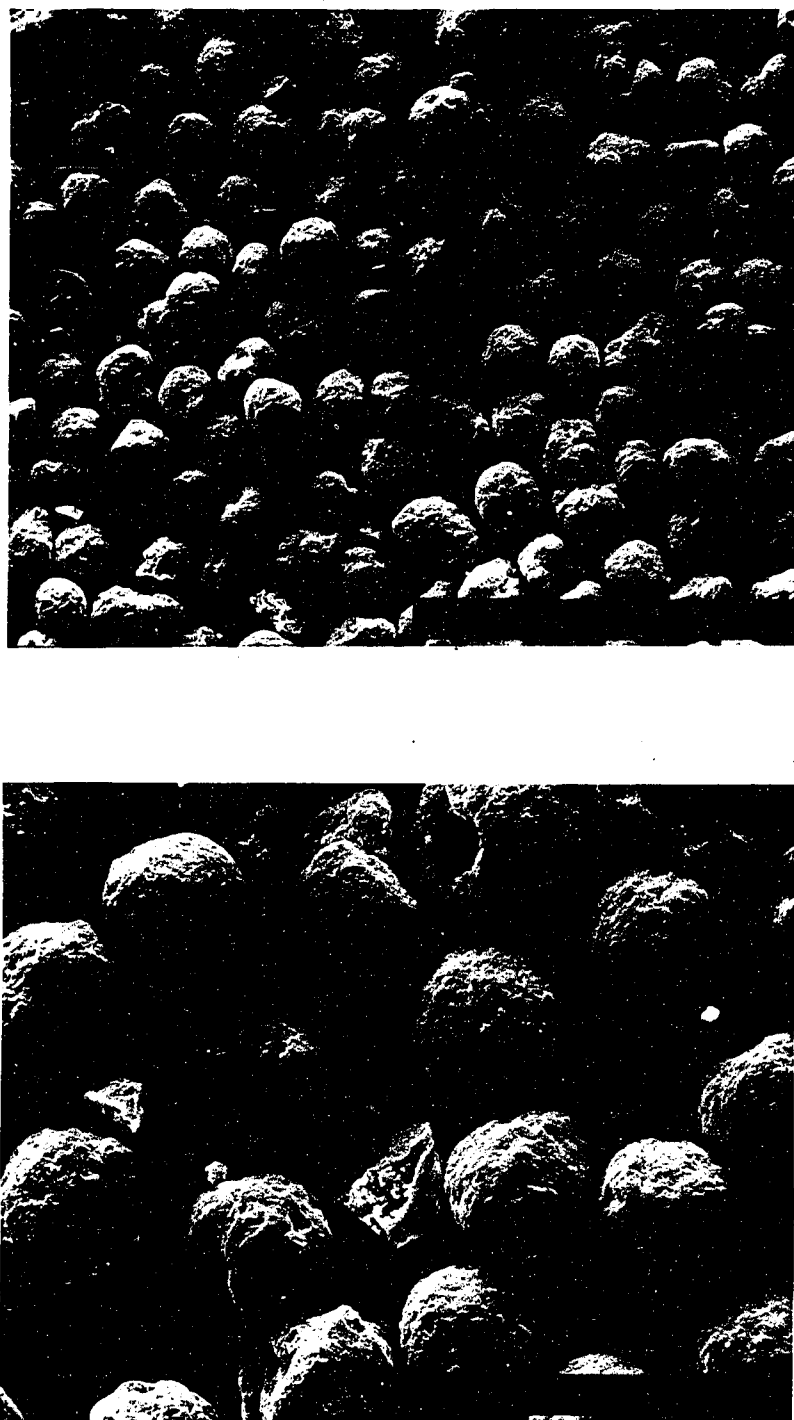


FIGURE 11. 1. Scanning electron micrographs of Versal GH after removal of fines; $d_p = 37\text{-}44\text{ }\mu\text{m}$; Magnification: Top = 200x; Bottom = 500x.

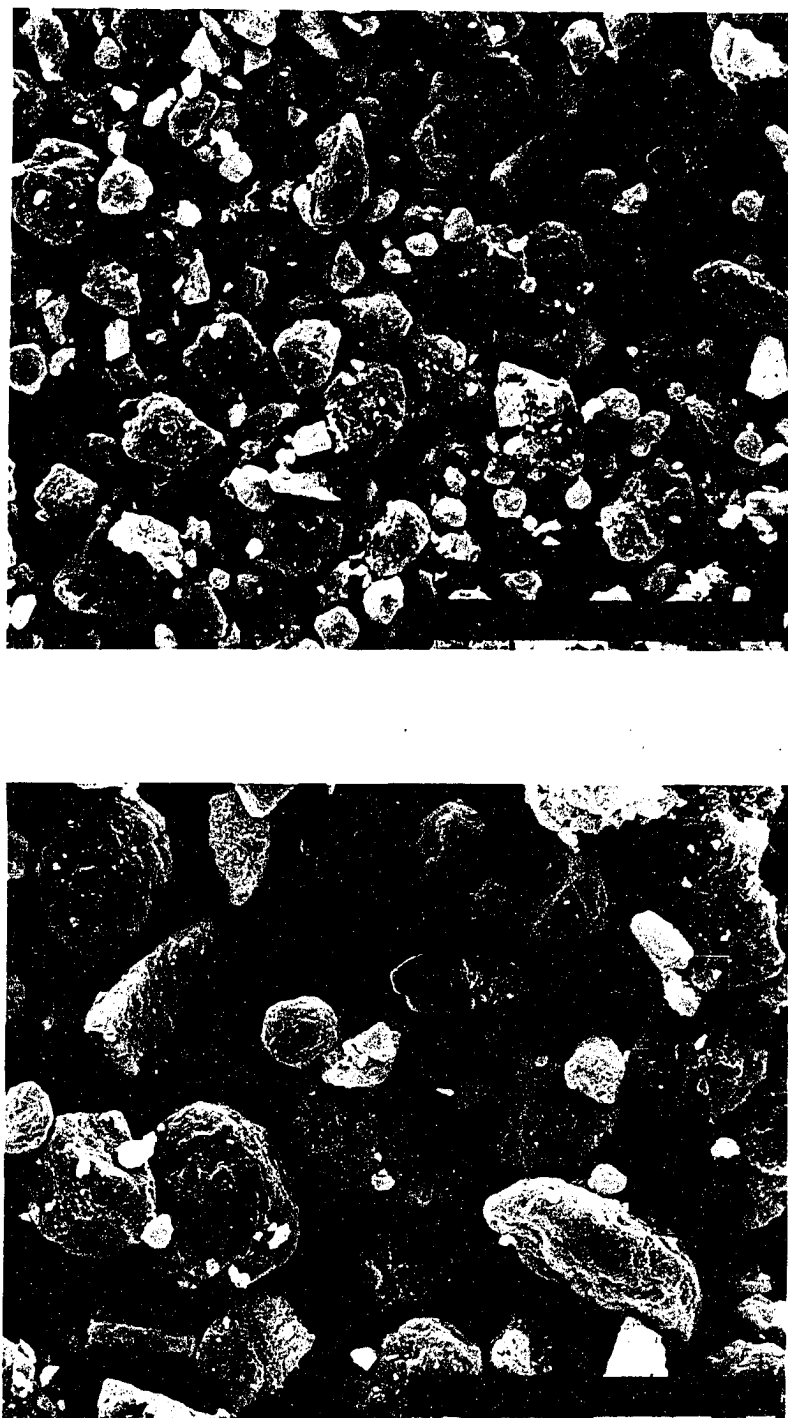


FIGURE 11. 2. Scanning electron micrographs of Versal GH after removal of fines; $d_p = 10\text{-}15\text{ }\mu\text{m}$; Magnification: Top = 1000x; Bottom = 2000x.

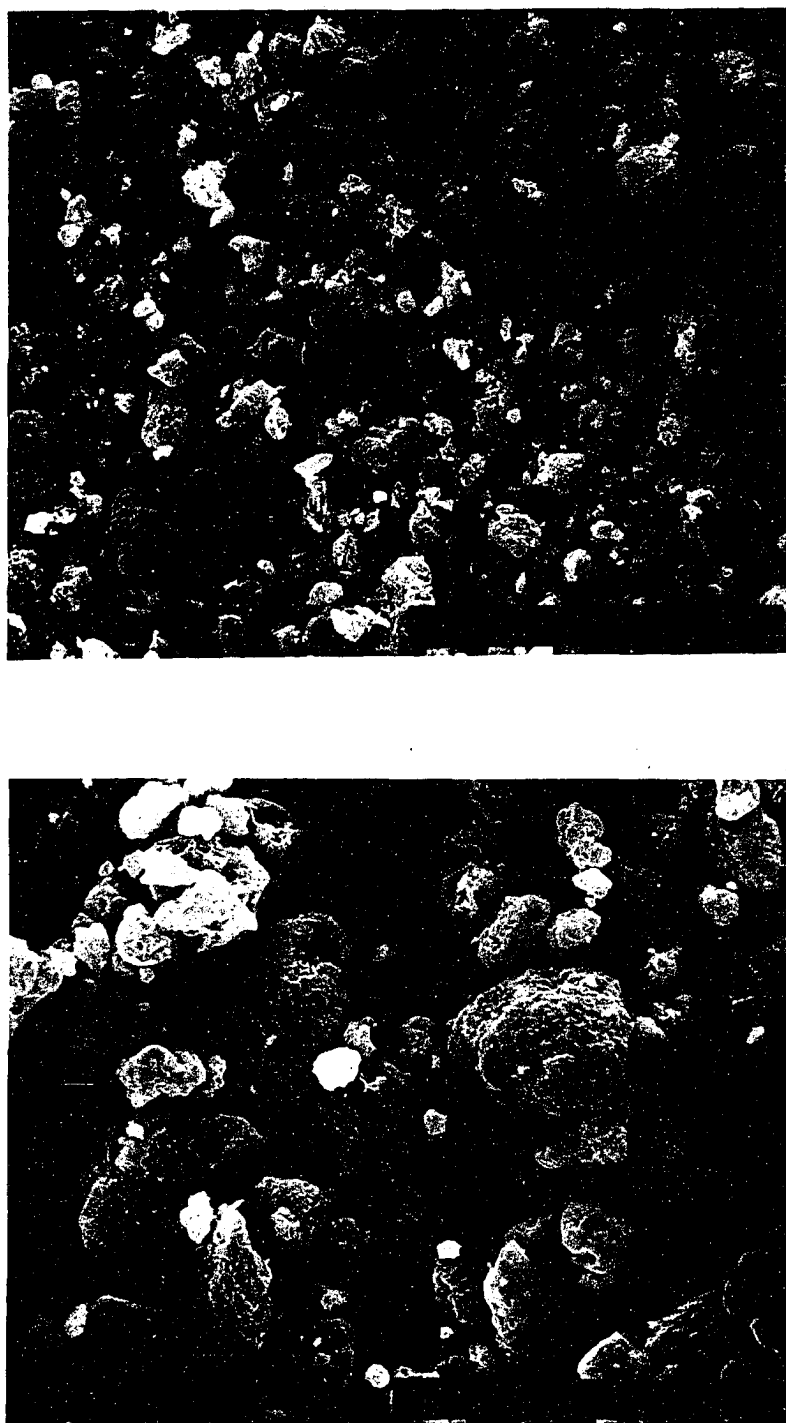


FIGURE 11. 3. Scanning electron micrographs of Versal GL after removal of fines; $d_p = 10\text{-}15\text{ }\mu\text{m}$; Magnification: Top = 1000x; Bottom = 2000x.



FIGURE 11. 4. Scanning electron micrographs of Versal GH ("air-classified") with fines; $d_p = 15 \mu\text{m}$; Magnification: Top = 1000x; Bottom = 2000x.



FIGURE 11. 5. Scanning electron micrographs of Versal GH ("air-classified") after removal of fines; $d_p = 15 \mu\text{m}$; Magnification: Both at 1000x.

slurry reservoir to the empty HPLC column). As can be seen, an additional gram of the denser Versal GH is needed to pack a 15 cm column compared to Versal GL or a commercially available silica.

The pH values of the water suspensions of the $\gamma\text{-Al}_2\text{O}_3$ samples obtained from LaRoche Chemicals, Inc. and a commercially available SiO_2 sample are given in Table 11.3. These values are normally reported for a 10% slurry of the adsorbent. However, due to the limited amount of $\gamma\text{-Al}_2\text{O}_3$ sample provided for the smaller diameter particles, a 5% slurry was used. From Table 11.3, it is seen that all the samples received from LaRoche Chemicals, Inc. can be classified (approximately) as neutral aluminas.

B. Particle Diameter, Particle Size Distribution And Particle Shape

The importance of d_p and PSD for obtaining highly-efficient HPLC columns is well documented [1-3]. At present, most commercially available HPLC columns are packed with particles having diameters between 3 and 10 μm . It is necessary to have a narrow PSD to obtain efficient HPLC columns, preferably within $\pm 1.5 d_p$ to $\pm 2 d_p$. Particle shape is not as important and both spherical and irregularly-shaped particles of similar diameter can be packed to give columns of comparable efficiency.

Scanning electron micrographs of the different Versal aluminas are illustrated in Figs. 11.1-11.5. These were obtained using a JEOL JSM-T300 Scanning Microscope at an accelerating voltage of 15 kV (Department of Geology and Geophysics, LSU; Operator: Gary Lovell). Scanning electron micrographs have the advantage of providing a visual appearance of the particles from which the particle shape and PSD can be deduced.

Figures 11.1-11.3 show the SEM of Versal GH and Versal GL aluminas sized by sieving and after removal of the fines. As can be seen, the more strongly bound fines

TABLE 11.3. pH of 5.0% slurry with water of various adsorbent.

$\gamma\text{-Al}_2\text{O}_3/\text{SiO}_2$ type	d_p (μm)	% Al_2O_3 or SiO_2	pH
I. $\gamma\text{-Al}_2\text{O}_3$			
A. Sized by sieving			
Versal GL	37-44	5.0	7.73
	10-15	5.0	8.05
Versal GH	37-44	5.0	8.58
	10-15	5.3	8.51
	5-10	5.4	8.39
B. Sized by "air classification"			
Versal GH			
With fines	15	5.1	8.36
Without fines	15	5.0	8.25
II. IMPAQ RG2010Si ^a	8.8	5.0	5.88

^a The manufacturer's reported pH for a 10% slurry is 5.1.

could not be removed. The presence of fines can result in higher column backpressures when packed using the high-pressure slurry-packing procedure since the fines can subsequently dislodge and plug the column frits or fill the interstitial volume. Another very obvious feature of the SEM is the very wide PSD for all these adsorbents. This is especially true for the 10-15 μm Versal GH and Versal GL aluminas (Figs. 11.2 and 11.3, respectively). For the 37-44 μm Versal GH alumina (Fig. 11.1), a narrower PSD is observed (excluding fines). Since the SEM for Figs. 11.1-11.3 were obtained for the adsorbents after removal of the fines, a much worse PSD is to be expected for the original lot. As described later, the procedure used to remove the fines from the adsorbent prior to packing appears to work very well. With regard to the particle shape, Fig. 11.1 shows that the 37-44 μm Versal GH alumina is highly spherical in nature. However, the 10-15 μm Versal GH and Versal GL aluminas (Figs. 11.2 and 11.3, respectively) are somewhat irregularly-shaped, although still approximately spherical. This difference in shape between the 37-44 μm and 10-15 μm particles may be due to the fact that the smaller particles were prepared by crushing the larger materials. According to LaRoche Chemicals, Inc., the original Versal GH alumina has a mean particle size of 45 μm , with 100% having diameters less than 125 μm and 1% having diameters less than 8 μm .

The SEM of Versal GH alumina sized via air classification is given in Figs. 11.4 and 11.5. This method of sizing gives a much narrower PSD (a definite advantage over the sieving method), but still fails to remove the fines. From Fig. 11.5, it is seen that there are still lots of fines left after "air classification", especially at the surface of the particles. Most of the fines can be removed by slurrying with methanol and decanting the supernatant, but this additional step still fails to completely remove the fines. This can clearly be seen in Fig. 11.5, where the fines were removed by repetitive slurrying of the sample (with sonication of the slurry for at least 15 minutes) and decanting of the

supernatant three times. As in Fig. 11.4, the majority of the remaining fines in Fig. 11.5 appears to be adhering to the surface of the bigger particles ($d_p \approx 15 \mu\text{m}$). However, we anticipate that upon slurry-packing these materials (which is done at very high pressure, *e.g.* 10000 psi), the fines will detach and result in a higher column backpressure and lower column efficiency. The particle shape of the Versal GH aluminas in Figs. 11.4 and 11.5 are similar to those in Fig. 11.2.

Figure 11.6 shows SEM for a commercially available silica. As can be seen, the material is also irregular in shape. Similar to the Versal aluminas seen earlier (Figs. 11.1-11.5), the silica sample is characterized by a relatively wide PSD, although almost no fines are present, and the silica surface is very smooth (*i.e.*, without any adhering fines similar to that in Figs. 11.4 and 11.5).

Based on the information described above, we propose the following steps for preparing (HPLC) chromatographic-grade alumina for particles with diameters between 5-10 μm .

1. Prepare the sample by sieving.
2. Remove the fines by slurring in methanol.
3. Air classify.

C. Optimization Of HPLC Column Packing Procedure For LaRoche Aluminas And A Control Silica

A list of the different HPLC columns packed so far is given in Tables 11.4A and 11.4B. Table 11.4A is for columns that were slurry-packed, while Table 11.4B lists columns that were dry-packed. Initially, a mobile phase consisting of hexane/0.05% acetonitrile was used for all normal-phase chromatographic runs [4]. Thus, before any chromatographic measurements can be done, the columns had to be conditioned using the procedure described earlier. This has the disadvantage of being both time consuming and uses up a lot of expensive organic solvents. Since the main objective



FIGURE 11. 6. Scanning electron micrographs of IMPAQ RG2010Si after removal of fines; $d_p = 8.8 \mu\text{m}$; Magnification: Both at 1000x.

TABLE 11.4A. Summary of results for HPLC columns prepared using the high-pressure slurry-packing procedure. ^a

Column Number ^b	Column Length (cm)	Adsorbent (γ -Al ₂ O ₃ or SiO ₂) ^c	d _p (μ m)	Slurry Liquid ^d	% γ -Al ₂ O ₃	Packing Pressure ^e (psi)	Blocked? ^f	t _R for Toluene (min)	As 0.1 (b/a)	N ^g	h	Expected N for 25 cm Column ^h
I. HPLC: Rainin Rabbit HP												
1A	10	Versal GL	37-44	A (1:2)	11	8540	Yes	—	—	—	—	—
2A	10	Versal GH	37-44	A (1:3)	15	7320	No	1.581	2.5	63	39.2	158
3A	10	Versal GL	37-44	A (1:2)	15	6100	No	1.926	1.2	474	5.2	1 180
4A	10	Versal GL	37-44	A (1:2)	13	6100	No	1.835	3.1	189	13.1	471
5A	10	Versal GH	10-15	A (1:1)	15	6100	No	1.738	0.4	431	18.6	1080
6A	10	Versal GL	10-15	A (1:3)	15	7320	No	With peak splitting. Peak apex distorted.				
7A	10	Versal GL	10-15	A (1:3)	15	6100	No	1.788				
8A	10	Versal GH	5-10	A (1:3)	15	7320	No	1.815	0.3	448	29.8	1120
9A	10	SiO ₂	8.8	A (1:1)	15	7320	No	1.665	2.2	801	14.2	2000
10A	15	SiO ₂	8.8	A (1:3)	15	8540	No	2.443	3.9	421	40.5	702
11A	10	Versal GL	10-15	A (1:1)	15	10980	Yes ?	HPLC backpressure limit exceeded.				
12A	5	Versal GH	10-15	A (1:1)	15	10980	No	0.875	0.5	279	14.3	1400
13A	5	Versal GH	5-10	A (1:1)	15	10980	No	0.816	3.3	44	152	219
14A	5	Versal GL	10-15	A (1:1)	?	10980	Yes ?	HPLC backpressure limit exceeded.				
15A*	5	Versal GL	10-15	A (1:2)	15	8540	No	2.018	3.1	116	34.5	580
								(Backpressure too high)				
16A	10	Versal GH	5-10	A (1:3)	14	9760	No	1.806	0.5	1190	11.2	2980
17A	10	Versal GH	10-15	A (1:3)	15	9760	No	1.706	0.5	624	12.8	1560
18A	10	Versal GH	5-10	B (1:1:3)	15	10370	No	1.803	0.4	With peak splitting.		
19A	10	Versal GH	5-10	B (1:1:3)	15	10980	No	1.871	2.3	1160	11.5	2900
20A	10	Versal GH	10-15	B (1:1:3)	15	10980	No	1.906	1.2	1900	4.2	4760
21A	15	SiO ₂	8.8	B (1:1:1)	15	10980	No	2.341	6.2	70	244	116
22A	15	SiO ₂	8.8	B (1:1:3)	15	10980	Yes?	HPLC backpressure limit exceeded.				
23A	15	SiO ₂	8.8	B (1:1:3)	15	10980	No	3.360	2.1	215	79.3	358
24A*	10	Versal GL	37-44	B (1:1:3)	15	7320	Yes?	HPLC backpressure limit exceeded.				
25A*	10	Versal GL	37-44	B (1:1:3)	15	6100	No	1.405	2.3	17	142	44

TABLE 11.4A (continued).

Column Number ^b	Column Length (cm)	Adsorbent (γ -Al ₂ O ₃ or SiO ₂) ^c	d _p (μm)	Slurry Liquid ^d	% γ -Al ₂ O ₃	Packing Pressure ^e (psi)	Blocked? ^f	t _R for Toluene (min)	As 0.1 (b/a)	N ^g	h	Expected N for 25 cm Column ^h
II. HPLC: Perkin Elmer Series 400												
1A	10	Versal GL	37-44	A (1:2)	11	8540	Yes	—	—	—	—	—
2A	10	Versal GH ⁱ	37-44	A (1:3)	15	7320	No	1.795	2.3	95.0	26.0	237
								1.819	2.1	91.3	27.0	229
								1.795	2.5	82.6	29.9	206
3A	10	Versal GL ⁱ	37-44	A (1:2)	15	6100	No	1.979	1.4	551	4.5	1380
								1.952	1.4	508	4.9	1270
								1.983	1.4	482	5.1	1210
4A	10	Versal GL ⁱ	37-44	A (1:2)	13	6100	No	2.591	3.0	148	16.7	370
								2.604	3.0	149	16.6	372
								2.596	3.0	152	16.2	381
26A*	10	SiO ₂	8.8	MeOH	15	5490	No	1.45	1.1	472	24.1	1180
27A*	10	SiO ₂	8.8	MeOH	14	6100	No	1.35	2.3	230	49.4	575
28A*	10	SiO ₂	8.8	MeOH	10	+6710	No	1.38	2.4	364	31.2	911
29A*	10	SiO ₂	8.8	MeOH	10	+6100	No	1.25	> 4	—	—	—
30A*	10	SiO ₂	8.8	MeOH	10	+6100	No	1.37	> 4	—	—	—
31A*	10	Versal GH	15	C	15	+7320	No	1.10	2.6	358	18.6	896
32A*	10	Versal GH	15	C	15	+10980	No	1.30	1.8	851	7.8	2140

TABLE 11.4A (continued).

Column Number ^b	Column Length (cm)	Adsorbent (γ -Al ₂ O ₃ or SiO ₂) ^c	d_p (μ m)	Slurry Liquid ^d	% γ -Al ₂ O ₃	Packing Pressure ^e (psi)	Blocked? ^f	t_R for Toluene (min)	As 0.1 (b/a)	N ^g	h	Expected N for 25 cm Column ^h
33A*	15	Versal GH	15	C	15	10980	No	Column was only 2/3 full.				
34A*	15	Versal GH	15	C	14	10980	No	1.82	1.41	2200	4.5	3700
35A*	15	Versal GH	15	C	15	10980	No	1.88	0.87	1510	6.6	2520
36A*	15	Versal GH	15	C	14	10980	No	1.85	1.88	1010	9.9	1680
37A*	15	Versal GH	15	C	14	10980	No	1.89	2.49	1000	10.0	1670
38A*	15	SiO ₂	8.8	C?	15	+6100	No	2.12	1.28	1620	10.5	2710
39A*	10	SiO ₂	8.8	C?	15	6100	No	1.23	1.68	517	22.0	1290

^a Test solute used was toluene, with 100% hexane/0.05% acetonitrile as mobile phase at 1.0 mL/min, unless indicated othrewise.

^b Column numbers ending with " * " suggest that the different chromatographic parameters reported was obtained using 100% methanol as mobile phase.

^c SiO₂ = IMPAQ RG2010Si.

^d A: MeOH/CHCl₃; B: MeOH/Dioxane/CHCl₃; C: 1:1 EtOH/CHCl₃/saturated with diiodomethane. Note: MeOH = methanol, CHCl₃ = chloroform, EtOH = ethanol.

^e A "+" before the packing pressure listed suggest that the column was packed by increasing the inlet pressure gradually within 15 seconds. Numbers without "+" suggest that the adsorbent was subjected to a sudden increase in pressure.

^f A "Yes" means that no flow was achieved upon connecting the column to the HPLC; a "Yes?" suggest that flow was obtained, however the column backpressure increased and exceeded 6000 psi; while a "No" suggest that flow was achieved without exceeding the set maximum HPLC backpressure (6000 psi).

^g Calculated using the Foley-Dorsey Equation.

^h Calculated from the value of h, assuming a column length of 25 cm.

ⁱ Determination of chromatographic parameters done in triplicate.

TABLE 11.4B. Summary of results for columns prepared using the dry-fill packing procedure ($d_p = 37\text{-}44\ \mu\text{m}$) ^a

Column Number ^b	Column Length (cm)	Adsorbent (γ -Al ₂ O ₃ or SiO ₂)	t _R (min)	As _{0.1} (b/a)	N ^c	h	Expected N for 25 cm column ^d
I. "Tap-Fill" Method							
1B	10	Versal GL	1.820	2.6	6.5	380	18
			1.886	2.5	7.4	330	19
			1.866	2.5	7.2	350	18
2B	10	Versal GL	No improvement.				
II. "Lateral Tapping" Method							
3B*	10	Versal GH	1.321	1.4	154	16.0	386
4B*	10	Versal GH	1.336	1.4	139	17.8	347
5B*	10	Versal GL	With peak splitting.				
6B*	10	Versal GL	With peak splitting.				
7B*	15	Versal GL	With peak splitting.				
8B*	15	Versal GH	With peak splitting.				

^a Test solute used was toluene, with 100% hexane/0.05% acetonitrile as mobile phase at 1.0 mL/min. HPLC used: Perkin Elmer Series 400.

^b Column numbers ending with " *" indicate that chromatographic data were obtained using 100% methanol as mobile phase.

^c Calculated using the Foley-Dorsey Equation.

^d Calculated from the value of h, assuming a column length of 25 cm.

was to determine how well the column was packed, only the chromatographic parameters for an unretained solute are needed. And since toluene is unretained, it is expected that the values of $As_{0.1}$, N and h for toluene will be unaffected by the mobile phase used. Pure methanol was then used as mobile phase to evaluate column packing efficiency, and since the column was packed using methanol as push liquid, toluene can be injected to the column right after the column was slurry-packed. In the results that follow, *data obtained via this faster procedure are denoted by the addition of an asterisk (*) to the column numbers, e.g. "15A*" in Table 11.4A.*

1. Versal GL

$$d_p = 10-15 \text{ } \mu\text{m}$$

A serious problem encountered in slurry-packing the Versal GL alumina was its limited pressure stability. For the sample with d_p between 10-15 μm (which was sized by sieving), a packing pressure greater than approximately 7320 psi could not be used. For example, columns 11A and 14A in Table 11.4A, which were both slurry-packed at 10980 psi, were both blocked since upon connection to an HPLC, the column backpressure immediately went above 6000 psi (the set maximum HPLC pressure limit). This implies that the alumina sample could not withstand this high a packing pressure and was crushed into smaller particles producing fines which clogged the column. It is assumed here that the fines originally present in the material before packing were not enough to block the column since at the same inlet pressure, no clogging of the column was observed for the Versal GH alumina of similar particle diameter. Thus, the Versal GH alumina is mechanically more pressure stable. However, using a packing pressure of 7320 psi or lower (columns 6A and 7A in Table 11.4A) appears to be too low for preparing a tightly-packed bed, since the peaks obtained for toluene were both broad and tailed, with peak splitting (Fig. 11.7 for the

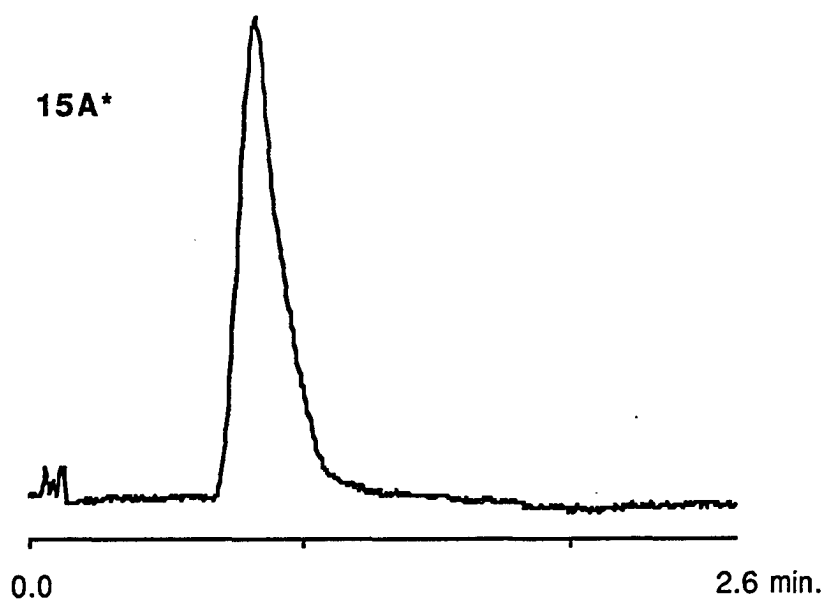
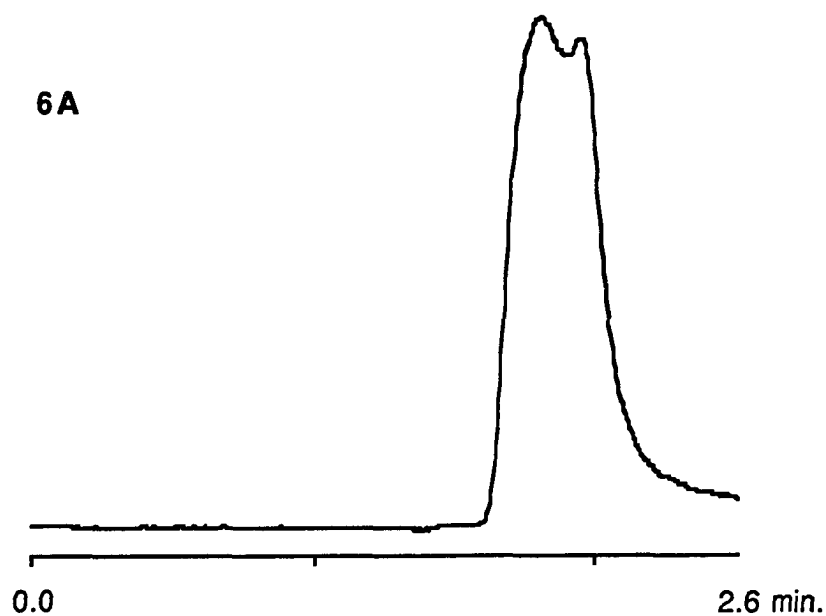


FIGURE 11.7. Chromatograms for toluene illustrating the column performance of 10-15 μm Versal GL aluminas slurry-packed at an inlet pressure of 7320 psi (6A) and 8540 psi (15A*).

toluene peak for column 6A). Using an intermediate packing pressure of 8540 psi (column 15A* in Table 11.4A) seems to produce a more tightly packed bed than that for columns 6A and 7A as seen in the better peak shape for toluene in Fig. 11.7. However, the peak is still tailed ($As_{0.1} = 3.1$) and the column unacceptable ($h = 34.5$). Also, an inlet pressure of 8540 psi may be beyond the pressure limit of the 10-15 μm Versal GL alumina since the HPLC column backpressure obtained was relatively high (1880 psi with 100% methanol at 1.0 mL/min). Since column 15A* is only 5 cm in length, a still higher HPLC backpressure would be obtained for longer columns. Complicating the situation is the fact that it is not possible to absolutely determine whether or not the high h value for column 15A* is due to a loosely packed bed since as can be seen in the SEM for 10-15 μm Versal GL in Fig. 11.3, the PSD is very wide with approximately 50% of the particles having diameters less than 10 μm .

In slurry-packing the 10-15 μm Versal GL alumina, the adsorbent was subjected to a sudden increase in pressure (*i.e.*, pressurization of the packer to the desired setting was done with the on/off valve closed). An alternative slurry packing technique that might be useful involves a gradual increase in packing pressure (*e.g.* over 15 seconds). This approach could be used to pack columns at a high packing pressure (> 8540 psi), thus producing a more tightly-packed bed, but at the same time minimizing the possibility of crushing the adsorbent from the sudden impact of the particles with the column frit and other adsorbent. If a tightly-packed bed of Versal GL can be prepared, then the only limiting factor for preparing a good column will be the PSD. Although we were not able to successfully pack a Versal GL column using this proposed strategy, we believe our failure is due at least in part to the difficulty in generating a gradual increase in pressure with our column packer.

Whether or not the adsorbent was crushed at a given packing pressure was determined indirectly based on the corresponding HPLC column backpressure measured

afterwards. To more accurately determine the pressure limit of a given adsorbent, it is probably best to compare SEM of the material before and after packing. However, this additional step is both time consuming and expensive.

In terms of the slurry solvent, the less dense Versal GL alumina was easier to pack (compared to the more dense Versal GH) using the balanced-density method. The use of halogenated alkanes is not necessary, and a 1:1 methanol/chloroform mixture seems appropriate. The particles do begin to settle within approximately one minute. However, no serious sedimentation problem is expected especially if slurry-packing is carried out as fast as possible (*i.e.*, from pouring the slurry into the reservoir and packing), since the material settles at a slow rate. If necessary, one can always resort to a 1:2 or 1:3 methanol/chloroform mixture, although the wetting properties of these solvents for alumina is expected to decrease. Also, the lower density of Versal GL alumina would allow it to be easily packed using the upward mode with just methanol as slurry solvent.

$$d_p = 37-44 \mu m$$

Dry-packing results. Normally, particles with $d_p > 20 \mu m$ are dry-packed. Two dry-filling packing procedure were used, both involving incremental addition of the adsorbent. The first method utilizes simultaneous vertical and lateral tapping while rotating the column [2]. As can be seen for columns 1B and 2B in Table 11.4B, this method produces terrible columns for Versal GL ($h > 300$). This can be explained by the fact that Versal GL does not settle in by itself (relative to Versal GH), and is light enough to rebound to a great extent during the vertical tapping step which loosens the packed bed.

The second method employs lateral tapping alone, thus eliminating the rebounding effect resulting from vertical tapping. According to Davies [5], this procedure produces more efficient columns than the procedure which involves both vertical and lateral

tapping. However, it still did not improve the packing characteristics of Versal GL. This is illustrated in Fig. 11.8, which shows very broad, distorted peaks with shoulders in the front for columns 5B*, 6B* and 7B* (see also Table 11.4B). Again, the inability of the 37-44 μm Versal GL to provide symmetrical peaks when dry-packed with only lateral tapping is most likely due to the fact that the particles are not heavy enough to settle efficiently.

Slurry-packing results. According to Snyder and Kirkland [2], porous particles with $d_p < 30 \mu\text{m}$ should not be dry-packed unless they have a narrow PSD ($\leq 2 d_p$). Thus, since the 37-44 μm Versal GL alumina is only slightly larger than the 30 μm cutoff, slurry-packing procedures were tried in an attempt to achieve better packing efficiency than had been attained with dry packing.

Unfortunately, like the 10-15 μm Versal GL alumina, the 37-44 μm GL alumina was also mechanically fragile. Packing pressures of 8540 and 7320 psi (for columns 1A and 24A* in Table 11.4A, respectively) resulted in total column blockage. When the packing pressure was reduced to 6100 psi, the blockage no longer occurred. Of the three 10 cm columns packed at this pressure (columns 3A, 4A and 25A* in Table 11.4A and Fig. 11.9), column 3A had a reduced plate height of 5.2.

Although it is not known from direct evidence (SEM) whether any fracturing of the material occurred at 6100 psi, the indirect evidence (observed HPLC column backpressures) suggests that the fracturing of the GL is minimal for a packing pressure of 6100 psi. At a flow rate of 1.0 mL/min., the backpressure for column 3A was 980 psi using hexane/0.05% acetonitrile as mobile phase, and 1900 psi with 85% isooctane, 15% ethanol/0.3% water (Rainin data). For column 4A, the backpressure obtained was 310 psi with 100% hexane/0.05% water, while that for column 25A* was 2930 psi with 100% methanol.

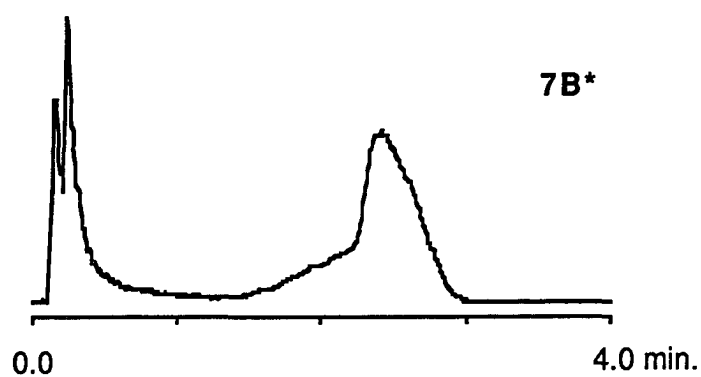
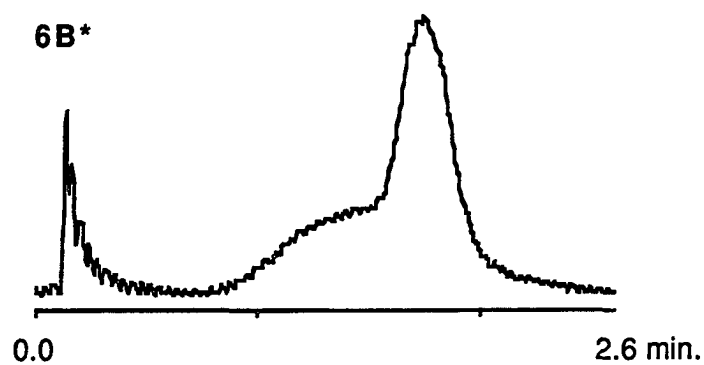
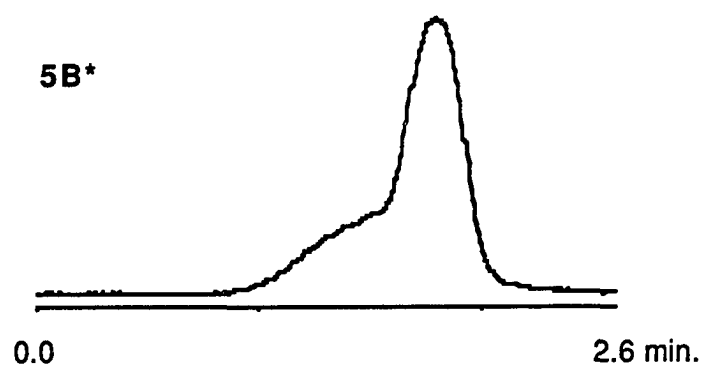


FIGURE 11.8. Chromatograms for toluene illustrating the column performance of 37-44 μm Versal GL aluminas prepared by the dry-fill packing procedure involving "lateral tapping" only.

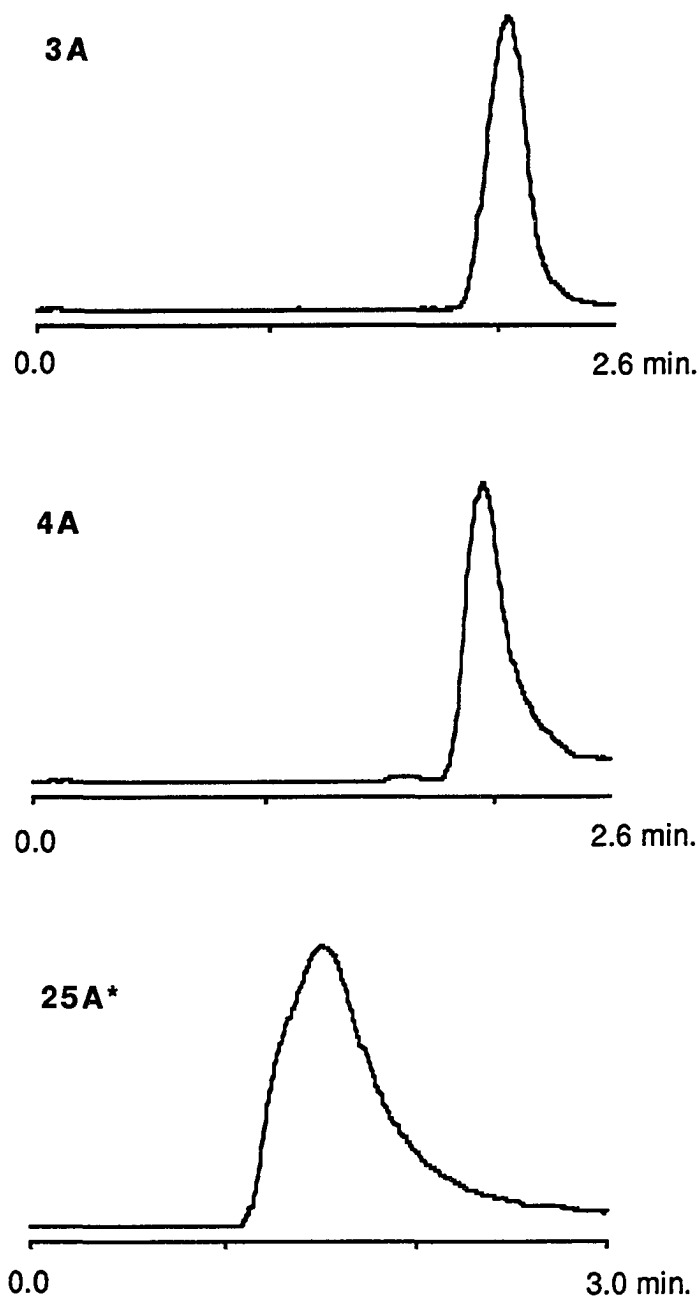


FIGURE 11.9. Chromatograms for toluene illustrating the column performance of 37-44 μm Versal GL aluminas slurry-packed at an inlet pressure of 6100 psi.

The reduced plate height of 5.2 for column 3A is not that impressive, but it does suggest that a tightly packed bed was achieved, even though the PSD is wide. Unfortunately, a comparison of the results obtained for columns 3A and 4A suggest that packing efficiency of 44 μm Versal GL alumina is not likely to be sufficiently reproducible under these conditions, since even though both columns were packed in an identical fashion, one had a reduced plate height (h) of 5.2 while the other's was 13.1. The separation of the test mixture using column 3A is shown in Figs. 12.6 and 12.7.

2. Versal GH

$d_p = 5\text{-}10\ \mu\text{m}$ and $10\text{-}15\ \mu\text{m}$

The 5-10 μm and 10-15 μm sample lots of Versal GH aluminas were sized by sieving, and as illustrated in Fig. 11.2, approximately half of the particles in the 10-15 μm Versal GH has $d_p < 10\ \mu\text{m}$. Also, a lot of fines are present which can lead to higher column backpressures. Although SEM for the 5-10 μm sample were not obtained, the situation is expected to be similar (if not worse).

In terms of pressure stability, Versal GH is far superior to Versal GL. Based solely on HPLC column backpressure data, the Versal GH can withstand a packing pressure of 10,980 psi (the highest packing pressure attainable with the slurry packer). Using hexane/0.05% acetonitrile as mobile phase at 1.0 mL/min, the observed column backpressures were 180 and 240 psi for columns 13A (5 cm) and 19A (10 cm), respectively, and 120 and 100 psi for columns 12A (5 cm) and 20A (10 cm), respectively (Table 11.4A). The first two columns were packed with 5-10 μm Versal GH, while the last two with 10-15 μm Versal GH. With 85% isooctane, 15% ethanol/0.3% water as mobile phase, the HPLC column backpressure for column 20A (10 cm) was 190 psi at a mobile phase flow rate of 1.0 mL/min, while that for a 25 cm Unisphere neutral alumina was 260 psi at 1.25 mL/min. Much lower column

backpressures are expected for the Versal GH columns with better quality Versal alumina (*i.e.*, lots with narrower PSD and without fines). Assuming that both 5-10 μm and 10-15 μm Versal GH aluminas are not fracturing at 10980 psi (which can be confirmed by comparing SEM of the material before and after packing), it is possible that an even higher packing pressure might produce even more efficient columns since the column bed will be more tightly packed. Although we can pack additional columns with Versal GH at higher pressures up to 15000 psi, we were not able to do so because the gas regulator we have (Victor Equipment Co., Denton, TX) delivers a maximum compressed air pressure of only 90 psi, which when amplified corresponds only to a packing pressure of 10980 psi.

Both the 5-10 μm and 10-15 μm Versal GH aluminas were slurry-packed by first pressurizing the packer to the desired setting, then immediately opening the on/off valve. This subjects the particles to a sudden increase in pressure with the incoming materials being slammed to either the column frit or other packed adsorbents. Since Versal GH appears to be pressure stable, this should be the best pressurization technique to use, which offers the advantage of packing the material as quick and as compact as possible.

An obvious problem observed when slurry-packing these small diameter Versal GH aluminas was the very fast settling rate of the particles in the slurry mixture compared to Versal GL and a commercially available silica of similar particle diameter. This is due to the higher density of Versal GH. As such, the particles begin to settle immediately upon removal of the slurry from the ultrasonic bath. Thus, although the mixture can be shaken manually before pouring into the slurry reservoir, and despite the speed with which the packing can be performed, some settling and sizing will still occur before pressure can be applied. This leads to a non-uniform bed (in terms of packing density and permeability), one that is not packed as tightly as possible. Therefore, it is

necessary to use the balanced-density technique (*i.e.*, a high density slurry solvent) in order to pack columns efficiently with a down-flow slurry packer.

Figure 11.10 shows the peak shapes of toluene for columns 13A, 16A and 19A (listed in Table 11.4A), which were all slurry-packed with 5-10 μm Versal GH aluminas. As can be seen, the best two columns (16A and 19A) were prepared by employing both a high packing pressure (necessary to obtain a tightly-packed bed) and a high-density slurry solvent (to minimize sedimentation). However, both columns are still unacceptable since the reduced plate heights obtained were 11.2 and 11.5 for columns 16A and 19A, respectively. Although column 13A was packed using a pressure of 10980 psi, it still had a very high (bad) reduced plate height of 152 because a 1:1 methanol/chloroform mixture was used as slurry solvent, which is not as dense as the slurry solvents used for columns 16A and 19A (1:3 methanol/chloroform and 1:1:3 methanol/dioxane/chloroform, respectively).

The peak shapes of toluene for columns packed with 10-15 μm Versal GH are shown in Figs. 11.11 and 11.12. Figure 11.11 shows the peak shapes for columns packed using methanol/chloroform as slurry solvent, and as can be seen, columns 5A, 12A and 17A are all unacceptable. Again, it is obvious that both a high packing pressure and a high-density slurry solvent are required to pack high-efficiency columns. All toluene peaks are fronted ($As_{0.1}$ was either 0.4 or 0.5) and the best column (17A, prepared using 1:3 methanol/chloroform as slurry solvent and a packing pressure of 9760 psi) had a reduced plate height of 12.8 (still unacceptably high).

Figure 11.12 shows the chromatogram from the best column packed. This is for a 10 cm column, slurry-packed with 10-15 μm Versal GH using a packing pressure of 10980 psi and a slurry solvent consisting of 1:1:3 methanol/dioxane/chloroform. As seen in Table 11.4A, column 20A has a reduced plate height of 4.2 and an asymmetry ratio of 1.2.

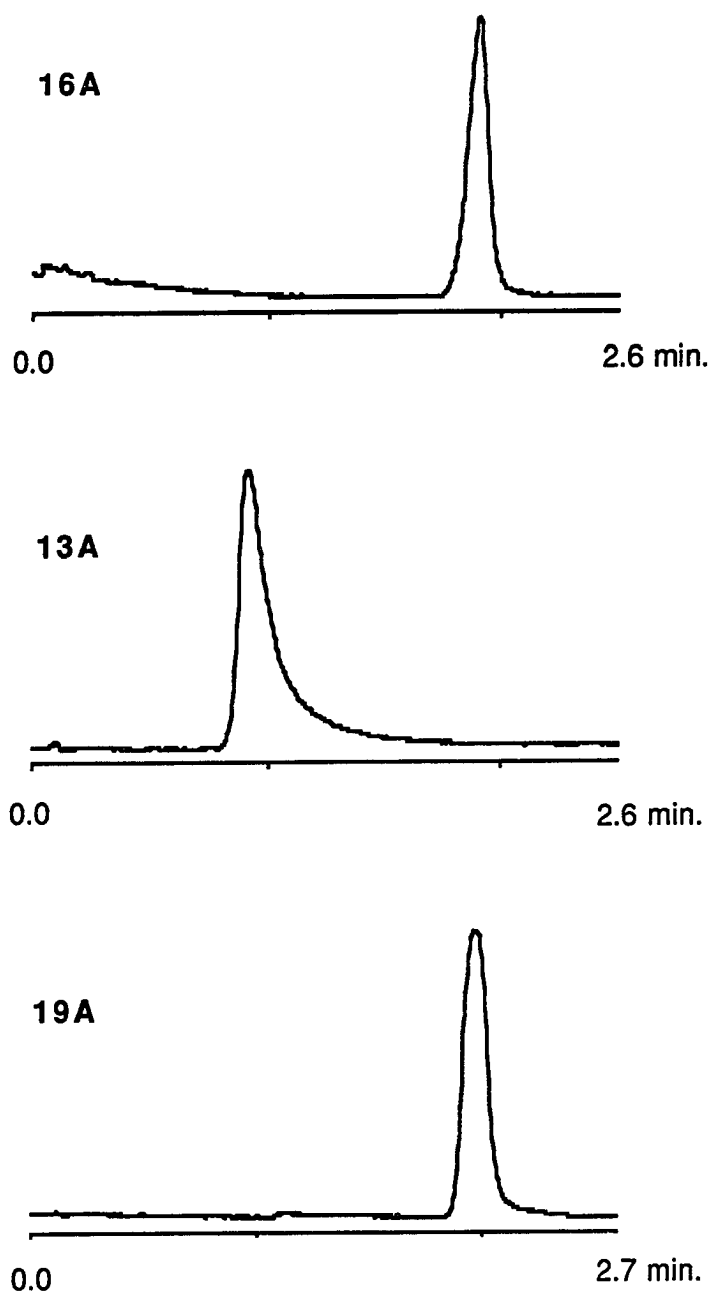


FIGURE 11.10. Chromatograms for toluene illustrating the column performance of 5-10 μm Versal GH aluminas slurry-packed at an inlet pressure of 9760 psi (16A) and 10980 psi (13A and 19A).

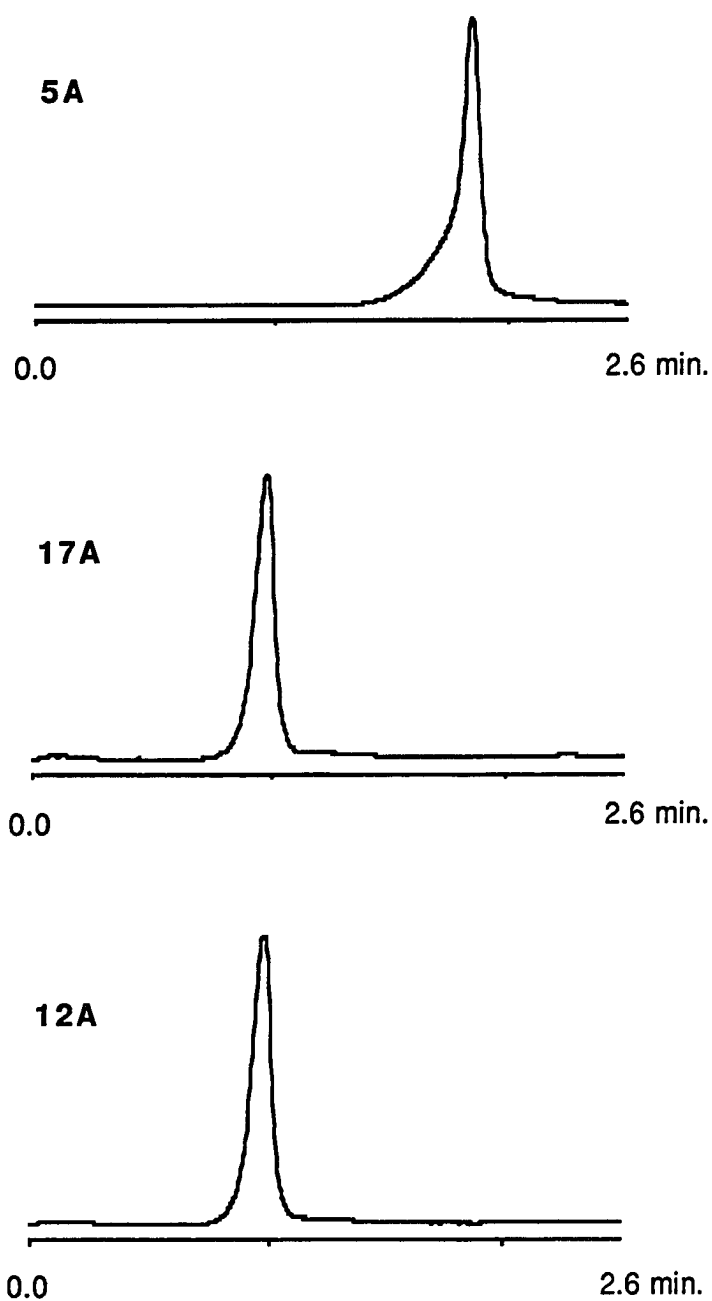


FIGURE 11.11. Chromatograms for toluene illustrating the column performance of 10-15 μm Versal GH aluminas slurry-packed at an inlet pressure of 6100 psi (5A), 9760 psi (17A) and 10980 psi (12A).

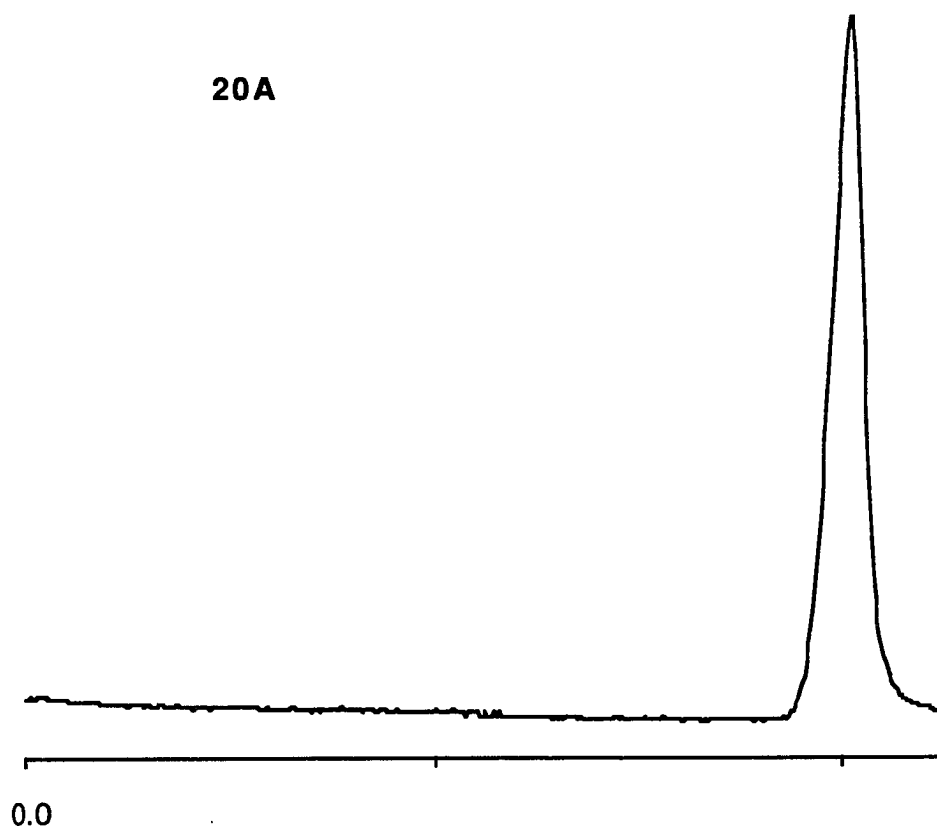


FIGURE 11.12. Chromatogram for toluene illustrating the column performance of 10-15 μm Versal GH alumina slurry-packed at an inlet pressure of 10980 psi (20A).

$d_p = 15 \mu\text{m}$ ("air-classified")

This sample was "air-classified", and although it has a much narrower PSD relative to the previous Versal GH aluminas prepared by sieving (Fig. 11.4), fines are still present which can block the column when slurry-packed. However, similar to the results obtained for the 5-10 μm and 10-15 μm Versal GH, these fines did not appear to block the columns (31A*-37A* in Table 11.4A). For example, columns 34A* and 35A* (the best two columns prepared for the 15 μm Versal GH) exhibited HPLC backpressures of 150 and 140 psi, respectively, with 85% isooctane, 15% ethanol/0.3% water at 1.0 mL/min.

The pressure stability of the 15 μm Versal GH was similar to that of the 5-10 μm and 10-15 μm samples. Thus, it apparently can withstand a packing pressure of 10980 psi or greater. More efficient columns of the air-classified 15 μm Versal GH were therefore prepared as before for the 5-10 and 10-15 μm Versal GH by employing both a high packing pressure and a high-density slurry solvent. Since the 15 μm Versal GH is expected to have a higher settling rate compared to the 5-10 μm and 10-15 μm Versal GH discussed earlier, a denser slurry solvent consisting of 1:1 ethanol/chloroform saturated with diiodomethane (balanced-density technique) was used for all the columns packed. However, it is not known as to how effectively this slurry solvent wets the material. Column 31A* (Table 11.4A) has the lowest efficiency ($h = 18.6$) for all the 15 μm columns because a packing pressure of only 7320 psi was employed compared to 10980 psi for the other columns. Thus, the bed was not packed as tight as possible. Increasing the pressure gradually during packing does not (conclusively) offer any advantage as seen from the results for column 32A*. Thus, sudden pressurization seems to be the best approach and this method produced the two best columns for the lot (columns 34A* and 35A* with h values of 4.5 and 6.6, respectively). However, these columns are still of poorer chromatographic quality compared to column 20A in terms of

both packing efficiency and peak asymmetry. The values for $As_{0.1}$ are 1.41 and 0.81 for columns 34A* and 35A*, respectively.

The major difference between columns packed at 10980 psi for the "air-classified" Versal GH and similarly sized Versal GH prepared by sieving was the backpressure resistance offered by the column bed during slurry packing. The 15 μm alumina did not seem to offer any resistance at all during the process, as evidenced from the shorter time interval between strokes and from the high velocity of the slurry liquid being sprayed at the outlet compared to the 5-10 μm and 10-15 μm materials, wherein the liquid came out either as a relatively low-velocity jet or drop by drop. This low resistance could be due to three factors, namely (i) that the packing pressure applied was not high enough to compact the bed, (ii) the lower amount of fines present for the "air-classified" sample, and (iii) that the slurry solvent did not effectively wet the material leading to particle agglomeration. No experiments were performed to verify the third possibility, however, this can easily be carried out by packing a column using 100% methanol as slurry solvent and comparing the HPLC backpressure obtained. We believe the main reason that a column better than 20A did not result with the 15 μm air-classified Versal GH was the excessive nonpolarity of the slurry solvent, which promoted particle agglomeration.

The results for columns 34A*-37A* clearly show the poor reproducibility obtained for the slurry-packing procedure used since these columns were supposedly packed at identical conditions. The reduced plate heights for the columns ranged from 4.5 (column 34A*) to 10.0 (column 37A*).

$$d_p = 37-44 \mu\text{m}$$

The experimental results indicate that unlike the 37-44 μm Versal GL, similarly sized Versal GH (prepared by sieving) are more effectively dry-packed than slurry-packed. Although the 37-44 μm Versal GH is more pressure stable than Versal GL, a

less efficient column was packed at 7320 psi. As seen in Table 11.4A and Fig. 11.13, the only slurry-packed Versal GH column (2A) has an h value of 39.2 and is tailed ($As_{0.1} = 2.5$). The HPLC backpressure recorded for this column was 40 psi using 100% hexane/0.05% acetonitrile as mobile phase at 1.0 mL/min, indicating that the column was not clogged. The very fast settling rate for this material would explain the high reduced plate height obtained. However, at present it is not known whether or not using a higher packing pressure would produce a more efficient column.

Unlike Versal GL, the 37-44 μm Versal GH is heavy enough to settle very quickly, forming a more tightly-packed bed easily prepared by dry-packing. The results for columns 3B* and 4B* clearly illustrates this (Table 11.4B), although the columns are still very inefficient. Columns 3B* and 4B* had h values of 16.0 and 17.8, respectively, although both columns did produce fairly symmetrical peaks ($As_{0.1} = 1.4$). Figure 11.14 shows the toluene peak shapes obtained for columns 3B* and 4B*, which were both dry-packed using lateral tapping only. A split peak was obtained for column 8B* in Table 11.4B because this column was dry-packed utilizing half the number of lateral taps (compared to columns 3A* and 4A*) per incremental addition of packing material.

3. IMPAQ RG2010Si

No acceptable HPLC column was ever packed for the 8.8 μm silica purchased from The PQ Corporation (Conshohocken, PA). Using the balanced-density technique seems to be unnecessary since the silica particles appear to have a low density and the settling rate of the material is similar to that of Versal GL. Thus, a 1:1 or even 1:3 methanol/chloroform mixture should be adequate. Alltech Associates, Inc. (Deerfield, IL) prescribed the use of 100% ethanol as both slurry solvent and push liquid. Using 1:1 ethanol/chloroform saturated with diiodomethane is inappropriate (see columns

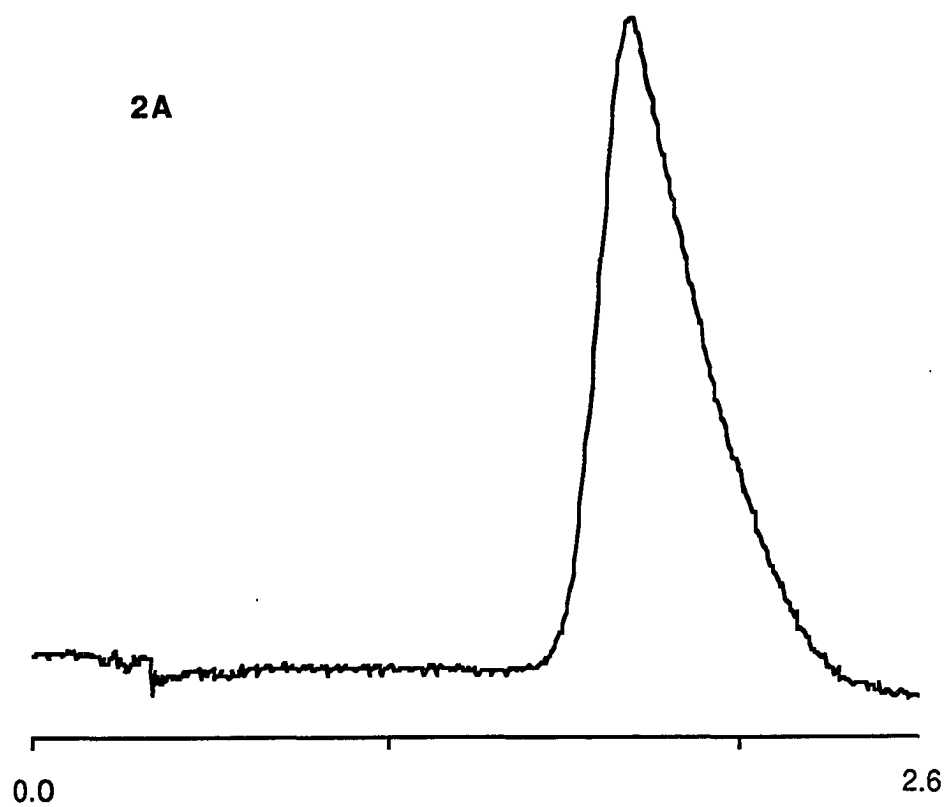


FIGURE 11.13. Chromatogram for toluene illustrating the column performance of 37-44 μm Versal GH alumina slurry-packed at an inlet pressure of 7320 psi (2A).

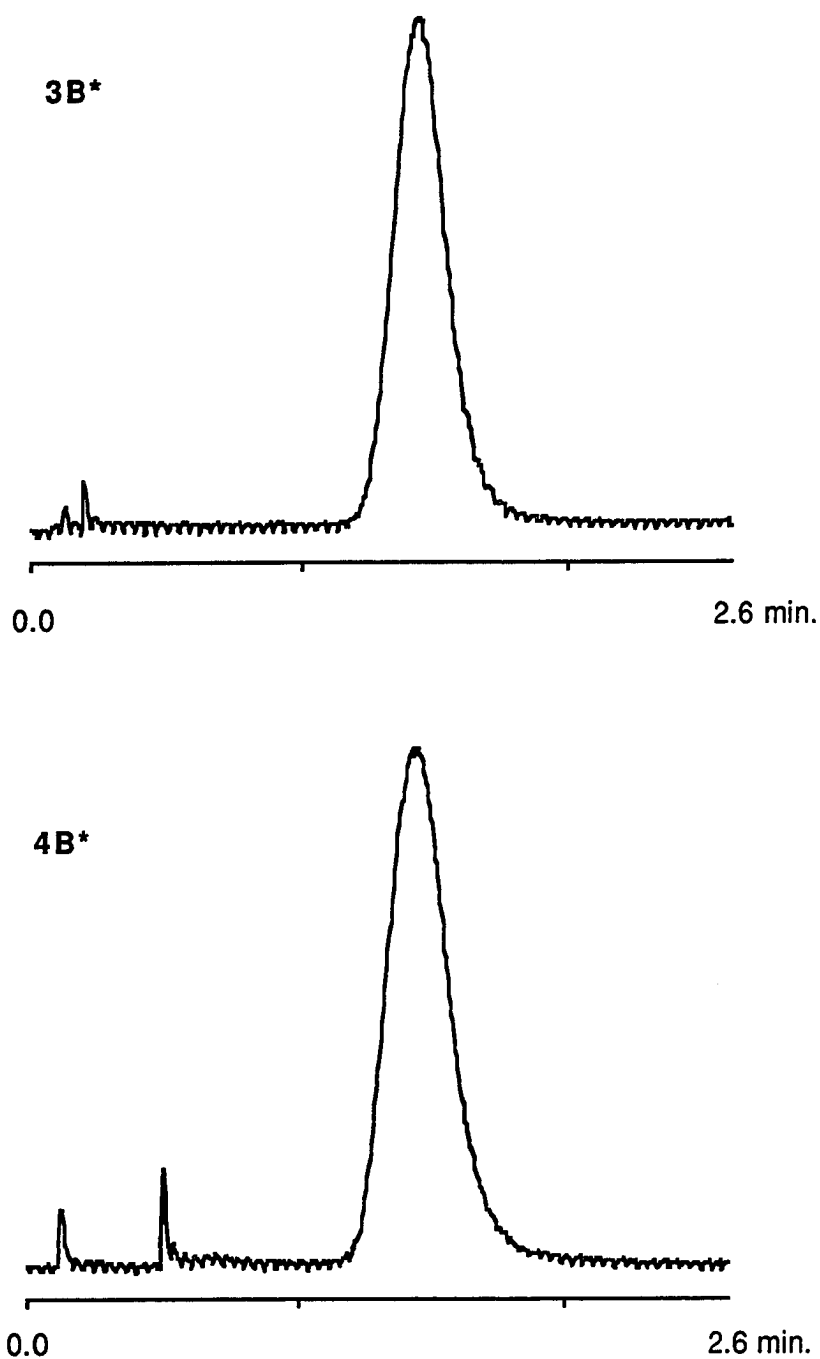


FIGURE 11.14. Chromatograms for toluene illustrating the column performance of 37-44 μm Versal GH aluminas prepared by the dry-fill packing procedure involving "lateral tapping" only.

38A* and 39A* in Table 11.4A) since a very thick slurry was formed, suggesting that the slurry solvent did not effectively wet the silica resulting in particle agglomeration. Thus, it was necessary to add enough ethanol before packing.

The major obstacles encountered with the silica were the selection of the packing pressure and the decision of whether or not to pressurize and release when slurry-packing. A packing pressure of 10980 psi appears to crush the material, as observed for columns 22A (which was totally blocked), and 21A and 23A. Using 100% hexane/0.05% acetonitrile at 1.0 mL/min, the recorded HPLC column backpressures were 2530 and 1570 psi, respectively. According to Neil Miller [6], the maximum packing pressure should not exceed 4500 psi, and pressurization and depressurization of the column packer should be done gradually. Unfortunately, these alternatives were not investigated, but we are optimistic that an efficient HPLC IMPAQ RG2010Si column will be packed in the future. At present, the best silica column packed (column 38A* in Table 4A) has a reduced plate height of 10.5 and an asymmetry ratio of 1.28. Pressurization of the column packer was achieved by gradually increasing to 6100 psi within 15 seconds. However, depressurization was done abruptly by closing the on/off valve. Unfortunately, the slurry solvent composition is known imprecisely since the original solvent used (1:1 ethanol/chloroform saturated with diiodomethane) formed a very thick paste, necessitating the addition of an undetermined volume of ethanol to form a thinner slurry.

REFERENCES FOR CHAPTER XI

1. Knox, J.H. *J. Chromatogr. Sci.* **1977**, *15*, 352-364.
2. Snyder, L.R.; Kirkland, J.J. *Introduction to Modern Liquid Chromatography*, 2nd ed.; John Wiley & Sons, Inc.: New York, 1979; Chapter 7.
3. Dewaele, C.; Verzele, M. *J. Chromatogr.* **1983**, *260*, 13-21.
4. Meyer, V.R. *Practical High-Performance Liquid Chromatography*; John Wiley & Sons Ltd.: New York, 1988; Chapter 8.
5. Davies, R.D. *J. High Res. Chromatogr., Chromatogr. Commun.* **1981**, *4*, 270-275.
6. Miller, N.T., The PQ Corporation, personal communication by J.P. Foley.

CHAPTER XII

CHROMATOGRAPHIC CHARACTERISTICS OF PACKED VERSAL HPLC COLUMNS

Chromatographic Characteristics Of Various Aluminas

The chromatographic characteristics of the various packed columns of Versal GH and GL, and a commercially available alumina column (Unisphere neutral alumina) were determined using a test mixture consisting of toluene, nitrobenzene, o-nitroaniline, m-nitroaniline and p-nitroaniline, and 85% isooctane, 15% ethanol/0.3% water as mobile phase. The resulting chromatograms are shown in Figs. 12.1-12.9 for three Versal GH columns (20A, 34A* and 35A* in Table 11.4A), a Versal GL column (3A), and a Unisphere neutral alumina column.

Figures 12.1 and 12.2 show the chromatograms for column 20A, the best column that was slurry-packed. Column 20A was packed with 10-15 μm Versal GH, prepared by sieving. As can be seen, all the peaks except for the first two are well resolved and the separation is comparable to that obtained for the Unisphere column (Figs. 12.8 and 12.9). However, the peaks obtained for the Unisphere column are narrower and better resolution is obtained for peaks 1 and 2. As seen in Table 12.1, this reflects the fact that the packing efficiency of the Unisphere column is better than that of Versal GH, as indicated by a reduced plate height for toluene of 2.9 for the Unisphere column compared to 4.9 for Versal GH (20A).

Because of the better packing efficiency of the Unisphere column, the h values of the other compounds (nitroanilines) are all better for the Unisphere alumina than that for Versal GH, except for p-nitroaniline where h was 6.0 for Versal GH and 6.8 for the Unisphere. We believe that the packing efficiency is limited by the quality of alumina used (PSD for Versal GH is too wide, due to inadequate sizing), and not by any

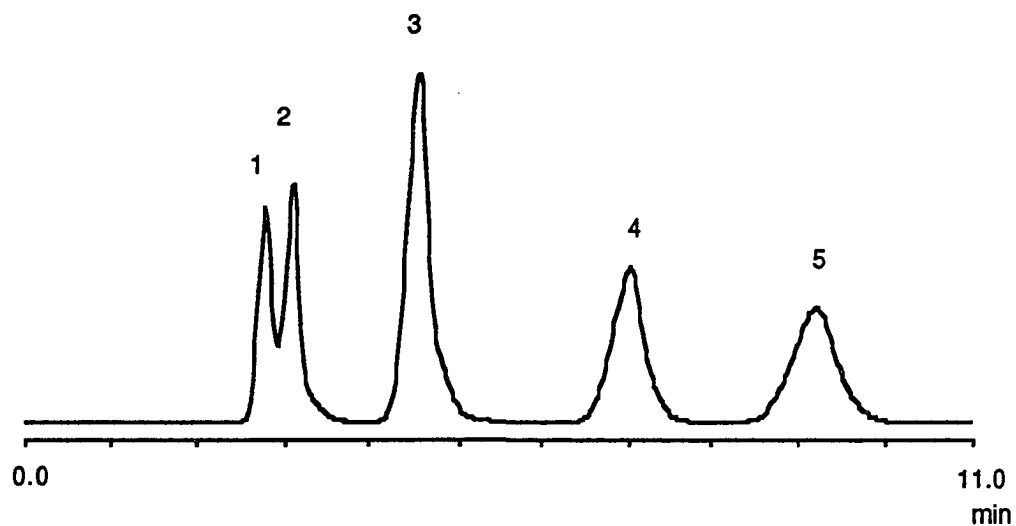


FIGURE 12.1. Normal-phase separation of benzene derivatives for 100 x 4.6 mm Versal GH Alumina (20A in Table 11.4A; d_p : 10-15 μm). Flow rate: 0.5 mL/min. Column backpressure: 120 psi. Solute identification: 1- Toluene; 2 - Nitrobenzene; 3 - o-Nitroaniline; 4 - m-Nitroaniline; 5 - p-Nitroaniline.

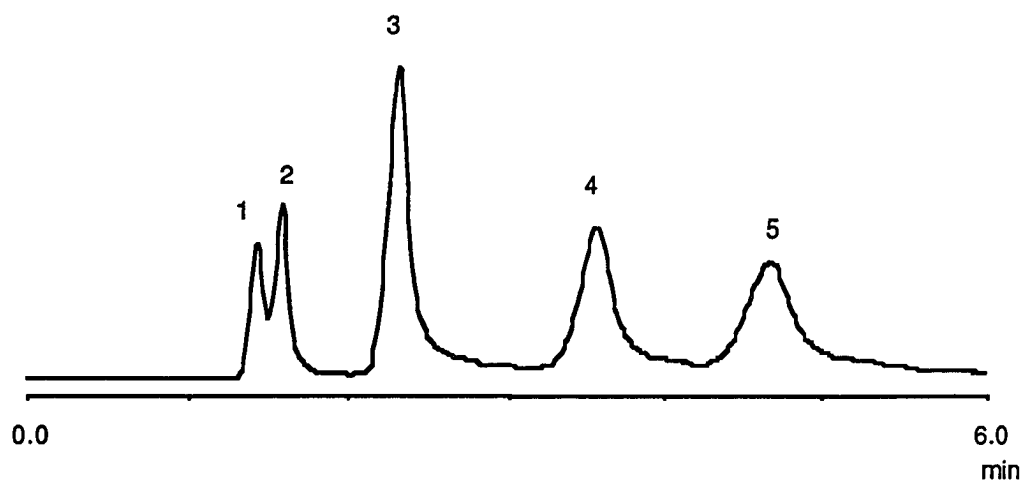


FIGURE 12.2. Same as in Fig. 12.1. Flow rate: 1.0 mL/min

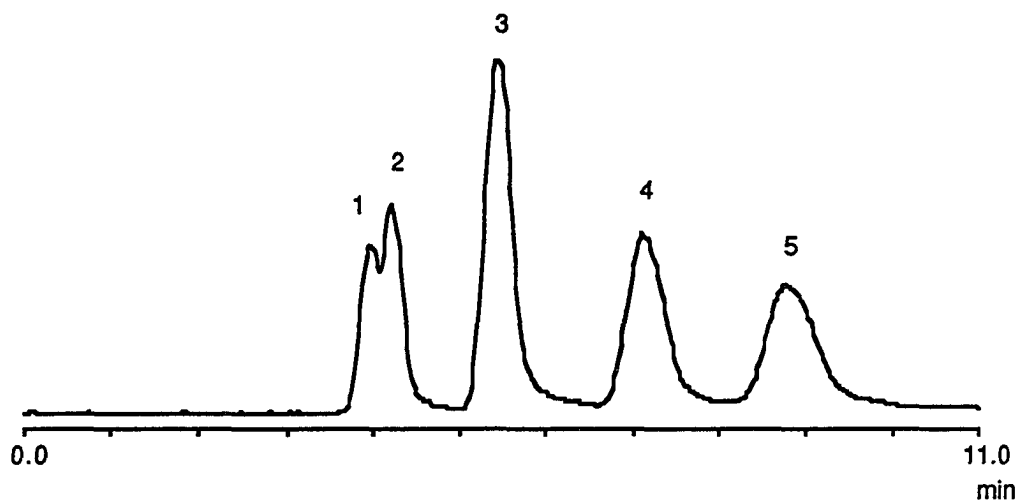


FIGURE 12.3. Normal-phase separation of benzene derivatives for 150 x 4.6 mm Versal GH Alumina (34A* in Table 11.4A; d_p : 15 μm). Flow rate: 0.5 mL/min. Column backpressure: 90 psi. Solute identification: 1- Toluene; 2 - Nitrobenzene; 3 - o-Nitroaniline; 4 - m-Nitroaniline; 5 - p-Nitroaniline.

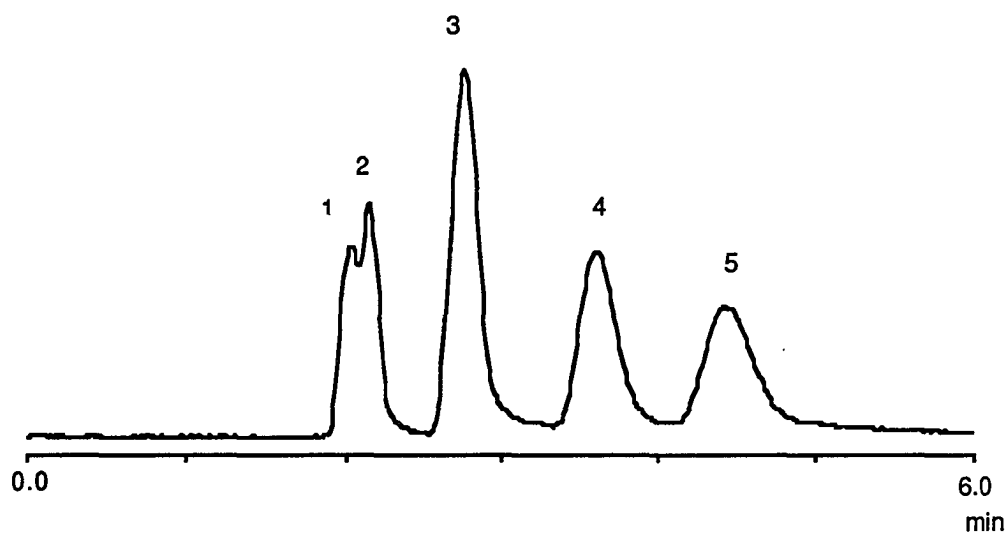


FIGURE 12.4. Same as in Fig. 12.3. Flow rate: 1.0 mL/min. Column backpressure: 160 psi.

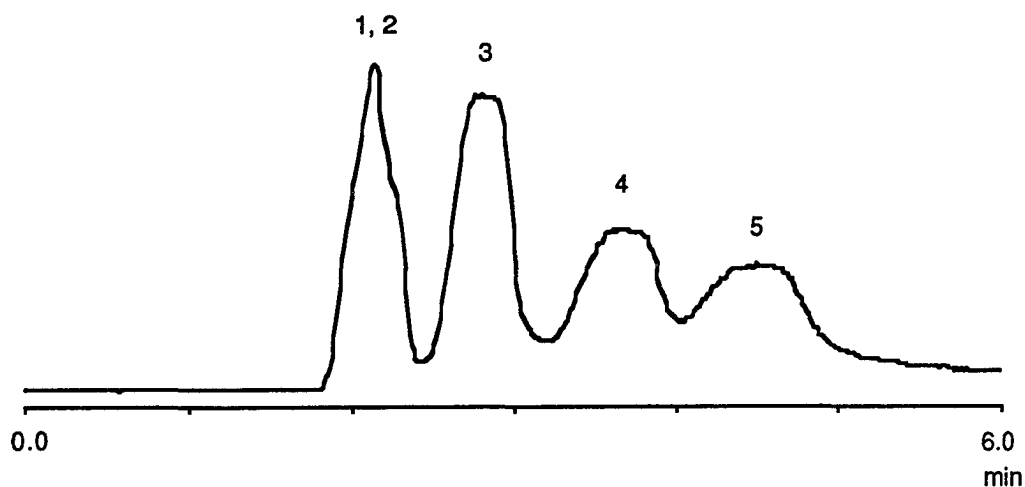


FIGURE 12.5. Normal-phase separation of benzene derivatives for 150 x 4.6 mm Versal GH Alumina (35Å* in Table 11.4A; d_p : 15 μm). Flow rate: 1.0 mL/min. Column backpressure: 150 psi. Solute identification: 1- Toluene; 2 - Nitrobenzene; 3 - o-Nitroaniline; 4 - m-Nitroaniline; 5 - p-Nitroaniline.

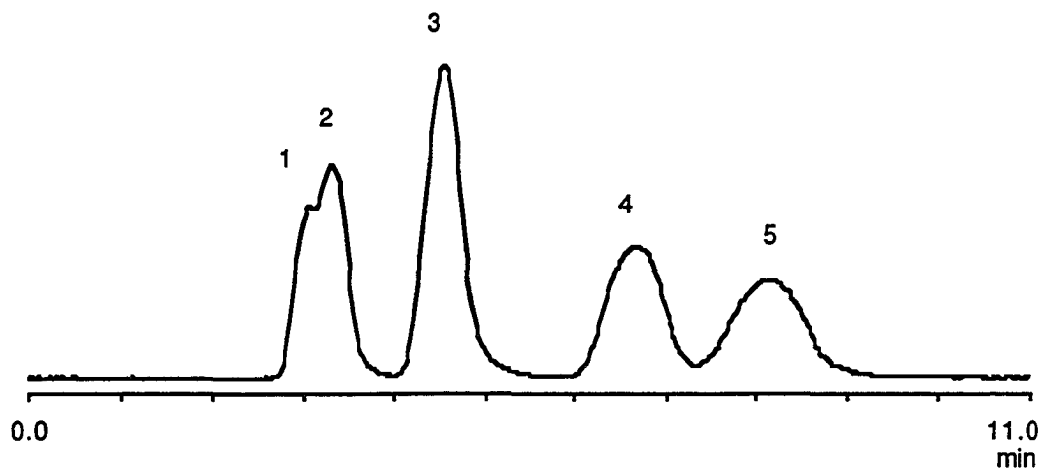


FIGURE 12.6. Normal-phase separation of benzene derivatives for 100 x 4.6 mm Versal GL Alumina (3A in Table 11.4A; d_p : 37-44 μm). Flow rate: 0.5 mL/min. Column backpressure: 920 psi. Solute identification: 1- Toluene; 2 - Nitrobenzene; 3 - o-Nitroaniline; 4 - m-Nitroaniline; 5 - p-Nitroaniline.

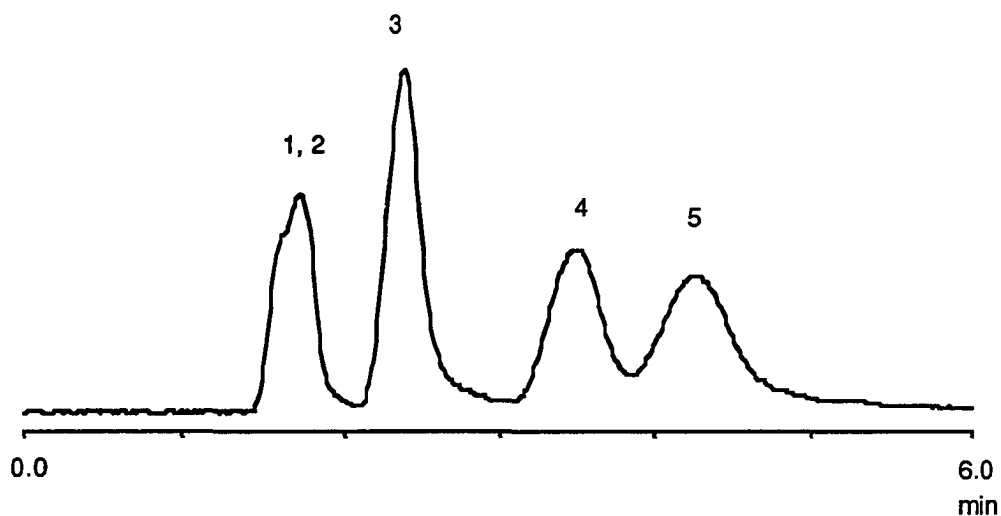


FIGURE 12.7. Same as in Fig. 12.6. Flow rate: 1.0 mL/min. Column backpressure: 1900 psi.

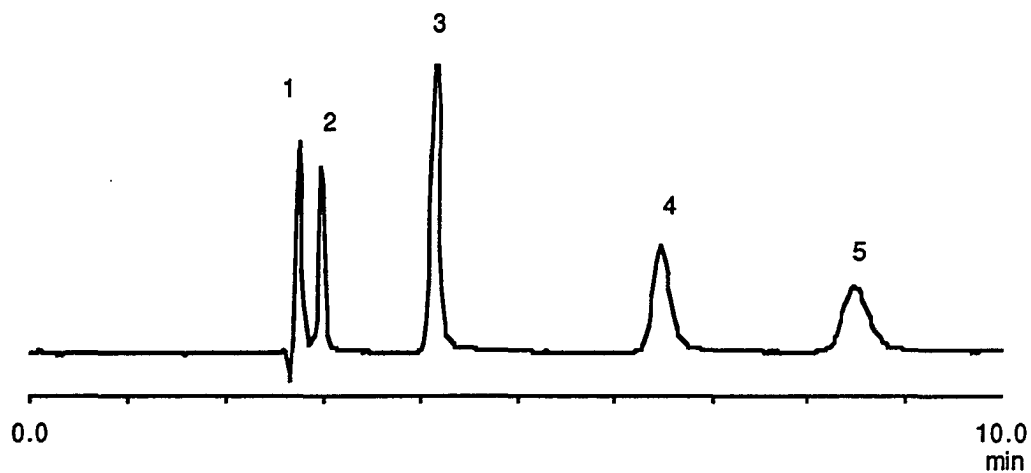


FIGURE 12.8. Normal-phase separation of benzene derivatives for 250 x 4.6 mm Unisphere Neutral Alumina (SN 580ATC; d_p : 10 μm). Flow rate: 1.25 mL/min. Column backpressure: 260 psi. Solute identification: 1- Toluene; 2 - Nitrobenzene; 3 - o-Nitroaniline; 4 - m-Nitroaniline; 5 - p-Nitroaniline.

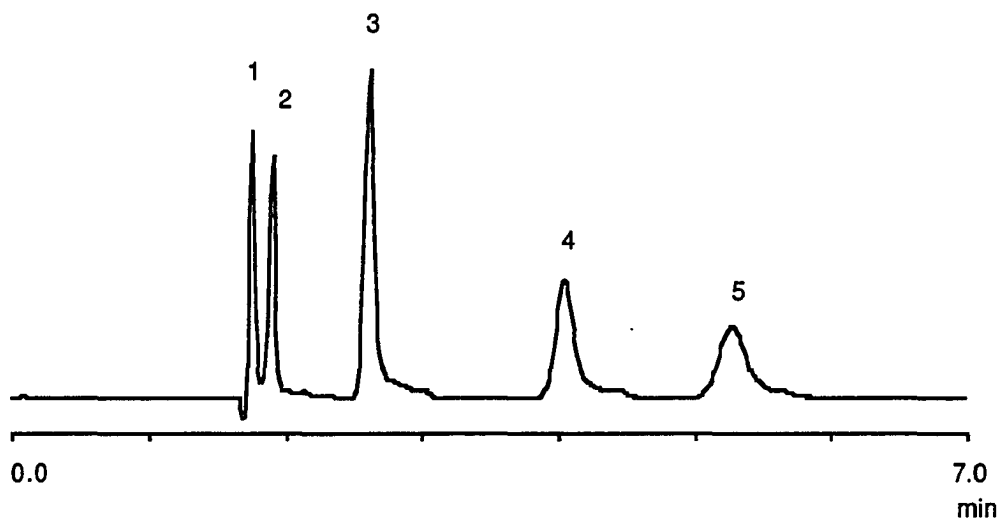


FIGURE 12.9. Same as in Fig. 12.8. Flow rate: 2.0 mL/min. Column backpressure: 380 psi.

TABLE 12.1. Peak asymmetry ($As_{0.1}$) and column efficiency (N and h) of benzene derivatives for Versal GH (column 20A) and Unisphere neutral aluminas at 25.0 ° C. ^a

Solute	<u>$As_{0.1}$</u>		<u>$N_{0.5}$</u>		<u>h</u>	
	<u>Versal GH Alumina</u>	<u>Unisphere Neutral Alumina</u>	<u>Versal GH Alumina</u>	<u>Unisphere Neutral Alumina</u>	<u>Versal GH Alumina</u>	<u>Unisphere Neutral Alumina</u>
Toluene	1.47	1.25	1620	8610	4.9	2.9
o-Nitroaniline	1.34	1.44	1620	6960	5.0	3.6
m-Nitroaniline	1.15	1.39	1420	4700	5.6	5.3
p-Nitroaniline	1.06	1.31	1330	3700	6.0	6.8

^a The mobile phase used was 85% isooctane, 15% ethanol/0.3% water at 1.0 mL/min for Versal GH alumina and 2.0 mL/min for Unisphere alumina.

deficiencies in our procedures. Thus, if better Versal GH alumina is used (*i.e.*, with narrower PSD), results similar to that for the Unisphere column should be possible. It is also, therefore, reasonable to assume that the mass transfer characteristics of Versal GH are at the least comparable if not better than that of the Unisphere alumina. Further evidence of this is shown in Tables 12.2-12.4, where the data reported for Versal GH and GL are for columns 3A and 20A, respectively, under the conditions of Table 11.4A. For basic compounds, at least, the Versal GH, Unisphere, and Versal GL aluminas appear to provide very similar interactions.

Table 12.2 shows the different retention factors (k') for nitrobenzene and the nitroanilines at different temperatures (15.0, 25.0, 35.0 and 45.0° C). It is seen that as expected, k' decreases slightly with increasing temperature. More importantly, however, is the similarity of the retention factors obtained for Versal GH and Unisphere aluminas. For example, at 25.0° C, retention factors for *p*-nitroaniline are 2.232 ± 0.017 and 2.289 ± 0.028 for the Versal GH and Unisphere columns, respectively. Retention factors were between 15% and 25% lower for the Versal GL column.

Column selectivity for the different benzene derivatives at different temperatures for the Versal GH, Unisphere, and Versal GL aluminas are listed in Table 12.3. Selectivity values were calculated using Eqn. 4.1. As can be seen from Table 12.3, the selectivity values for the two columns were similar, although in all cases selectivity was slightly greater for the Unisphere column. As an example, the selectivity between *m*-nitroaniline and *o*-nitroaniline at 25.0° C was 2.35 and 2.69 for the Versal GH and Unisphere aluminas, respectively. Another consistent similarity between the two columns is the temperature dependence of selectivity for the three pairs of solutes. For the *o*-nitroaniline/nitrobenzene and *p*-nitroaniline/*m*-nitroaniline pairs, column selectivity increases with increasing temperature, while for the *m*-nitroaniline/*o*-nitroaniline pair,

TABLE 12.2. Retention factors (k') of benzene derivatives for Versal GH (column 20A), Unisphere and Versal GL (column 3A) aluminas at different temperatures. ^a

Solute	Temperature (°C)	Retention Factor (k') ^b		
		Versal GH Alumina	Unisphere Neutral Alumina	Versal GL Alumina ^c
Nitrobenzene	15.0	0.129	0.102	—
	25.0	0.115	0.085	0.08
	35.0	0.104	0.075	—
	45.0	0.090	0.068	—
o-Nitroaniline	15.0	0.676	0.611	—
	25.0	0.629	0.544	0.50
	35.0	0.585	0.486	—
	45.0	0.540	0.465	—
m-Nitroaniline	15.0	1.641	1.694	—
	25.0	1.480	1.461	1.20
	35.0	1.344	1.263	—
	45.0	1.214	1.175	—
p-Nitroaniline	15.0	2.379	2.559	—
	25.0	2.232	2.289	1.68
	35.0	2.111	2.035	—
	45.0	1.980	1.983	—

^a The mobile phase used was 85% isooctane, 15% (premixed 99.7% ethanol/0.3% water) at 1.0 mL/min for Versal aluminas and 2.0 mL/min for Unispherealumina.

^b Based on four k' measurements except for the Versal GL (two measurements).

^c Data are less precise due to the uncertainties in t_m resulting from severe peak overlap.

TABLE 12.3. Selectivity (α) of benzene derivatives on Versal GH (column 20A), Unisphere and Versal GL (column 3A) aluminas at different temperatures. ^a

Compound pair	Temperature (° C)	Selectivity (α)		
		Versal GH Alumina	Unisphere Neutral Alumina	Versal GL Alumina ^b
o-Nitroaniline/Nitrobenzene	15.0	5.24	5.99	6.18
	25.0	5.47	6.40	
	35.0	5.62	6.48	
	45.0	6.00	6.84	
m-Nitroaniline/o-Nitroaniline	15.0	2.43	2.77	2.40
	25.0	2.35	2.69	
	35.0	2.30	2.60	
	45.0	2.25	2.53	
p-Nitroaniline/m-Nitroaniline	15.0	1.45	1.51	1.41
	25.0	1.51	1.57	
	35.0	1.57	1.61	
	45.0	1.63	1.69	

^a The mobile phase used was 85% isooctane, 15% (premixed 99.7% ethanol/0.3% water) at 1.0 mL/min for Versal aluminas and 2.0 mL/min for Unisphere neutral alumina.

^b Data are less precise due to the uncertainties in t_m resulting from severe peak overlap.

TABLE 12.4. Thermodynamic retention parameters of benzene derivatives for Versal GH (column 20A) and Unisphere neutral aluminas. ^a

Compound	$-\Delta H^\circ$ (kcal·mol ⁻¹)	$-(\Delta S^\circ/R + \ln \phi)$	R ²
I. Versal GH Alumina			
Nitrobenzene	2.15	5.79	0.994
m-Nitroaniline	1.82	2.68	0.999
o-Nitroaniline	1.35	2.75	0.998
p-Nitroaniline	1.11	1.07	1.000
II. Unisphere Neutral Alumina			
Nitrobenzene	2.45	6.58	0.986
m-Nitroaniline	2.27	3.44	0.980
o-Nitroaniline	1.70	3.47	0.968
p-Nitroaniline	1.61	1.88	0.944

^a Data obtained from van't Hoff plots (Eqn. 5.4), where temperatures of 15.0, 25.0, 35.0 and 45.0° C were used. The mobile phase used was 85% isooctane, 15% (premixed 99.7% ethanol/0.3% water) at 1.0 mL/min for Versal GH alumina and 2.0 mL/min for Unisphere alumina.

selectivity decreases with increasing temperature, for both Versal GH and Unisphere aluminas.

Table 12.4 gives the thermodynamic parameters obtained for the different benzene derivatives for the Versal GH and Unisphere columns. As seen from the table, the standard enthalpies of transfer for Versal GH and the Unisphere columns are very similar for each of the four test compounds, although the values for the Unisphere column are slightly more negative. For example, ΔH° for p-nitroaniline is -1.11 and -1.61 kcal/mol for the Versal GH and Unisphere columns, respectively, consistent with literature values for alumina. Values for ΔS° could not be deconvoluted from ϕ , the phase ratio, since V_S , the volume of stationary phase available to the test solutes, was not known.

Figures 12.3-12.5 show how poor packing efficiency leads to poor chromatographic separations. The chromatograms in Figs. 12.3 and 12.4 are for column 34A* in Table 11.4A, which is packed with 15 μm Versal GH and has a reduced plate height of 4.5 for toluene. Although the nitroanilines are all baseline resolved, the resolution between toluene and nitrobenzene (peaks 1 and 2) is much worse compared to that obtained for column 20A (Figs. 12.1 and 12.2). The chromatogram obtained for column 35A*, which is packed with 15 μm Versal GH and has a reduced plate height of 6.6 for toluene, is significantly poorer as seen in Fig. 12.5. Peaks 1 and 2 are overlapping, and now the nitroanilines are no longer baseline resolved. Also, the peaks for the nitroanilines are very broad with flat tops.

The only chromatographic separations obtained for Versal GL are illustrated in Figs. 12.6 and 12.7. This is for column 3A which contains 37-44 μm Versal GL with a reduced plate height of 5.2 for toluene. As shown, Versal GL alumina is potentially a good normal-phase adsorbent, provided that the problems of mechanical instability/poor packing efficiency can be overcome. Given the similarity in the selectivities provided by

Versal GH, Unisphere, and Versal GL aluminas (Table 12.3), the Versal GL can be expected to provide similar normal-phase separations, provided that the mobile phase strength is reduced slightly to compensate for the slightly lower retention observed with the Versal GL (Table 12.2).

CONCLUSIONS

The conclusions listed incorporate the results obtained from Chapters XI and XII. Due to their much greater mechanical stability, the Versal GH aluminas are significantly more promising than the GL aluminas as stationary phase adsorbents in HPLC. The Versal GH alumina provided retention and selectivities very similar to that of a commercial grade HPLC alumina originally produced by Alcoa and now made by Biotage. The limited amount of data obtained for the Versal GL alumina (due to the difficulty of packing it) indicates that it provides selectivity similar to the Versal GH and the Unisphere aluminas, although it was found to be slightly less retentive. Unfortunately, the packing of the Versal GL aluminas into usable HPLC columns is problematic. At low pressures where they are mechanically stable, the GL alumina particles cannot be consistently packed with good (adequate) efficiency. At the (higher) pressures necessary for efficient column packing, GL aluminas fracture, producing fines which result in total column blockage. Finally, although the GH materials can be packed satisfactorily in the downward-flow mode using a density-balanced slurry (using halogenated solvents), the costly, somewhat tedious density-balanced approach will probably not be necessary if an upward-flow packing mode is employed.

CHAPTER XIII

SUMMARY AND CONCLUSIONS

A. Polymer-Coated Unisphere Aluminas For Reversed-Phase Liquid Chromatography

The chromatographic properties of three types of polymer-coated aluminas (Unisphere Al-PBD, Unisphere Al-C₁₈ and Unisphere Al-CN, and to a limited extent Millipore Al-PBD) were evaluated and compared to those of conventional, covalently bonded silica-based stationary phases (Microsorb and LiChrospher Si-C₁₈) in terms of the solvent strengths of acetonitrile and methanol, methylene and polar group selectivity, active sites participation in solute retention, thermodynamic performance, kinetic performance (van Deemter relationships), column stability and column re-equilibration kinetics after gradient elution. The different Unisphere polymer-coated aluminas used in the study are commercially manufactured by Biotage, Inc.

During the evaluation of the solvent strengths of MeCN and MeOH for the different column types, it was observed that a better linear correlation was obtained from plots of $\log k'$ vs. ϕ than from the corresponding plots of $\log k'$ vs. $E_T(30)$ solvent polarity. However, in both situations a quadratic function best describes the relationship between $\log k'$ and either ϕ or $E_T(30)$ solvent polarity. An independent survey of published results by researchers who advocate the use of the $E_T(30)$ solvent polarity scale over ϕ , however, reveals that results similar to those obtained in this study are not unique. Limitations in using the S value (Eqn. 3.2) as a measure of solvent strength in RPLC were also identified, and to a first approximation the prediction of solvent strength based solely on the S value is valid provided comparisons are made for the same solute and the same organic solvent using a similar range of mobile phase composition. Hence, it is

reasonable to assume that the S parameter can be used to compare the solvents strengths of the same organic solvent for different columns.

Based on the comparison of S and ϵ values (Eqns. 3.2 and 3.7, respectively), a greater difference in solvent strength between MeCN and MeOH was observed for all the polymer-coated aluminas employed (*i.e.*, MeCN was observed to be a stronger solvent while MeOH a weaker solvent for the alumina-based phases compared to the Si-C₁₈). This trend was attributed to the presence of residual C=C bonds on the stationary phase surface of the aluminas (from incomplete crosslinking and polymerization of the "parent" polymer during stationary phase synthesis), which will interact more with the π electrons of MeCN via π - π interaction. It was also determined that for the polymer-coated aluminas, the difference in solvent strength between MeCN and MeOH was maximum between *ca.* 40-70% organic solvent. A similar distinct maxima was not that obvious for the Si-C₁₈ phases. Finally, this region where the greatest difference in solvent strength between MeCN and MeOH was observed coincides almost exactly to that range wherein the greatest difference in concentrations of free MeCN and free MeOH occurs. The latter observation supports the hypothesis that solute retention in RPLC is controlled predominantly by the volume fraction of free organic solvent (*i.e.*, MeCN and MeOH).

The larger difference in solvent strength between MeCN and MeOH on the polymer-coated aluminas implies that a wider polarity range of solutes can be eluted on these columns than on the Si-C₁₈ stationary phases. This could be done using a two-stage gradient consisting of water to MeOH in the first stage, and MeOH to MeCN in the second stage. Such a gradient represents a significantly larger change in mobile phase strength for the polymer-coated aluminas than for the Si-C₁₈ columns, on which MeCN and MeOH have been shown to be of very similar solvent strength. Note that the dramatic change in mobile phase strength during this two-stage gradient is further

amplified, because the difference in solvent strength between MeCN and MeOH will be particularly large for large molecules that would be expected to elute during the final stage. Analysis of the results from such an investigation will provide concrete evidence supporting the observed greater difference in solvent strength between MeCN and MeOH for the polymer-coated aluminas.

In general, for similar solutes at the same temperature and mobile phase composition, α_{CH_2} values obtained for all polymer-coated aluminas and Si-C₁₈ stationary phases were approximately equal, although in certain solute types the α_{CH_2} values for the Si-C₁₈ columns were slightly higher. This trend, coupled with the less retentive nature of the various alumina-based columns, suggest a potentially important advantage of polymer-coated aluminas, namely that for a given homologous series it should be possible to employ a weaker mobile phase on the polymer-coated columns, thereby achieving higher methylene selectivity with equivalent retention, particularly when MeCN is used as the organic modifier. Assuming the efficiency of the alumina-based columns is comparable to that of silica-based C₁₈ columns, the greater methylene selectivity achieved via a more aqueous mobile phase is a significant advantage, as the polymer-coated columns would thereby provide better resolution of a homologous series. Similarly, using polymer-coated aluminas is advantageous over Si-C₁₈ columns since at equal methylene selectivities, shorter analysis time will be involved for the alumina-based columns.

A detailed examination of the relative retentions of toluene and benzene for both types of columns reveals that the various polymer-coated aluminas are slightly less hydrophobic than the Si-C₁₈ phases, consistent with the more retentive nature and higher $-\Delta H^\circ$ values observed for the Si-C₁₈. However, a comparison of the hydrophobic and polar group selectivity values obtained for each column used in the study indicates the highly hydrophobic nature of these phases (*i.e.*, for all the alumina- and silica-based

phases). For the different polymer-coated aluminas, higher polar group selectivity values were obtained for the Al-CN phase (with the greatest difference observed for the -NO₂ group), while approximately equal polar group selectivities were observed for both Al-PBD and Al-C₁₈. The higher polar group selectivity values obtained for the Al-CN stationary phase is most likely due to the more polar nature of the coating due to the presence of -CN groups on the stationary phase surface, which apparently interacts more with the polar groups of the test probes used, especially -NO₂. The concentration of these cyano groups, however, seems to be just enough to manifest the higher polar group selectivities for the Al-CN column, and still maintain a hydrophobicity similar to that of Al-PBD and Al-C₁₈. Finally, at equal % organic solvent, the Si-C₁₈ polar group selectivity values obtained were in general slightly higher than those observed for the different polymer-coated aluminas.

Unfortunately, polar group selectivities were determined only for the MeOH/H₂O solvent system. It would be interesting to know how similar polar group selectivity values for both the polymer-coated aluminas and Si-C₁₈ would compare for the MeCN/H₂O solvent system. Such results are important especially since it was determined that MeCN is a weaker solvent on the aluminas than on the silicas.

Similar to the conclusions made earlier regarding methylene group selectivity, although the Si-C₁₈ polar group selectivity values obtained were in general slightly larger than similar values for the polymer-coated aluminas, use of a weaker mobile phase on the aluminas will result in similar if not larger polar group selectivity values with equivalent or even smaller retention due to the less retentive nature of these columns. Thus, the use of polymer-coated alumina stationary phases may result in better separation resolution assuming the column efficiencies of the alumina- and silica-based columns are comparable.

In terms of the effect of mobile phase composition and temperature on stationary phase selectivity, it was determined that both methylene and polar group selectivity values increase with decreasing % organic solvent in the mobile phase. Also, higher methylene selectivity are obtained for MeOH/H₂O relative to MeCN/H₂O. Finally, methylene selectivity decreases slightly with increasing column temperature.

Based on the elution order of aniline and phenol, it appears that the different polymer-coated aluminas used in the study are more suitable for the separation of basic samples compared to the different Si-C₁₈ columns employed. This implies that the polymer-coating process utilized for the synthesis of the alumina-based stationary phases effectively shields the -OH groups of the alumina support, rendering these groups inaccessible for the solutes during the chromatographic separation.

Evaluation of the kinetic performance of the polymer-coated aluminas and Si-C₁₈ phases reveals that at optimum linear velocity, comparable reduced plate heights were obtained for the Al-PBD, Al-CN and Si-C₁₈ columns, although *h* values for the retained solutes are slightly better for the silica-based stationary phase. Reduced plate height for the Si-C₁₈ was 2.3 while those for the aluminas ranged from 2.8 to 3.0. However, the minimum *h* values obtained for the Al-C₁₈ were unacceptable, 8.0 and 12.8 for acetone and toluene, respectively. It was hypothesized that the poor column efficiency of the Al-C₁₈ phase may be due to the inherent difficulty involved in obtaining a thin, uniform coating for this stationary phase. Unfortunately, no direct evidence was provided for this hypothesis. It was also determined that in general *u*_{opt} for the aluminas are slightly lower ranging from 0.12 to 0.31 mm/s (0.10 to 0.25 mL/min). The optimum linear velocity was slightly higher for the Microsorb Si-C₁₈ ranging from 0.34-0.67 mm/s, equivalent to flows of 0.25-0.50 mL/min. Finally, examination of the van Deemter plots for the aluminas relative to that for the Si-C₁₈ reveals a broader minimum for the unretained solute (acetone), while the retained solutes displayed a more rapid loss in

efficiency (increase in plate height) with increasing linear velocities, which is almost linear.

The lower u_{opt} values, larger h values at u_{opt} , and the more rapid loss in column efficiency with increasing mobile phase flow rate observed for the polymer-coated aluminas compared to the Si-C₁₈ columns impose a very serious drawback in the possibility of utilizing the alumina-based columns for rapid chromatographic analysis. At practical flow rates (2.00 mL/min for the polymer-coated aluminas and 1.0 mL/min for the Si-C₁₈), h values ranged from 5.7 to 11.5 for Al-PBD and Al-CN, 26.7 to 30.3 for Al-C₁₈, and 3.0 to 5.4 for the Si-C₁₈ columns. Hence, although methylene selectivity values were larger for the polymer-coated aluminas compared to the Si-C₁₈ columns at equivalent retention (*i.e.*, analysis time), the difference in α_{CH_2} seems to be inadequate to provide better R_s values for the polymer-coated aluminas at practical flow rates. Therefore, for the Unisphere columns to be advantageous over conventional Si-C₁₈ in terms of analysis time, the van Deemter minimum for the aluminas should be made broader, and the column efficiencies improved by at least a factor of 6.

It should be noted that if the Unisphere columns are made more efficient than its silica-based counterpart, better R_s values, and shorter analysis time (achieved by using higher flow rates) are easily attainable for the aluminas since normalized ΔP values for the Unisphere phases were observed to be less than that of the Si-C₁₈ phases at the same flow rate and mobile phase composition, with the difference in magnitude greater at elevated flow rates. Utilization of the polymer-coated aluminas would also result in lesser consumption of organic solvent while at the same time resulting in better, if not similar, R_s values relative to the Si-C₁₈ phase. Making these apparent advantages a reality would render the Unisphere polymer-coated aluminas more attractive to use in RPLC, especially in preparative LC.

Finally, the effects of the magnitude of the gradient step, flow rate and temperature on column re-equilibration after gradient elution in RPLC for the various Unisphere polymer-coated aluminas and Si-C₁₈ columns were evaluated. Except for gradient runs started with 100% H₂O, it was shown that flushing the column with at least 20 column volumes of starting mobile phase is enough to fully equilibrate any reversed-phase liquid chromatographic stationary phase (at least for the Si-C₁₈ and polymer-coated aluminas employed in the study). However, a very large amount of starting mobile phase was necessary to equilibrate both Si-C₁₈ and Al-PBD phases for gradients started with 100% water. This trend occurred since complete removal or replacement of the partitioned organic solvent (*i.e.*, organic solvent within the stationary phase) is very difficult for the 100% organic solvent to 100% H₂O reverse step gradient, due mainly to the polarity difference of the latter two solvents. This is a result of the poor water wettability of the nonpolar stationary phase, hence, the stationary phase tends to resist replacement of the partitioned organic solvent with water. For the effect of flow rate on column re-equilibration, it was observed that to a first approximation, the volume of mobile phase needed to equilibrate the stationary phase was independent of flow rate. Hence, it is recommended that the stationary phase be flushed with the new mobile phase using the highest flow rate allowable, which was shown to result in a significant decrease in re-equilibration time. Similar to the results obtained for the effect of flow rate, no definite conclusions can be made regarding the effect of temperature since the RCV values obtained fluctuated over an average range of only about 5 column volumes for both Si-C₁₈ and polymer-coated aluminas. A comparison of the mobile phase volumes necessary to equilibrate the different stationary phases at 15.0 and 55.0° C, however, reveals a general decrease in re-equilibration volume with increasing temperature. In relation to this, although increasing temperature during column re-equilibration may not definitely lead to a significant reduction in RCV, increasing temperature will reduce the

viscosity of the mobile phase allowing the use of even higher flow rates for column re-equilibration relative to that obtained at room temperature. Therefore, it is reasonable to conclude that employing both high flow rate and high temperature will facilitate faster column re-equilibration after gradient elution. It should be noted, however, that the latter recommendation assumes minimal temperature effects on the selectivity of the stationary phase.

B. Versal Aluminas For Normal-Phase Liquid Chromatography

The primary objectives of this part of the research were to optimize the slurry-packing procedure for Versal GL and GH aluminas (produced commercially by LaRoche Chemicals, Inc.) for applications in normal-phase liquid chromatography, and to determine and compare the chromatographic properties of the packed Versal aluminas.

Due to their much greater mechanical stability, the Versal GH aluminas are significantly more promising than the GL aluminas as stationary phase adsorbents in HPLC. The Versal GH alumina provided retention and selectivities very similar to that of a commercial grade HPLC alumina originally produced by Alcoa and now made by Biotage. The limited amount of data obtained for the Versal GL alumina (due to the difficulty of packing it) indicates that it provides selectivity similar to the Versal GH and the Unisphere aluminas, although it was found to be slightly less retentive.

Unfortunately, the packing of the Versal GL aluminas into usable HPLC columns is problematic. At low pressures where they are mechanically stable, the GL alumina particles cannot be consistently packed with good (adequate) efficiency. At the (higher) pressures necessary for efficient column packing, GL aluminas fracture, producing fines which result in total column blockage. Finally, although the GH materials can be packed satisfactorily in the downward-flow mode using a density-balanced slurry (using

halogenated solvents), the costly, somewhat tedious density-balanced approach will probably not be necessary if an upward-flow packing mode is employed.

APPENDIX

MISCELLANEOUS FIGURES

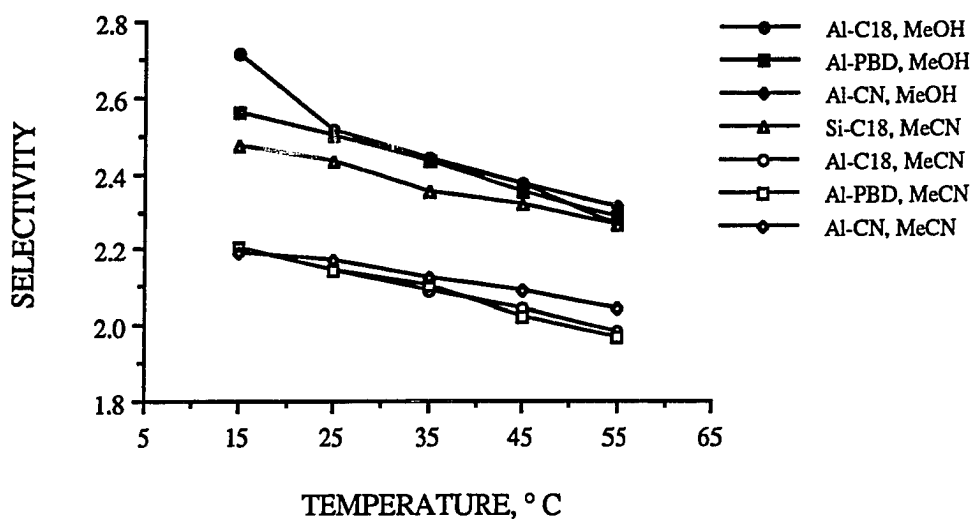


FIGURE A.1. Plot of data in Table 5.2, illustrating the effect of temperature on α_{CH_2} for the n-alkylphenones for the various polymer-coated aluminas and LiChrospher Si-C₁₈ column.

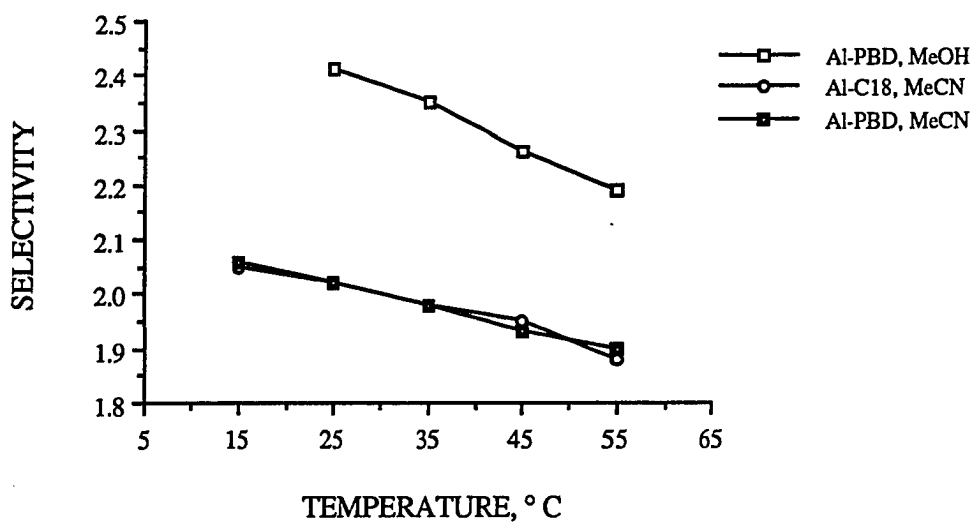


FIGURE A.2. Plot of data in Table 5.3, illustrating the effect of temperature on α_{CH_2} for the n-alkylbenzenes for the Unisphere Al-PBD and Al-C₁₈ columns with 30% organic solvent as mobile phase.

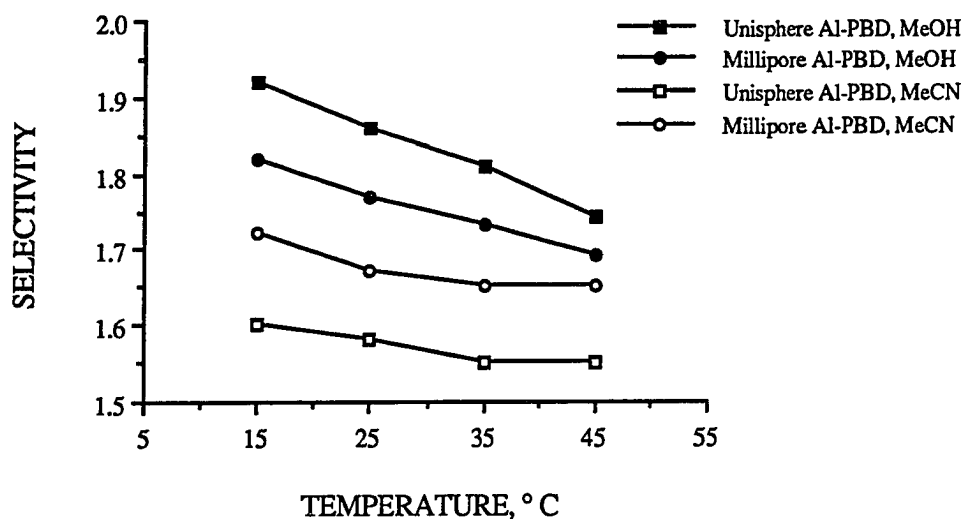


FIGURE A.3. Plot of data in Table 5.4, illustrating the effect of temperature on α_{CH_2} for the n-alkylbenzenes for the Unisphere and Millipore Al-PBD phase with 60% organic solvent as mobile phase.

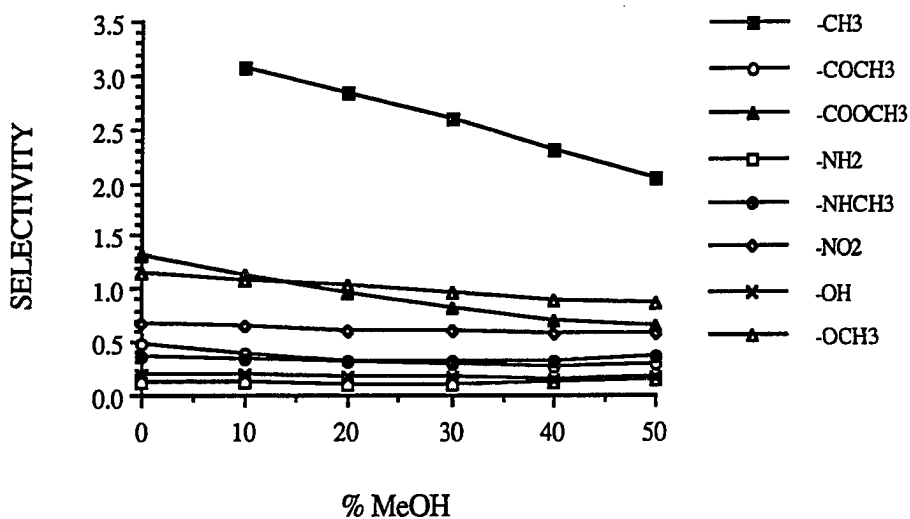


FIGURE A.4. Plot of data in Table 6.5, illustrating the effect of mobile phase composition (organic solvent = MeOH) on group selectivity for the Al-PBD phase.

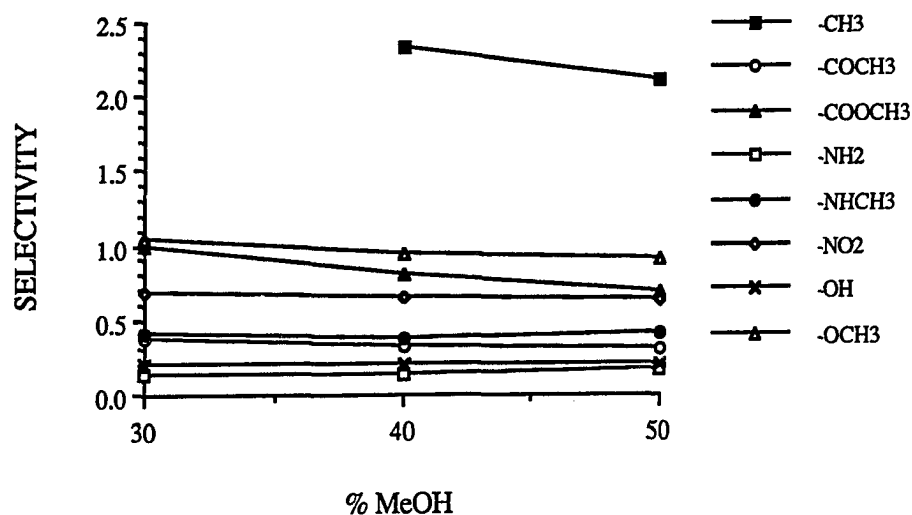


FIGURE A.5. Plot of data in Table 6.6, illustrating the effect of mobile phase composition (organic solvent = MeOH) on group selectivity for the Al-C₁₈ phase.

VITA

The author was born on August 3, 1961 in Manila, Philippines, and grew up in Los Baños - a small, charming town located south of Manila, nestled on the foothills of Mount Makiling, famous for its many hot springs and the University of the Philippines. He attended Maquiling Elementary School, the University of the Philippines Rural High School, and in 1983 obtained his B.S. in chemistry degree from the University of the Philippines at Los Baños. While in college, he performed research on the microbial extraction of trace metals under the guidance of Professor Maria Cristina D. Padolina.

After graduation, the author was employed as a research assistant at the National Crop Protection Center, conducting research on mycotoxin analysis in cereals and legumes. Then in 1984 to 1987, he served as an instructor in chemistry at the University of the Philippines at Los Baños, handling sophomore and senior analytical chemistry laboratory courses. Aside from teaching, he was also a member of the Analytical Services Laboratory, in charge of amino acid analyses. In 1985 he was married to Raquel J. dela Cueva from Santo Tomas, Batangas, and a food technology graduate from the University of the Philippines at Los Baños.

In pursuit of further knowledge in analytical chemistry, he left family and friends behind, and was admitted at the chemistry graduate program of Louisiana State University in 1987. He specialized in chromatography and conducted research under the supervision of Professor Joe P. Foley. While at LSU, the author presented eight scientific papers at various national and international meetings, and had one publication.

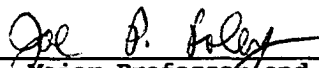
DOCTORAL EXAMINATION AND DISSERTATION REPORT

Candidate: Rene V. Arenas

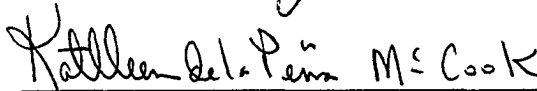
Major Field: Chemistry (Analytical)

Title of Dissertation: Novel Alumina-Based Stationary Phases for
Liquid Chromatography

Approved:

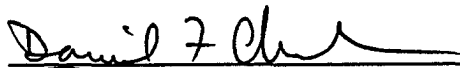


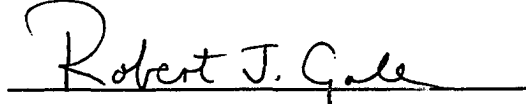
Major Professor and Chairman

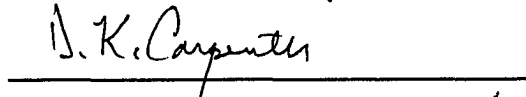


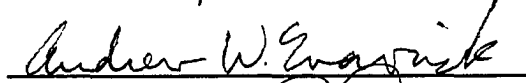
Dean of the Graduate School

EXAMINING COMMITTEE:











Date of Examination: